

https://dspace.org/

# The effects of lightning in shallow coal mines: an engineering study.

**Geldenhuys, Hendrik Jacobus.**

**1995**
https://hdl.handle.net/10539/25064

Downloaded from a DSpace repository. https://dspace.org/

# THE EFFECTS OF LIGHTNING IN SHALLOW COAL MINES - AN ENGINEERING STUDY

**Hendrik Jacobus Geldenhuys**

A thesis submitted to the Faculty of Engineering, University of the Witwatersrand, in fulfilment of the requirements for the degree of Doctor of Philosophy in Electrical Engineering.

JOHANNESBURG

February 1995

# DECLARATION

I declare that this thesis is my own, unaided work. It is being submitted for the degree of Doctor of Philosophy in the University of the Witwatersrand, Johannesburg. It has not been submitted before for any degree or examination in any other University.



20th day of February 1995

## ABSTRACT

Lightning causes electrical shocks to people, the premature ignition of explosives, and the ignition of methane underground in coal mines. This study examines this problem using a theoretical study and the results of an extensive measurement programme that was conducted in several coal mines. The work that has been done, particularly in South Africa, is also reviewed.

Two mechanisms are responsible for the penetration of lightning surge currents into the underground workings. A direct strike to the service structures leading into a shaft is one of the two mechanisms, and the second is that resulting from lightning strikes to the strata above the underground workings.

The frequency and amplitude with which such surges can be expected is quantified using the theoretical study. This model correlates well with the observed frequencies of the empirical studies.

The sensitivity of methane to lightning-type sparks is investigated. Currents as low as 10 mA have been proved to be capable of igniting methane. The sensitivity of conventional detonators is also investigated. The thesis proposes a generalised test which can be applied to both the low-impedance protection method and a high-impedance protection method. The test methodologies have been generalised to make provision for any new innovative detonators that may be used by the industry.

A risk evaluation of mines is developed which allows a mine to be categorised according to the likelihood of lightning causing an accident in a mine.

The South African Recommended Practice for avoiding such accidents is also reviewed.

**For Elmarie**

# ACKNOWLEDGEMENTS

Appreciation is extended to the following organisations and individuals:

The National Energy Council of South Africa - for supporting some of the work reported in this thesis.

The South African Government Mining Engineer and staff - for assisting with the investigations.

The various mining companies that were involved in the measurement programme.

Members of the Lightning and Stray Current Subcommittee, including

Mr J Raath
Mr D Bakker
Mr J B Jackson.

My colleagues at the CSIR who supported the execution of the various measurement programmes.

Prof. Jan Reynders, my study leader.

In particular, my wife and family for their support and understanding.

CONTENTS Page

DECLARATION . . . . . ii
ABSTRACT . . . . . iii
ACKNOWLEDGEMENTS . . . . . v
CONTENTS . . . . . vi
LIST OF FIGURES . . . . . vi
LIST OF TABLES . . . . . vii
LIST OF SYMBOLS . . . . . .

CHAPTER 1: LIGHTNING-INDUCED INCIDENTS IN SHALLOW COAL MINES . . . . . 1

1 INTRODUCTION . . . . . 1

2 THE EXPLOSION HAZARDS ADVISORY COMMITTEE OF THE SOUTH AFRICAN COAL-MINING INDUSTRY . . . . . 2

3 INCIDENTS IN SOUTH AFRICAN COLLIERIES . . . . . 2

3.1 Examples of a detonator explosion . . . . . 5
3.2 Example of a methane explosion . . . . . 7

4 INTERNATIONAL EXPERIENCE . . . . . 8

5 CODE OF PRACTICE FOR THE AVOIDANCE OF HAZARDS UNDERGROUND IN COLLIERIES DUE TO LIGHTNING . . . . . 9

5.1 Earthing of metal work . . . . . 9
5.2 The cessation of handling of explosives when there is a lightning warning 9
5.3 The integrity of the insulation of the detonator electrical circuit . . . . . 11
5.4 Separation of the blasting area from the service structures . . . . . 11

6 THE AIM OF THE STUDY . . . . . 11

6.1 Understanding and quantifying the basic mechanisms through which lightning can enter a mine . . . . . 11
6.2 The sensitivity of detonators and methane . . . . . 12
6.3 The evaluation of mine risk and the Code of Practice . . . . . 12

CHAPTER 2: MECHANISMS WHEREBY LIGHTNING DISCHARGES MAY PENETRATE INTO AN UNDERGROUND MINE . . . . . 13

1 INTRODUCTION . . . . . 13

2 A DIRECT STRIKE TO THE STRUCTURES AT A SHAFT ENTRANCE - A SIMPLE MODEL . . . . . 14

2.1 An analytical model of the surge propagation . . . . . 15

2.2 The frequency of strikes to a shaft = frequency of surges . . . . . 16
2.3 The frequency of voltage surges on the conveyor belt . . . . . 17
2.4 The voltage on a conveyor belt required to set off a detonator in a work face . . . . . 18

2.4.1 Coupling between the conveyor structure and the detonator circuit . . . . . 18
2.4.2 The resistance of the conveyor structure to earth . . . . . 18

2.5 The frequency (risk) of surges in detonator circuits . . . . . 19

3 A DIRECT STRIKE TO THE SURFACE ABOVE A WORKING AREA (COUPLING BY CONDUCTION THROUGH THE STRATA) - A SIMPLE MODEL . . . . . 21

3.1 Current density (J) . . . . . 22
3.2 Current through a 3 m x 5 m rectangular face ($I_F$) . . . . . 22
3.3 The effect of the orientation of the strike relative to the exploder-to-face direction . . . . . 22

4 THE EFFECT OF THE ASSUMPTIONS MADE IN THE MODEL ON THE EXPECTED FREQUENCY OF LIGHTNING CURRENTS . . . . 24

4.1 Uniformity of the strata structure . . . . . 24
4.2 Disregarding skin effect . . . . . 24
4.3 Current through a 3 m x 5 m rectangular face ($I_F$) is equal to the current through a detonator circuit . . . . . 25

5 THE FREQUENCY OF OCCURRENCE OF CURRENTS LARGER THAN A CERTAIN VALUE IN A PARTICULAR FACE . . . . . 25

6 THE RADIATION MECHANISM - ENERGY TRANSFERRED TO A VULNERABLE CIRCUIT BY ELECTROMAGNETIC COUPLING . 30

6.1 The magnetic field . . . . . 30
6.2 A typical configuration . . . . . 32

7 COMPARISON BETWEEN THE MAGNETIC INDUCTION MECHANISM AND THE RESISTIVE CONDUCTION MECHANISM 33

7.1 The conduction mechanism . . . . . 33
7.2 The magnetic induction mechanism . . . . . 34

CHAPTER 3: THE EFFECT OF STRATA LAYERS ON THE PENETRATION OF CURRENT INTO DETONATION CIRCUITS . . . . 35

1 INTRODUCTION . . . . . 37

2 A SIMPLE SPHERICAL MODEL . . . . . 37

3 THE STRATA MODEL . . . . . 38

4 EVALUATION AND SELECTION OF A FIELD CALCULATION PROGRAMME . . . . . 40

5 TYPICAL RESULTS FROM THE FIELD CALCULATION PROGRAMMES . . . . . 42

6 DATA OF INTEREST TO THIS STUDY . . . . . 45

7 CALCULATION OF THE FREQUENCY ($N_r$) AT WHICH LIGHTNING SURGES OF MORE THAN A CERTAIN MAGNITUDE WILL OCCUR IN A DETONATOR CIRCUIT . . . . . 47

7.1 The number of events . . . . . 47
7.2 The probability $P_r(r)$ . . . . . 48
7.3 Results from the example . . . . . 49

8 RESULTS: THE EFFECT OF DIFFERENT MODEL PARAMETERS . . . . . 52

8.1 Depth of the coal seam - peak current amplitude at the work face . . . . 52
8.2 Depth of the coal seam - surge current frequency . . . . . 54

8.3 The resistivity of the strata . . . . . 56

8.3.1 $\rho_1 = \rho_2$ - the same resistivity above and below the coal seam 56
8.3.2 The effect of the resistivities of the surface layer and the deep strata where $\rho_1$ is not equal to $\rho 2$ . . . . . 59

8.4 The effect of the resistivity of the coal seam . . . . . 62

8.5 The effect of the thickness of the coal seam . . . . . 65

CHAPTER 4: THE "ACCURATE" MEASUREMENT OF SURGES UNDERGROUND . . . . . 67

1 INTRODUCTION . . . . . 68

2 HISTORY OF MEASUREMENTS . . . . . 68

3 THE RESEARCH STATION . . . . . 68

3.1 The underground station . . . . . 70
3.2 The surface station . . . . . 71

3.2.1 Power to the surface station . . . . . 71
3.2.2 Control of the surface station . . . . . 72
3.2.3 Recording at the surface station . . . . . 72

4 LOCATIONS AND CONFIGURATIONS OF THE RESEARCH STATIONS . . . . . 73

4.1 Installation at Springbok Collier . . . . . 73
4.2 Installation at Greenside Colliery . . . . . 76

5 RESULTS OBTAINED FROM THE MEASUREMENT PROGRAMME . . . . . 78

5.1 Results from Configuration 1 . . . . . 79
5.2 Results from Configuration 2 . . . . . 81
5.3 Results from Configuration 3 . . . . . 81
5.4 Results from Configuration 4 . . . . . 83
5.5 Results from Configuration 5 . . . . . 84

5.5.1 Results from Springbok Colliery . . . . . 84
5.5.2 Results from Greenside Colliery . . . . . 86

6 A COMPARISON BETWEEN THE RESULTS FROM GREENSIDE COLLIERY AND THE SIMPLE SPHERICAL MODEL . . . . . 87

7 GENERAL DISCUSSION OF RESULTS . . . . . 90

7.1 The induction mechanism . . . . . 90
7.2 Vertical and horizontal voltage gradient . . . . . 90

CHAPTER 5: THE FUSE SURGE DETECTOR MEASURING PROGRAMME
. . . . . 90
1 INTRODUCTION . . . . . 90

2 THE OBJECTIVES OF THE FSD PROGRAMME . . . . . 90

3 THE CONSTRUCTION AND DESIGN OF THE FSD . . . . . 90

3.1 Sensitivity of the FSD . . . . . 90
3.2 The equivalent median lightning current . . . . . 93
3.3 The function of the gas arresters . . . . . 94
3.4 Corrosion-resistant FSDs . . . . . 94
3.5 Indication of blown fuses and intrinsic safety . . . . . 95

4 METHOD OF INSTALLING FSDs IN TYPICAL WORK-FACE CONFIGURATIONS . . . . . 95

4.1 Collieries in which FSDs were installed . . . . . 97

5 RESULTS FROM THE BLOWN FSDs IN COLLIERIES . . . . . 98

6 LIGHTNING FLASH DENSITY . . . . . 101

7 NORMALISED FREQUENCY OF SURGES IN THE VARIOUS MINES . . . . . 102

8 RESULTS: SOME COMPARISONS . . . . . 104

8.1 The configuration of Faces 1 and 2 . . . . . 104
8.2 Comparison with the simple model . . . . . 105
8.3 Comparison between the mines and depth dependence . . . . . 106

CHAPTER 6: METHANE SENSITIVITY TO LIGHTNING-INDUCED SPARKS . . . . . 108

1 INTRODUCTION . . . . . 108

2 THE NATURE OF LIGHTNING SPARKS UNDERGROUND . . . . 108

2.1 Sparking on the strata surface . . . . . 108
2.2 Sparking involving conductors . . . . . 109

3 LITERATURE SURVEY . . . . . 111

3.1 Energy . . . . . 112
3.2 Current . . . . . 112
3.3 Rate of energy dissipation . . . . . 112
3.4 Electrode material and shape . . . . . 113

4 THE CSIR EXPERIMENT . . . . . 113

4.1 The experimental arrangement . . . . . 113
4.2 Results from the CSIR experiment . . . . . 116

5 CONCLUSIONS . . . . . 118

**CHAPTER 7: THE SENSITIVITY OF CONVENTIONAL DETONATORS** . . . . . 119

1 **CONSTRUCTION OF A CONVENTIONAL ELECTRIC DETONATOR** . . . . . 120

1.1 **The operating mechanisms** . . . . . 120
1.2 **Delay element and base charge** . . . . . 120
1.3 **Housing** . . . . . 120
1.4 **Static protection** . . . . . 120

2 **TYPES OF DETONATORS TESTED** . . . . . 120

3 **SPARKS TO THE FUSE HEAD** . . . . . 121

4 **LIGHTNING-TYPE IMPULSE CURRENT IN NORMAL MODE** . . . 123

5 **BREAKDOWN VOLTAGE FROM THE TUBE TO THE ELECTRICAL CIRCUIT** . . . . . 125

**CHAPTER 8: THE LIGHTNING SURGE VOLTAGE REQUIRED TO SET OFF AN ELECTRICAL DETONATOR** . . . . . 128

1 **INTRODUCTION** . . . . . 128

2 **AN EQUIVALENT ELECTRICAL CIRCUIT FOR DETERMINING THE CURRENT THAT LIGHTNING INDUCES INTO A DETONATOR CIRCUIT** . . . . . 129

2.1 **The current flow between the two detonators $I_F$** . . . . . 131
2.2 **The current flow between the exploder and the detonators in the work face** . . . . . 131

3 **THE IMPEDANCE (TIME AND CURRENT) BEHAVIOUR OF THE ELEMENTS OF A DETONATOR CIRCUIT UNDER LIGHTNING CURRENT IMPULSES** . . . . . 132

3.1 **Explosives** . . . . . 132

3.1.1 The DC resistivity of two commercial explosives . . . . . 132
3.1.2 The impulse impedance behaviour of explosives . . . . . 134
3.1.3 Calculated (expected) resistance based on the DC resistivity measurements 135
3.1.4 Experimental results . . . . . 135

4 THE IMPULSE IMPEDANCE BEHAVIOUR OF COAL . . . . . 140

4.1 The experimental set-up . . . . . 140
4.2 Experimental results . . . . . 142

5 THE IMPULSE IMPEDANCE BEHAVIOUR OF A DETONATOR IN AN EXPLOSIVES-COAL INSTALLATION . . . . . 145

5.1 The experimental results . . . . . 145

5.1.1 Time dependence of impedance . . . . . 147
5.1.2 Voltage dependence of current . . . . . 147

5.2 Ageing of the test configuration . . . . . 152
5.3 Effect of polarity . . . . . 152
5.4 An empirical mathematical relationship between current and voltage . . 152

6 GENERALISATION OF THE RESULTS . . . . . 153

6.1 Explosives-detonator-coal model . . . . . 153
6.2 Comparison with the Oettlé model . . . . . 153
6.3 A model for the exploder and the detonator . . . . . 155

7 THE VOLTAGE AND ELECTRIC FIELD GRADIENT REQUIRED TO SET OFF DETONATORS . . . . . 157

7.1 Face (top to bottom) . . . . . 157

7.1.1 Five detonators in parallel in series with five parallel detonators . . . . . 157
7.1.2 Type 0 detonator: . . . . . 157
7.1.3 Type 1 detonator . . . . . 158

7.2 15 parallel detonators in series with a shot exploder . . . . . 159

7.2.1 Type 0 detonato . . . . . 159
7.2.2 Type 1 detonator . . . . . 159

7.3 The minimum voltage and minimum electric field gradient . . . . . 160

CHAPTER 9: AN IMPROVED ELECTRICAL SAFETY SPECIFICATION FOR COLLIERY DETONATORS . . . . . 161

1 INTRODUCTION . . . . . 161

2 HISTORIC SAFETY TESTS . . . . . 162

3 INSULATION PROTECTION AND SHORT-CIRCUIT PROTECTION . . . . . 163

4 A LIGHTNING SENSITIVITY TEST . . . . . 164

5 SPARK PENETRATION TEST168

6 METHODS OF APPLYING THE TESTS . . . . . 168

6.1 Common-mode test . . . . . 169

CHAPTER 10: A LIGHTNING-RISK INDEX FOR A MINE

1 INTRODUCTION . . . . . 172

2 TYPES OF HAZARDS . . . . . 173

2.1 Methane . . . . . 172
2.2 Detonators/explosives . . . . . 173

3 A PROPOSED RISK INDEX . . . . . 173

3.1 Ng - lightning flash density . . . . . 175
3.2 N(d) - Surge frequency at depth (d) . . . . . 175
3.3 $K_p$ - the effect of strata resistivity . . . . . 176
3.4 $K_t$ - The effect of coal-seam thickness . . . . . 177

4 RISK INDEX ANALYSIS USED IN MINES ON THE FUSE SURGE DETECTOR PROGRAMME . . . . . 179

5 RISK INDEX . . . . . 183

5.1 Accident statistics . . . . . 184

6 THE RISK OF AN UNDERGROUND DETONATOR ACCIDENT . . 185

7 DISCUSSION . . . . . 186

CHAPTER 11: RECOMMENDATIONS AND FINALE . . . . . 187

1 AMENDMENTS TO THE CODE OF PRACTICE . . . . . 188

1.1 Mine risk index . . . . . 188
1.2 Detonators . . . . . 188
1.3 Connection of detonators . . . . . 189

3 FURTHER WORK REQUIRED TO REFINE THE FINDINGS OF THIS THESIS . . . . . 192

3.1 The frequency of surges - model . . . . . 192
3.2 Coal resistivity and the Oettlè model . . . . . 192
3.3 The effect of underground structures on the distribution of lightning surge currents . . . . . 193
3.4 The effect of the mined-out section on current distribution . . . . . 193
3.5 Depths exceeding 100 m . . . . . 194
3.6 Extrapolation of the effects of resistivity and coal seams . . . . . 194
3.7 Methane - lightning sensitivity . . . . . 194

4 HIGHLIGHTS OF THE THESIS . . . . . 194

REFERENCES . . . . . 195

## LIST OF FIGURES


| Figure No. | | Page |
|---|---|---|
| 1.1A | A plan giving a view of the area in a mine where four faces detonated inadvertently in September 1980 | 13 |
| 1.1B | Detailed plan of the section in which detonations occurred at two faces, showing the faces and interconnections between the detonators. | 13 |
| 1.2 | Performance of the CSIR lightning warning unit. | 14 |
| 2.1 | A simplified diagram depicting how lightning surges may enter collieries | 16 |
| 2.2 | A simple equivalent electrical model of the case where lightning strikes a shaft entrance | 20 |
| 2.1 | A simplified diagram depicting how lightning surges may enter collieries | 13 |
| 2.2 | A simple equivalent electrical model of the case where lightning strikes a shaft entrance | 14 |
| 2.3 | The voltage surge U and the current $I_C$ injected into the underground structure as a function of the lightning current $I_L$ and the resistance of the earth electrode $R_E$ at the shaft entrance | 16 |
| 2.4 | The frequency with which surges are induced into detonator circuits when lightning strikes the shaft entrance, calculated for $N_g = 1$. | 20 |
| 2.5 | The physical model of lightning current penetrating the earth | 21 |
| 2.6 | The frequency of lightning-induced currents in a face calculated for different seam depths. The results are normalized to one face and Ng = 1 and $I_L$ = 34 kA. | 28 |
| 2.7 | The maximum current in face as a function of the coal seam depth calculated for lightning currents of different magnitude | 29 |
| 2.8 | Model of lightning current | 30 |

2.9 The $A^2$ s induced through the magnetic induction mechanism compared with the resistive conduction mechanism. This comparison has been made using the median lightning strike of Figure 2.8 as a function of distance from the flash. . . . . 35

3.1 The basic model for evaluating computer programmes . . . . . 36

3.2 A simplified model of the configuration of the strata in a typical South African mine . . . . . 38

3.3 Boundaries of the simplified model . . . . . 39

3.4 The positioning of boundary elements on the model analysed. . . . . 42

3.5 The equipotential contours up to 1 500 m (seam depth (d) = 15 m and seam thickness (t) = 5 m) . . . . . 42

3.6 The equipotential contours to a depth of 500 m (seam depth (d) = 15 m and seam thickness (t) = 5 m) . . . . . 43

3.7 The equipotential contours to a depth of 50 m (seam depth = 15 m and seam thickness = 5 m) . . . . . 43

3.8 The electric field gradient vertically down the symmetrical axis. . . . . 44

3.9 The potential horizontally above the coal seam ($U_T$) and the potential just below the coal seam ($U_B$). (I = 1 A, seam depth (d) = 15 m, and seam thickness (t) = 5 m) . . . . . 45

3.10 The voltage difference between $U_T$ and $U_B$ directly vertical ($U_V$) and the voltage difference diagonally across $U_D$. The "face-to-exploder" distance ($d_F$) is 30 m and can be compared to the potential of the boundary just above the coal seam ($U_T$). Seam depth (d) = 15 m and seam thickness (t) = 5 m . . . . . 46

3.11 The lightning current required to set off a Type 0 Detonator as a function of the distance between the strike and the work face (r). The probability of a particular strike exceeding this value of current is plotted on the same axis. Seam depth d = 15 m. Seam thickness t = 5 m.

3.12 The probability at a defined distance times the area associated with that distance. . . . . 50

3.13 The diagonal voltage difference ($U_D$) for coal seams at different depths (d).
t = 5 m, $\rho_C$ = 3 000 Ω.m, and I = 1 A. . . . . 52

3.14 The peak of the diagonal voltage difference $U_D$ as a function of the seam depth (d).
t = 5 m, $\rho$ = 3 000 Ω.m, I = 1 A, and $\rho_1 = \rho_2$ = 400 Ω.m. . . . . 54

3.15 The frequency of surges exceeding the sensitivity of Type 0 (0/d) detonators as a function of the depth of the coal seam (d).
t = 5 m, $\rho$ = 3 000 Ω.m, and $\rho_1 = \rho_2$ = 400 Ω.m . . . . . 55

3.16 The maximum of the diagonal voltage difference ($U_D$) in the case where the resistivities of the surface layer and deep strata are the same, $\rho_1 = \rho_2$.
t = 5 m, d = 30 m, $\rho_C$ = 3 000 Ω.m, I = 1 A. . . . . 56

3.17 The frequency of surges exceeding the sensitivity of Type 0 detonators as a function of strata resistivity. The resistivity of the surface layer and the resistivity of the deep strata are the same, $\rho_1 = \rho_2$.
t = 5 m, d = 30 m, $\rho_C$ = 3 000 Ω.m . . . . . 57

3.18 The maximum of the diagonal voltage difference ($U_D$) as a function of the resistivity of the surface layer ($\rho_1$).
t = 5 m, d = 30 m, $\rho_c$ = 3 000 Ω.m, I = 1 A. . . . . 58

3.19 The maximum of the diagonal voltage difference ($U_D$) as a function of the resistivity of the deep strata ($\rho_2$).
t = 5 m, d = 30 m, $\rho_1$ = 3 000 Ω.m, I = 1 A . . . . . 59

3.20 The frequency of surges exceeding the sensitivity of Type 0 detonators as a function of the resistivity of the surface layer ($\rho_1$).
t = 5 m, d = 30 m, $\rho_1$ = 3 000 Ω.m . . . . . 60

3.21 The frequency of surges exceeding the sensitivity of Type 0 detonators as a function of the resistivity of the deep strata ($\rho_2$).
t = 5 m; d = 30 m; $\rho_1$ = 3 000 Ω.m . . . . . 61

3.22 The maximum of the diagonal voltage difference ($U_D$) as a function of the resistivity of the coal seam ($\rho_2$).
t = 5 m, d = 30 m, $\rho_1 = \rho_2$ = 400 Ω.m, I = 1 A . . . . . 62

3.23 The frequency of surges exceeding the sensitivity of Type 0 detonators as a function of the the resistivity of the coal seam ($\rho_C$).
A : is the frequency of the voltage required to set off a detonator (taken as being 38 kV).
B : is the frequency where the effect of the resistivity of the coal seam on the detonator current is taken in consideration, according to Figure 8.26. . . 63
t = 5 m, d = 30 m, $\rho_1 = \rho_2 = 400$ Ω.m

3.24 The maximum diagonal voltage difference ($U_D$) for different thicknesses of coal seams (t).
A : the voltage across a 2.5 section of the coal seam
B : the voltage across the total seam
d = 30 m, $\rho_1 = \rho_2 = 400$ Ω.m, I = 1 A . . . . . 65

3.25 The frequency of surges exceeding the sensitivity of Type 0 detonators as a function of the thickness of the coal seam (t).
A : only the voltage across a typical work face (2.5 m) is taken into account
B : if the voltage across the total thickness of the coal seam is taken into account
d = 30 m; $\rho_1 = \rho_2 = 400$ Ω.m; $\rho_C = 3\,000$ Ω.m . . . . . 66

4.1 A schematic diagram of the research station showing
- the circuit configuration at the work face
- the instrumentation boxes underground
- the installation at the surface, i.e. the recording station, flash counter and video camera . . . . . 68

4.2 A functional diagram of the surface recording station. Information was recorded by the event recorder (on paper) and by the digital storage oscilloscope in a bubble memory. . 69

4.3 Measuring circuit configurations used in the research programme . . . . . 72

4.4 A diagram showing the measuring installation used at Springbok Colliery. This shows the layout with only one instrument box. . . . . 73

4.5 The strata at Springbok Colliery (taken from Geological Borehole No. 226). At the actual research station, the depth of the No. 2 seam is 46 m.
The coal seams are bordered by sedimentary layers. . . . . 74

4.6 Earth resistivity measurements made, using the Venner method, at the research station in Springbok Colliery for the period that the station operated. . . . . 74

4.7 The underground research station at Greenside Colliery. A special borehole was drilled for the optic-fibre cable between the installation and the surface. . . . . 75

4.8 The strata at Greenside Colliery (from Geological Borehole Sample No. BH1). The depth of the research station is 23 m and it was the No. 5 seam that was being mined.
The coal seams are bordered by sedimentary layers. . . . . 76

4.9 Earth resistivity measurements above the research station at Greenside Colliery, taken at various times during the period that the research station was operated at this site (Jan. 1986 to July 1989) . . . . . 76

4.10 Monthly and total seasonal lightning flash density at the recording station for 1986/87, 1987/88 and 1988/89. . . . . 77

4.11 The position and amplitude of the surges relative to the Greenside Research Station . . 87

4.12 The waveshape of the surge of 31/8/88 . . . . . 87

4.13 The waveshape of the surge of 28/11/88 . . . . . 88

5.1 Drawing of the physical layout of the FSD . . . . . 91

5.2 The fuse current of nichrome wire of various diameters. The fuse currents of Type 0 and Type 1 detonators are also shown. . . . . 92

5.3 The installation of FSDs in a particular area of a mine. Note that the "first fuse" detects currents in the face and the "second fuse" detects current from the face to the exploder. . . . . 96

5.4 The normalised frequency of 3 A of Face 1, vertical or horizontal and Face 2 at the various mines. . . . . 104

5.5 The predicted frequencies (Geldenhuys et al, Oct. 1987) at diagonal faces at depths of 20 m and 80 m. The average results of all the mines in the FSD programme are plotted on the same axis as the line marked with *.
+ These points are frequencies that have been observed in particular mines. . . . . 105

5.6 The normalised frequencies of 3 A, 7 A and 10 A that blew fuses in Face 2 (diagonal current) in the various mines. . . . . 106

5.7 The normalised frequencies of 3 A, 7 A and 10 A that blew fuses in Face 2, plotted against the average depth of the FSD installation in the various mines. The maximum frequency of a specific current versus depth is also shown through the interconnecting lines. . . . . 107

6.1 The potential induced into the roof of an underground working.
$P_1 = P_2$, t = 3 m, $\rho_C$ = 3 000 Ω.m, $\rho_1 = \rho_2$ = 400 Ω.m. . . . . 110

6.2 The cross-section of the 2.5 m diameter tunnel in which the experiment was conducted. The electrode spark gap and the manhole through which the wires were fed into the tunnel are also shown. . . . . 114

6.3 The equivalent circuit diagram of the high-voltage impulse circuit. The HV-DC charging unit could charge the capacitor up to 40 kV . . . . . 115

6.4 The ignition (YES) and the non-ignition (NO) data points obtained from the CSIR experiment. The lines are drawn on the boundaries of ignition or non-ignition for the three gaps tested. The waveshapes have a time-to-half value of 50 μs. The electrodes are of steel. . . . . 116

6.5 The minimum ignition peak current required to ignite of an air-methane mixture as a function of the spark gap length. The waveshape has a time-to-half value of 50 μs. Steel electrodes were used. . . . . 118

7.1 The construction of an electrostatically-protected electrical detonator. . . . . 120

7.2 The electrical equivalent circuit of a conventional electrical detonator . . . . . 121

7.3 Electrical sparking to the fuse-head test configuration. The high-voltage impulse current was limited by a resistor and the waveshape was 0.5/700 μs. . . . . 122

7.4 The normal mode of current flow through a detonator . . . . . 124

7.5 The impulse breakdown voltage of the different detonator types. A 1.2/50 μs waveshape was used. The tube was positive and the wires negative. The line represents one standard deviation. . . . . 125

7.6 The impulse breakdown voltage of the different detonator types. A 1.2/50 μs waveshape was used. The tube was negative and the wires positive. The line represents one standard deviation. . . . . 126

8.1 A schematic representation of the voltage and current induced by lightning in an underground coal-seam mining operation. . . . . 128

8.2 An electrical equivalent representation of the detonator-exploder configuration. . . . . 129

8.3 The electrode configuration used to measure the resistance through a stick of explosives . . . . . 131

8.4 A schematic diagram showing the dummy explosive cartridge tamped inside a metal tube. A detonator was placed inside the explosive as in normal practice and an high-voltage impulse was applied between the detonator and the metal pipe. . . . . 133

8.5 Oscillogram showing the applied voltage waveshape and measured impulse current on Ajax (before breakdown) . . . . . 134

8.6 Oscillogram showing the applied voltage (top), which breaks down and collapses to almost 0 V, with an associated step in current (bottom). The impedance after breakdown is also shown. . . . . 136

8.7 Oscillogram of voltage impulse applied to Coalex.
A - before breakdown. B - after breakdown. . . . . 137

8.8 Physical dimensions of the coal block from Greenside Colliery . . . . . 138

8.9 The physical layout of the experiment. . . . . 139

8.10 The impulse generator circuit used in the experiment. The generator has a rating of 50 kV per stage. Up to four stages were used. C = .14 $\mu$F per stage. . . . . 139

8.11 The resistivity as a function of field strength, as measured on the coal block from Sigma Colliery (in a uniform current density field). The results from both positive and negative impulses are shown. Measurements were taken at 2 $\mu$s, 5 $\mu$s and 10 $\mu$s after the impulse peak. . . . . 140

8.12 The resistivity as a function of field strength, as measured on the coal block from Greenside Colliery (in a uniform current density field). Measurements were taken at 2 $\mu$s, 5 $\mu$s and 10 $\mu$s after the impulse peak. . . . . 141

8.13 The current density as a function of field strength, as measured on the coal block from Sigma Colliery (in a uniform current density field). The results from both the positive and negative impulses are shown. Measurements were taken at 2 $\mu$s, 5 $\mu$s and 10 $\mu$s after the impulse peak. . . . . 141

8.14 The current density as a function of field strength, as measured on the coal block from Greenside Colliery (in a uniform current density field). Measurements were taken at 2 $\mu$s, 5 $\mu$s and 10 $\mu$s after the impulse peak. . . . . 142

8.15 A cross-sectional schematic diagram showing how the dummy explosive-detonator circuit was constructed in the CSIR HV laboratory. . . . . 143

8.16 Zone 1: The current impulse waveshape resulting from the application of a 20 kV peak 1/50 $\mu$s impulse to the configuration of Figure 8.15 (Impulse No. 20 of Table 8.4). Positive voltage polarity was applied to the detonator. . . . . 146

8.17 Transition from Zone 1 to Zone 2: The current impulse waveshape resulting from the application of a 40 kV peak 1/50 $\mu$s impulse to the configuration of Figure 8.15 (Impulse No. 22 of Table 8.4). Positive voltage polarity was applied to the detonator. . . . . 147

8.18 Zone 2: The current impulse waveshape resulting from the application of a 100 kV peak 1/50 $\mu$s impulse to the configuration of Figure 8.15 (Impulse No. 9 of Table 8.4). Positive voltage polarity was applied to the detonator. . . . . 148

8.19 The applied voltage peak versus the peak current measured through the detonator circuit for the sequence of impulses as applied in Table 8.4. Note the difference between the first and second series of tests. . . . . 149

8.20 Mathematical regression line fitted to the data of Figure 8.19. . . . . 150

8.21 Comparison between the experimental data and the Oettlé model. . . . . 152

8.22 The Oettlé model used for various coal resistivities . . . . . 153

8.23 The impulse impedance model for a detonator in explosives in coal and a model for an exploder standing on the mine floor . . . . . 154

8.24 The detonator-explosion-coal impulse impedance model showing the sparkover at 20 kV due to the explosives insulation characteristic . . . . . 154

8.25 The minimum voltage required to set off a detonator in the face top-to bottom configuration. . . . . 159

8.26 The minimum voltage required to set off a detonator in the face-to-exploder configuration. . . . . 159

8.27 The minimum electric field gradient required to set off a detonator in the two configurations analysed. . . . . 160

9.1 A "French" test performed on a conventional electrical detonator. $R_i$ = internal resistance of the capacitor; L = circuit stray resistance . . . . . 162

9.2 A schematical circuit diagram of a lightning-sensitivity test set-up for detonators. . . . 164

9.3 The equivalent test resistance, $R_T$, for the diagonal configuration. . . . . 166

9.4 The frequency of surges in the case where the current induced into a detonator circuit and where the current is kept constant, as reference I = 7 A.
The second curve is the case where the voltage is kept constant, as reference V = 38 kV.
t = 3 m; d = 30 m; $\rho = \rho_2 = 400$ Ω.m . . . . . 167

9.5 Different designs of detonators:
(i) Multi-wire, T-off
(ii) Multi-wire, in out
(iii) Transformer coupled
(iv) Conventional design . . . . . 169

9.6 Common-mode test configuration for detonators connected in series and in parallel . . 170

10.1 The frequency of surges exceeding Type 0 detonator sensitivity, as a function of mine depth. The data points are shown and the curve is the regression line. . . . . 175

10.2 The correction factor, $K_\rho$ that makes provision for the effect of strata resistivity. The thick line represents the case where the resistivity above and below the coal seam is the same. . . . . 177

10.3 The correction factor, $K_t$ that makes provision for the effect of coal-seam resistivity. . 178

10.4 The linear regression between the predicted frequency of the model and the frequency measured by the 3 A FSD. . . . . 181

10.5 The linear regression between the predicted frequency of the model and the measured frequency of the 7 A FSD. . . . . 182

10.6 The linear regression between the predicted frequency of the model and the measured frequency of the 10 A FSD. . . . . 182

11.1 The lightning surge current flow between the face and the exploder. Connecting the exploder cable to the top is preferred. . . . . 189

LIST OF TABLES


| | | |
|---|---|---|
| **Table 1.1** | Summary of lightning-related incidents in South African collieries | 3 |
| **Table 2.2** | Skin depth at f = 10 kHz (permeability assumption $u_r = 1$) | 25 |
| **Table 2.3** | The frequency of surges exceeding the value of $I_F$. $N_g = 1$ and $I_L = 34$ kA. | 27 |
| **Table 2.4** | The maximum of $I_F$ as a function of depth and lightning current | 29 |
| **Table 3.1** | The outer hemispherical boundary potential determined by equation 3.2 | 41 |
| **Table 4.1** | Surges recorded at Springbok Colliery in Configuration 1 | 79 |
| **Table 4.2** | Summary of the surges recorded in Configuration 1. | 79 |
| **Table 4.3** | Summary of the surges recorded in Configuration 2. | 80 |
| **Table 4.4** | Surges recorded at Springbok Colliery in Configuration 3 | 81 |
| **Table 4.5** | Summary of the surges recorded in Configuration 3. | 82 |
| **Table 4.6** | Surges recorded at Springbok Colliery in Configuration 4 | 83 |
| **Table 4.7** | Summary of the surges recorded in Configuration 4 | 83 |
| **Table 4.8** | Surges recorded at Springbok Colliery in Configuration 5 | 84 |
| **Table 4.9** | Summary of the surges recorded in Configuration 5 | 85 |
| **Table 4.10** | Surges recorded at Greenside Colliery in Configuration 5 during the 1988/89 season | 86 |
| **Table 4.11** | Statistical summary of the surges recorded in Configuration 5 at Greenside Colliery | 88 |
| **Table 4.12** | Data for the three flashes | 89 |
| **Table 5.1** | The fuse current rating of the different fuses in the FSD | 97 |
| **Table 5.2** | Mines in which FSDs were installed. The last column shows the total exposure at each mine: number of faces installed x flash density, accumulated for the total period | 98 |
| **Table 5.3** | The average and minimum depths and thicknesses of coal seams at locations where FSDs were installed in the various mines | 99 |
| **Table 5.5** | Results obtained during six thunderstorm seasons, 1986/87 to 1990/92. The fuses blown were in the vertical configuration | 100 |
| **Table 5.6** | Results obtained during six thunderstorm seasons, 1986/87 to 1990/91. The fuses blown were in the horizontal configuration | 100 |

The fuses blown were in the horizontal configuration . . . . . 100

5.7 Results obtained during six thunderstorm seasons, 1986/87 to 1990/2. The fuses blown were in the face-to-exploder-bolt configuration . . . . . 102

5.8 Lightning ground flash densities ($N_g$) at the Greenside, Sigma, Welgedacht, Delmas and Matla Collieries . . . . . 102

5.9 Normalised frequencies for Face 1, vertical . . . . . 103

5.10 Normalised frequencies for Face 1, horizontal . . . . . 103

5.11 Normalised frequencies for Face 2 . . . . . 103

5.12 Normalised frequencies for Face 2 at the individual mines

6.1 Ionisation radius of a lightning current of 100 kA versus strata resistivity . . . . . 109

6.2 The maximum voltage difference induced into the roof of a 15-m deep coal seam and a 30-m deep coal seam by a lightning current of 100 kA. . . . . 110

6.3 The voltage current, pulse duration and peak current required to ignite methane-air mixtures in a 1.25 mm gap, taken from Bartels (1975). . . . . 113

6.4 The values of R and the RC time constant assuming C = 10 pF . . . . . 115

7.1 Different types of conventional detonators tested . . . . . 121

7.2 Results of electrical sparking to the detonator fuse head. The voltage applied had a peak of 6 kV and a 0.5/700 $\mu$s waveshape. . . . . 123

7.3 The peak current and energy required to set off the different types of detonators . . . . . 124

8.1 Measurements obtained with the Hipotronics Megohm meter . . . . . 132

8.2 Impedance in Figure 8.5 against time . . . . . 134

8.3 Physical dimensions of the coal blocks used in the experiment. . . . . 138

8.4 The impulses applied to the coal block in chronological order. + Indicates the positive polarity applied to the detonator. . . . . 144

8.5 Face (top to bottom): The voltage, electric field gradient and equivalent test parameters required to set off a detonator, for different coal resistivities . . . . . 156

8.6 Face to exploder. The voltage, electric field gradient and equivalent test parameters required to set off a detonator, for different coal resistivities . . . . . 158

9.1 The energy dissipated in a detonator with a bridge-wire resistance of 1.41 Ω and different lead wire resistances. . . . . 163
9.2 The equivalent test resistance, $R_T$, obtained from the vertical and diagonal detonator analysis in Chapter 8, for Type 0 (7 A) and Type 1 (32 A) detonators. . . . . 165

10.1 The factors analysed in Chapter 3. The ranges of the factors are given and their relative effect on the frequency that surges will occur. . . . . 173

10.2 The predicted frequency of surges occurring in mines where the FSD programme was used. Resistivity data was only available in some of the mines and $K_\rho$ was calculated only for these mines. . . . . 179

10.3 The predicted frequency ($N_g$ = 1) versus the observed frequency of surges in the mines taking part in the FSD programme. . . . . 180

10.4 Results of the linear regression between the predicted and FSD-measured results ($y = mx + C$) . . . . . 180

10.5 Accident statistics from the Government Mining Engineer, Eastern Transvaal area for the period 1/1/88 to 30/9/94. This represents a total of 176 000 man years . . . . . 184

10.6 The risk index of the mines involved in the FSD measurement programme. . . . . 185

## LIST OF UNIQUELY DEFINED SYMBOLS

| Symbol | Quantity |
|---|---|
| A | Area ..... $m^2$ |
| B | Magnetic flux density ..... T |
| E | Electric field strength ..... V/m |
| f | Frequency ..... Hz |
| I | Electric current ..... A |
| $I_L$ | Lightning current ..... A |
| J | Electric current density ..... $A/m^2$ |
| $N_s$ | Frequency of surges in a coal face ..... Surges/year |
| $N_g$ | Lightning flash density ..... $flashes/km^2$ |
| P | Point in space |
| R | Resistance ..... Ω |
| t | Time ..... s |
| U | Voltage ..... V |
| V | Volt |
| X | Distance ..... m |
| $Z_t$ | Time-dependent impedance ..... Ω |
| $Z_\omega$ | Frequency-dependent impedance ..... Ω |
| $\alpha$ | Impulse impedance ..... Ω |
| $\epsilon$ | Permittivity ..... F/m |
| $\epsilon_o$ | Permittivity of free space ..... $8.85 \times 10^{-12}$ F/m |
| $\epsilon_R$ | Relative permittivity |
| $\mu$ | Permeability ..... H/m |
| $\mu_o$ | Permeability of free space ..... $4\pi \times 10^{-7}$, H/m |
| $\omega$ | Angular frequency ..... Radians/s |
| $\rho$ | Resistivity ..... Ω.m |
| $\pi$ | Pi |
| $\beta$ | Magnetic flux density ..... Weber per $m_2$ |
| $\Phi$ | Magnetic flux ..... Weber |

# CHAPTER 1

# LIGHTNING-INDUCED INCIDENTS IN SHALLOW COAL MINES

## 1 INTRODUCTION

During mining and tunnelling operations underground in shallow coal mines, incidents or disturbances have occurred which were frequently related to lightning storms being present on the surface. These incidents included electrical shocks, visible sparking from underground equipment, the premature detonation of explosives, and methane explosions.

This thesis is aimed in particular at quantifying the risk of lightning underground in collieries in engineering terms, and proposes practical measures to manage the risk.

## 2 THE EXPLOSION HAZARDS ADVISORY COMMITTEE OF THE SOUTH AFRICAN COAL-MINING INDUSTRY

The South African coal-mining industry has experienced a large number of incidents. These incidents were particularly prevalent in shallow collieries and are of great concern to the mining industry. A number of wide-ranging investigations were initiated and these culminated, in 1978, in the formation of a Subcommittee of the Explosives Hazards Advisory Committee of the South African Coal Mining Research Controlling Council (CMRCC). The task of this Subcommittee was to carry out an in-depth study of the problem and to formulate appropriate safety measures. This thesis is a continuation of the initial work done.

The Subcommittee concluded that a number of actions had to be taken to improve the safety of personnel and equipment in coal mines, including:

- The compilation of a safety code (The South African Coal Mining Research Controlling Council, 1981)

- The Development and implementation of a "Lightning Warning System" in affected mines (Eriksson et al, 1984)

- The introduction and use of a "Stat Safe" detonator for use in all affected mines.

# 3 INCIDENTS IN SOUTH AFRICAN COLLIERIES

Table 1.1 is a summary of a number of incidents in South African collieries (up to 1984). It is worth noting that accidents involving the ignition of explosives are much more frequent than accidents involving methane explosions. In the former type of accident, only one person was usually involved and it is only in rare cases that a person was killed. However, although methane explosions are less frequent, when they do occur the consequences are much more devastating, often killing even tens of miners in a single incident.

Since the measures recommended by the CMRCC were implemented, the number of incidents has been greatly reduced. Cloete (1994) of the Office of the Inspector of Mines for the Eastern Transvaal reported that no incidents have been reported in the last six years.

Methane explosions are caused when methane is allowed to accumulate in concentrations between 5 % and 15 % $CH_4$ and, to prevent these explosions, it is very important to prevent these concentrations of methane. This is usually done by providing adequate ventilation throughout the mine.

When an ignitable concentration of methane occurs, it can be ignited by either mechanical friction, open flames, or electric sparks. Lightning is a potential source of electric sparks and the visible sparks observed underground are a potential source of ignition.

**Table 1.1** Summary of lightning-related incidents in South African collieries

| Date | Incident | Remarks | Fatalities and Injuries (when available) |
|---|---|---|---|
| Aug. 1972 | Methane explosion | Worked-out section, 100 m depth, dyke | - |
| Jan. 1974 | Methane explosion | 80 m depth, dyke | 13 killed |
| Jan. 1975 | Shothole detonation | - | No injury |
| Dec. 1976 | Methane explosion | 100 m depth, dyke | - |
| Oct. 1977 | Methane explosion | - | - |
| Nov. 1979 | Shothole detonation | - | - |
| Feb. 1980 | Methane explosion | Sealed vertical shaft | - |
| April 1980 | Shothole detonation | Shocks recorded | 1 killed |
| Sep. 1980 | Shothole detonation | Shocks recorded, sparks observed, 42 - 50 m depth | - |
| Dec. 1980 | Shothole detonation | - | - |
| Feb. 1982 | - | Electric shock, flash observed between borehole and power cable, 34 m depth | No injury |
| March 1982 | - | Electric shocks, 25 m depth | - |
| Nov. 1983 | Methane explosion | Sinking incline shaft | 1 killed, 1 injured |
| Dec. 1983 | Shothole detonation | Near borehole, flashes observed, 20 m depth | - |
| Feb. 1984 | Shothole detonation | Near borehole | - |

## 3.1 Examples of a detonator explosion

The most extensive accident caused by the premature detonation of explosives occurred in South Africa in 1980. From an analysis of the accident, it is assumed that it had been caused by a lightning strike to the headgear of the shaft, rather than a lightning strike to the surface above the working area.

Figures 1.1 (A and B) are schematic drawings of the south end of the mine where the incident occurred. A comprehensive report on the incident was compiled by the Inspector of Mines (De Wet, 1980).

The accident occurred while a lightning storm was active on the surface. Four charged faces in three different sections of the mine (shown in Figure 1.1A) detonated spontaneously. It can be seen in this figure that as much as 300 m separates the different locations where detonators were ignited prematurely. From analyses made later (in Chapters 2 and 3), it is evident that it is only when a surge is conducted through the underground structures that simultaneous accidents can occur at sites that are as much as 800 m apart.

The depth of the seam (No. 2 seam) in the mine being worked was about 48 m. When the accident occurred, the working faces were in different phases of preparation. In one case, the miner had just interconnected the detonator wires, while in other cases, the exploder cables had been connected to the detonators at the face, but had not yet been connected to the exploder. A schematic drawing of the section where detonations occurred at two faces is given in Figure 1.1B. All the faces were within a distance of 30 m from electrical equipment that was bonded to the power system earth via their trailing cables.

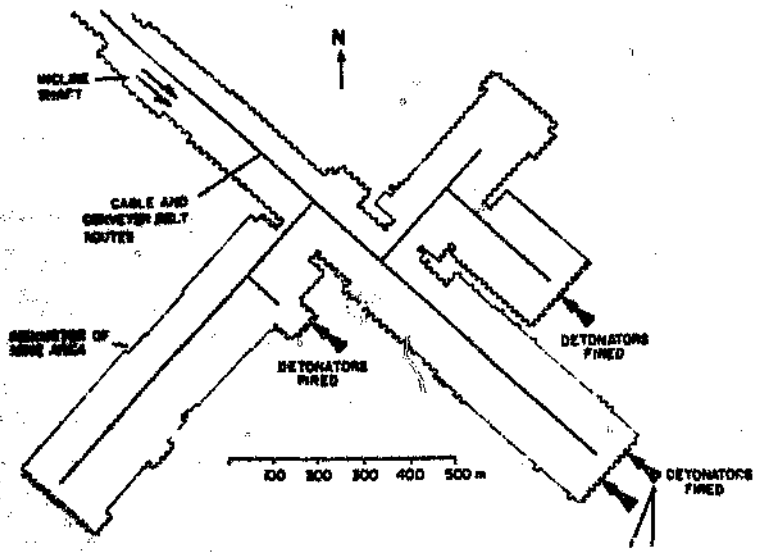



**Figure 1.1A** A plan giving a view of the area in a mine where four faces detonated inadvertently in September 1980

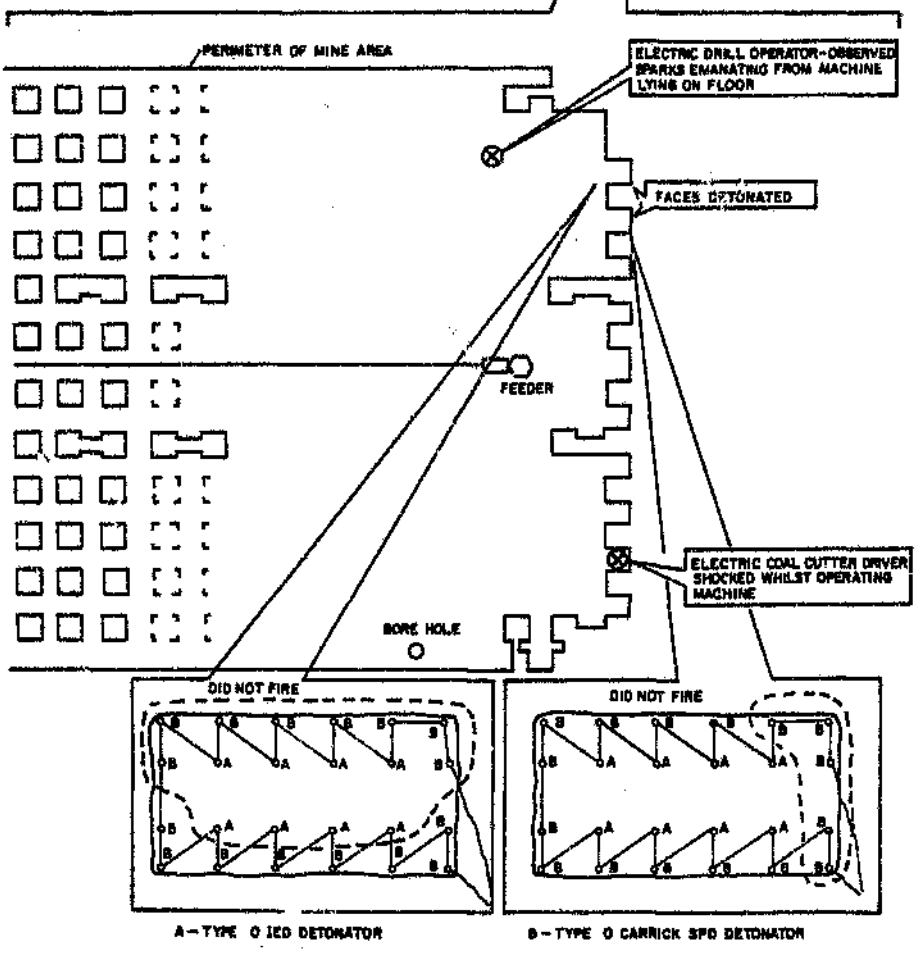



**Figure 1.1B** Detailed plan of the section in which detonations occurred at two faces, showing the faces and interconnections between the detonators.

## 3.2 Example of a methane explosion

An accident that occurred while a new inclined shaft was being sunk in a mine is used here as an example of an explosion caused by lightning igniting methane. The explosion occurred at approximately 16:45 on Sunday 6 November 1983.

The events leading up to the explosion were as follows:

A lightning storm was approaching the shaft area from a distance. At approximately 30 minutes before the accident, the lightning tripped the overhead medium-voltage power supply line, leaving the shaft without power. Being a Sunday afternoon, only two labourers were on duty at the shaft which meant that there was nobody in a position to request that the power be restored.

The shaft is in an area with a relatively high level of methane emission. On the day that the accident was investigated, methane could be observed bubbling from the floor of the mine about halfway down the shaft. The power interruption caused by the lightning stopped the temporary ventilation system that had been installed to enable the shaft to be sunk. This, in turn, allowed methane to accumulate in the middle of the shaft.

The storm moved into the direct vicinity of the shaft 30 minutes after the power interruption. It is assumed that a strike from the storm struck the highest security light (33 m high) at the entrance of the shaft. This could have caused a spark somewhere in the middle of the shaft where the methane had accumulated to flammable concentrations.

From observations of the temperature to which various objects had been exposed, it was decided that the main explosion had taken place in the middle of the shaft. The explosion did not propagate all the way down to the bottom of the shaft.

One of the labourers was in the middle of the shaft, at the highest temperature zone. He was killed. The second labourer was in the bottom of the shaft. He survived the accident with only his eardrums being ruptured.

Fortunately, this explosion took place in an area of the mine where there was no coal dust. Many methane explosions ignite coal dust, causing further explosions, normally resulting in much more severe explosions (Landman, 1992).

It is interesting to note that, in this case, lightning was both the primary cause and the secondary cause of the explosion. It first interrupted the ventilation and then ignited the methane.

# 4 INTERNATIONAL EXPERIENCE

Marshall (1941) points out that several blasting accidents occurred between 1915 and 1940 in spite of all precautions being taken and the issue of safety instructions. For many years, the exact cause of premature explosions during electric storms was a complete mystery and all that was known was that "static charges set off the detonator somehow".

Marshall also reported on some field experiments where the standard detonators used at that time were connected to an aerial. A lightning strike more than 2 km away caused 47 out of 50 detonators to ignite. He described a shunt to the detonator metal tube which was used as a protection measure and which completely protected the detonators from this failure mechanism. It is clear from his description of the experiment that the detonators used then were extremely sensitive to static and lightning.

The question of detonator shells that are made of, or covered with, dielectric material will be dealt with in Chapter 9. It is interesting to note that this idea was mentioned by Marshall and by Forsyth (1959) but that it had not been practical or economical to manufacture such detonators then.

The most comprehensive analysis published to date on the issue of lighting setting off detonators was carried out by Berger (1977), focusing on tunnelling accidents that had been reported by Fourestier (1950). Berger postulates two mechanisms through which induction can take place through lightning either striking the equipment at a tunnel entrance, or penetrating through the rock strata.

Berger's postulation of induction through the strata via resistive conduction is broadly the basis of much of the analysis done in this thesis. However, rather different techniques and approaches are taken to arrive at evaluations. This thesis is based on a much deeper analysis and on data measured in the field.

Very little is mentioned in the international literature on the risk of methane being set off by lightning. Golde (1973) mentions it (almost incidentally) in Chapter 9.4 of his book *Lightning Protection*, on the lightning protection of mining and blasting. However, this risk is a major concern in South African collieries; this type of accident seldom occurs but when they do occur they lead to a number of fatalities. One such event caused the death of 37 miners.

The problem of lightning setting off electrical detonators goes back many years, but accidents are still reported (ICI, Sep. 1983 and Santis, 1988). A significant step taken recently in improving the electrical detonator safety was the introduction of transformer-coupled detonators. Geldenhuys (1980) showed that even very large unipolar discharges

(> 2 000 A) cannot set off such detonators if the current is passing through the primary circuit.

# 5 CODE OF PRACTICE FOR THE AVOIDANCE OF HAZARDS UNDERGROUND IN COLLIERIES DUE TO LIGHTNING

Resulting from the work of the Lightning and Stray Current Research Subcommittee of the Explosion Hazards Advisory Committee of the Coal Mining Research Controlling Council, the above-mentioned code was published in 1981.

The code was produced by a group of practical mine engineers and lightning experts. It was based largely on their experience and knowledge and was synthesised through their "gut feelings" into the code. This code was published timeously and it laid an excellent base for the reduction of lightning incidents in coal mines.

The main recommendations of this code were:

## 5.1 Earthing of metal work

The code recommends the extensive bonding and earthing of the underground service structures, such as the conveyor-belt structure, the electrical cables, and ventilation pipes. This recommendation was made to minimise the potential between the mine strata and the structures in order to prevent electrical sparking which may set off methane.

Earthing of the structures and services at the shaft entrance was recommended to reduce the surge voltages that may be created by lightning striking the mine structures on the surface then being conducted into the underground workings via the conveyor-belt structure and other structures.

## 5.2 The cessation of handling of explosives when there is a lightning warning

The South African Mines and Works regulations require that all charging of explosives should cease when a thunderstorm is ***in the vicinity of a working face in a colliery***. To effectively implement this precaution, the warning process must be automatic. For this reason, it was recommended that an effective lightning warning instrument had to be installed at mines which had histories of accidents, or in mines where the working areas

and depths were similar to those of mines where incidents had happened.

Through the initiative of the committee, the CSIR developed a lightning warning unit (Eriksson et al, 1984). Units were installed in more than 30 coal mines in the Eastern Transvaal. Figure 1.2 shows the performance of this warning unit during a typical thunderstorm. The data on the top part of the figure represent lightning strikes in real time. The distance along the Y axis of the figure represents the distance in kilometres of the lightning strikes from the location of the warning unit. The bottom three lines show the operation of the warning unit.

The green alarm switched on at about six minutes after the automatic operation of the warning unit, the amber alarm at 17 minutes and the red alarm at about 21 minutes.

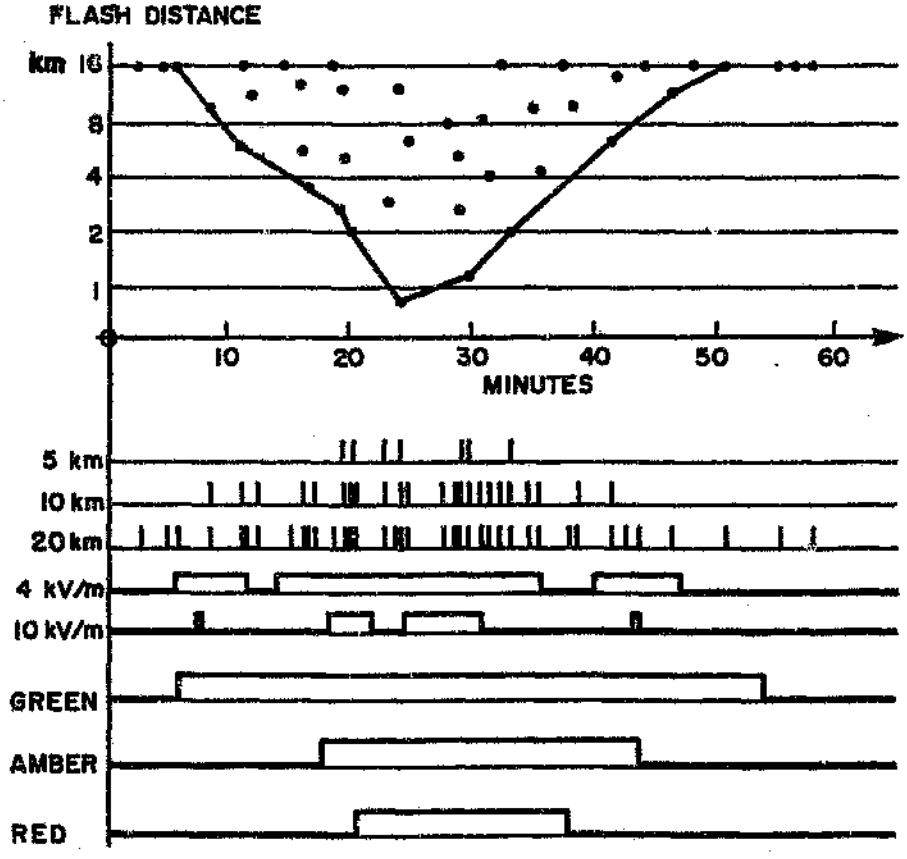



**Figure 1.2** Performance of the CSIR lightning warning unit during an approaching storm.

- The top diagram shows the approach of the storm
- Registration of lightning flashes at 5 km, 10 km, and 20 km, I,
- Electric field measurements that exceed the set values of 4 and 10 kV/m.
- Green, amber and red are the three alarm levels of the warning unit

The concept of using lightning warning units to protect blasting operations has also been propagated in the USA (Santis, 1989).

The potential effectiveness of this approach was demonstrated (ironically) when there was a premature detonation of explosives at a mine where a lightning warning unit had been installed (Naude, 1985). The warning instrument sounded an alarm but, unfortunately, the telephone to the underground section was engaged. The warning could not be relayed to the section of the mine in time and a detonator was set off by the storm. Better communication procedures were subsequently recommended.

## 5.3 The integrity of the insulation of the detonator electrical circuit

The code recommended that the integrity of the detonator wires be maintained. Only blasting cable in good condition should be used. The bare ends of the detonators should never be allowed to come in contact with the work face or the floor.

## 5.4 Separation of the blasting area from the service structures

It was recommended that the service equipment, such as coal drills, shuttle cars, etc. be withdrawn to no less than 25 m from the face before charging takes place.

# 6 THE AIM OF THE STUDY

As indicated above, much is understood about the problem, but very little has been quantified in engineering terms. The aim of this thesis is to advance this quantification of the mechanisms and the risks involved.

## 6.1 Understanding and quantifying the basic mechanisms through which lightning can enter a mine

The core of this thesis is the quantification of the above basic mechanisms to obtain engineering quantities and models.

Chapter 2 focuses on three mechanisms through which lightning can possibly enter into a mine. The mechanisms are compared to determine their relevance to the induction process.

The models in Chapter 2 are somewhat simplistic. Through laboratory testing and from models in literature combined with computer-based numerical modelling, one of the mechanisms discussed in Chapter 2 is refined in Chapter 3 to a level where the absolute and relative frequencies of detonator accidents can be determined.

## 6.2 The sensitivity of detonators and methane

The threshold levels that are of concern in determining the frequency of accidents obviously depend on the "object" at risk, the detonator or methane-gas mixture. For this reason, the sensitivity of both detonators and methane was studied. The results are reported in Chapters 6 and 7.

Electrical detonators are traditionally constructed by an electrical bridge wire coated with a thermally sensitive explosive. By passing current through the bridge wire thereby heating it, the explosion is initiated. The detonator canister is invariably made of metal, specifically of copper in fiery coal mines.

New types of detonator are gradually becoming available. These detonators often use electronic timing circuits to improve the timing of sequential firing. The body of the detonator may be made of plastic. The bridge wire of the detonator may not be of the conventional design.

The traditional approach to ensuring the lightning and electrostatic safety of detonators does not necessarily apply any more. This thesis suggests a specific battery of tests for the use of alternatively designed detonators.

The energy/spark conditions required to set off a methane-air mixture sparks that originate from ordinary electrical apparatus are well known. This is widely adopted in intrinsically-safe codes of practice. Very little has been reported in the literature about lightning-like sparks. Chapter 6 deals with the sensitivity of methane-air mixtures to the type of sparks caused by lightning.

## 6.3 The evaluation of mine risk and the Code of Practice

The understanding of the basic mechanisms and the sensitivity of detonators and methane allows the refinement of the code of practice. The implications of the models will be examined and comments are made in the final chapter on improvements to the code of practice.

Not all mines are exposed to the same risk. Factors such as

- $N_g$ - lightning flash density
- strata resistivity
- mining depth
- coal-seam resistivity and thickness

all play a role in making a particular mine more or less hazardous because of lightning. An evaluation algorithm has been developed in Chapter 10 which will allow management to determine the risk to which a mine is exposed. This also allows informed decision making on the measures required in a particular mine to reduce the risk to acceptable levels.

# CHAPTER 2

# MECHANISMS WHEREBY LIGHTNING DISCHARGES MAY PENETRATE INTO AN UNDERGROUND MINE

## 1 INTRODUCTION

In this thesis, three possible ways are examined by which lightning may enter an electrical circuit underground in a mine. Two of these mechanisms are graphically illustrated in Figure 2.1.

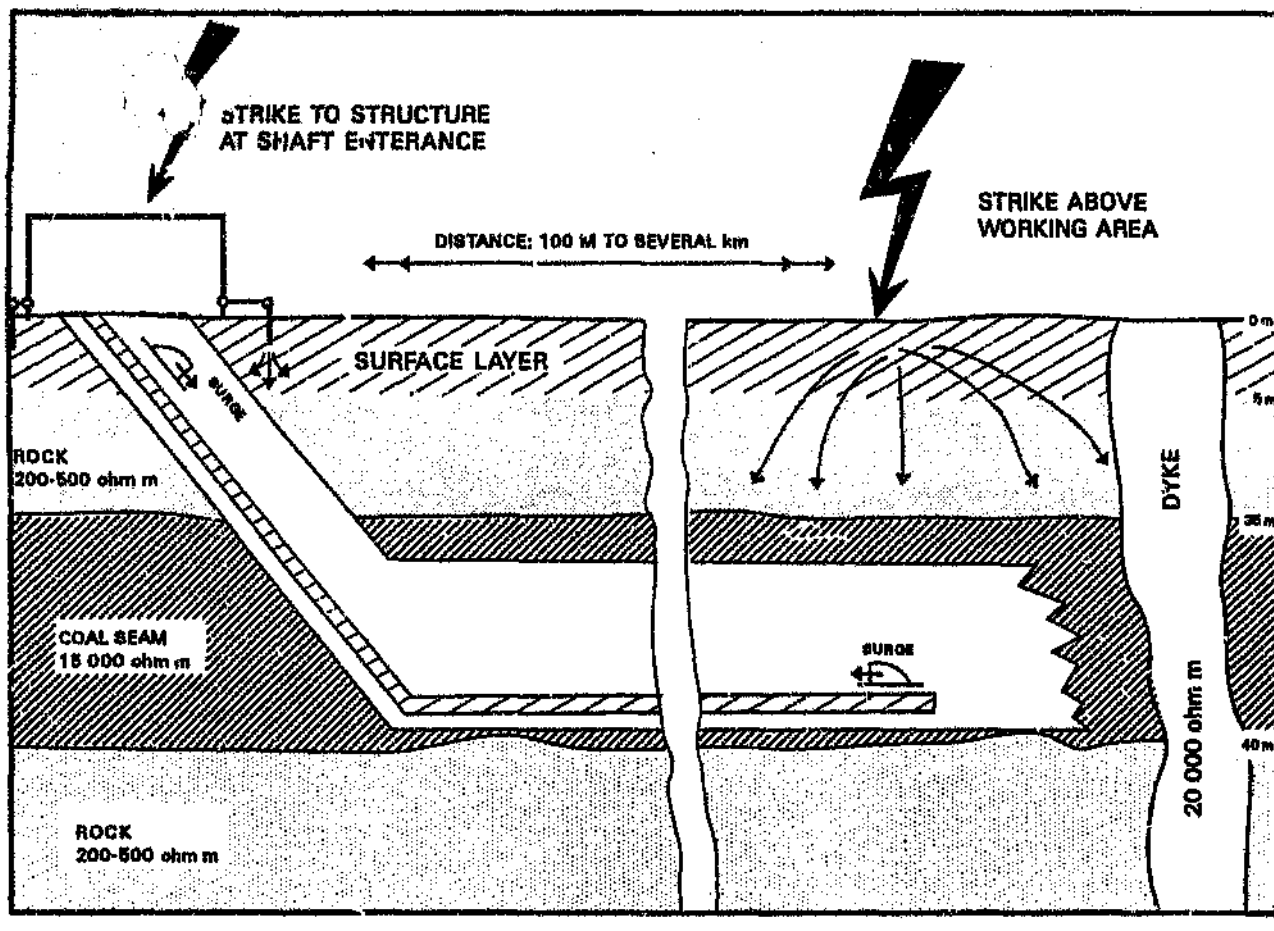



Figure 2.1 A simplified diagram depicting how lightning surges may enter collieries

The mechanisms are:

- A direct strike to the structures at a shaft entrance. The surge is then conducted into the mine via underground services, e.g. the electrical cables, waterpipes and conveyor-belt structures.

- A direct strike to the surface above a working area. The lightning current is resistively conducted and coupled to any vulnerable circuits.

- A direct strike to the surface above a working area. Energy is coupled to vulnerable circuits via magnetic induction.

## 2 A DIRECT STRIKE TO THE STRUCTURES AT A SHAFT ENTRANCE - A SIMPLE MODEL

When lightning strikes the structures at a shaft entrance, some of the current will be dissipated (injected) into the ground via the earth electrode at the shaft entrance. Some of the current will propagate down into the mine via the conveyor structures as illustrated in Figure 2.2.

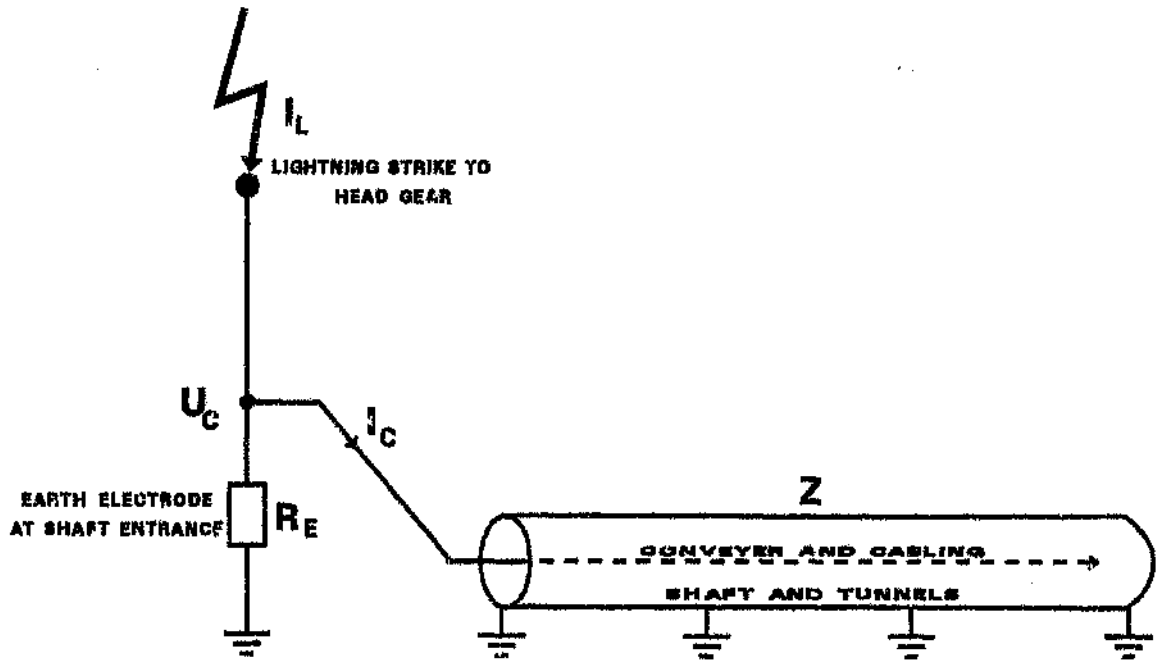



**Figure 2.2** A simple equivalent electrical model of the case where lightning strikes a shaft entrance

## 2.1 An analytical model of the surge propagation

The voltage rise (U) of the structures at the shaft entrance can be calculated as follows:

$$U = I_L \left( \frac{R_E Z}{R_E + Z} \right) \quad \ldots\ldots\ldots\

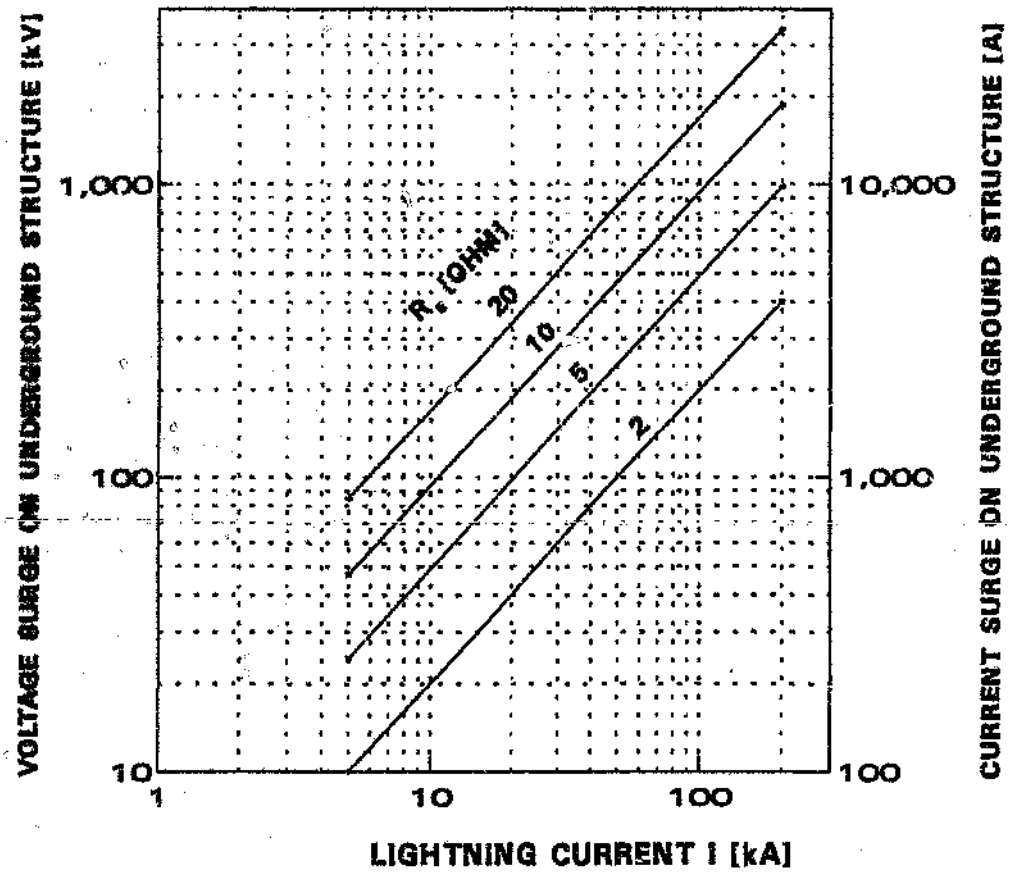



**Figure 2.3** The voltage surge U and the current $I_C$ injected into the underground structure as a function of the lightning current $I_L$ and the resistance of the earth electrode $R_E$ at the shaft entrance. Assuming Z = 100 Ω.

## 2.2 The frequency of strikes to a shaft = frequency of surges

The frequency of surges caused by this mechanism can be calculated as follows:

The attractive radius $r_a$ of the headgear of a shaft can be calculated according to Eriksson (1986) by

$$r_a = 14\ h^{0.7}\ [m] \quad \ldots\ldots\ldots\ldots\ldots\ldots\ldots\ldots\ldots\ldots\ldots\ldots\ldots\ldots\ldots\ldots\ldots\ldots\ 2.3$$

where h = the height of the headgear at the shaft

The number of strikes per year to such a structure (N) is given by

$$N = \pi \cdot N_g \cdot r_a^2 \cdot 10^{-6} \text{ [flashes per year]} \quad \ldots\ldots\ldots\ldots\ldots\ldots\ldots\ldots \quad 2.4$$

where $N_g$ = flash density per year

Assume h = 20 m for a typical shaft and $N_g$ = 1 flash per year per km$^2$, then:

$r_a$ = 114 m
N = 0.0409 flashes/year

## 2.3 The frequency of voltage surges on the conveyor belt

The number of flashes per year can be converted to an average frequency of a voltage surge of a certain magnitude occurring, as follows:

The flashes to the structure have a probability of being of a certain magnitude, as represented by the Cigré distribution. Anderson (1982) derived an equation that closely models this distribution:

$$P(I_L) = \frac{1}{1 + \left[\frac{I_L}{31}\right]^{2.6}} \quad \ldots\ldots\ldots\ldots\ldots\ldots\ldots\ldots\ldots\ldots\ldots\ldots \quad 2.5$$

$I_L$ in kA.

The voltage on the conveyor belt is given by

$$U_C = I_L \left[\frac{R_E Z}{R_E + Z}\right]$$

By substituting 2.1 (for $I_L$) into equation 2.5, we can derive the probability of a particular strike to the structure producing a certain voltage on the conveyor ($U_C$):

$$P(U_C) = \frac{1}{1 + \left[\frac{U_C (R_E + Z)}{31 \cdot R_E Z}\right]^{2.6}} \quad \ldots\ldots\ldots\ldots\ldots\ldots\ldots\ldots\ldots\ldots \quad 2.6$$

The frequency ($N_s$) at which a particular surge voltage will occur on the conveyor structure is

$$N_s = N \times P(U_c) \quad \text{2.7}$$

## 2.4 The voltage on a conveyor belt required to set off a detonator in a work face

In section 1.1 the surge voltage on the underground conveyor structure is derived. To be a risk to the detonator circuit, the voltage on the conveyor structure has to be transferred to the detonator circuit. It is shown in Chapter 8 that Type O detonators are sensitive to voltages between 20 kV and 90 kV (depending on the resistivity of the medium in which the detonator is placed).

To quantify the risk associated with this mechanism, some assumptions are made. These are discussed below.

### 2.4.1 Coupling between the conveyor structure and the detonator circuit

Coupling of the voltage on the conveyor structure to the detonator circuit is indirect, through the resistivity of the strata. This effect has not been analysed. To perform such an analysis would require a complex 3D field plotting exercise. This analysis is beyond the scope of this thesis. The physical separation of the conveyor structure from the detonator circuit will effectively reduce the transfer of the induced surge to the detonator circuit. In order to indicate how the problem should be solved and in order to make some progress in this thesis an assumption is made which is believed to be conservative:

If the conveyor belt can be modeled as a simple spherical resistive electrode the potential from the edge of the conveyor falls away as a function of (1/x) where x is the physical dimension of the conveyor-electrode.

The detonator circuit is in the area where the potential falls away as (1/x) (x is large, several 100 m, and the dimension of the detonator circuit is relatively small, approximately 15 m compared to x). The detonator circuit will always be more than 25 m away from the closest conveyor structure in accordance with the Code of Practice. The effect is illustrated in Figure 2.3b. It will be conservative to assume that 25% of the conveyor voltage is transferred to the detonator circuit (i.e. less than 25% will be transferred in reality.) In Figure 2.3b 15% (x=30 m), at most, of the voltage falls within the electrode dimension.

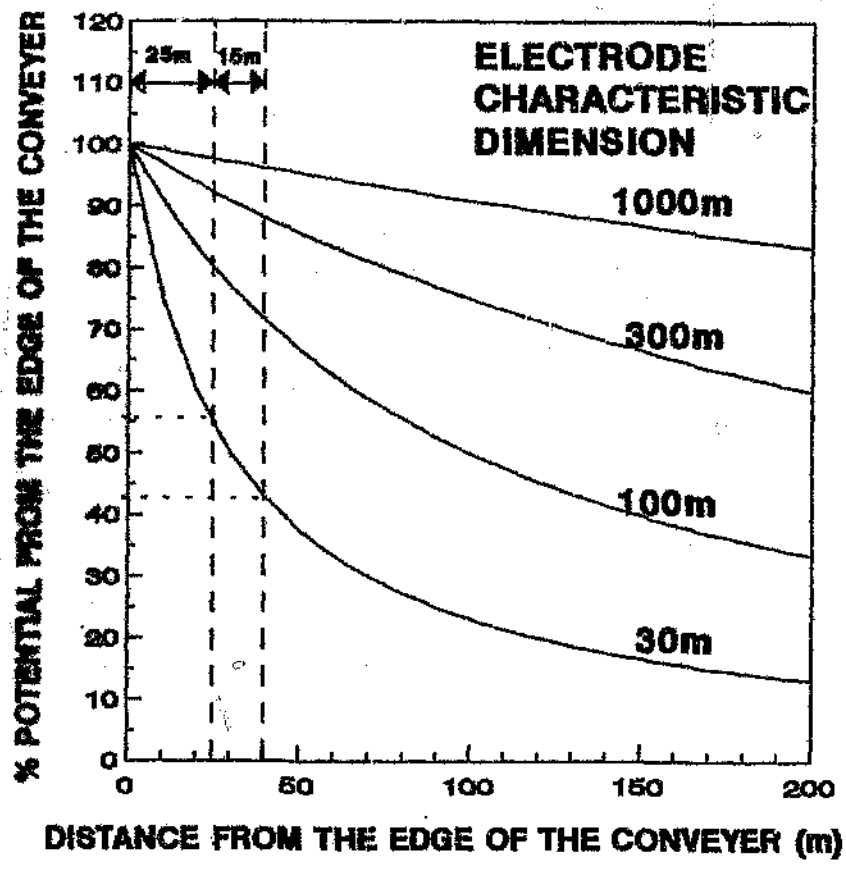



**Figure 2.3b** The potential fall from the edge of a simple hemispherical electrode. To illustrate what can be expected around a conveyer structure and the field in which the detonator circuit will lie.

### 2.4.2 The resistance of the conveyor structure to earth

In the model of Figure 2.2, it is assumed that the conveyor structure has no conductive connection to earth. This, of course, is not the case. The conveyor structure is continuously in contact with the workings surrounding it. In addition, the Code of Practice recommends that the conveyor structure be earthed at regular intervals, using roofbolts.

The floor of the mine is normally wet sandstone which has a relatively low resistivity, typically of 400 Ω.m. Such a floor will result in a conveyor-to-earth resistance of around 8 Ω per 100 m of conveyor structure. This result in a lossy transmission line.

Furthermore several different conveyor structures run from the shaft in different directions, effectively reducing the surge impedance seen by the surge that travels underground.

It is outside of the scope of this thesis to analyze all these effects, they will require a substantial study by it self. The effects mentioned here are compensated for by assuming that $R_g$ will be reduced by a factor of two (due to the earthing effect of the conveyor and

the multiple conveyor structures.)

Taking both of the above factors (2.4.1 and 2.4.2) into consideration, the voltage ($U_D$) induced into a detonator circuit is eight times less than the voltage ($U_C$) on the conveyor structure, i.e.

$$U_D = U_C / 8 \quad \ldots\ldots 2.8$$

## 2.5 The frequency (risk) of surges in detonator circuits

The frequency of surges $N_D$ ($U_D$) having a certain magnitude being induced into detonator circuits can be deduced by substituting equation 2.8 into equation 2.6.

$$N_D(U_D) = \frac{N}{1 + \left[\frac{0.258\ U_D\ (R_E + Z)}{R_E\ Z}\right]^{2.6}} \quad \ldots\ldots 2.9$$

Equation 2.9 was plotted in Figure 2.4 using different resistances for the earth electrodes in a shaft.

It is shown in Chapter 8 that a voltage of between 20 kV and 90 kV is required to set off a Type O detonator (depending on the resistivity of the strata in which the detonator is located).

Example

If the risk ($N_D$) of a detonator being set off is to be reduced to a frequency below one in a thousand occurrences in one year on the Highveld, with $N_g = 8$, then

$$N_D < \frac{1}{1000}$$

Figure 2.4 is based on $N_g = 1$; this is therefore equivalent to $N_D$ in Figure 2.4 divided by eight.

$$N_D < 1.25 \times 10^{-4} \text{ (Figure 2.4)} \quad \ldots\ldots 2.10$$

If the coal resistivity is 3 000 Ω.m, the corresponding voltage will be 38 kV (see Chapter 8).

These two values are plotted in Figure 2.4 and indicate that the electrode resistance required is less than 2 Ω.

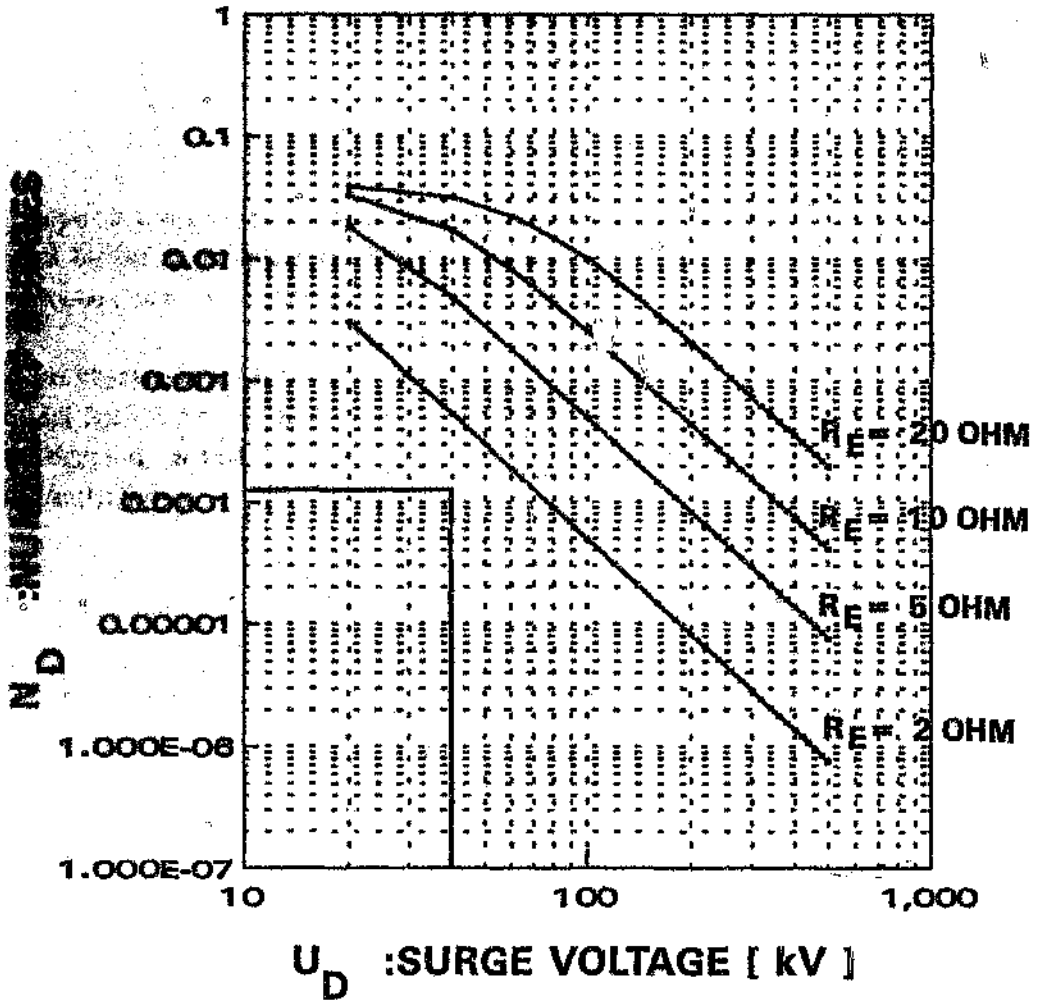



Figure 2.4 The frequency with which surges are induced into detonator circuits when lightning strikes the shaft entrance, calculated for $N_g = 1$.
Mast height at shaft entrance h = 20 m.

# 3 A DIRECT STRIKE TO THE SURFACE ABOVE A WORKING AREA (COUPLING BY CONDUCTION THROUGH THE STRATA) - A SIMPLE MODEL

The second mechanism postulated here by which lightning can penetrate into electrical circuits underground is that of the direct conduction of the lightning current through the strata. This section contains a simple model based on the conduction mechanism.

The analysis is concentrated on current in the beginning of this section. The model is then explored further to calculate the expected frequency of occurrence of current surges underground due to this mechanism.

The basic physical characteristics of the model are shown in Figure 2.5. It is assumed in the model that the earth is homogeneous with a resistivity, $\rho$. Another assumption made is that lightning current will spread homogeneously outward from the point of strike (hemispherically).

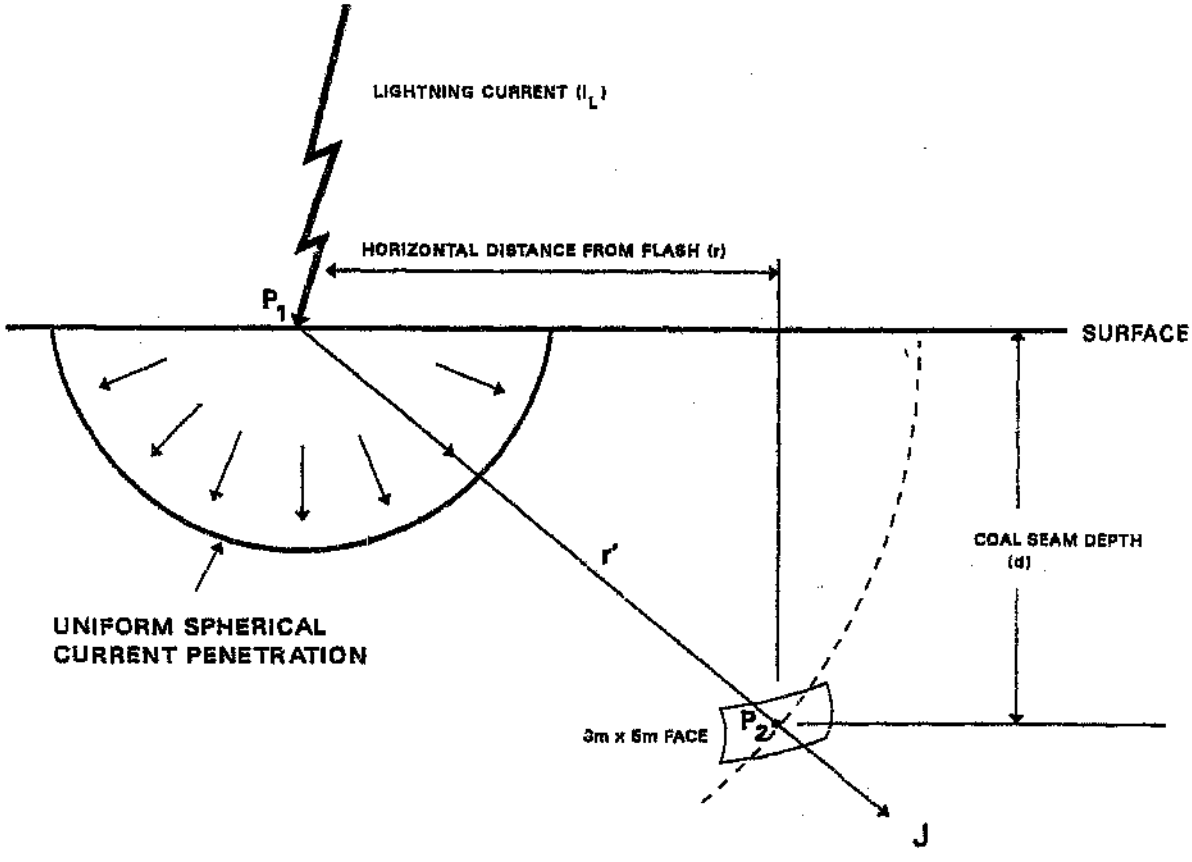



**Figure 2.5** The physical model of lightning current penetrating the earth

## 3.1 Current density (J)

The current density at a certain point produced by a lightning flash current ($I_L$) is denoted as J. The horizontal distance between the point and the flash is r and the depth of the point is d. J is then given by:

$$J = \frac{I_L}{A} \quad [A/m^2] \qquad \text{2.11}$$

where A is the surface of the hemisphere which has its centre at $P_1$, and the surface going through $P_2$.

$$r' = \sqrt{r^2 + d^2} \quad [m] \qquad \text{2.12}$$

$$J = \frac{I_L}{2\pi\,(r^2 + d^2)} \quad [A/m^2] \qquad \text{2.13}$$

## 3.2 Current through a 3 m x 5 m rectangular face ($I_F$)

In order to convert current density into the current flowing into the detonator circuit ($I_F$), the following assumption is made: the current produced by the current density through the surface area of a typical face is the current that will flow through the detonator circuit.

This results in

$I_F = (3 \times 5)\, J$ [A]
$I_F = 15\, J$ [A] ..... 2.14

## 3.3 The effect of the orientation of the strike relative to the exploder-to-face direction

The position of a particular flash relative to the face-exploder orientation effects the magnitude of the surge through the face; if it is exactly orthogonal, it will not produce a nett surge but if it is in line with the face-exploder orientation it will produce the maximum surge.

Both the horizontal orientation as well as the depth of the face have a similar effect. The

depth effect is not analysed as in the practical case in SA, common depths of seams are around 30 m. At this depth, the vertical effect has little effect at the boundary where the face will still be affected by a relatively distant flash.

The occurrence of a flash relative to a specific face-exploder orientation (in plan) is random. The flash current density at the face-exploder ($J_F$) can be broken up in two orthogonal components, namely ($J_{FN}$) the component normal to the exploder-face connection and ($J_{FP}$) the component which is parallel to the exploder-face connection. It is obvious that it is $J_{FP}$ which affects detonator circuits, and it is this component which should be taken into consideration when calculating the frequency of lightning currents penetrating into detonator circuits. If R, the distance between the flash and the face, is much larger than the exploder-to-face distance, then

$$J_{FP} = J_F \text{ Cos } \theta \qquad \ldots\ldots\ldots\ldots\ldots\ldots\ldots\ldots\ldots\ldots\ldots\ldots\ldots\ldots 2.15$$

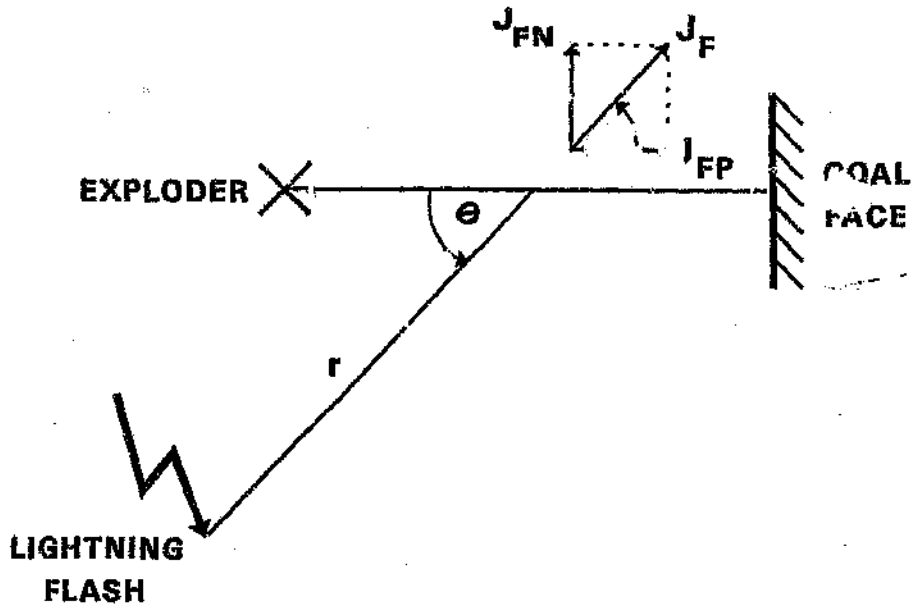



**Figure 2.6** The effect of the position of the strike relative to the exploder-to-face direction

The occurrence of $\theta$ is totally random. The average effect on the overall frequency of currents in the face can be calculated as follows:

$$I_{av(average)} = \frac{2}{\pi} I_p \int_0^{\frac{\pi}{2}} \cos\theta \, d\theta = .637 \, I_p \quad \ldots\ldots\ldots 2.16$$

This results in

$$I_{p(average)} = 1.507 \times 15 \, I \, [A] = 9.6 \, I \, [A] \quad \ldots\ldots\ldots 2.17$$

$$I_p = 9.6 \frac{I_z}{2\pi(r^2 + d^2)} \; [A] \quad \ldots\ldots\ldots 2.18$$

# 4 THE EFFECT OF THE ASSUMPTIONS MADE IN THE MODEL ON THE EXPECTED FREQUENCY OF LIGHTNING CURRENTS

## 4.1 Uniformity of the strata structure

The actual underground strata structure is not uniform because of the presence of different resistivity layers, mining cavities and dykes. These can either increase or decrease the value of $N_g$, depending on the non-uniformity of the strata, and will, therefore, affect the slope of the relationship $N_g \times I_p$ (in the cut-off current area), and cause more high-current surges than expected.

## 4.2 Disregarding skin effect

The skin depth is calculated in Table 2.2 for various resistivities at 10 kHz according to (Hayt (1974)):

$$\delta = \frac{1}{\sqrt{\pi f \mu / \rho}}$$

Table 2.2 Skin depth at f = 10 kHz (permeability assumption $\mu_r = 1$)

| Soil resistivity (Ω.m) | 200 | 500 | 1 000 | 2 000 |
|---|---|---|---|---|
| Skin depth (m) | 71 | 113 | 159 | 225 |

The main component of energy in a lightning strike lies in the frequency band of 10 kHz. It can be seen from Table 2.4 that the skin depth at 10 kHz will have a minor reducing effect on $N_g$ in shallow mines (20 m - 60 m). Soil resistivities are invariably higher than 200 Ω.m.

### 4.3 Current through a 3 m x 5 m rectangular face ($I_F$) is equal to the current through a detonator circuit

This is obviously a simplification - the current will depend on the nature of the actual detonator installation and the resistivities of the strata surrounding the detonator circuit. The difference between the actual detonator circuit and the model should be of a roughly constant nature.

## 5 THE FREQUENCY OF OCCURRENCE OF CURRENTS LARGER THAN A CERTAIN VALUE IN A PARTICULAR FACE

The average number of lightning flashes N within a certain radius (R) from a particular point is:

$$N = \pi r^2 Ng \times 10^{-6} \quad \ldots\ldots\ldots\

$$r = \sqrt{\frac{9.6\, I_L}{2\pi I_F} - d^2} \qquad \ldots\ldots\ldots\

$$I_F = \frac{9.6 I_L}{2\pi d^2} \quad \ldots\ldots\ldots\

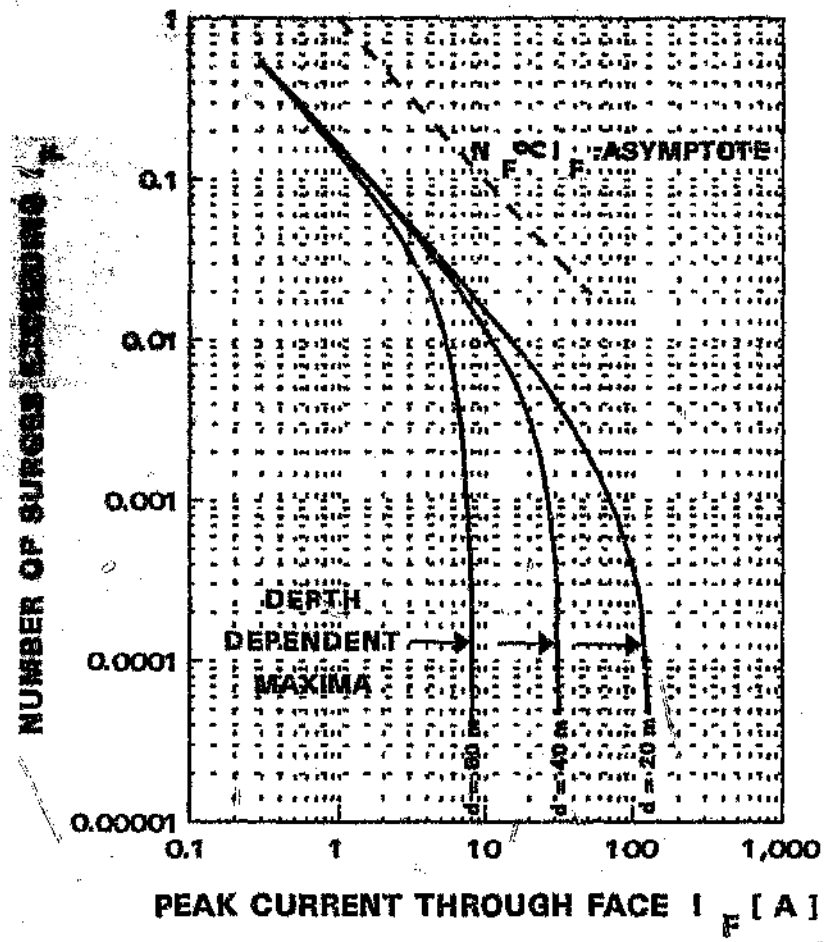



**Figure 2.6** The frequency of lightning-induced currents in a face calculated for different seam depths. The results are normalized to one face and Ng = 1 and $I_L$ = 34 kA.

Table 2.4 gives values at selected depths to illustrate the effect of equation 2.20. This result is plotted in Figure 2.7.

**Table 2.4** The maximum of $I_p$ as a function of depth and lightning current

| Lightning current (kA) | | Maximum face current $I_p$ max [A] at depth [m] | | | | | | |
|---|---|---|---|---|---|---|---|---|
| $I_L$ | P(I) | 20 | 40 | 60 | 80 | 100 | 120 | 150 |
| 4 | 98 % | 15.3 | 3.82 | 1.70 | .95 | .61 | .42 | .27 |
| 34 | 50 % | 130 | 32.5 | 14.4 | 8.12 | 5.19 | 3.61 | 2.31 |
| 100 | 3 % | 382 | 95.5 | 42.4 | 23.9 | 15.3 | 10.6 | 6.79 |
| 200 | .1 % | 764 | 191 | 84.9 | 47.8 | 30.6 | 21.2 | 13.58 |

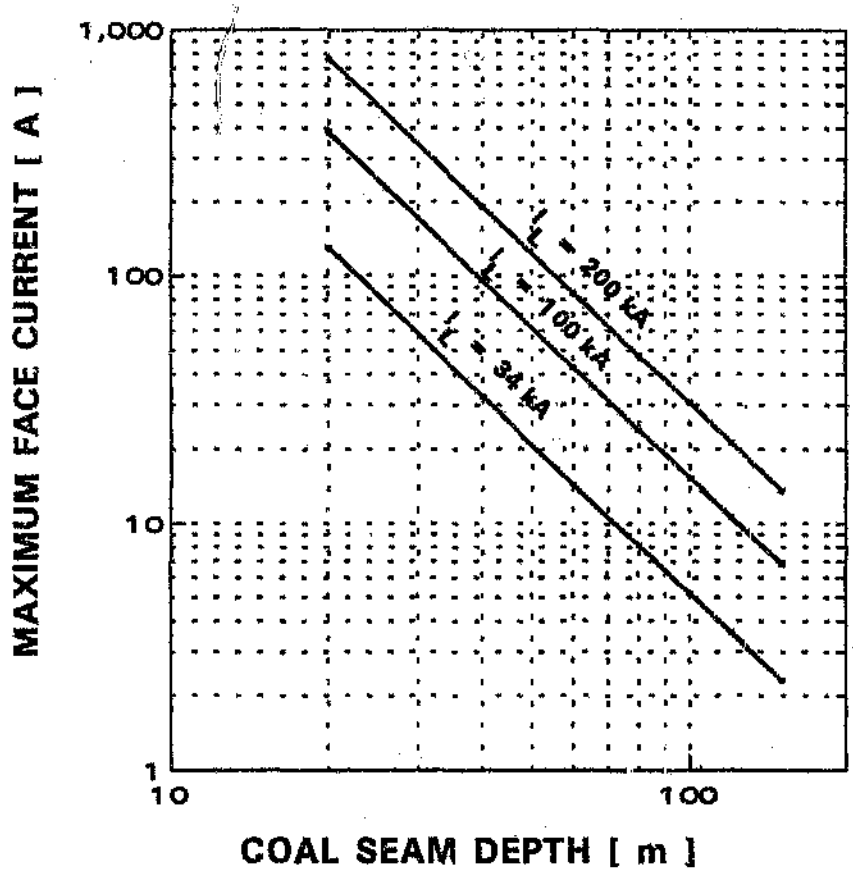



**Figure 2.7** The maximum current in a face as a function of the coal seam depth calculated for lightning currents of different magnitude

# 6 THE RADIATION MECHANISM - ENERGY TRANSFERRED TO A VULNERABLE CIRCUIT BY ELECTROMAGNETIC COUPLING

The purpose of this part of the thesis is to examine under what conditions electromagnetic radiation would be capable of igniting a detonator.

Because of the nature of the lightning discharge and the low-impedance nature of a detonator circuit, magnetic induction dominates electromagnetic coupling. For this reason, only magnetic coupling is considered.

## 6.1 The magnetic field

To allow a simple analysis of the coupling mechanism, we assume a model for the lightning strike (as shown in Figure 2.8), namely a peak value of $I_L$ and a linear rise-and-fall slope with a time-to-peak of 2 $\mu$s and a time of 100 $\mu$s for the tail to go down to zero.

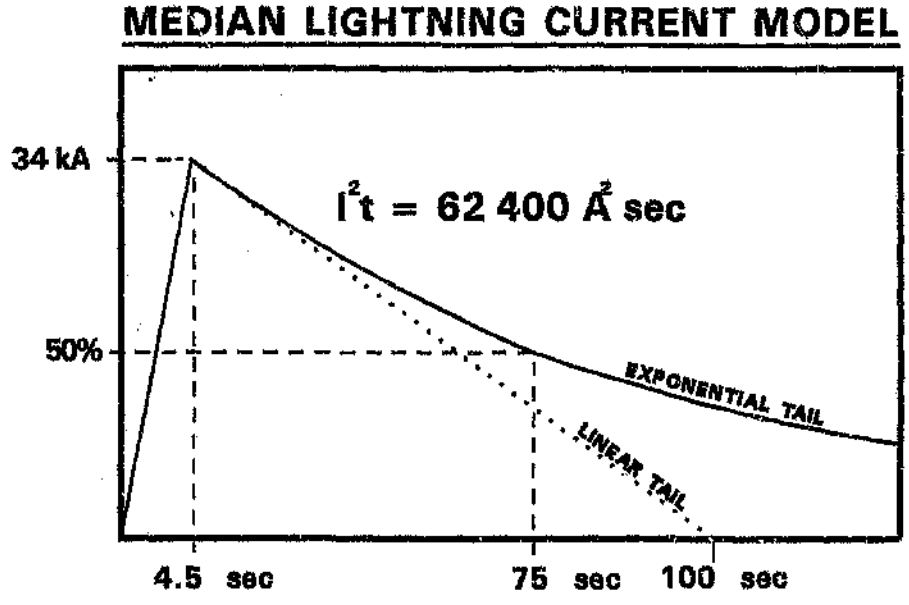



**Figure 2.8** Model of lightning current

The choice of the rise times and fall times is broadly in line with the median lightning strike given by Anderson (1980).

The magnetic field intensity produced by a infinitely long straight filament of current is:

$$B = \frac{\mu_0 \mu_r I_L}{2 \pi r} \quad \ldots\ldots 2.25$$

where r is the distance from the filament.

$$B = \frac{2 \times 10^{-7} \mu_r I_L}{r} \quad \ldots\ldots 2.26$$

The voltage induced (U) in a loop with a cross-sectional area of A is:

$$U = \frac{d\phi}{dt} \quad \ldots\ldots 2.27$$

where $\phi$ is the total magnetic flux through area A.

In this example calculating U can be broken up into two parts, one while the current is rising and another when the current is decreasing. There is also only one loop in the coil.

The magnetic flux in the loop is

$$\phi = B.A.$$

where A is the cross-sectional area of the loop.

$$= \frac{2 \times 10^{-7} \mu_r I_L A}{r} \quad \ldots\ldots 2.28$$

and the voltage is

$$U = \frac{2 \times 10^{-7} \mu_r A}{r} \frac{\Delta I_L}{\Delta t} \quad \ldots\ldots 2.29$$

where $\Delta t$ is the rise time of the lightning current $I_L$.

The current in the circuit (ignoring the inductance):

$$I = \frac{2 \times 10^{-7} \mu_r A}{r.R} \frac{\Delta I_L}{\Delta t} \quad \ldots\ldots 2.30$$

where R is the total circuit resistance

## 6.2 A typical configuration

Assume that there are three rows of five detonators each (a total of 15 detonators). The resistance per detonator is 2 Ω and the total resistance of the circuit is therefore

$$R = 3 \times 5 \times 2 = 30\ \Omega \quad \ldots\ldots\ldots\

$$= \left[\frac{2 \times 10^{-7}\ \mu_r\ I_L\ A}{rR}\right]^2 \times \left[\frac{1}{\Delta t_r} + \frac{1}{\Delta t_f}\right] \quad \text{2.36}$$

The maximum distance (r) over which such an induction can set off a detonator is calculated by substituting:

$\mu_r$ = 1
$I_L$ = 90 000 A (95 % probability)
A = 15 m²
R = 30 Ω
$\Delta t_r$ = 4.5 μs
$\Delta t_f$ = 100 μs

$$I^2\Delta\ t = \frac{1}{d^2} \times 18.8 = 2.5mJ$$

$$r = 86.7\ m \quad \text{2.37}$$

# 7 COMPARISON BETWEEN THE MAGNETIC INDUCTION MECHANISM AND THE RESISTIVE CONDUCTION MECHANISM

The median lightning current model of Figure 2.8 is used as a basis for comparison. The criterion used for comparison is the action integral ($A^2$ s) that the particular mechanism can induce at the same distance (d) from the lightning strike.

with $I_L$ = 34 000 A
and $T_{50}$ = 75 μs = time to 50 % of peak value.

## 7.1 The conduction mechanism

From equation 2.14, the current induced into a detonator circuit is

$$I_P \text{ max} = 15\ I_L/2\pi r^2$$

$$I_p \text{ max} = \frac{81.2\times10^3}{r^2} \quad \text{2.38}$$

The $A^2s$ for an exponentially decaying impulse is

$$\int I^2\,dt = 1.44\, I_p^2\, T_{50}/2 \quad \text{2.39}$$

$$= .72\, T_{50}\, I_p^2$$

$$= .72\,(75\,\mu) \times (81.2 \times 10^3/r^2)^2$$

$$= \frac{356\times10^3}{r^4}$$

## 7.2 The magnetic induction mechanism

From equation 2.36:

$$I^2\,\Delta t = \left[\frac{2\times10^{-7}\,\mu_r\, I_L\, A}{rR}\right]^2 \left[\frac{1}{\Delta t_r} + \frac{1}{\Delta t_f}\right] \quad \text{2.40}$$

where

$\mu_r = 1$
$I_L = 34\,000$ A
$A = 15$ m$^2$
$R = 30\ \Omega$
$\Delta t_r = 4.5\ \mu s$
$\Delta t_f = 100\ \mu s$

$$= \left[\frac{11.6\times10^{-6}}{r^2}\right] \times 232\ .\ 10^3$$

$$= \frac{2.68}{r^2}$$

From Figure 2.9, it is evident that the conduction mechanism is dominant in the range where energy transfer is sufficient to set off detonators.

It is concluded from this example that the magnetic induction process can be ignored for the purpose of this study. For this reason, this thesis, focuses only on the conduction mechanism.

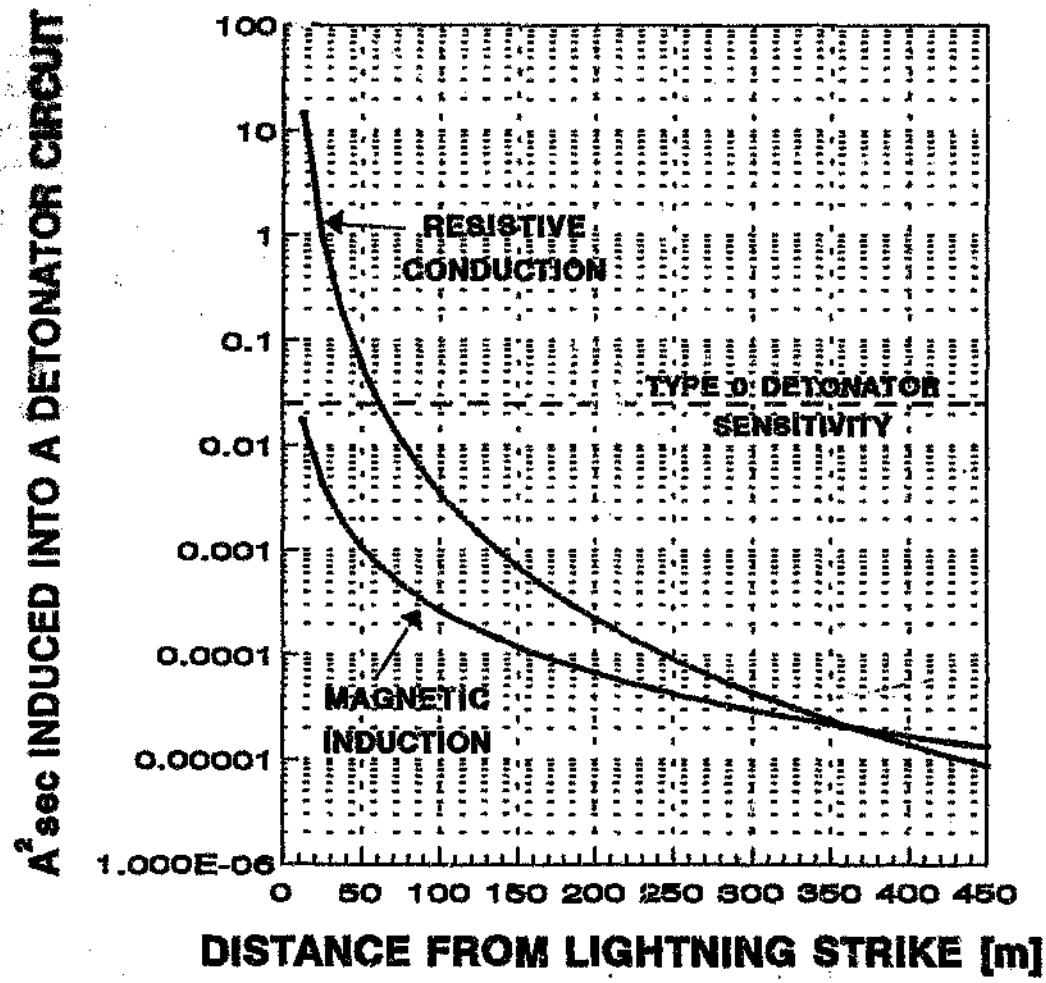



**Figure 2.9** The $A^2$ s induced through the magnetic induction mechanism compared with the resistive conduction mechanism. This comparison has been made using the median lightning strike of Figure 2.8 as a function of distance from the flash.

# CHAPTER 3

# THE EFFECT OF STRATA LAYERS ON THE PENETRATION OF CURRENT INTO DETONATION CIRCUITS

## INTRODUCTION

[illegible] the mechanism by which lightning strikes the surface above a [illegible] the current penetrates the circuit via conduction through the strata. [illegible] for the mechanism is proposed in Chapter 2. This chapter uses [illegible] but a field calculation computer-based programme is used to [illegible] complex strata have on the penetration process.

## A SIMPLE SPHERICAL MODEL

Figure 3.1 shows the basic physical model used. Lightning current ($I_L$) is injected into the centre of a hemisphere. A vertical line through this point represents a symmetrical axis. For the purpose of analysis, this axis forms the basis of a cylindrical co-ordinate system. This model was used to determine the accuracy of computer programmes that were considered for possible use.

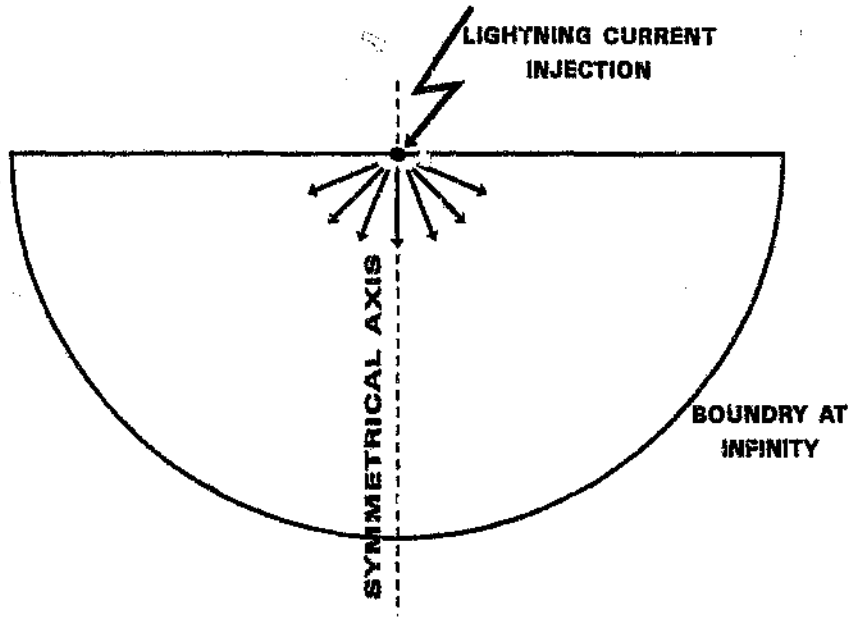



**Figure 3.1** The basic model for evaluating computer programmes

Analytical equations are available for this model. The electric field (E) at any point p in the hemisphere is

$$E_p = \frac{I_L \rho}{2\pi r^2} \quad \ldots\ldots 3.1$$

where r = the distance from the current injection point to point p
and ρ = soil resistivity.
The voltage (U) at p is

$$U = \frac{\rho I}{2\pi r} \quad \ldots\ldots 3.2$$

The resistance between a hemisphere with radius r and infinity is

$$R = \frac{\rho}{2\pi r} \quad \ldots\ldots 3.3$$

The voltage between any two hemispheres with radii $r_0$ and $r_1$ is

$$V = \frac{\rho I_L}{2\pi} \left[ \frac{1}{r_0} - \frac{1}{r_1} \right] \quad \ldots\ldots 3.4$$

The resistance between any two hemispheres with radii $r_0$ and $r_1$ is

$$R = \frac{\rho}{2\pi} \left[ \frac{1}{r_0} - \frac{1}{r_1} \right] \quad \ldots\ldots 3.5$$

# 3 THE STRATA MODEL

The actual configuration of the strata in typical South African mines is very complex. For the purpose of the analysis in this thesis it has been simplified to the configuration given in Figure 3.2.

The strata consist of a single layer of uniform resistivity ($\rho_1$) above the coal seam, the coal seam with uniform resistivity ($\rho_c$) and, finally, the deep strata with uniform resistivity ($\rho_2$).

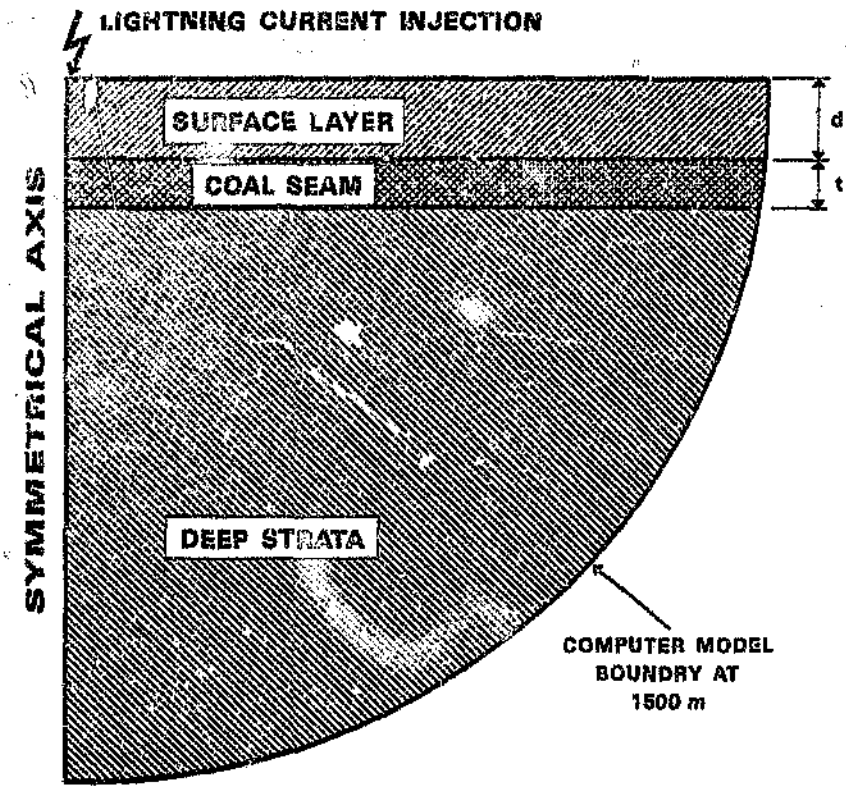



**Figure 3.2** A simplified model of the configuration of the strata in a typical South African mine

The boundary of the model was chosen to be relatively far away from the area of interest, at 1 500 m. This is approximately ten times further than any distance of real interest.

The dimensions of interest are shown in Figure 3.3:

| | | |
|---|---|---|
| d | = | the depth of coal seam |
| t | = | the thickness of coal seam (this is assumed to be 3 m in this chapter, unless otherwise specified) |
| r | = | the horizontal distance between the work face and a lightning strike |
| $d_F$ | = | the distance from the face to the exploder (this is assumed to be 30 m throughout this chapter) |
| $U_T(r)$ | = | the voltage at the top of the coal seam |
| $U_B(r)$ | = | the voltage at the bottom of the coal seam |
| $U_V(r)$ | = | $U_T(r) - U_B(r)$ ..... 3.6 |
| | = | the voltage vertically across the coal seam |
| $U_D(r)$ | = | $U_T(r) - U_B(r + d_F)$ ..... 3.7 |
| | = | the voltage diagonally across the coal seam. This represents the maximum voltage induced into an exploder-detonator circuit. |

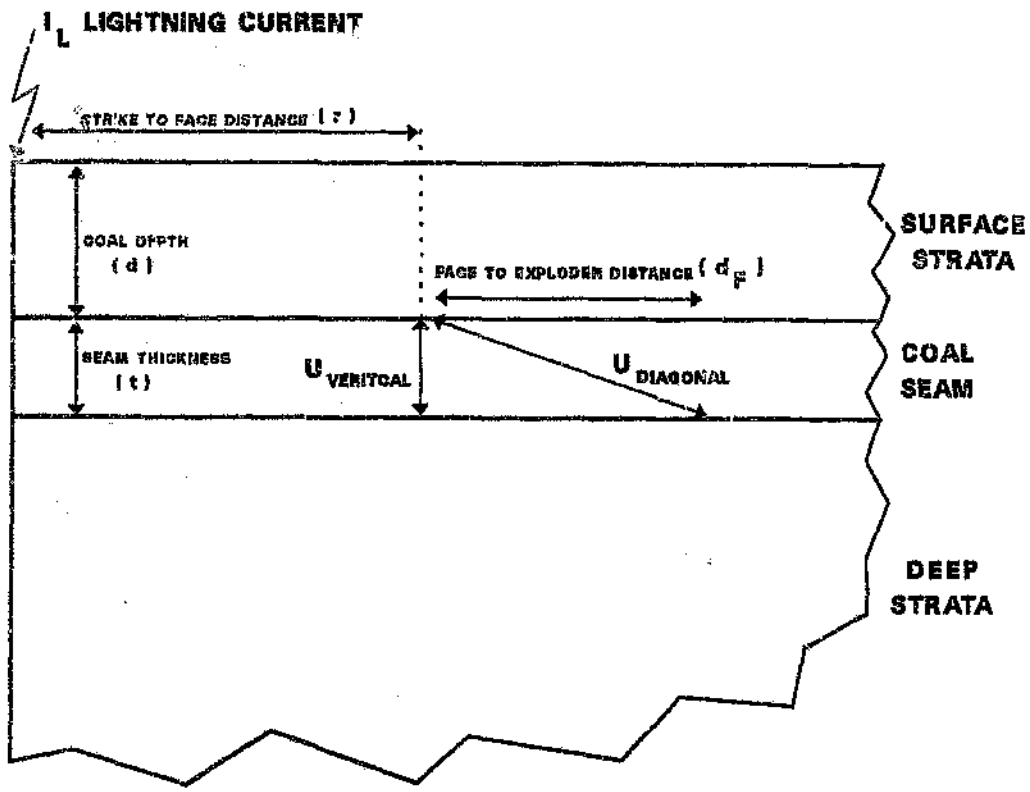



**Figure 3.3** Boundaries of the simplified model

# 4 EVALUATION AND SELECTION OF A FIELD CALCULATION PROGRAMME

Compared to the calculations of electrostatic fields usually ma when designing HV equipment, this model has distinctly different features:

- A current source injects current into a resistive medium at a distinct point that is relatively small.
- The boundary potential at infinity is not defined; in fact, no boundary potential is defined. The point of concern is not necessarily where the highest electrostatic fields are present (i.e. the high electrostatic fields that would normally interest a designer of HV equipment), the magnitudes of interest could be several orders of magnitude less than the highest field present in the analysis.

Three different commercially available field calculation programmes were evaluated to solve this problem:

(1) MacNeal-Schwendler Corporation's package: Maggie

(2) Ansoft Corporation's package: Maxwell
(3) Integrated Engineering Software's package: Electro

The first two packages are based on the finite-element method and the last package is based on the boundary-element method (charge simulation).

Both of the finite-element packages failed to correctly calculate simple examples that are analytically known.

Two analyses were done, the first where the outer boundary is set at infinity (equal to 0 V), and the second where an outer spherical boundary is given at the correct calculated potential. In the first case, the programs gave results which were wrong by orders of magnitude. In the second case, the programs only had to interpolate correctly between two boundaries; these results were wrong, the error was as much as 25 %.

The same analyses were repeated using the boundary-element method. In the case where the outer boundary was set at infinity (equal to 0 V), the boundary-element method gave errors of 20 % of the expected value.

In the case where a spherical boundary is given (set at the correct calculated potential), the boundary-element method gave errors of 1 % of the expected value.

For this application, the boundary-element method proved to be the only method that could be used to solve the problem. The reason for this is to be found in the fundamental method of calculation.

The error in the finite-element method (Kuffel and Zaengl, 1984) depends on the element dimension and the derivatives of the potential. In this problem, the field has maximum divergence and the solution has to be accurate over several orders of magnitude of potential. The approximations used in the packages are probably of the first order or, at most, second order, and are not capable of dealing with the demands set out above.

In contrast, the boundary-element method is based on the fundamental physical phenomena selected to suit the dimensions of the problem. The influence of a boundary element (even if it is very far away) can be determined accurately because the dimension is known accurately. Therefore, accuracy depends only on the extent to which the boundary elements are appropriately placed and estimated.

# 5 TYPICAL RESULTS FROM THE FIELD CALCULATION PROGRAMMES

A geometrical configuration was set up in Electro. This is shown in Figure 3.4. It consisted of the following:

- An outer hemispherical boundary was set at 1 500 m
- The strata configuration shown in Figures 3.2 and 3.3 was used
- The current was injected via a 1 m spherical electrode at the centre of the sphere.

Boundary elements were placed on the boundaries of the half sphere as shown in Figure 3.4. Boundary elements were also placed on the boundary between the coal layer and the surface and the deep strata. An analysis was performed to determine where the elements should be placed. If insufficient elements were used, the curves resulting from the analysis were irregular and the number of elements was increased to improve the curves.

A current of 1 A was injected at the centre of the sphere. The potential of the outer hemispherical boundary at 1 500 m (determined by equation 3.2) was set to the values shown in Table 3.1.

**Table 3.1** The outer hemispherical boundary potential determined by equation 3.2

| $\rho$ ($\Omega$.m) | U (V) |
|---|---|
| 200 | 0.0212 |
| 400 | 0.0425 |
| 800 | 0.0850 |
| 1 600 | 0.1700 |

The programme can calculate the vector field of the electric field and the scalar field of potential.

Figures 3.5 to 3.7 show the results of the case where the seam depth is 15 m and the seam thickness is 5 m.

Figure 3.8 shows the magnitude of the electric field along the symmetrical axis. It is interesting to note that this magnitude is proportional to the resistivity in the vicinity - resulting in an increase in the field across the coal seam. This effect is also apparent in Figure 3.7; note the closeness of the spacing of the equipotential contours through the coal strata.

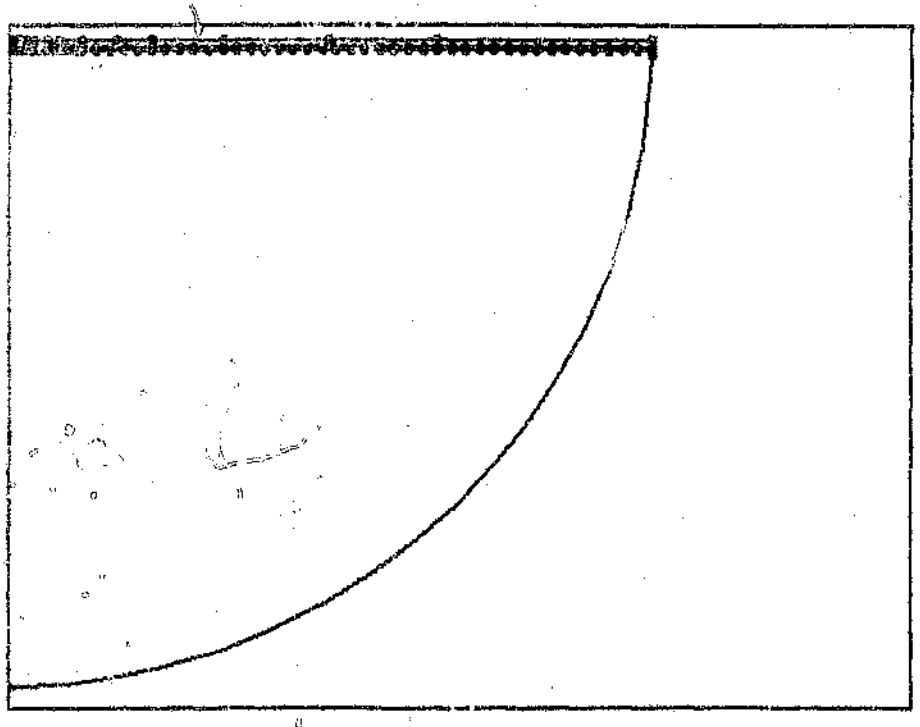


**Figure 3.4** The positioning of boundary elements on the model analysed.

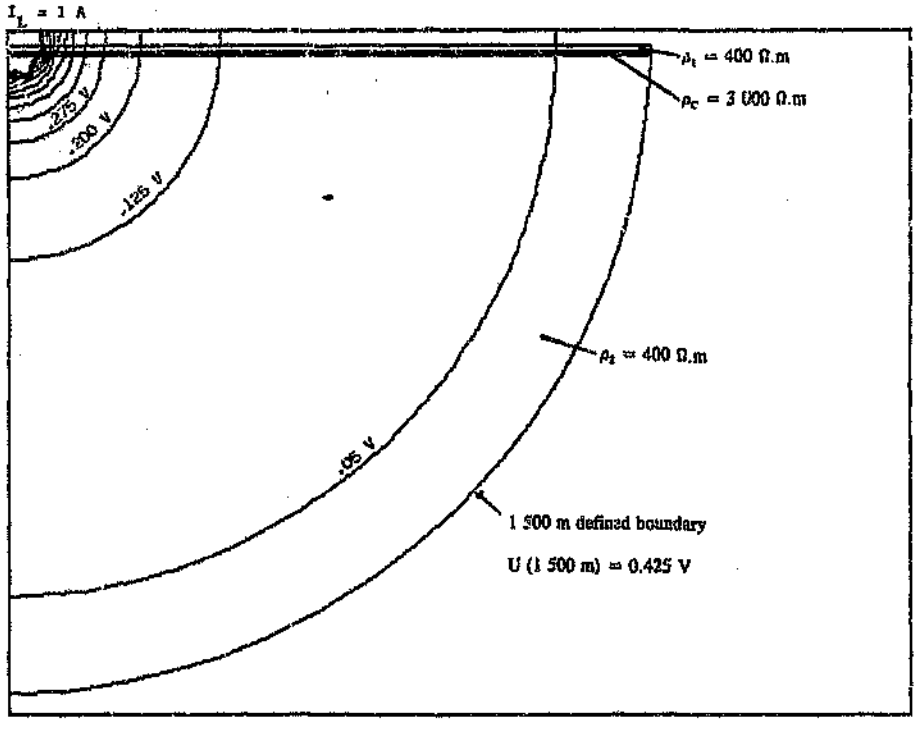



**Figure 3.5** The equipotential contours up to 1 500 m (seam depth (d) = 15 m and seam thickness (t) = 5 m)

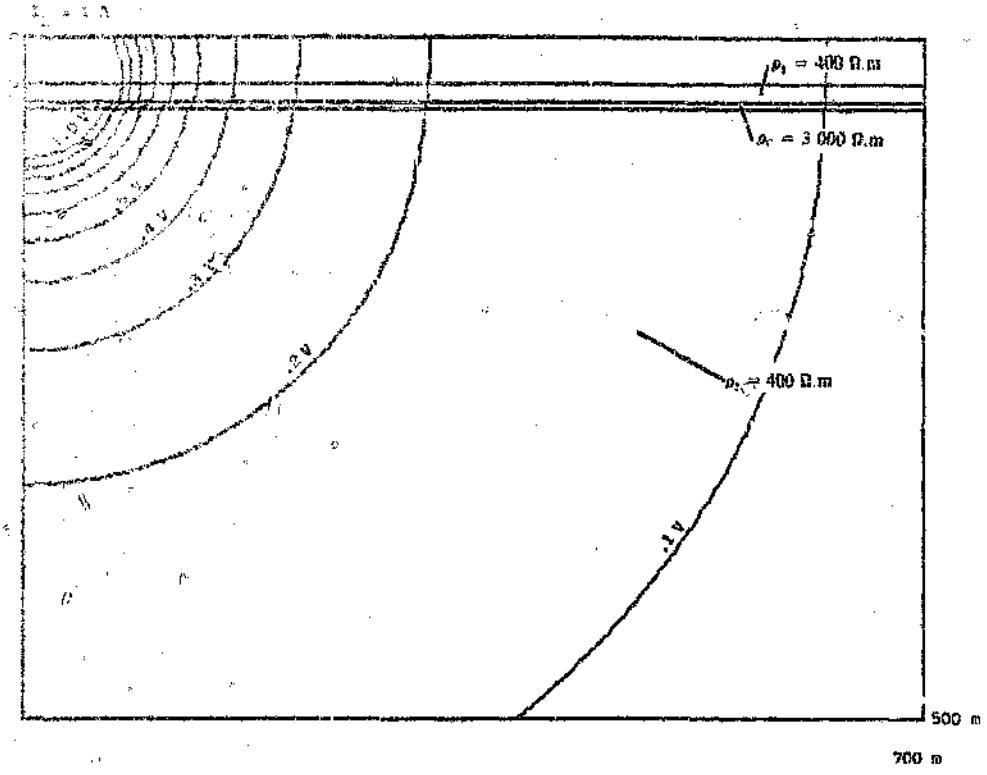



**Figure 3.6** The equipotential contours to a depth of 500 m (seam depth (d) = 15 m and seam thickness (t) = 5 m)

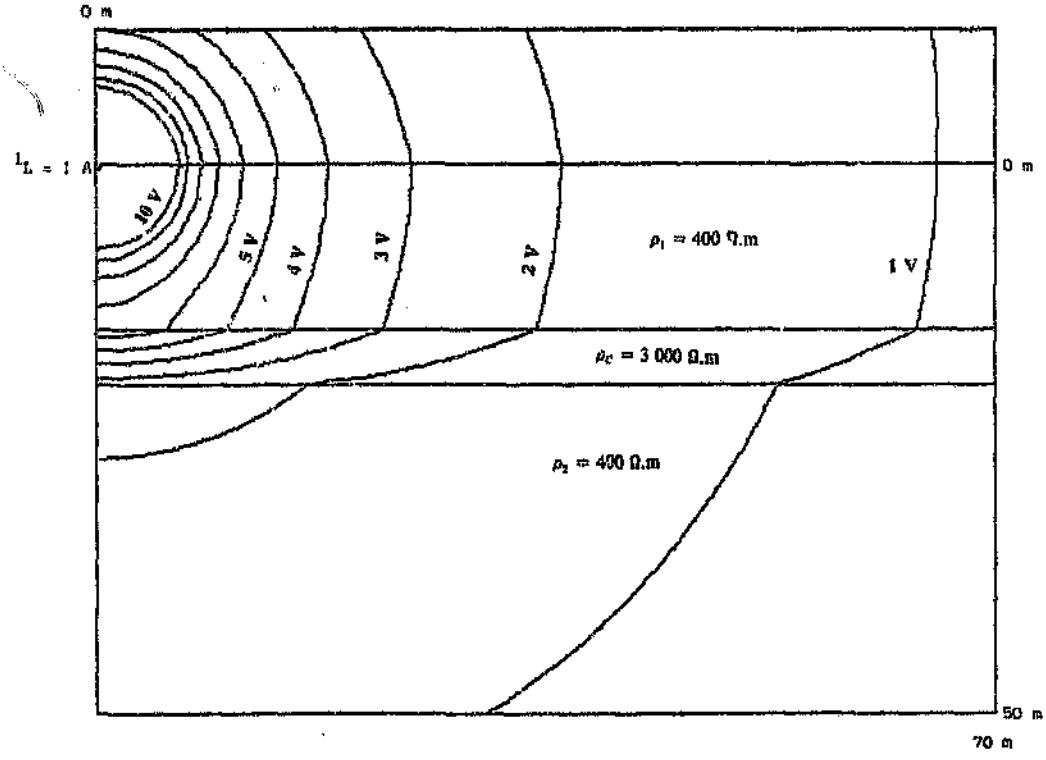



**Figure 3.7** The equipotential contours to a depth of 50 m (seam depth = 15 m and seam thickness = 5 m)

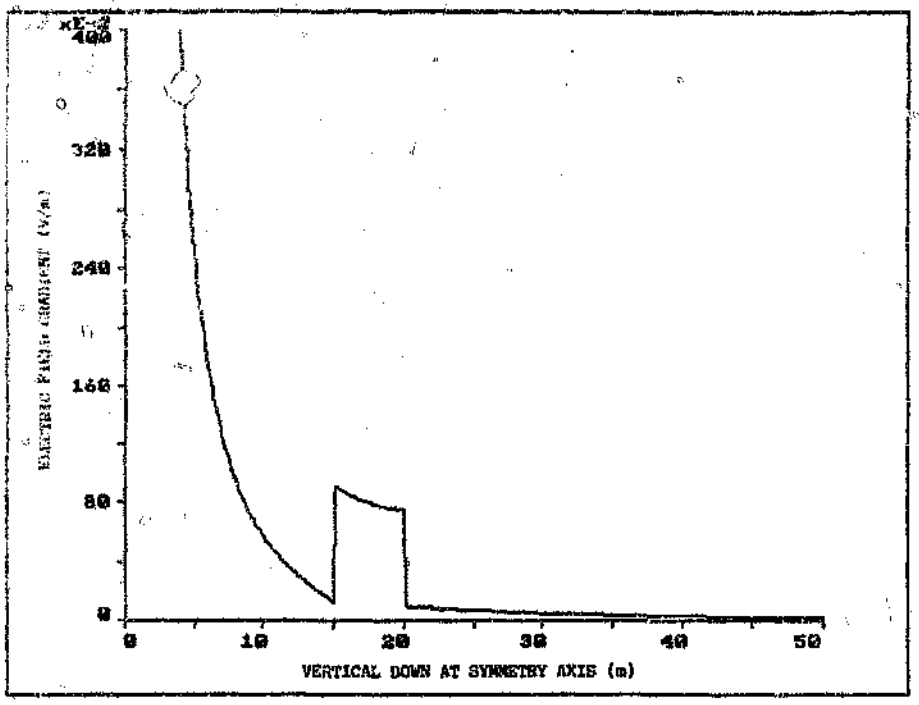



**Figure 3.8** The electric field gradient vertically down the symmetrical axis. (For an injected current of 1.0 A.)

The voltage ($U_i$) produced is shown on the equipotential contours. The voltage ($U_L$) produced by a lightning strike of a specific magnitude can be calculated by

$$U_L = I_L U_i \quad \ldots\ldots\ldots\

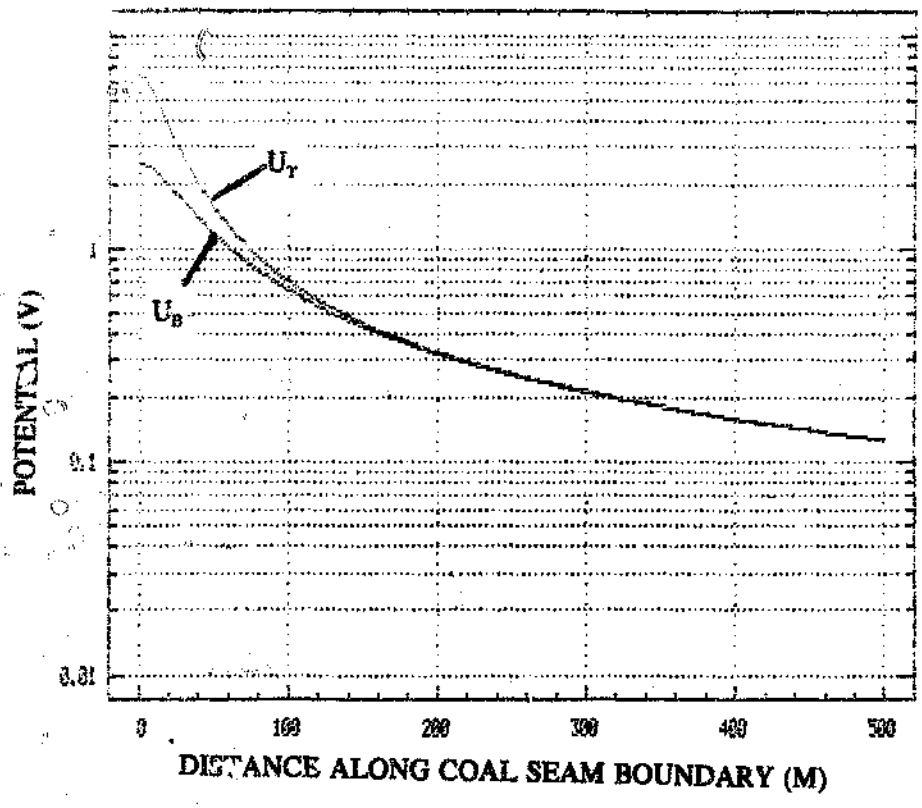



**Figure 3.9** The potential horizontally above the coal seam ($U_T$) and the potential just below the coal seam ($U_B$). ($I_L$ = 1 A, seam depth (d) = 15 m, and seam thickness (t) = 5 m)

$U_V$ and $U_D$ were determined thereafter using equations 3.6 and 3.7. The results of this example are shown in Figure 3.10.

The maximum voltage produced by a given magnitude of lightning current can be determined using the results of Figure 3.10. Comparisons between different strata configurations can be made based on the maximum of Figure 3.10, i.e. the maximum of $U_V$ and $U_D$. However this is not necessarily related to the frequency that surges will occur, i.e. the risk associated with a particular strata configuration.

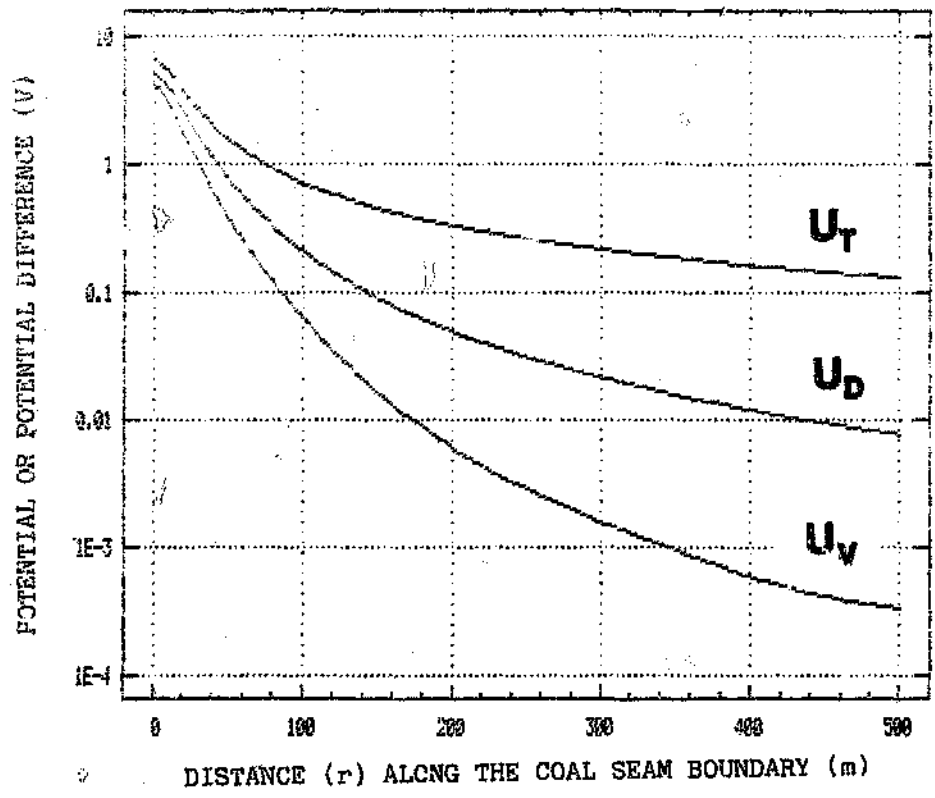



**Figure 3.10** The voltage difference between $U_T$ and $U_B$ directly vertical ($U_V$) and the voltage difference diagonally across $U_D$. The "face-to-exploder" distance ($d_E$) is 30 m and can be compared to the potential of the boundary just above the coal seam ($U_T$).
Seam depth (d) = 15 m and seam thickness (t) = 5 m

# 7 CALCULATION OF THE FREQUENCY ($N_E$) AT WHICH LIGHTNING SURGES OF MORE THAN A CERTAIN MAGNITUDE WILL OCCUR IN A DETONATOR CIRCUIT

## 7.1 The number of events

If it is assumed that the probability ($P_E(r)$) of a particular lightning flash striking at a certain distance (r) from a work face and setting off a detonator is known, the number of events ($N_E$) exceeding this magnitude is given by

$$N_F = N_g \times 2\pi \int_0^{\infty} r \times P_F(r)dr \quad \ldots\ldots 3.9$$

or can be approximated by

$$N_F = N_g \times 2\pi \sum_0^{\infty} r \times P_F(r) \times \Delta r \quad \ldots\ldots 3.10$$

## 7.2 The probability $P_F(r)$

The vertical voltage ($U_V$) and the diagonal voltage ($U_D$) required to set off a detonator is studied in Chapter 8 where Figures 8.25 and 8.26 show the surge voltage peak required to set off a detonator as a function of the resistivity of the coal seam.

Because the diagonal voltage $U_D$ is much larger than the vertical voltage $U_V$ (see Figure 3.10), the diagonal voltage is always the critical factor. For this reason only the diagonal voltage/risk is analysed.

From Figure 8.26 it can be seen that the diagonal voltage $U_D$ required (in the present example) to set off a detonator in a coal seam resistivity of 3 000 Ω.m is 38 kV.

Figure 3.10 gives the relationship between $U_D$ and $I_L$:

$$U_D\,(r,I_L) = I_L \times f(r) \quad \ldots\ldots 3.11$$

The lightning current ($I_{LF}$) corresponding to 38 kV at a distance (r) from a work face is

$$I_{LF} = \frac{38kV}{f(r)} \quad \ldots\ldots 3.12$$

The probability of a particular lightning flash exceeding a certain magnitude was expressed in an analytical equation by Anderson (1982), as

$$P(I_L) = \frac{1}{1 + \left[\frac{I_L}{31}\right]^{2.6}} \quad \ldots\ldots 3.13$$

The probability $P_F(r)$ of a particular flash at a distance r setting off a detonator can be calculated by substituting equation 3.12 into equation 3.13.

$$P_F(r) = \frac{1}{1 + \left[\frac{38}{31 \times f(r)}\right]^{2.6}} \quad \ldots\ldots 3.14$$

Equations 3.9 and 3.10 now become

$$N_F = N_g \times 2\pi \int_0^{\infty} \frac{r}{1 + \left[\frac{38}{31 \times f(r)}\right]^{2.6}} \quad \ldots\ldots 3.15$$

and

$$N_F = N_g \times 2\pi \sum_0^{\infty} \frac{r \times \Delta r}{1 + \left[\frac{38}{31 \times f(r)}\right]^{2.6}} \quad \ldots\ldots 3.16$$

## 7.3 Results from the example

In Equation 3.16, its various parts have physical meaning.

Figure 3.11 shows the lightning current required (at a certain distance) to set off a detonator. It also shows the probability of the occurrence of a strike exceeding the required magnitude. When a strike occurs close to the work face, the minimum current is relatively low (± 9 kA). The probability of such a low-amplitude strike occurring is very high, almost 1. However, when a strike is far away (± 200 m), almost 900 kA is required to set off a detonator. Such a strike has never been recorded. The probability (according to Anderson (1982)) is accordingly low.

A probability times the area associated to which that probability applies is shown in Figure 3.12. The probability is initially high but the area is low. Eventually, the area is high but the probability is very low. $N_F$ is the integral under the curve of Figure 3.12. This was numerically evaluated and the result for this example is

$N_F = 0.00603$ events in one year, and $N_g = 1$

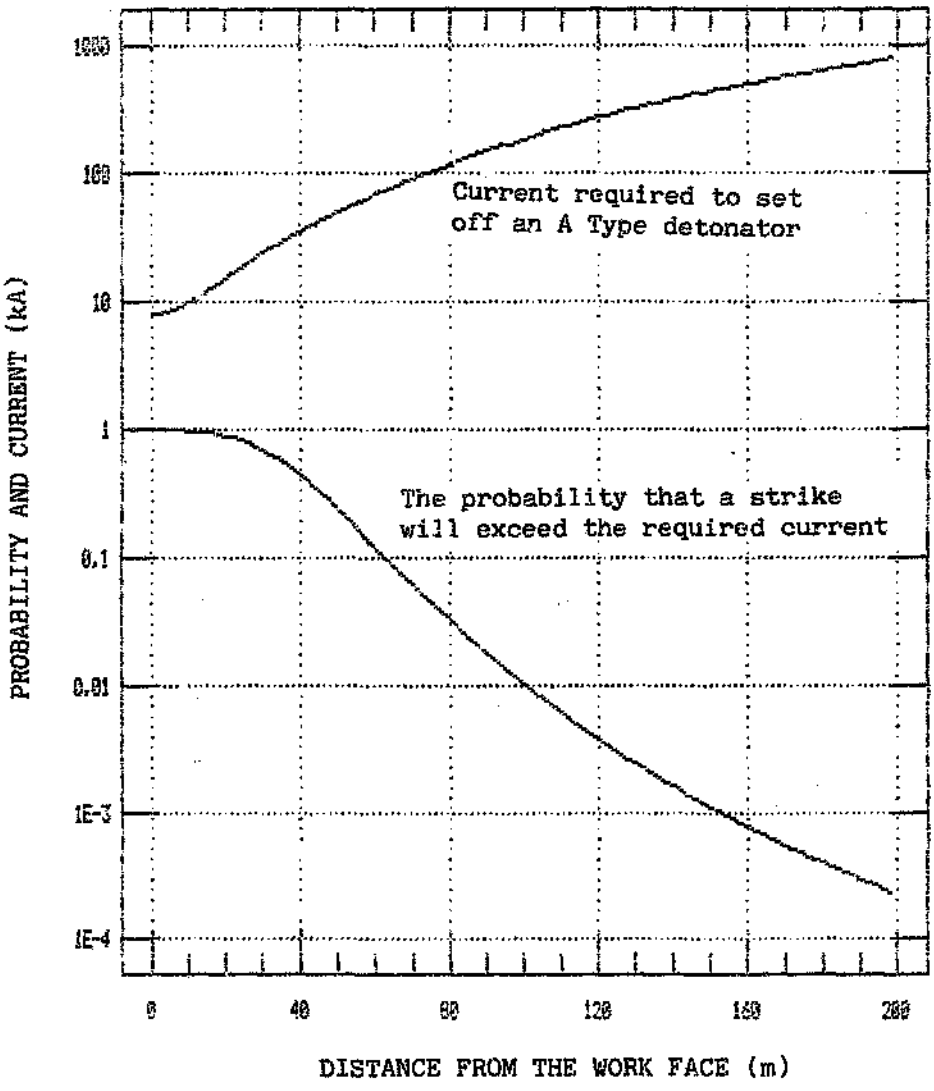



**Figure 3.11** The lightning current required to set off a Type 0 Detonator as a function of the distance between the strike and the work face (r). The probability of a particular strike exceeding this value of current is plotted on the same axis.
Seam depth d = 15 m. Seam thickness t = 5 m.

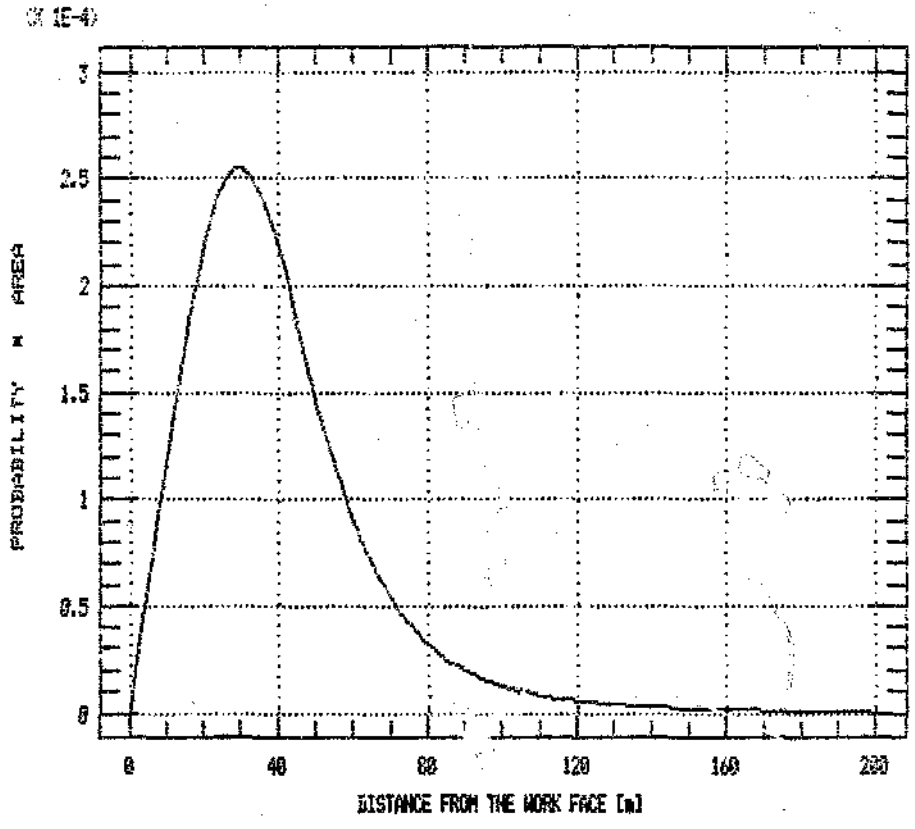



**Figure 3.12** The probability at a defined distance times the area associated with that distance.

# 8 RESULTS: THE EFFECT OF DIFFERENT MODEL PARAMETERS

This section gives the results of the analysis, i.e. the effect of different characteristics of different mines on the analysis. This is quantified via the peak current produced for such a situation as well as the frequency ($N_F$) at which surges of a dangerous magnitude will occur.

The analysed characteristics of the mine are:

- Depth of the coal seam
- Resistivity of the strata
- Resistivity of the coal seam
- Thickness of the coal seam.

## 8.1 Depth of the coal seam - peak current amplitude at the work face

From the simple model of Chapter 2, it is expected that the depth of a coal seam will have a very big effect on the probability of a detonator being set off by lightning. A series of analyses was conducted to study the effect of seam depth. In all cases, the seam thickness (t) = 5 m, and the resistivity ($\rho_C$) = 3 000 Ω.m.

The diagonal voltage difference ($U_D$) for seam depths of 15 m, 30 m, 60 m and 100 m was calculated. The result is shown in Figure 3.13.

The maximum of the diagonal voltage difference $U_D$ is an indication of the maximum current that can be expected at that depth. The maximum of $U_D$ is plotted in Figure 3.14 as a function of seam depth. If we assume that the highest possible amplitude of a lightning strike will be 200 kA, this strike will produce a maximum diagonal voltage difference at a depth of 100 m of $U_D$ = 200 kA x 0.211 = 42.2 kV.

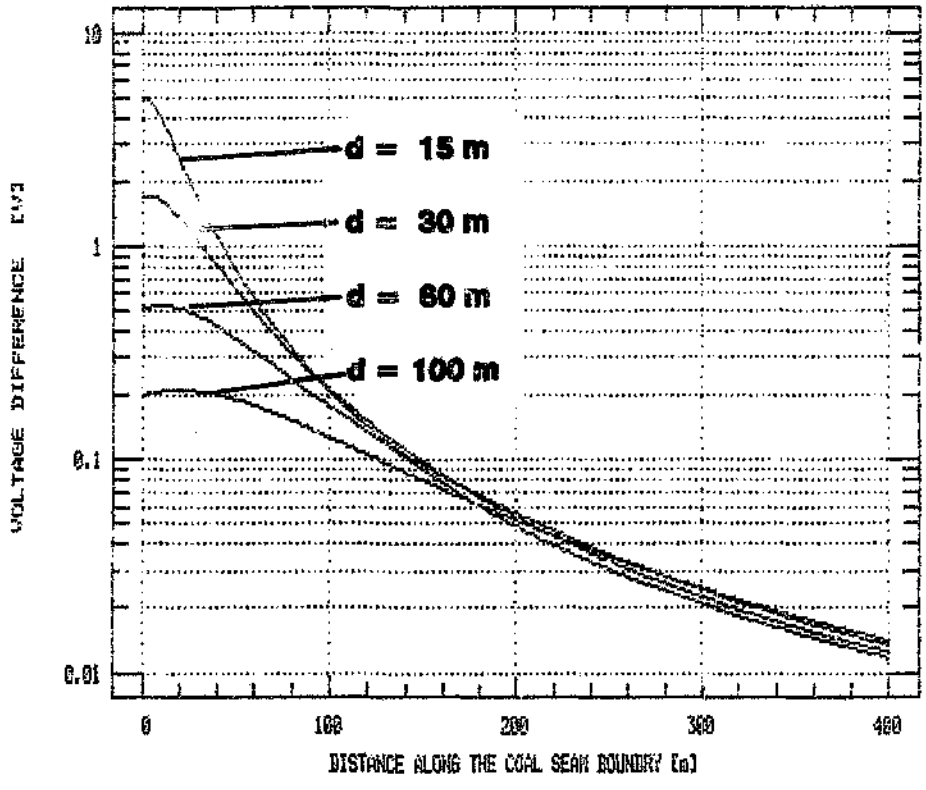



**Figure 3.13** The diagonal voltage difference ($U_D$) for coal seams at different depths (d). t = 5 m, $\rho_C$ = 3 000 Ω.m, and $I_L$ = 1 A

In an attempt to compare this result with the simple model of Chapter 2, the following reasoning was followed:

From Chapter 8, it was determined that 38 kV is required to set off a Type 0 detonator via the diagonal voltage configuration. This will produce a peak of 7 A. From Chapter 2, the maximum current was determined as

$$I_{max} = \frac{15\, I_L}{2\pi d^2} \qquad \ldots\ldots 2.24$$

In the present analysis, $I_L$ = 1 A.

The relationship between $I_{max}$ and $V_{max}$ can be assumed to be

$$R = \frac{38\ kV}{7\ A} = 5.4\ k\Omega \quad \ldots\ldots 3.17$$

$$V_{max} = I_{max} R \quad \ldots\ldots 3.18$$

$$V_{max} = \frac{5.4 \times 10^3 \times 15\ I_L}{2\pi d^2} \quad \ldots\ldots 3.19$$

$$V_{max} = \frac{1.29 \times 10^4}{d^2} \quad \ldots\ldots 3.20$$

This equation is plotted in Figure 3.14. There is an strong correlation between the shape of the two curves. By applying a constant correction factor of 0.14, the two curves almost coincide exactly.

## 8.2 Depth of the coal seam - surge current frequency

The true basis of risk evaluation, however, is the number of surges that can exceed the sensitivity of the detonator used in the mine. The frequency of surges exceeding the sensitivity of the Type 0 detonator was calculated using the method given earlier in this chapter for seam depths of 15 m, 30 m, 60 m and 100 m.

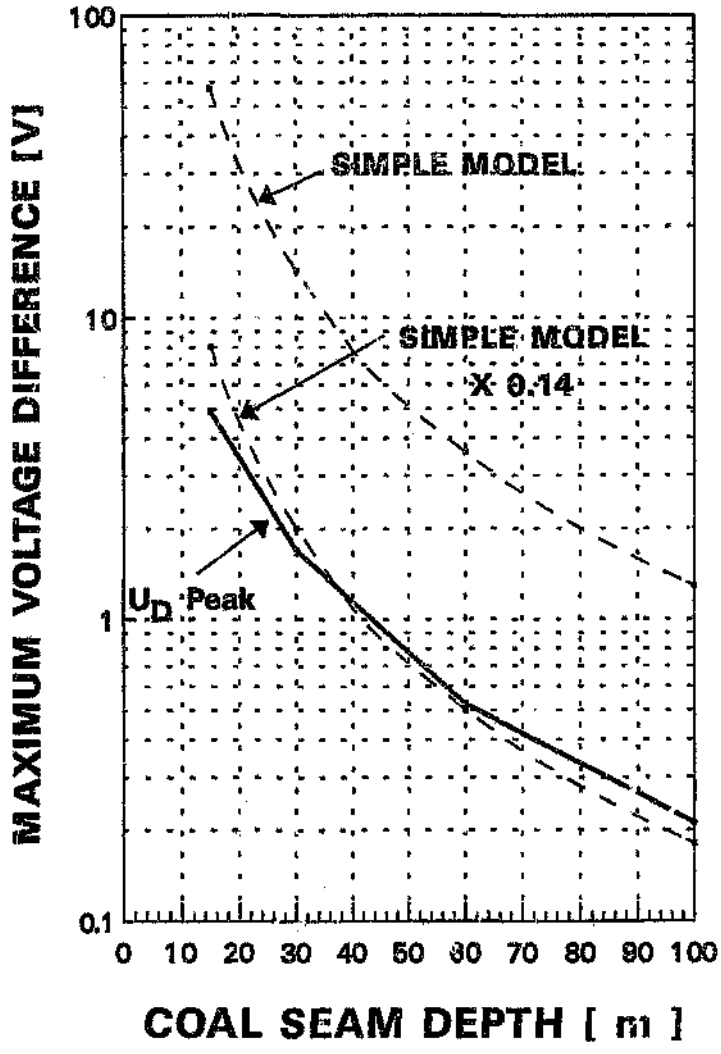



**Figure 3.14** The peak of the diagonal voltage difference $U_D$ as a function of the seam depth (d). $t = 5$ m, $\rho = 3\,000\ \Omega.m$, $I = 1$ A, and $\rho_1 = \rho_2 = 400\ \Omega.m$.

The frequency reduction due to depth does not quite follow the inverse squared relationship of equation 2. However, the effect of depth is very significant. Going from a depth of 15 m to 100 m (6.67 times deeper), the number of surges (exceeding the sensitivity of "0" detonators) is reduced by 22.3 times. The result if plotted in Figure 3.15.

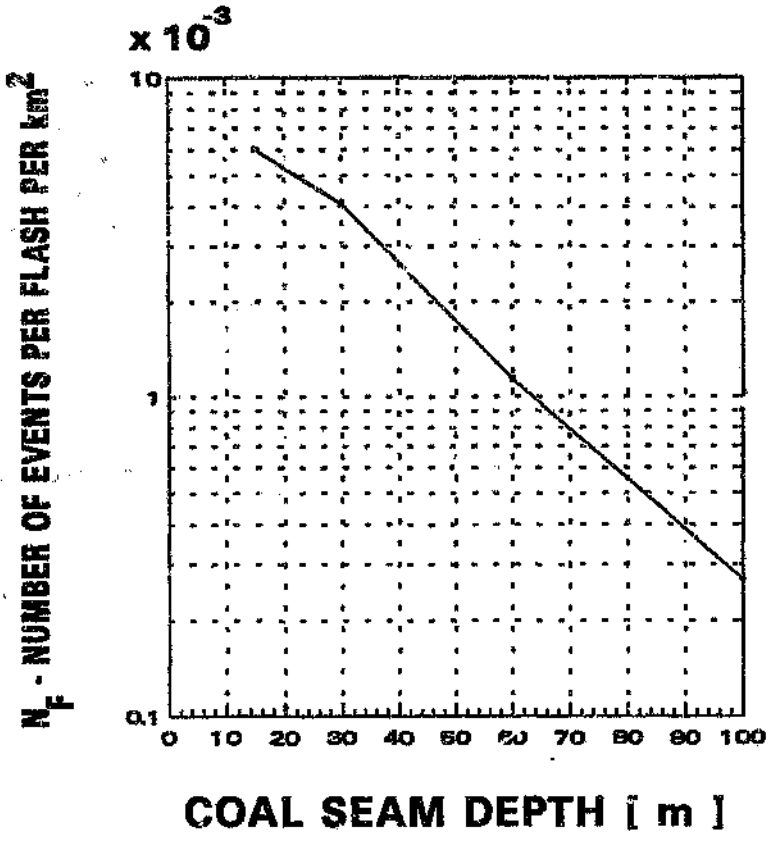



**Figure 3.15** The frequency of surges exceeding the sensitivity of Type 0 detonators as a function of the depth of the coal seam (d). t = 5 m, $\rho$ = 3 000 Ω.m, and $\rho_1 = \rho_2$ = 400 Ω.m

## 8.3 The resistivity of the strata

### 8.3.1 $\rho_1 = \rho_2$ - the same resistivity above and below the coal seam

The simplest point to start the analysis is to assume $\rho_1 = \rho_2$. The result of the maximum diagonal voltage ($U_D$) is shown in Figure 3.16. The ratio between resistivity variation (200 Ω.m : 1 600 Ω.m = 1:8) is much more than the ratio of increase, $U_D$, which was 3.57 times.

Again the most important comparison is that of the frequency at which the sensitivity level of the detonator is exceeded. A comparison between 200 Ω.m : 1 600 Ω.m gives an

increase of the ratio in $N_p$ to 1 : 8.78. The risk variation is slightly more than the proportional change in resistivity. (The result is shown in Figure 3.17.)

Mathematically, the change in frequency can be expressed as

$$N_2 : N_1 = \left[\frac{\rho_1}{\rho_2}\right]^{1.04} \quad \ldots\ldots\ldots\

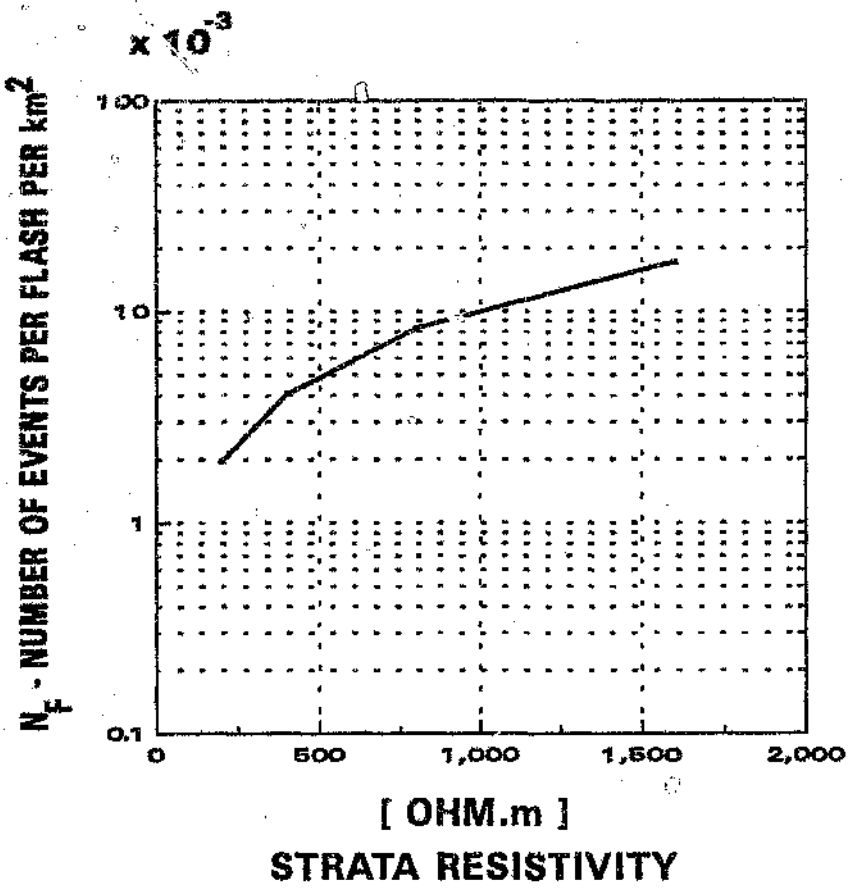



**Figure 3.17** The frequency of surges exceeding the sensitivity of Type 0 detonators as a function of strata resistivity. The resistivity of the surface layer and the resistivity of the deep strata are the same, $\rho_1 = \rho_2$.

| | | |
|---|---|---|
| t | = | 5 m |
| d | = | 30 m |
| $\rho_c$ | = | 3 000 Ω.m |

### 8.3.2 The effect of the resistivities of the surface layer and the deep strata where $\rho_1$ is not equal to $\rho_2$

Peak amplitude

Figures 3.18 and 3.19 give the peak diagonal voltage difference ($U_D$) as a function of the resistivity of the surface layer $\rho_1$ and the resistivity of the deep strata, calculated for specific values of the alternate parameter. From the figures, it is apparent that the deep strata resistivity ($\rho_2$) has very little effect on $U_D$.

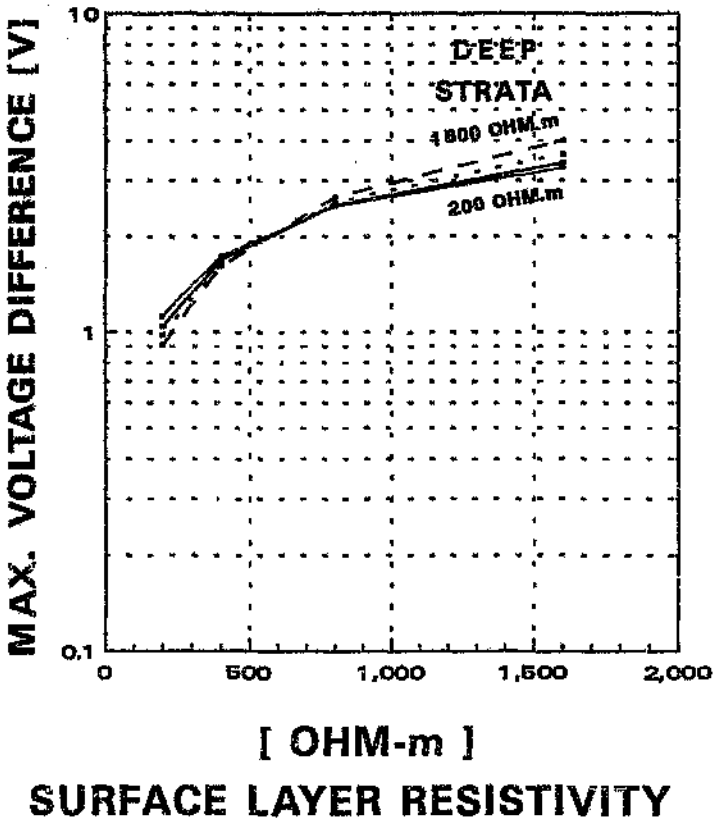



**Figure 3.18** The maximum of the diagonal voltage difference ($U_D$) as a function of the resistivity of the surface layer ($\rho_1$).

| | | |
|---|---|---|
| t | = | 5 m |
| d | = | 30 m |
| $\rho_2$ | = | 3 000 Ω.m |
| I | = | 1 A. |

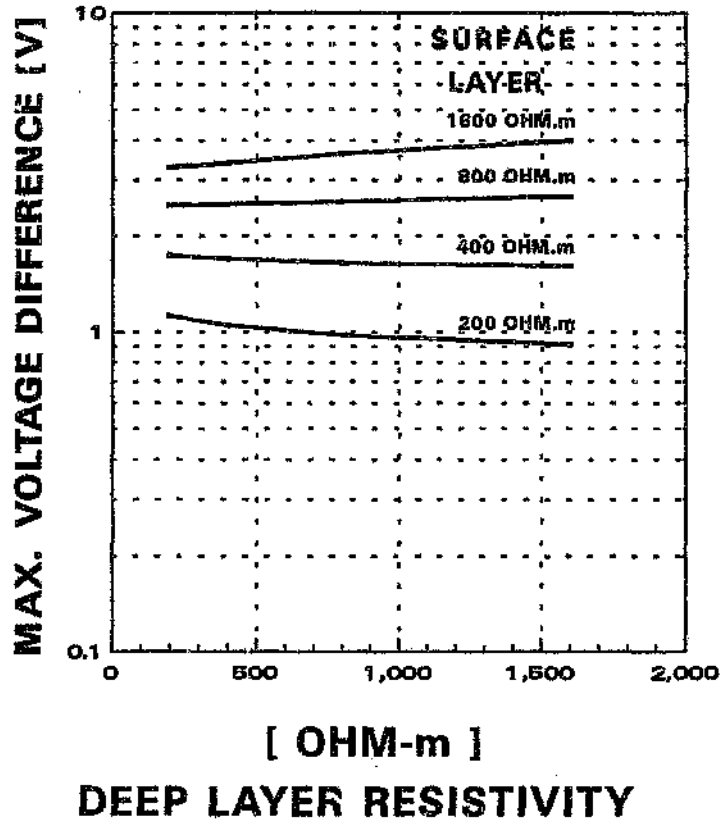



**Figure 3.19** The maximum of the diagonal voltage difference ($U_D$) as a function of the resistivity of the deep strata ($\rho_2$).

| | | |
|---|---|---|
| t | = | 5 m |
| d | = | 30 m |
| $\rho_1$ | = | 3 000 Ω.m |
| I | = | 1 A |

Frequency

In contrast to the peak voltage, the frequency with which surges occur depends both on the resistivity of the deep strata as well as the resistivity of the surface layer. An extensive attempt was made to find an empirically derived regression equation between $N_f$ and $\rho_1$ and $\rho_2$. This attempt did not give results that would be used to interpolate the results. The frequency with which surges exceed the sensitivity of the Type 0 detonator is shown in Figure 3.20 as a function of the resistivity of the surface layer. In Figure 3.21, it is shown as a function of the resistivity of the deep strata.

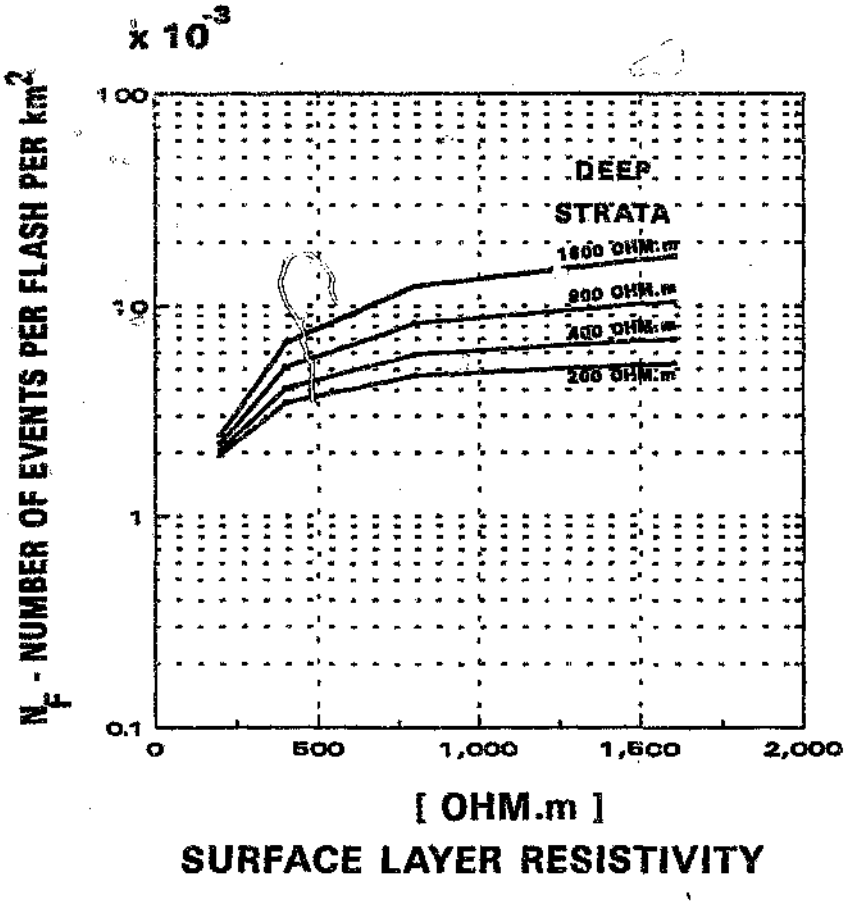



**Figure 3.20** The frequency of surges exceeding the sensitivity of Type 0 detonators as a function of the resistivity of the surface layer ($\rho_1$).

| | | |
|---|---|---|
| t | = | 5 m |
| d | = | 30 m |
| $\rho_1$ | = | 3 000 Ω.m |

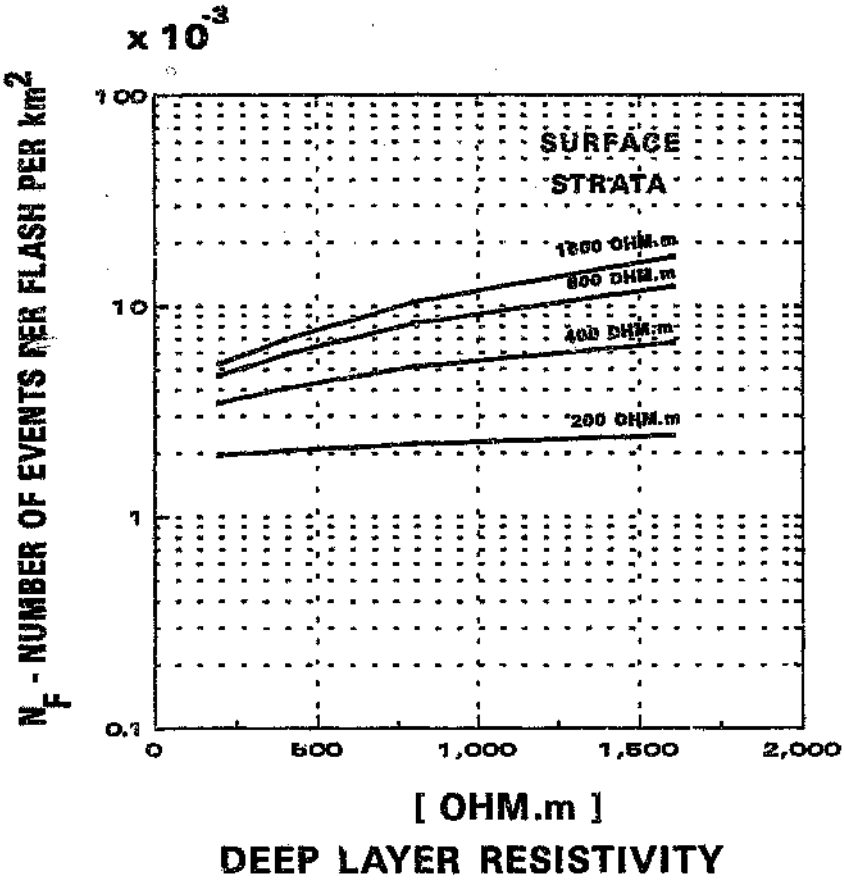



**Figure 3.21** The frequency of surges exceeding the sensitivity of Type 0 detonators as a function of the resistivity of the deep strata ($\rho_2$).

$t = 5$ m; $d = 30$ m; $\rho_1 = 3\,000\ \Omega.m$

## 8.4 The effect of the resistivity of the coal seam

Peak voltage

The diagonal voltage difference ($U_D$) was calculated as a function of the resistivity of the coal seam. The result is shown in Figure 3.22. As expected, the voltage increases with the increase in resistivity. However, this does not mean that the current in a detonator circuit increases. It is shown in Figure 8.26 in Chapter 8 that, due to the increase in resistivity, an increased voltage is required to set off a detonator in surroundings of higher resistivities.

Frequency

The frequency of surges exceeding 38 kV was first calculated and the result is shown by Curve A of Figure 3.23. This results in an increase in frequency as the resistivity of the seam increases. However, the results of Figure 3.26 were incorporated into Curve B of Figure 3.23, taking the effect of surrounding resistivity on the detonator current into account. When this is done, it actually results in a decrease in the risk as resistivity increases.

The implications of this result are important: if the hole for the explosives is drilled into the coal, or just above the coal into the surface layer (which may have a low resistivity), it could make an enormous difference to the risk to which the operation is exposed.

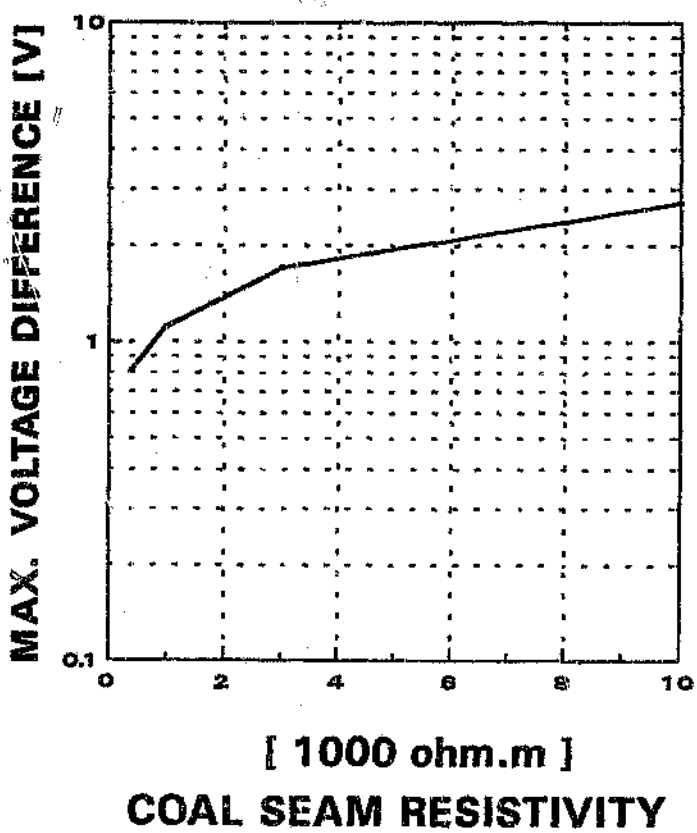



Figure 3.22 The maximum of the diagonal voltage difference ($U_D$) as a function of the resistivity of the coal seam ($\rho_2$).
t = 5 m, d = 30 m, $\rho_1 = \rho_2 = 400$ Ω.m, I = 1 A

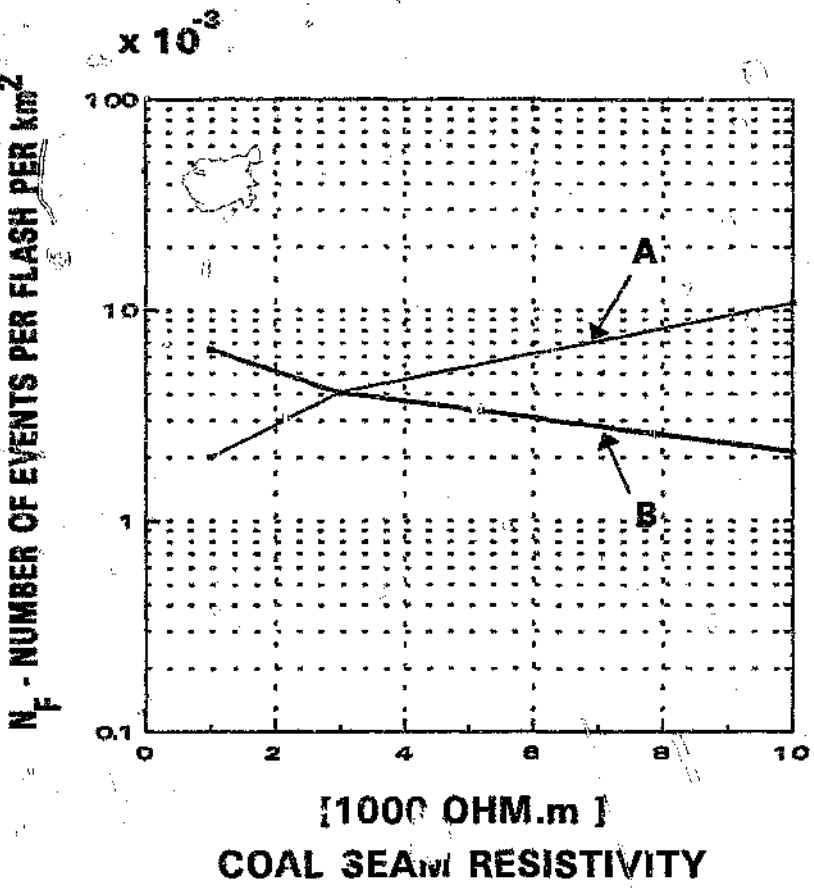



**Figure 3.23** The frequency of surges exceeding the sensitivity of Type 0 detonators as a function of the the resistivity of the coal seam ($\rho_C$).

A : is the frequency of the voltage required to set off a detonator (taken as being 38 kV).

B : is the frequency where the effect of the resistivity of the coal seam on the detonator current is taken in consideration, according to Figure 8.26.

| | | |
|---|---|---|
| t | = | 5 m |
| d | = | 30 m |
| $\rho_1 = \rho_2$ | = | 400 Ω.m |

## The effect of the thickness of the coal seam

The maximum diagonal voltage difference ($U_D$) across the total thickness of the seam is [illegible] Curve B of Figure 3.24. At a practical work face, it is unrealistic to assume that [illegible] thickness of the coal seam will be mined. To compensate for the actual height [illegible] the work face, the voltage across only 2.5 m of the seam was calculated. This is shown by Curve A of Figure 3.24.

The frequency of surges exceeding the sensitivity of Type 0 detonators was calculated. Taking, the voltage across the total seam, this is as shown by Curve B of Figure 3.25. However, it is more realistic to take the voltage across 2.5 m of the seam and the results of this are given by Curve A of Figure 3.25.

It can be argued that thick coal seams have a definite protective benefit. Unlike the variation of resistivity which could occur when drilling into low resistivity layers of the surface or deep strata, where there is a thick coal seam drilling will be into the coal only. This, in turn, may have a high resistivity which will reduce the induced current and will also have the effect of reducing the voltage "divider", as shown in Figure 3.24.

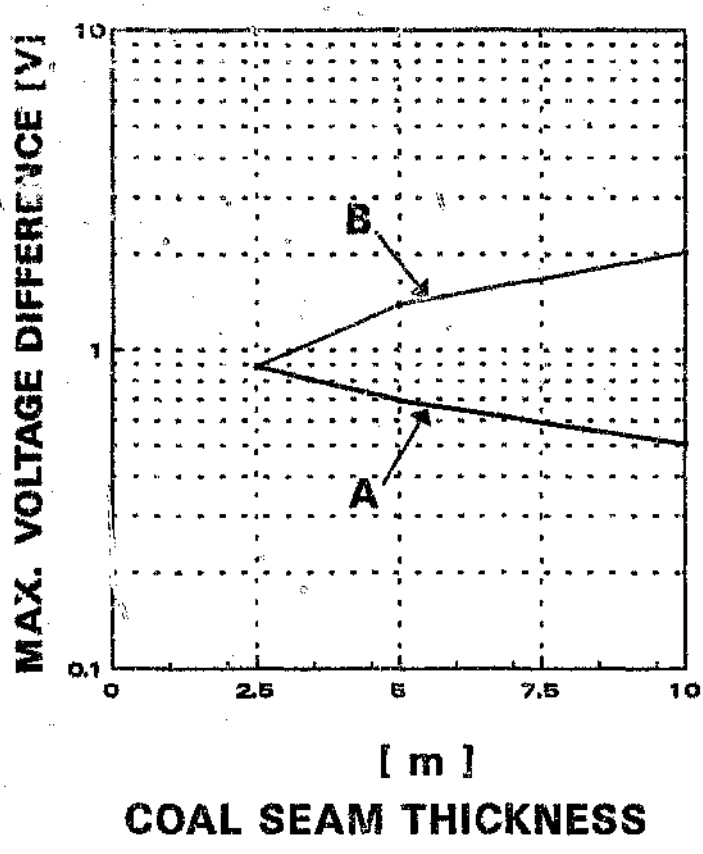



**Figure 3.24** The maximum diagonal voltage difference ($U_D$) for different thicknesses of coal seams (t).

A : the voltage across a 2.5 section of the coal seam
B : the voltage across the total seam
d = 30 m, $\rho_1 = \rho_2 = 400$ Ω.m, I = 1 A
$\rho_c = 3\,000$ Ωm

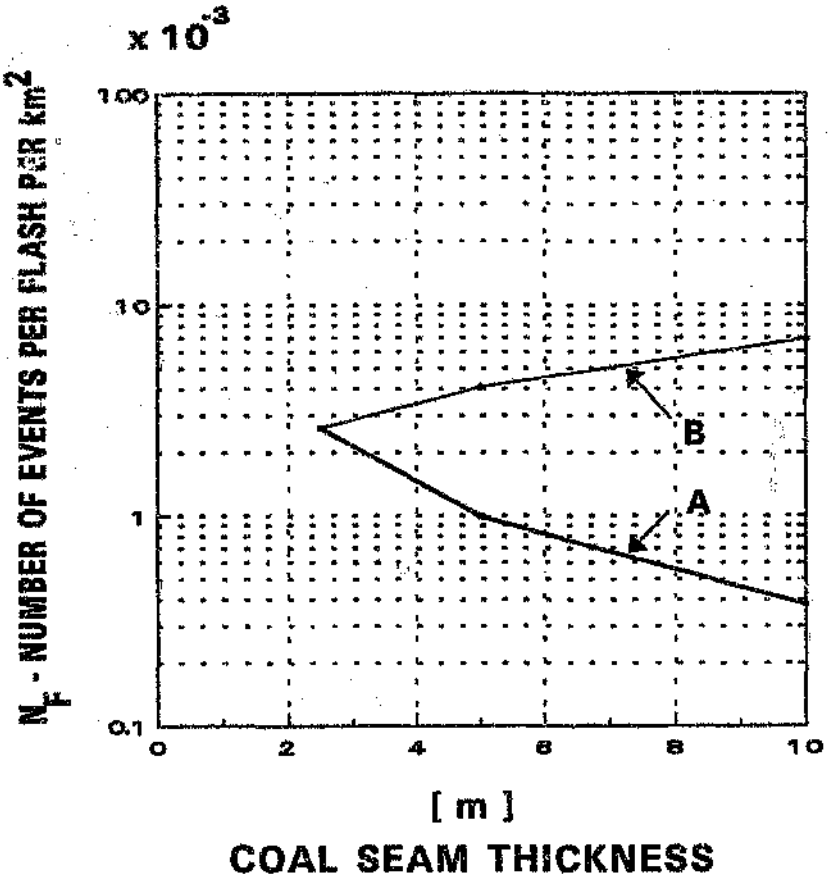



**Figure 3.25** The frequency of surges exceeding the sensitivity of Type 0 detonators as a function of the thickness of the coal seam (t).

A : only the voltage across a typical work face (2.5 m) is taken into account

B : if the voltage across the total thickness of the coal seam is taken into account

d = 30 m; $\rho_1 = \rho_2 = 400$ Ω.m; $\rho_C = 3\,000$ Ω.m

# CHAPTER 4

# THE "ACCURATE" MEASUREMENT OF SURGES UNDERGROUND

## 1 INTRODUCTION

An "accurate" measurement programme was undertaken to study the nature of surges that occur underground between the coal face and the conveyor structure, and the surges in typical detonator-exploder circuits. This measurement programme and the results obtained are described in this chapter.

## 2 HISTORY OF MEASUREMENTS

Surges in mining configurations have been recorded as far back as 1941 by Marshall. To study the problem in collieries in South Africa, the measurement of surges dates back to 1979 (Eriksson 1979, Bourne 1981, and Geldenhuys, August 1982). However, the measurements made then were limited because only the amplitude could be measured of either voltage or current. A proposal was therefore made to the Coal Mine Research Controlling Council to undertake another measurement programme that would be capable of measuring the waveshape of the surges. The proposal was accepted and an "accurate" measuring programme was started in 1985.

## 3 THE RESEARCH STATION

The research station was designed to

- measure the waveshape of surges on a digital storage oscilloscope;
- monitor storm activity and correlate lightning with the occurrence of surges;
- determine the position of strikes on the surface using a simple video-camera arrangement (this was only done in 1988/89).

To perform these functions, it was necessary to have real-time communication between the underground station and the surface recording station.

Two further requirements had to be met:

No electrical conducting wires could be allowed into the experimental set-up at the work face as they would distort the natural occurrence of surges in such circuits.

Because the experimental set-up was in a "fiery" mine, underground equipment had to be intrinsically safe.

To meet all these functions and criteria, the underground recording station was designed around a low-energy consumption, wide-bandwidth, analogue optic-fibre transmitter which could be powered from a NiCad battery for more than one week.

Schematic diagrams of the station layout are shown in Figures 4.1 and 4.2.

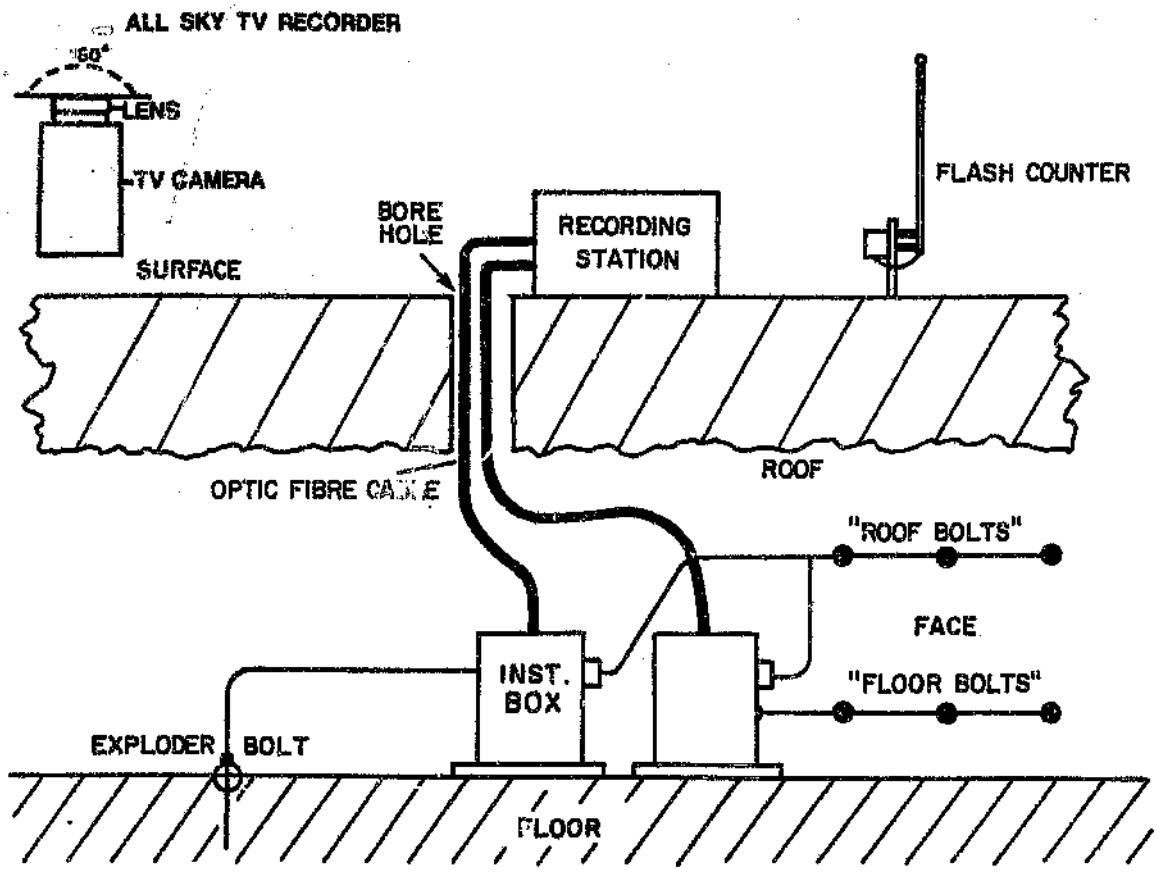



**Figure 4.1** A schematic diagram of the research station showing

- the circuit configuration at the work face
- the instrumentation boxes underground
- the installation at the surface, i.e. the recording station, flash counter and video camera

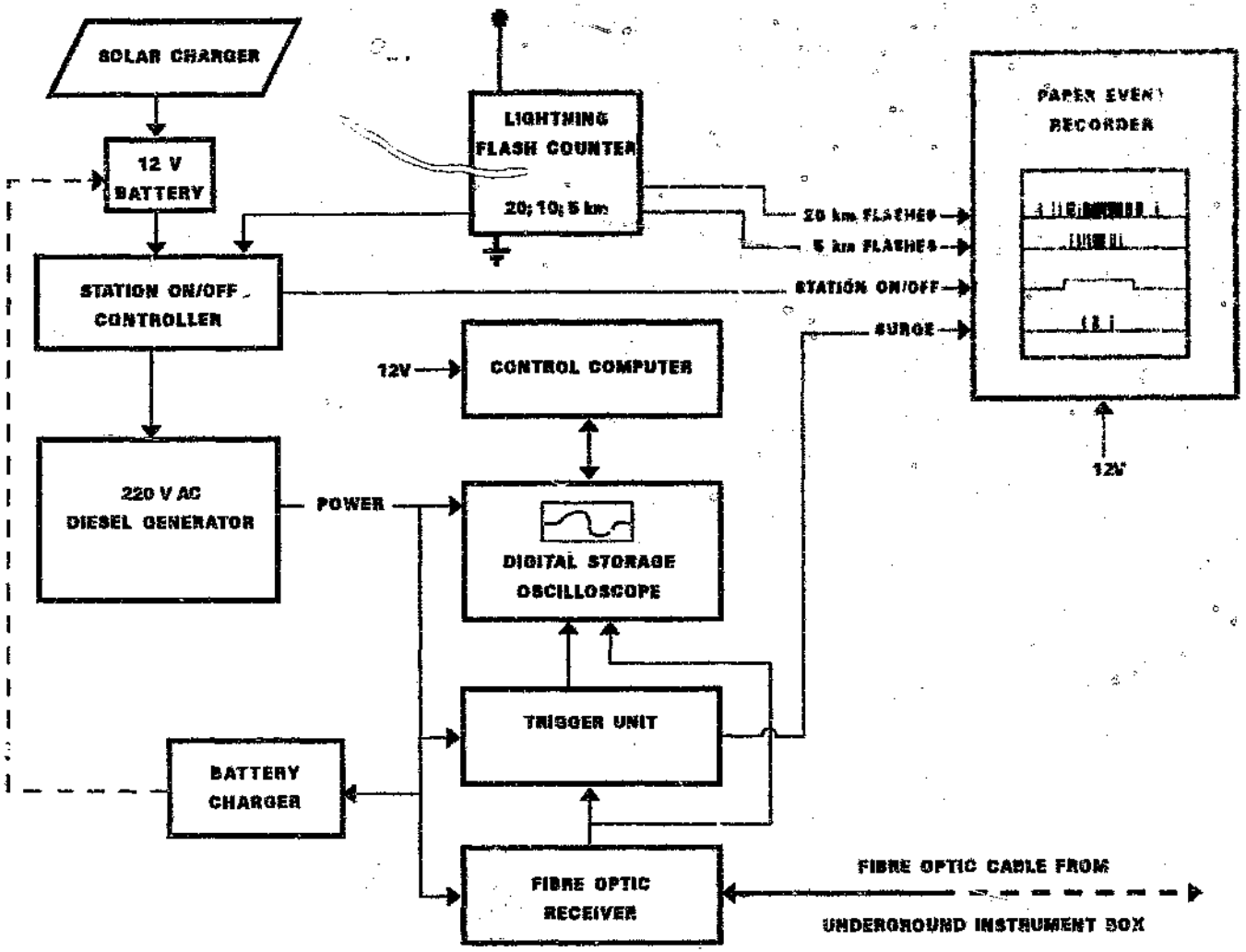



**Figure 4.2** A functional diagram of the surface recording station. Information was recorded by the event recorder (on paper) and by the digital storage oscilloscope in a bubble memory.

### 3.1 The underground station

A work face was constructed to be similar to that normally used in an explosives-blasting configuration (see figure 4.1) with a row of roof bolts near the roof of the face. The [illegible] represented by roof bolts having a length of 1.8 m. These roof bolts were [illegible] and, at the installation in Greenside Colliery, they were connected to [illegible] transmission boxes or an "exploder bolt" (which represented an exploder at a distance away from the point at which a miner would set off the charge). A second circuit was completed between a set of bolts close to the roof and a set of bolts close to the floor of the working face. This arrangement allowed current to flow vertically down the face and diagonally towards the exploder point. The various configurations that were used are shown in Figure 4.3.

The underground measuring unit could measure either open circuit voltage (10 MΩ input impedance voltage dividers) or short-circuit current (1 Ω shunts). Initially, only one unit was available (before February 1987).

A second unit was installed at the beginning of April 1987, making it possible to record two measurements simultaneously.

The output voltage of the voltage dividers (or current shunts) were fed into optic-fibre transmitters which converted the voltage signal into an optic signal and transmitted it to the surface (which could have been up to 200 m away).

The optic-fibre transmitter/receiver had a bandwidth of 20 Hz to 3 MHz, a gain of about 0.5 and a maximum input voltage of approximately 2 V. The underground units were battery-driven and had sufficient capacity to operate for a period of about nine days. The underground units were always switched on and the batteries were changed once a week. The equipment was intrinsically safe and the batteries were housed in flameproof enclosures so that they could be used in fiery mines.

### 3.2 The surface station

A schematic diagram of the surface station is shown in Figure 4.2.

The surface data-recording station performed the following functions:

- Monitoring lightning activity in the vicinity (using a lightning-flash counter)

- Recording the signals transmitted from the underground units, using a digital storage oscilloscope.

### 3.2.1 Power to the surface station

The power to the surface station was derived from two systems:

- A 12 V DC battery, used continuously for driving the chart recorder, the station controller and the oscilloscope controller. The battery was charged by a solar charger and by a diesel generator when the station was switched on.
- A 220 V AC diesel generator. This was switched on during storms and supplied the bulk power required for the oscilloscope and the TV recorder. This generator also boost-charged the battery.

### 3.2.2 Control of the surface station

The surface station was controlled by a station controller. The lightning flash counter (which had a radius of 20 km) was fed into the controller. As soon as a storm was detected in the vicinity of the station, the station controller switched the diesel generator on and kept it running until the storm had moved outside the range of the counter. The 220 V generator activated the oscilloscope controller and the oscilloscope.

### 3.2.3 Recording at the surface station

Four different recorders operated at the surface station:

- The event recorder was a simple paper-pen recorder which could be time-correlated. It recorded the lightning flashes that occurred at distances of 20 km and 5 km. It also recorded the on/off status and the times that surges were triggered.

- The controller of the oscilloscope and computer also functioned as a data logger. The switch-on and switch-off times of the station were recorded and the times that the oscilloscope were triggered could be printed by the computer printer.

- The oscilloscope recorded the signals received from underground and could store up to 21 triggered events in its bubble memory.

- A TV recorder which had a 360° view of the area was added to the system later. The sound of the thunder was also recorded to enable the location of a flash to be determined by means of the direction of the flash and the time-to-thunder. This system only operated successfully during the night.

# 4 LOCATIONS AND CONFIGURATIONS OF THE RESEARCH STATIONS

Research stations were located and operated at the following collieries:

| | |
|---|---|
| Landau Colliery | - for two months (6/3/86 to 25/4/86) |
| Springbok Colliery | - for two lightning seasons (2/10/86 to 29/2/88) |
| Greenside Colliery | - for one lightning season (10/3/88 to 30/4/89) |

Detailed CSIR reports were compiled giving the results of the research (Geldenhuys et al, 1986; Geldenhuys and Ballard, Jan. 1988; Ballard and Geldenhuys, 1988; Lagesse et al, 1989).

Different configurations were used during the three-year period. These are shown in Figure 4.3. Note that both voltage and current were measured.

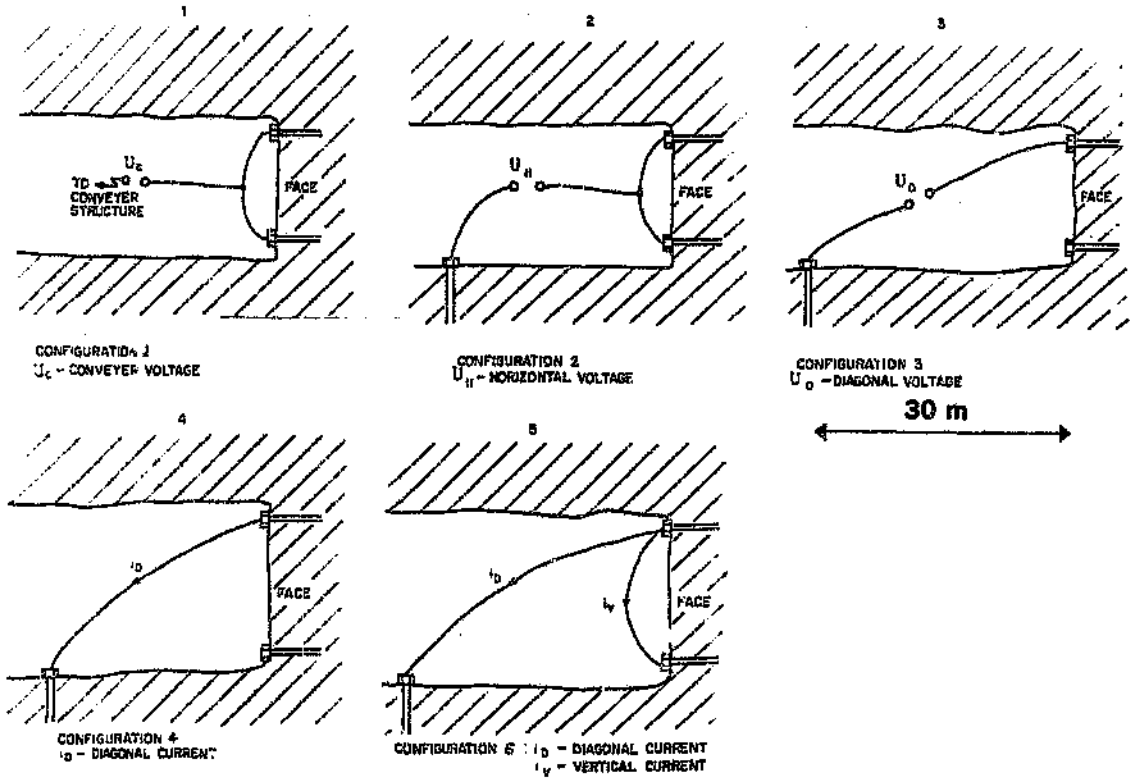



**Figure 4.3** Measuring circuit configurations used in the research programme

The configurations used at various locations in the mines are given in Tables 4.2, 4.3, 4.5, 4.7 and 4.9.

The installation at Landau Colliery operated for a very short period only and, for this reason, will not be discussed in much detail. The installation at Landau was at a depth of approximately 52 m in a coal-seam of about 3 m thick.

## 4.3 Installation at Springbok Colliery

The layout underground at Springbok Colliery is shown in Figure 4.4. More details about the area and the mine are contained in Appendix I.

The Springbok underground installation was at a depth of 46 m. The seam being mined was the No. 2 seam which had a thickness of 3 m. As can be seen from Figure 4.5, the No. 2 seam lies below seams numbered 3, 4 and 4a. The combined thickness of these seams above the No. 2 seam was 3.7 m. There are no high-resistivity strata layers of volcanic rock above the measuring site.

Two earth resistivity measurements were made at Springbok. The results are shown in Figure 4.6 where it can be seen that the surface resistivity (top 10 m - 20 m) is about 400 Ω.m to 500 Ω.m. The resistivity of the deeper strata is much higher, but impossible to quantify exactly.

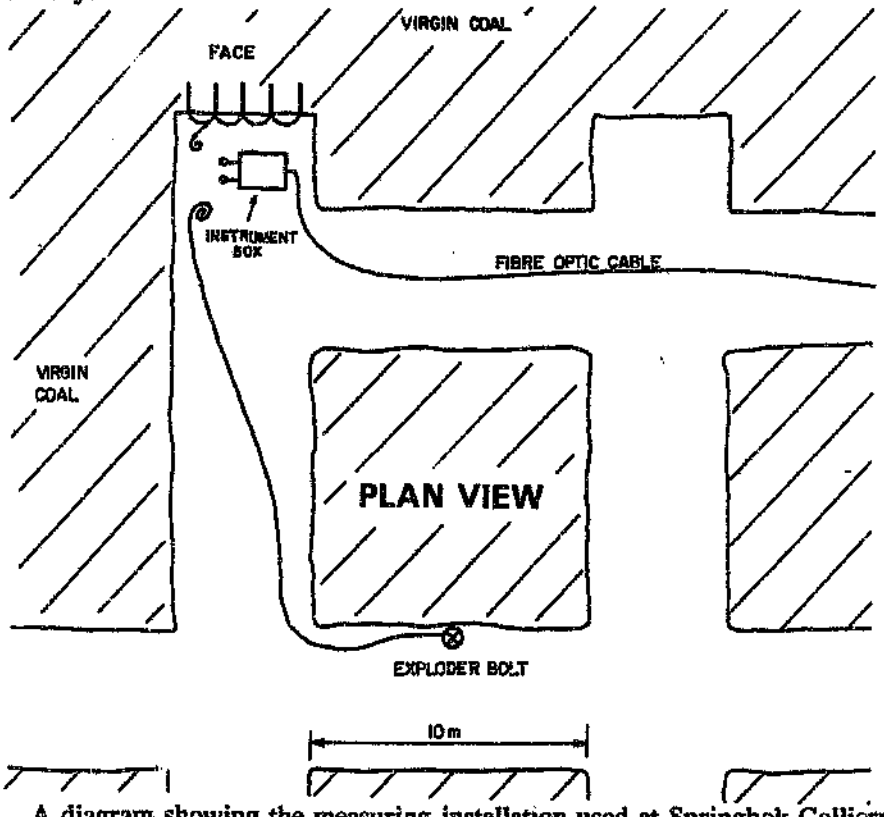



**Figure 4.4** A diagram showing the measuring installation used at Springbok Colliery. This shows the layout with only one instrument box.

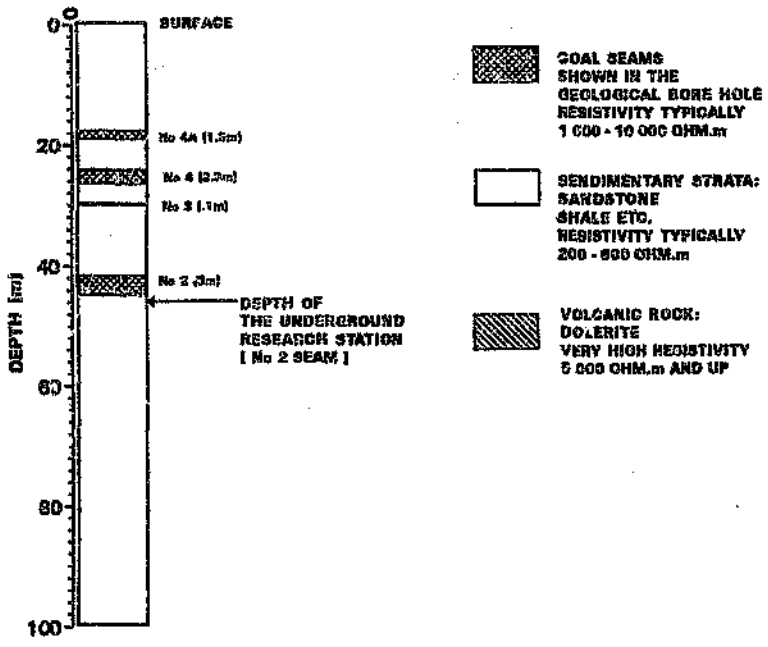



**Figure 4.5** The strata at Springbok Colliery (taken from Geological Borehole No. 226). At the actual research station, the depth of the No. 2 seam is 46 m. The coal seams are bordered by sedimentary layers.

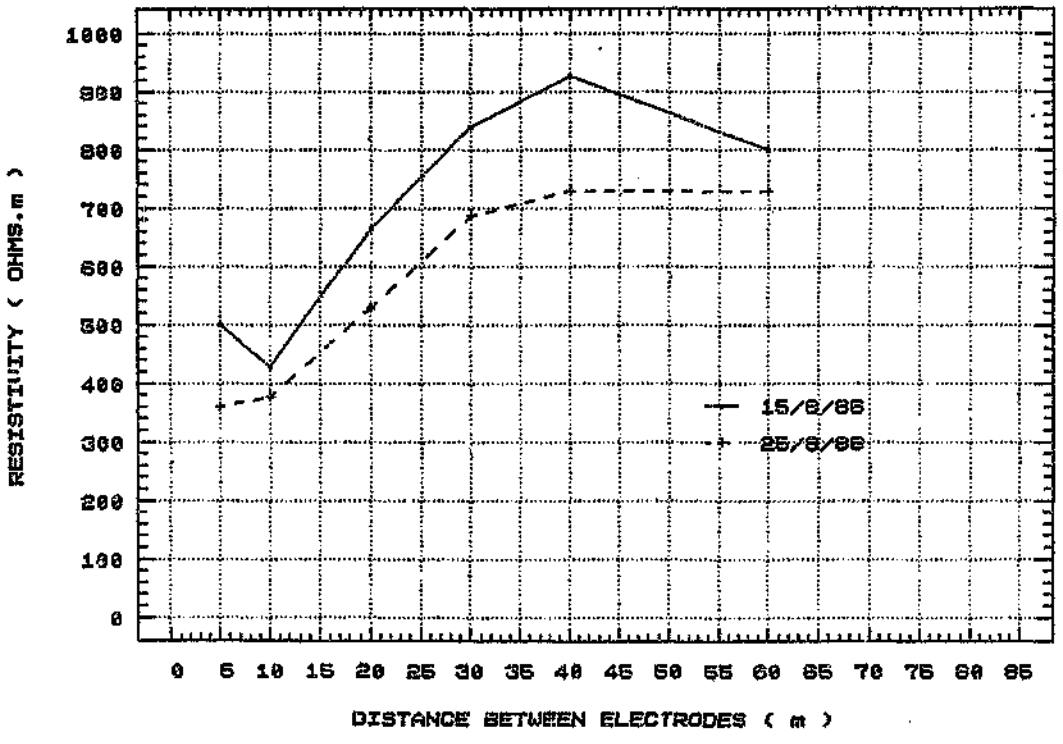



**Figure 4.6** Earth resistivity measurements made, using the Venner method, at the research station in Springbok Colliery for the period that the station operated.

## 4.2 Installation at Greenside Colliery

The layout underground at Greenside Colliery is shown in Figure 4.7. More details about the area and the mine are contained in appendix II.

This underground installation at Greenside colliery was at a depth of 23 m. The seam being mined was the No. 5 seam. It can be seen from Figure 4.8 that the No. 5 seam is the top seam and that it has a thickness of 2 m. There are no high-resistivity strata layers of volcanic rock over the measuring site.

Several earth resistivity measurements were taken at Greenside at different times through the seasonal cycle. The results are given in Figure 4.9. The surface resistivity varied between 300 Ω.m and 450 Ω.m. The deeper strata have much higher resistivities which are impossible to quantify exactly.

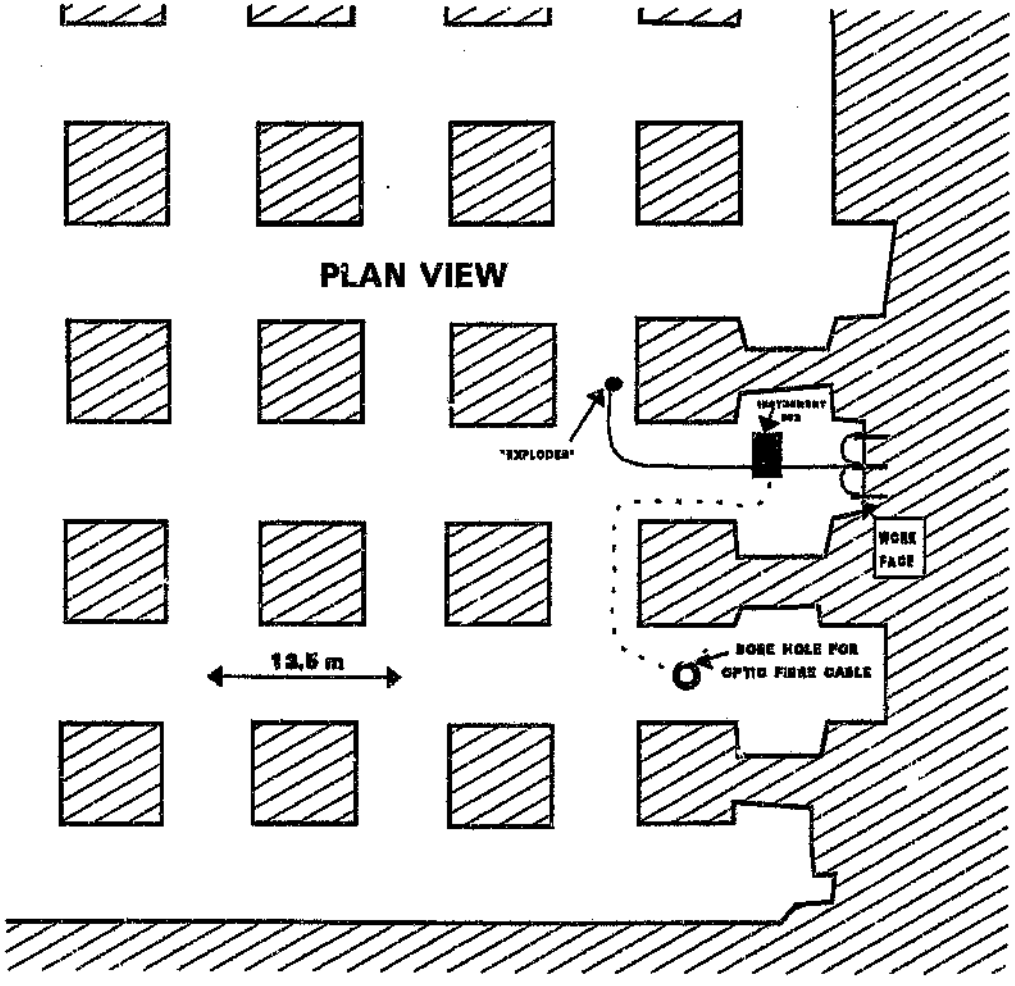



**Figure 4.7** The underground research station at Greenside Colliery. A special borehole was drilled for the optic-fibre cable between the installation and the surface.

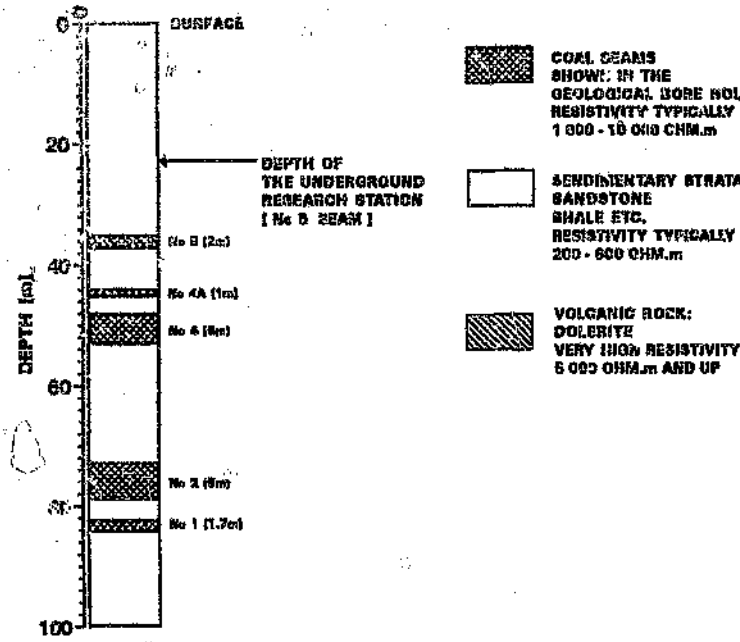



**Figure 4.8** The strata at Greenside Colliery (from Geological Borehole Sample No. BH1). The depth of the research station is 23 m and it was the No. 5 seam that was being mined. The coal seams are bordered by sedimentary layers.

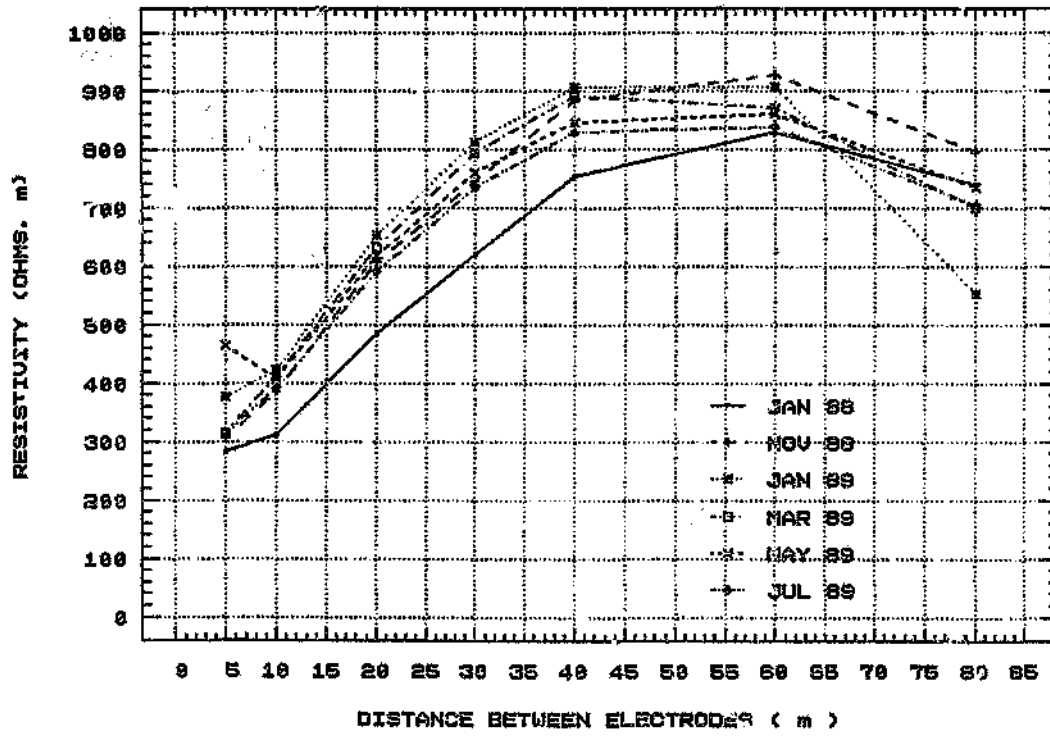



**Figure 4.9** Earth resistivity measurements above the research station at Greenside Colliery, taken at various times during the period that the research station was operated at this site (Jan. 1986 to July 1989)

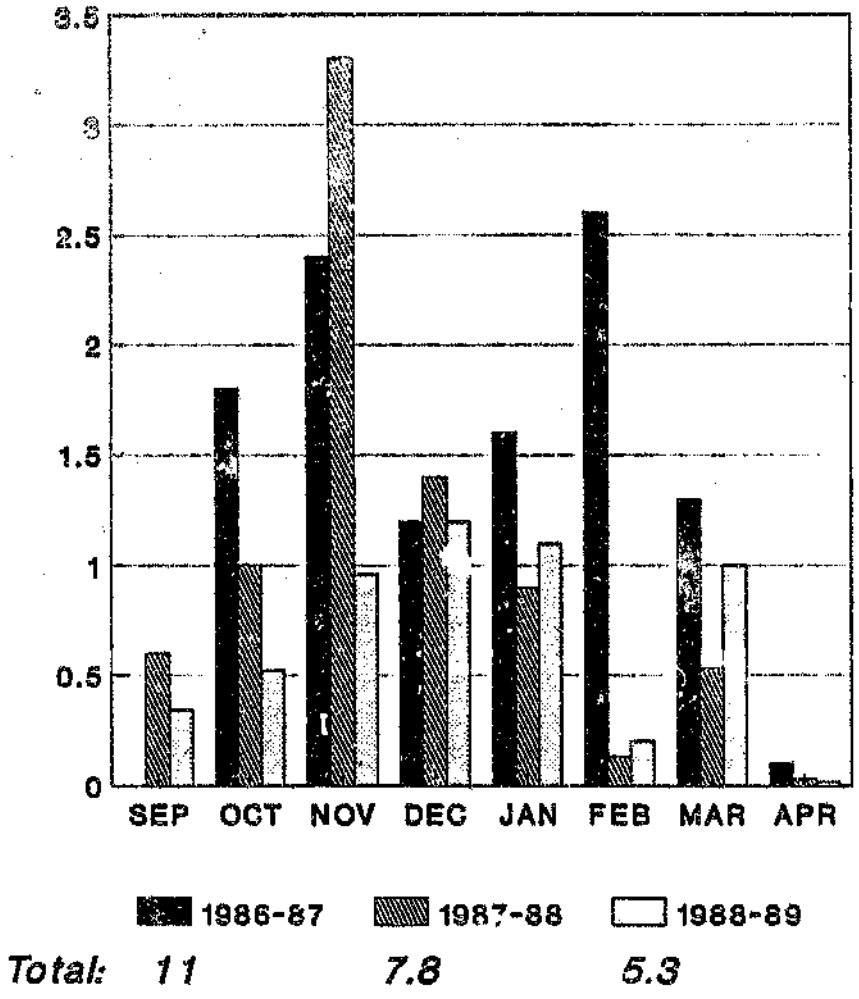



**Figure 4.10** Monthly and total seasonal lightning flash density at the recording station for 1986/87, 1987/88 and 1988/89.

## 5 RESULTS OBTAINED FROM THE MEASUREMENT PROGRAMME

The lightning flash density varied greatly during the three seasons. The lightning flash density (monthly and seasonal) recorded at the station is shown in Figure 4.10. It can be seen that the lightning activity was quite high in 1986/87, but, unfortunately, in 1988/89 it was quite low.

The results obtained are analysed in the following paragraphs in groups of the specific configurations that were employed.

## 5.1 Results from Configuration 1

Configuration 1 (Figure 4.3) was the first configuration installed at Landau Colliery following previous surge-counter installations that had been done in this fashion.

This configuration bonds directly to the conveyor structure. This will enhance surges originating from the conveyor structure. The surges recorded at Springbok Colliery in Configuration 1 are shown in Tables 4.1 and 4.2.

Many surges with amplitudes larger than 100 V were observed in this configuration: 133 surges per flash per km$^2$. However, the highest amplitude was only 773 V. These are regarded as quite small surges.

All the surges were of positive polarity. This implies that the conveyor structure is negative relative to the roof bolts in the coal face which is positive. This observation supports the theoretical expectation that lightning surges are "picked up" by the underground structure and then travel towards the coal face in question. However, none of them are suspected to have been lightning strikes to, or close to, the shaft entrance.

Typical waveshapes of the surges recorded in Configuration 1 are shown in Appendix III.

Table 4.1 Surges recorded at Springbok Colliery in Configuration 1

| Date | Log Sheets | Time | Peak I or V | Surges | Flash density |
|---|---|---|---|---|---|
| 11/3/86 | 7 | 15:30 | | 2 | .16 |
| 12/3/86 | 7 | 14:00 | ≈ 300 V | 1 | |
| 12/3/86 | 7 | 21:00-22:00 | | 5 | |
| 13/3/86 | 10 | 07:11 | + 136 V | 1 | .05 |
| | | | + 106 V | 1 | |
| | | | + 151 V | 1 | |
| | | | + 121 V | 1 | |
| | | | + 197 V | 1 | |
| | | | + 227 V | 1 | |
| | | | + 227 V | 1 | |
| | | | + 136 V | 1 | |
| | | | + 106 V | 1 | |
| | | | + 106 V | 1 | |
| | | | + 151 V | 1 | |
| | | | + 106 V | 1 | |
| | | | + 106 V | 1 | |
| | | | + 773 V | 1 | |
| | | | + 227 V | 1 | |
| | | | + 90 V | 1 | |
| | | | + 197 V | 1 | |
| | | | + 212 V | 1 | |
| | | | + 409 V | 1 | |
| | | | + 151 V | 1 | |
| Total | | | | 28 | .21 |

**Table 4.2** Summary of the surges recorded in Configuration 1.

| Period | Trigger level | No. of surges | Flash density | No. of surges/ Flash density |
|---|---|---|---|---|
| 6/3/86 - 25/4/86 at Landau Colliery | 100 V | 28 | 0.2 | 133 |

## 5.2 Results from Configuration 2

The underground mining operation in Landau Colliery was closed down in 1986. This meant that the experimental installation had to be moved to Springbok Colliery where incidents of lightning had also occurred.

The first configuration installed in Springbok was Configuration 2. It can be seen from Table 4.3 (in comparison to Table 4.2) that the frequency with which surges occurred in this configuration was very low. No surges were recorded in a reasonably significant period ($N_g$ = .51). This could have been because the short-circuit across the top and bottom of the work face could effectively also short-circuit the potential between the bottom of the face and the exploder point. If the various resistivities around the coal seam are taken into consideration, this explanation is feasible.

**Table 4.3** Summary of the surges recorded in Configuration 2.

| Period | Trigger level | No. of surges | Flash density | No. of surges/ Flash density |
|---|---|---|---|---|
| 2/10/86 - 9/11/86 Springbok Colliery | 100 V | 0 | 0.51 | < 1.96 |

## 5.3 Results from Configuration 3

In the light of the fact that no (or very few) surges were observed in Configuration 2, the installation at Springbok was changed to Configuration 3, i.e. the "vertical short-circuit" was disconnected.

Changing the configuration immediately had a huge effect. A large number of surges of relatively low magnitude were recorded. The results are shown in Table 4.4. Some of the waveshapes recorded are given in Appendix IV. The frequency with which surges occurred is summarised in Table 4.5.

**Table 4.4** Surges recorded at Springbok Colliery in Configuration 3

| Date | Log Sheets | Time | Peak I or V | Surges | Flash density |
|---|---|---|---|---|---|
| 15/11/86 | 26 | 18:00 - 21:00<br>14:00 - 15:30<br>18:00 - 20:00 | | 33<br>5<br>13 | .76 |
| 19/11/86 | 26B | 21:00 | | 61 | 1.1 |
| 20/11/86 | 27 | 15:15 | | 2 | .06 |
| 23/11/86 | 28 | 08:55<br>16:15 | | 1<br>1 | .43 |
| 27/11/86 | 29 | 01:00 - 02:00 | | 10 | .04 |
| 1/12/86 | 30<br>30<br>31 | 12:06<br>12:59<br>18:15 | | 26<br>9<br>62 | .01<br><br>.13 |
| 2/12/86 | 31 | | | 262 | |
| Some of the voltages of the surges are | | | | | |
| | 31 | 18:04<br>18:05<br>18:06<br>18:06:32<br>18:07<br>18:07:32<br>18:07:50<br>18:08<br>18:09<br>18:09:30<br>18:10 | 1 417 V<br>1 166 V<br>1 082 V<br>1 333 V<br>1 333 V<br>1 082 V<br>750 V<br>1 249 V<br>834 V<br>- 667 V<br>1 247 V | 1<br>1<br>1<br>1<br>1<br>1<br>1<br>1<br>1<br>1<br>1 | |
| 2/12/86 | 31 | 19:03<br>19:04<br>19:04:41<br>19:04:59<br>19:05<br>19:05:33<br>19:06<br>19:07 | 1 748 V<br>1 584 V<br>1 668 V<br>1 082 V<br>1 417 V<br>1 333 V<br>- 918 V<br>1 417 V | 1<br>1<br>1<br>1<br>1<br>1<br>1<br>1 | |
| 9/12/86 | 34 | 15:47<br>17:00 | | 2<br>6 | .08 |
| 19/12/86 | 38 | 13:45<br>14:25 | | 1<br>1 | .02 |

Table 4.5 Summary of the surges recorded in Configuration 3.

| Period | Trigger level | No. of surges | Flash density | No. of surges/ Flash density |
|---|---|---|---|---|
| 10/11/86 - 29/12/86 Springbok Colliery | 100 V | 582 | 2.8 | 208 |
| | 500 V | 8 | 1.15 | 7 |
| | 900 V | 0 | 0.27 | < 4 |

The voltage measured in Configuration 3 represents the voltage that drives the current diagonally in a typical detonator installation.

The storm records and surge data were carefully analysed. From the analysis, the following was observed:

- Surges can only be recorded during the period that the station is switched on during a storm.
- There was a very poor correlation between the lightning strikes recorded on the 20 km flash counter at the time of the surge.
- The magnitudes of the surges were all very similar and did not display the typical stochastic variation of lightning.
- The amplitudes of the surges (± 1 000 V) are relatively insignificant relative to the amplitude required to set off detonators.

For these reasons, not much significance is placed on the surges recorded in Configuration 3. With reference to Appendix IV, it can be noted that the waveshapes display the typical characteristics of surges on transmission lines, i.e. with positive and negative reflections. The durations are generally much shorter than those of a typical lightning current waveshape. This is possibly due to reflection effects. Generally, the appearance of the surges indicate that they did originate from lightning strikes.

No significant surges were recorded in Configuration 3.

## 5.4 Results from Configuration 4

To study the current that can be induced into a detonator circuit, the installation at Springbok was changed to Configuration 4.

The recordings made in Configuration 4 are listed in Table 4.6. The results are summarised in Table 4.7.

The biggest surge observed in Configuration 4 was a pulse of -3.3 A (estimated as it was an obscure reading). Some of the oscillographic records of Configuration 4 can be found in Appendix V.

Table 4.6 Surges recorded at Springbok Colliery in Configuration 4

| Date | Log Sheets | Time | Peak I | Surges | Flash density |
|---|---|---|---|---|---|
| 12/1/87 | 46 | 19:04 | | 1 | .24 |
| 15/1/87 | | 11:58 | | 1 | |
| 19/1/87 | 48 | 16:45 | | 16 | .17 |
| 21/1/87 | 49 | 16:38 | | 1 | .12 |
| 23/1/87 | 50 | 24:26 | | 3 | .44 |
| 25/1/87 | 50 | 18:19 | - 3.3 A | 5 | |
| 1/2/87 | 52 | 18:18<br><br><br><br>18:28 | + 360 mA<br>+ 418 mA<br>+ 57 mA<br>+ 86 mA | 1<br>1<br>1<br>1 | .52 |
| 4/2/87 | 54 | 13:57 | | 1 | .06 |

Table 4.7 Summary of the surges recorded in Configuration 4

| Period | Trigger level | No. of surges | Flash density | No. of surges/ Flash density |
|---|---|---|---|---|
| 5/1/87 - 4/2/87<br>Springbok Colliery | 0.1 A<br>1.0 A | 35<br>2 | 1.95<br>2.62 | 18<br>38 |

## 5.5 Results from Configuration 5

### 5.5.1 Results from Springbok Colliery

It was realised that two optic-fibre transducers would allow the study of both the diagonal and the vertical current induced in the work face. For this reason a second unit was constructed and installed in Springbok Colliery in February 1987.

The surges recorded at Springbok Colliery in Configuration 5 are listed in Table 4.8. The

atistical results are summarised in Table 4.9.

Table 4.8 Surges recorded at Springbok Colliery in Configuration 5

| Date | Log Sheets | Time | Peak Current | | Surges |
|---|---|---|---|---|---|
| | | | $I_p$ | $I_v$ | |
| 10/2/87 | 56 | | | | 1 |
| 14/2/87 | 57 | | | | 2 |
| 26/2/87 | 60 | | - 1.04 A<br>+ 0.11 A<br>+ 0.49 A<br>- 0.12 A | 0 A<br>0 A<br>0 A<br>0 A | 5 |
| 27/2/87 | 61 | | - 0.29 A | - 0.14 A | 1 |
| 7/3/87 | 63 | | | | 1 |
| 8/3/87 | 63 | | + 0.82 A<br>- 0.24 A | + 0.38 A<br>+ 0.04 A | 2 |
| 17/3/87 | 66 | | + 0.18 A | 0 A | 2 |
| 21/3/87 | 67 | | | | 1 |
| 87/88 Season | | | | | |
| 28/10/87 | 13 | 02:39 | + 0.44 A | 0 A | 1 |
| 29/10/87 | 14 | | - 0.68 A | 0 A | 1 |
| 10/11/87 | 17 | 12:46<br>12:51 | + 0.11 A<br>+ 0.13 A | 0 A | 2 |
| 17/11/87 | 19 | | - 0.28 A<br>- 0.21 A<br>+ 0.28 A<br>- 0.21 A | 0 A | 4 |
| 24/11/87 | 21 | 18:56 | | - 0.10 A | 1 |
| 3/12/87 | 23 | 17.03 | + 0.34 A<br>- 0.29 A | 0 A<br>0 A | 2 |
| 26/12/87 | 28 | | + 0.18 A | + 0.10 A | 1 |
| 14/1/88 | | | - 0.10 A | - 0.02 A | 1 |

*A = Diagonal current $I_D$
*B = Vertical current $I_v$

Table 4.9 Summary of the surges recorded in Configuration 5

| Period | Surge level | No. of surges | Flash density | No. of surges/ Flash density |
|---|---|---|---|---|
| 10/2/87 to 29/2/87 | 0.1 A<br>0.3 A<br>1 A | 28<br>5<br>0 | 9.2 | 3.04<br>0.54<br>< 0.10 |

Some of the oscillographic records of Configuration 5 at Springbok Colliery are attached as Appendix VI.

### 5.5.2 Results from Greenside Colliery

An opinion was expressed that, due to the depth of the coal seam and because of the overhead coal seams at Springbok Colliery, this site was not a particularly exposed site where many surges could be expected. This opinion was strengthened by the low number of significant surges that were recorded at Springbok Colliery. For this reason, the research station was moved to Greenside Colliery, to a much shallower depth (23 m) with no overlying coal seams.

The surges recorded at Greenside Colliery are listed in Table 4.10.

**Table 4.10** Surges recorded at Greenside Colliery in Configuration 5 during the 1988/89 season (continued on the next page)

| Date | Log Sheets | Time | Peak Current | | Surges |
|---|---|---|---|---|---|
| | | | $I_p$ | $I_v$ | |
| 31/8/88 | 1 | 17:29 | - 2.98 A | + 0.14 A | 1 |
| 12/11/88 | 15 | 19:23 | + 0.61 A | 0 A | 1 |
| 28/11/88 | 17 | 18:15 | + 2.80 A | 0 A | 1 |
| 16/12/88 | 21 | 20:58 | NA | | 1 |
| 14/3/89 | 39 | 20:45 | 10-20 A | NA | 1 |

| Date | Log Sheets | Time | Peak Current | | Surges |
|---|---|---|---|---|---|
| | | | $I_f$ | $I_v$ | |
| 25/3/89 | 41 | 16:20 | NA | NA | 8 |
| | | 16:25 | NA | NA | |
| | | 16:28 | NA | NA | |
| | | 16:35 | NA | NA | |
| | | 16:39 | NA | NA | |
| | | 16:58 | NA | NA | |
| | | 17:13 | NA | NA | |
| | | 17:24 | NA | NA | |

The statistical results are summarised in Table 4.11. Some of the oscillographic records are given in Appendix VI.

**Table 4.11** Statistical summary of the surges recorded in Configuration 5 at Greenside Colliery

| Date | Surge level | No. of surges | Flash density $N_g$ | Frequency No. of surges/$N_g$ |
|---|---|---|---|---|
| 10/3/88 to 30/4/89 | 0.6 A | 13 | 5.4 | 2.40 |
| | 1 A | 4 | | 0.74 |

# 6 A COMPARISON BETWEEN THE RESULTS FROM GREENSIDE COLLIERY AND THE SIMPLE SPHERICAL MODEL

With the aid of a video camera and by measuring the "time to thunder", the position of three of the bigger surges at Greenside Colliery could be plotted relative to the station. These results are given in Figure 4.11.

The oscillographic waveshapes of two of the surges are shown in Figure 4.11 and Figure 4.12.

Table 4.12 summarises the data pertaining to the three flashes that were captured by the video camera.

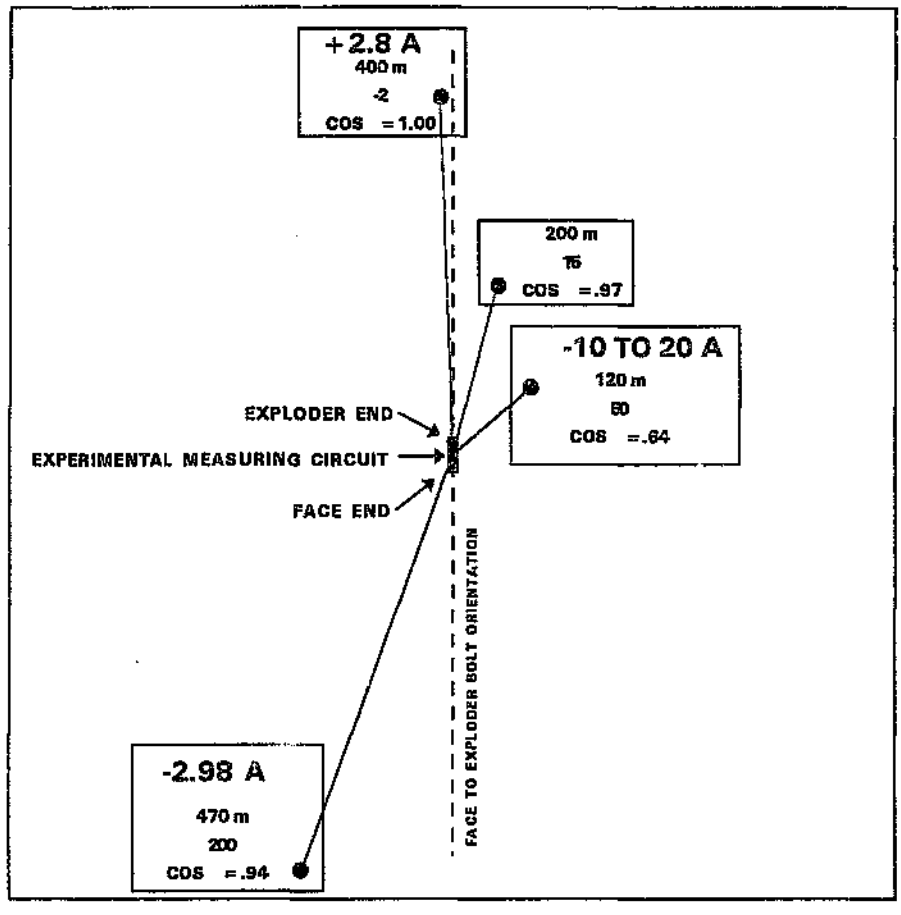


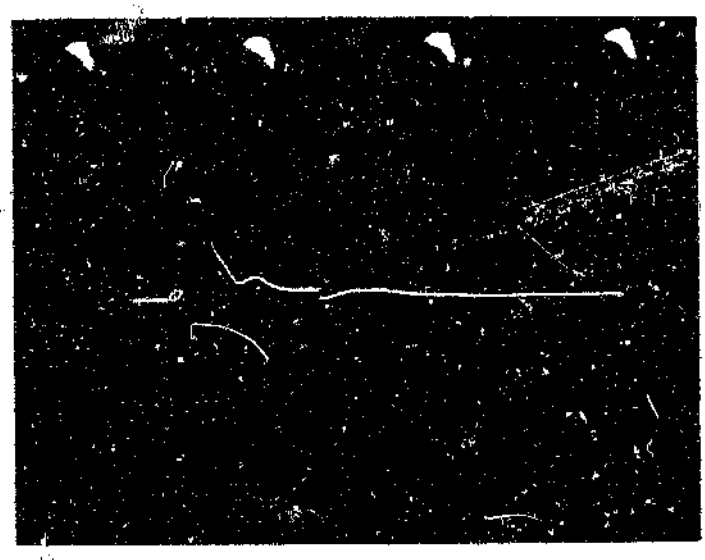

**Figure 4.11** The position and amplitude of the surges relative to the Greenside Research Station



$I_{peak}$ =-2.98 A

400 $\mu$s sweep

**Figure 4.12** The waveshape of the surge of 31/8/88 (see Table 4.12)



$I_{peak}$ = +2.80 A

400 $\mu$s sweep

**Figure 4.13** The waveshape of the surge of 28/11/88 (see Table 4.12)

Equation 4.1 derived from the simple spherical model can be rewritten as:

$$I_L = I_F \times 2\pi\ (d^2 + r^2)\ \cos\theta\ /\ 15 \quad \ldots\ldots 4.1$$

From the data we have: $I_F$, d, r and $\Theta$ are known and we can calculate $I_L$ from the equation. This will then derive the original lightning current that induced the surge in the first place.

This was done and the result is given in Table 4.12 as the equivalent lightning current.

**Table 4.12** Data for the three flashes

| Date | 31/8/89 | 28/11/89 | 14/3/89 |
|---|---|---|---|
| Peak current (A) | 2.98 | 2.80 | 15.00 |
| Seam depth (m) | 23 | 23 | 23 |
| Flash distance from the face (m) | 500 | 340 | 140 |
| Angle-to-face direction | 200 ° | - 2 ° | 50 ° |
| Cos $\theta$ | 0.94 | 1.00 | 0.64 |
| Equivalent lightning current (kA) | 294.00 | 136.00 | 92.60 |

The average value of the equivalent lightning current is 174.2 kA. This value is much higher than the median value for South Africa reported by Geldenhuys et al (Sept 1989).

If we assume that the three flashes represent the average lightning flash, we can calculate the ratio between the average South African distribution and the calculated average.

Ratio = 174.2 kA/45 kA = ± 4 times

This means that the factor 15 used in Equation 4.1 should actually be 60. The coupling in this particular case is therefore much more effective than the 15 m² used in Chapter 2. It was also shown by the Fuse Surge Detector (FSD) Programme (Chapter 5) that particularly high surge frequencies were recorded at Greenside.

# 7 GENERAL DISCUSSION OF RESULTS

## 7.1 The induction mechanism

The experimental configurations were mainly designed to observe phenomena associated with the mechanism where conduction takes place through the strata. From the results obtained, it is clear that this mechanism produces currents and voltages that are capable of setting off detonators and methane explosions.

The waveshapes observed often indicate that they are of the "reflection" type which indicate complex interactions between the underground strata and the conductors in the vicinity.

The observations reported in Figure 4.12 further confirm the conduction mechanism: the polarity difference between the results of 31/8/88 and 28/11/88 are exactly what are expected from the conduction mechanism.

## 7.2 Vertical and horizontal voltage gradient

From the results, it can be seen that very few current surges were observed in the vertical configuration compared to the number and amplitude of those in the diagonal configuration. This result is in line with the modelling results of Chapter 3 and suggest that the insulation effect of the coal layer is not prominent when the distance from the flash exceeds 200 m.

# CHAPTER 5

# THE FUSE SURGE DETECTOR (FSD) MEASURING PROGRAMME

## 1 INTRODUCTION

The accurate measurement programme gave results on the waveshape of surges and the mechanism through which surges occur in typical coal faces. To obtain a larger statistical picture of the phenomena, an alternative method of simultaneous measurements in many places had to be developed.

To do this, a simple and cheap device was developed, called the Fuse Surge Detector (FSD). The presence of a surge is detected by the fact that a fuse has blown.

## 2 THE OBJECTIVES OF THE FSD PROGRAMME

When the decision was taken to embark on the FSD programme, it was aimed at

- Reinforcing the simple model developed by Geldenhuys (1987), in particular, to see whether the asymptotic behaviour predicted by the model was observed. Another objective was to see whether a "maximum" asymptote was observed and to "calibrate" this model and any future models to be developed.

- Reinforcing the statistical chance of a lightning-induced surge occurring.

- Establishing the reduction in risk arising from changes in detonator sensitivity, e.g. between a detonator with a sensitivity of 8 A, 1/50 $\mu$s (Type 0) and a detonator with a sensitivity of 42 A, 1/50 $\mu$s (Type 1).

## 3 THE CONSTRUCTION AND DESIGN OF THE FSD

The physical construction of the FSD (Model 1) is shown in Figure 5.1

### 3.1 Sensitivity of the FSD

Different sensitivity levels are built into the FSD by connecting a group of fuses in series with different fusing levels. The magnitude of a surge is indicated by the highest rated fuse blown by the surg

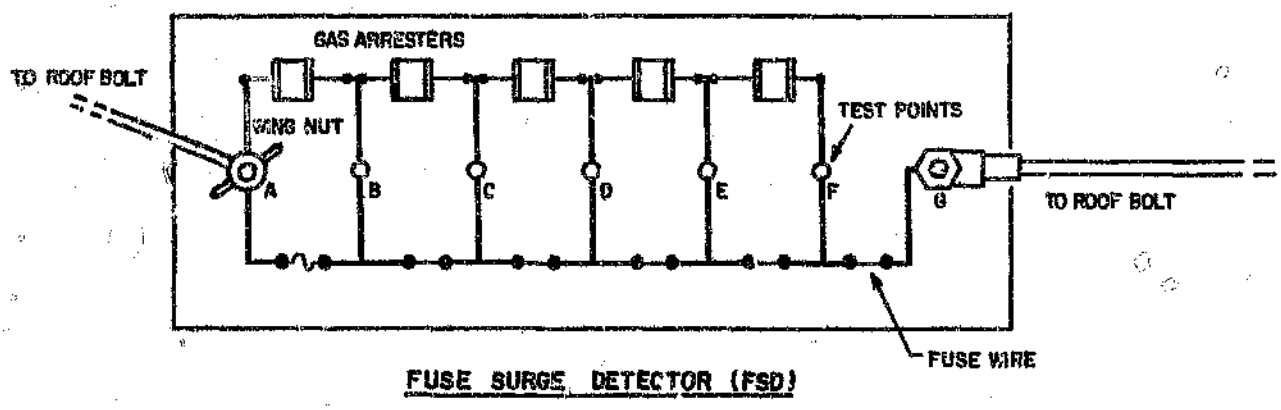



**Figure 1** Drawing of the physical layout of the FSD

With current pulses of sufficiently short duration to prevent the thermal conduction time constant playing a role, the sensitivity (s) of both the fusing of resistive wire and the initiation of electric detonators is

$$s = (k \int I^2\, dt) \,/\, d^3 \quad \ldots\ldots\ldots\

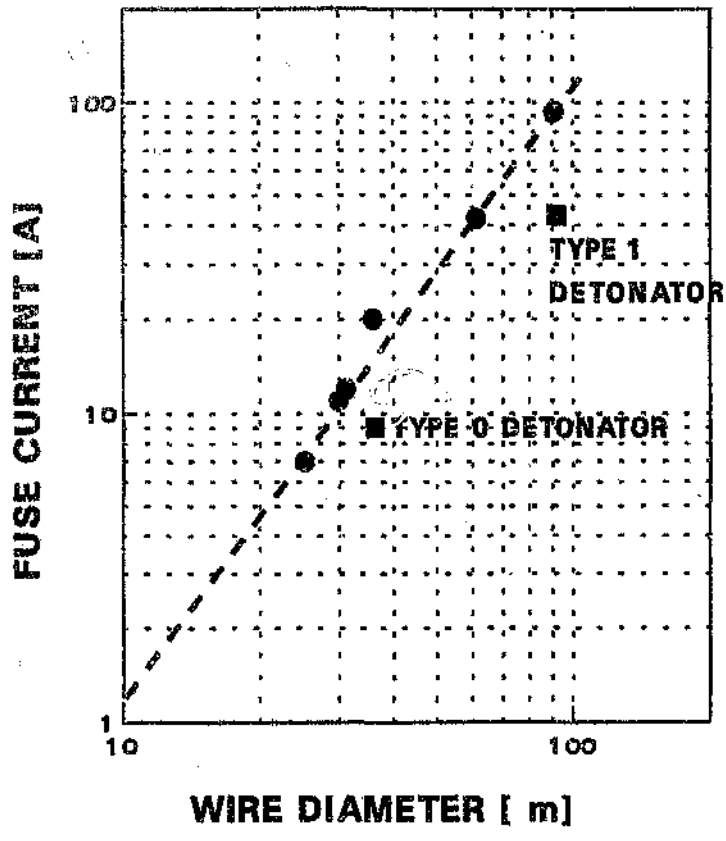



**Figure 5.2** The fuse current of nichrome wire of various diameters. The fuse currents of Type 0 and Type 1 detonators are also shown.

**Table 5.2** The fuse current rating of the different fuses in the FSD

| Fuse No. | Fuse type | Fuse current (1.2/44 μs current impulse) | Median lightning current (1/75 μs impulse) |
|---|---|---|---|
| A-B | IC aluminium track | 3 A peak | 2.30 A peak |
| B-C | Θ = 25 m nichrome wire | 7 A peak | 5.36 A peak |
| C-D | Θ = 30 m nichrome wire | 12 A peak | 9.19 A peak |
| D-E | Θ = 36 m nichrome wire | 20 A peak | 15.3 A peak |
| E-F | Θ = 61 m nichrome wire | 42 A peak | 32.2 A peak |
| F-G | Θ = 91 m nichrome wire | 93 A peak | 71.2 A peak |

Five of the six fuse wires are nichrome wire with lengths of 2 mm, but with different diameters, soldered onto a printed circuit board (see Table 5.2) Wires with diameters of less than 25 $\mu$m are almost impossible to handle and integrated circuits (ICs) with a thin aluminium track etched on a layer of silicon oxide were used to obtain a sensitivity level as low as 3 A peak. Commercially obtainable fuses were used in place of the IC in a later model of the FSD.

## 5.2 The equivalent median lightning current

The FSD is characterized by the peak current of a 1,2/44 $\mu$s waveshape. However the actual waveshape of lightning is quite different from this waveshape. An attempt is made in this section to arrive at an equivalent lightning peak current for the various sensitivity levels of the FSD.

It was shown earlier that the sensitivity of the FSD depends on

$$S \propto k \int i^2 \, dt \quad \ldots\ldots\ldots\ldots\ldots\ldots\ldots\ldots\ldots\ldots\ldots\ldots\ldots\ldots\ldots\ldots\ldots\ldots\ldots\ldots 5.2$$

$$= \int_0^\infty \left[ I \, e^{-\frac{t}{\tau}} \right]^2 dt \qquad \text{(integral of exponentially decaying impulse)}$$

$$= ( \tau \, I_0^2 ) / 2 \qquad \tau = \text{exponential time constant}$$

$$= ( 1.44 \, T_{50} \, I_0^2 ) / 2 \qquad T_{50} = \text{time to 50 \% of peak}$$

$$= .77 \, T_{50} \, I_0^2 \qquad \tau = 1.44 \, T_{50}$$

The median value of $T_{50}$ for the first lightning strokes is

$$T_{50} = 75 \, \mu s \quad \ldots\ldots\ldots\ldots\ldots\ldots\ldots\ldots\ldots\ldots\ldots\ldots\ldots\ldots\ldots\ldots\ldots\ldots\ldots\ldots 5.3$$

The ratio between the test waveshape current and median lightning current can therefore be determined by setting the action integrals ($I^2s$), for both the tests (1.2/44 $\mu$s) carried out

on the FSDs and the median lightning waveshape, equal to:

$$T_{50}\, I^2 = T'_{50}\, I'^2 \qquad \text{.....5.4}$$

$$I = \sqrt{\frac{T'_{50}}{T_{50}}} \times I'$$

$$I_L = \sqrt{\frac{44}{75}} \times I_{test}$$

$$I_L = .77\ I_{test}$$

This value is calculated and given in Table 5.2.

## 3.3 The function of the gas arresters

When a fuse wire fuses, the conductor is burnt away and may interrupt the flow of current through the FSD circuit. This mechanism can therefore protect fuses which are rated higher against fusing in an event where sufficient surge current is available to fuse such fuses. To prevent this, gas arresters were installed in parallel with the five lower-rated fuses. These arresters will be open-circuit as long as the fuse wire is intact. As soon as the fuse blows and a voltage difference of more than 90 V develops across the gas arrester, it will spark over and conduct almost like a short-circuit. The 90 V level may seem high and could be suspected of affecting the operation of the FSD. However, this is not believed to be the case, since the voltage driving the current is of relatively high magnitude as shown in this thesis.

## 3.4 Corrosion-resistant FSDs

When first attempting to make a low-cost detector, actual detonators were used (after removing the base charge). These attempts failed because the copper tubes could not stand the corrosion conditions underground. To solve this problem, the test points on the FSDs were made of stainless steel and the whole printed circuit board on which the fuses were mounted was enclosed in epoxy resin, which formed the body of the unit.

### 3.3 Indication of blown fuses and intrinsic safety

The first group of FSDs that were produced were checked for blown fuses by using a continuity tester.

A continuity tester was built into the second model FSDs. A LED flashing at intervals of two seconds then indicated that a fuse had been blown. This design of FSD was submitted to the SABS and was approved as an intrinsically safe device. This was necessary because the FSDs were located in "fiery" mines.

## 4 METHOD OF INSTALLING FSDs IN TYPICAL WORK-FACE CONFIGURATIONS

To study the occurrence of surges underground, some decisions had to be made on how the experimental equipment should be installed.

Figure 5.3 shows the configurations that were chosen. Two faces close to each other were selected. The purpose of the first one was to study the current induced between adjacent detonators in the same work face, vertically and horizontally. The purpose of the second one was to study the current induced between the work face and the point where the shot exploder would typically be placed.

Five areas were selected in each of the mines which were regarded as being particularly exposed. The experimental equipment was installed at two faces in each area (as shown in Figure 5.3). This meant that 15 FSDs were installed in each particular mine at a particular time.

Roofbolts were inserted into the holes and were fixed by means of a semi-conductive epoxy resin. The roofbolts substituted the normally charged-up holes in a blasting operation.

In retrospect, the installation between the work face and the exploder bolt could possibly have been better done by connecting only the top of the face and not the bottom as well.

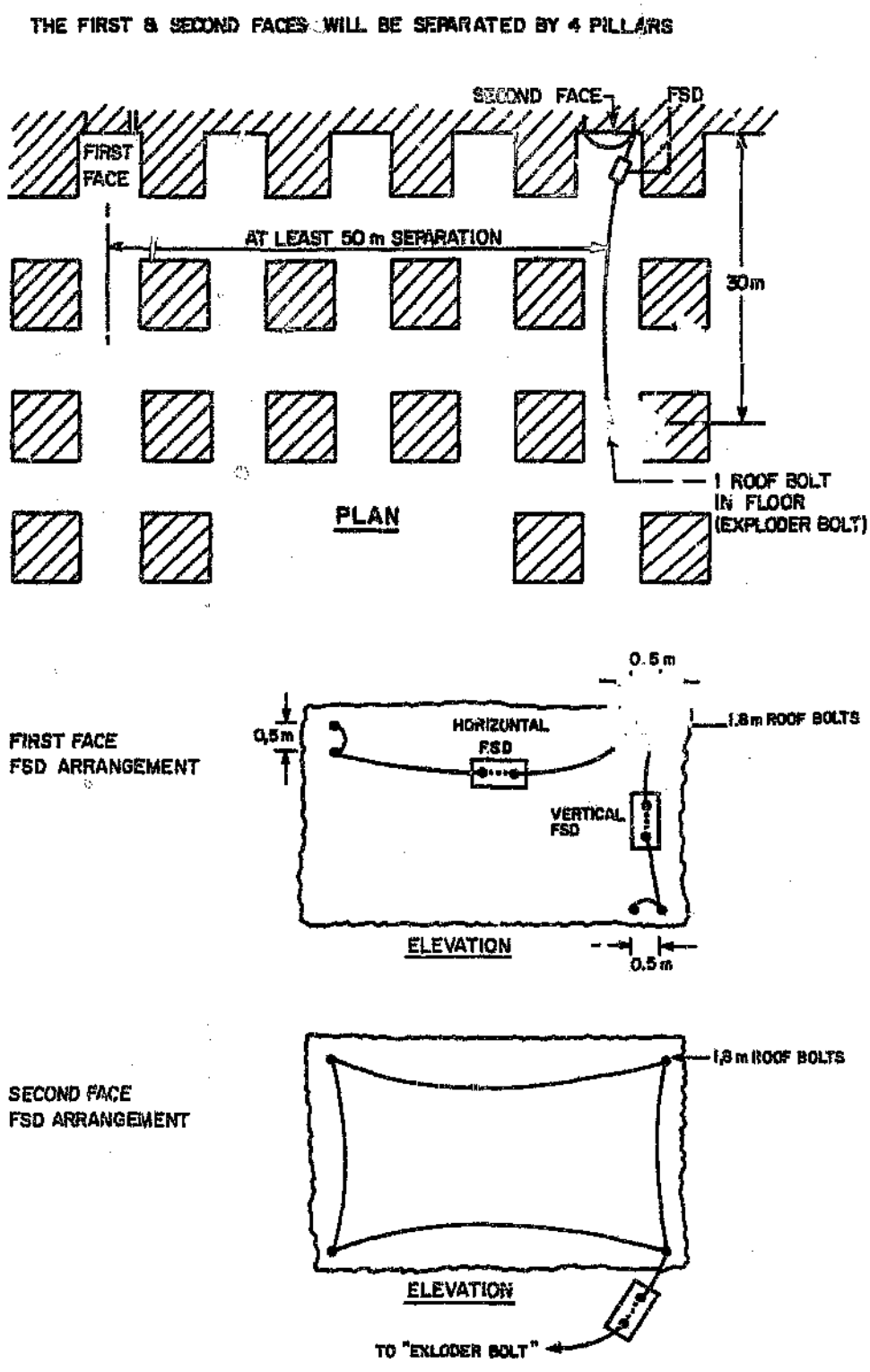



**Figure 5.3** The installation of FSDs in a particular [illegible] mine. Note that the "first face" detects currents in locally the work face and the "second face" detects current from the work face to the point where a exploder will normally be placed.

## 4.1 Collieries in which FSDs were installed

The mines in which FSDs were installed are listed below in Table 5.3

Table 5.3 gives the total exposure (number of fuses x flash density, accumulated for all the years) of FSDs in the various mines. Table 5.4 gives some important background information about the various mines in which FSDs had been installed.

**Table 5.3** Mines in which FSDs were installed. The last column shows the total exposure at each mine: number of faces installed x flash density, accumulated for the total period.

| Mine | 86/87 | 87/88 | 88/89 | 89/90 | 90/91 | 91/92 | Face x $N_g$ |
|---|---|---|---|---|---|---|---|
| 1. Arnot | 5 | 5 | 5 | 5 | 4 | 4 | 217.00 |
| 2. Delmas | 0 | 0 | 0 | 0 | 2 | 1 | 26.80 |
| 3. Douglas | 5 | 5 | 5 | 5 | 4 | 3 | 209.00 |
| 4. Goedehoop | 5 | 5 | 5 | 4 | 5 | 5 | 225.00 |
| 5. Greenside | 5 | 5 | 5 | 5 | 3 | 3 | 182.00 |
| 6. Kriel | 0 | 0 | 4 | 4 | 4 | 4 | 127.00 |
| 7. Landau | 5 | 5 | 3 | 5 | 0 | 0 | 136.00 |
| 8. Matla | 0 | 0 | 0 | 0 | 5 | 5 | 87.00 |
| 9. Sigma | 0 | 0 | 0 | 0 | 5 | 4 | 79.00 |
| 10. South Witbank | 0 | 0 | 0 | 4 | 5 | 5 | 123.00 |

Table 5.4 The average and minimum depths and thicknesses of coal seams at locations where FSDs were installed in the various mines

| Mine | Average depth (m) | Minimum and maximum depths (m) | Average seam thickness | Seam No. |
|---|---|---|---|---|
| Arnot | 63 | 47 - 72 | 2.8 | 2 |
| Delmas | 103 | - | 6.7 | NA |
| Douglas | 45 | 35 - 60 | 5.1 | 1 and 2 |
| Goedehoop | 45 | 32 - 62 | 3.2 | 2 |
| Greenside | 36 | 16 - 59 | 1.7 | 5 |
| Kriel | 47 | 44 - 56 | 3.9 | 4 |
| Landau | 48 | 26 - 85 | 6.2 | 2 |
| Matla | 48 | 45 - 57 | 6.6 | 4 |
| Sigma | 70 | 68 - 72 | 4.0 | 3 |
| South Witbank (Tavistock) | 54 | 45 - 64 | 4.6 | 4 |

The actual seam number of the Witbank coal field is important; the different layers are identified and numbered from the deepest seam, No. 1, to the most shallow seam, No. 5. When mining operations are carried out at Seam No. 1 or Seam No. 2, there are normally high-resistivity coal layers above the seam. If Seam No. 5 is mined, the implication is that there are no overlying layers of high-resistivity coal.

# 5 RESULTS FROM THE BLOWN FSDs IN COLLIERIES

The FSDs that blew during the six-year period are listed in Tables 5.5 to 5.7.

The various configurations are given separately, for example the "first face" arrangement, horizontal and vertical. Attention is focused on the "second face" data as this configuration was the most exposed.

Note that the results obtained will be less than the actual expected frequency. This is because the results depend on how regularly the FSDs were checked and how soon they were replaced after they had blown. If a second current impulse had passed through the same FSD while it was fused, the result would have been that two events were recorded as one. An effort was made to minimise this problem, but the success of the experiment depended on the conscientiousness of the miner who was responsible for the upkeep of the FSD.

**Table 5.5** Results obtained during six thunderstorm seasons, 1986/87 to 1990/92. The fuses blown were in the vertical configuration

| Colliery | Date | Type of installation | Rating of blown fuse (A) | | | | | |
|---|---|---|---|---|---|---|---|---|
| | | | 3 | 7 | 10 | 20 | 40 | 90 |
| Greenside | 20/11/86 | Face 1 vertical | x | | | x | x | x |
| Landau | 21/12/86 | " | x | x | | | | |
| Landau | 21/12/86 | " | x | | | | | |
| Greenside | 89/90 | Face 1 vertical | x | | | | | |
| Landau | 21/12/89 | " | x | | | | | |
| South Witbank | 2/3/90 | " | x | | | | | |
| South Witbank | 2/4/90 | " | x | | | | | |
| South Witbank | 3/11/89 | " | x | | | | | |
| Greenside | 90/91 | Face 1 vertical | x | | | | | |
| South Witbank | 90/91 | " | x | | | | | |
| South Witbank | 90/91 | " | x | | | | | |
| Arnot | 91/92 | Face 1 vertical | x | | | | | |
| Arnot | 3/92 | " | x | | | | | |
| Greenside | 92 | " | x | x | | | | |
| South Witbank | 12/91 | " | x | | | | | |
| South Witbank | 2/92 | " | x | | | | | |

**Table 5.6** Results obtained during six thunderstorm seasons, 1986/87 to 1990/91. The fuses blown were in the horizontal configuration

| Colliery | Date | Type of installation | Rating of blown fuse (A) | | | | | |
|---|---|---|---|---|---|---|---|---|
| | | | 3 | 7 | 10 | 20 | 40 | 90 |
| Landau | 21/11/86 | Face 1 horizontal | x | | | | x | x |
| Landau | 21/12/86 | " | x | | | | | |
| Landau | 10/2/87 | " | x | | | | | |
| Arnot | 14/11/88 | Face 1 horizontal | x | | | | | |
| Arnot | 16/1/89 | " | x | | | | | |
| Kriel | 23/1/91 | Face 1 horizontal | x | | | | | |
| South Witbank* | 90/91 | " | | | | | | x |
| South Witbank | 90/91 | " | x | | | | | |
| Van Dyk's Drift (Douglas) | 12/91 | Face 1 horizontal | x | | | | | |
| Van Dyk's Drift (Douglas) | 90/91 | " | x | | | | | |

* This result is suspect and is not included in the theoretical study.

**Table 5.7** Results obtained during six thunderstorm seasons, 1986/87 to 1990/2. The fuses blown were in the face-to-exploder-bolt configuration

| Colliery | Date | Type of installation | Rating of blown fuse (A) | | | | | |
|---|---|---|---|---|---|---|---|---|
| | | | 3 | 7 | 10 | 20 | 40 | 90 |
| Arnot | 9/4/87 | Face 2 | x | | | | | |
| Greenside | 20/11/86 | " | x | | | | x | x |
| Landau | 21/11/86 | " | x | | | | | |
| Landau | 21/11/86 | " | x | | | | | |
| Landau | 21/11/86 | " | x | | | | | |
| Landau | 21/12/86 | " | x | x | | | | |
| Landau | 26/3/87 | " | x | | | | | |
| Douglas | 87/88 | Face 2 | x | x | | | | |
| Douglas | 87/88 | " | x | x | x | | | |
| Greenside | 87/88 | " | x | x | | | | |
| Greenside | 30/11/87 | " | x | | | | | |
| Landau | 9/1/88 | " | x | | | | | |

| Colliery | Date | Type of installation | Rating of blown fuse (A) | | | | | |
|---|---|---|---|---|---|---|---|---|
| | | | 3 | 7 | 10 | 20 | 40 | 90 |
| Greenside | 88/89 | Face 2 | x | | | | | |
| Greenside | 89/90 | " | x | | | | | x |
| Kriel | 89/90 | " | x | x | | | | |
| Kriel | 3/11/89 | " | x | x | x | | | |
| Kriel | 28/11/89 | " | x | | | | | |
| South Witbank | 2/3/90 | " | x | | | | | |
| South Witbank | 2/3/90 | " | x | | | | | |
| South Witbank | 2/3/90 | " | x | | | | | |
| South Witbank | 3/11/89 | " | x | | | | | |
| South Witbank | 28/11/89 | " | x | | | | | |
| Goedehoop | 90/91 | Face 2 | | | | | | |
| South Witbank | 12/90 | " | x | | | | | |
| South Witbank | 90/91 | " | x | | | | | |
| South Witbank | 90/91 | " | x | | | | | |
| Arnot | 91/92 | Face 2 | x | | | | | |
| Arnot | 3/92 | " | x | | | | | |
| Arnot | 3/92 | " | x | | | | | |
| Greenside | 92 | " | x | x | x | | | |
| Greenside | 92 | " | x | x | | | | |
| Kriel | 91/92 | " | x | | | | | |
| Matla | 92 | " | x | | | | | |
| South Witbank | 91 | " | x | | | | | |
| South Witbank | 92 | " | x | x | | | | |
| South Witbank | 2/92 | " | x | | | | | |
| South Witbank | 92 | " | x | | | | | |

## 6 LIGHTNING FLASH DENSITY

The lightning flash density for the period of study was determined using the Cigré 20-km lightning flash counters. The results for this period are given in Table 5.8.

**Table 5.8** Lightning ground flash densities ($N_g$) at the Greenside, Sigma, Welgedacht, Delmas and Matla Collieries

| Mine | 1986/87 | 1987/88 | 1988/89 | 1989/90 | 1990/91 | 1991/92 | 11-year average* |
|---|---|---|---|---|---|---|---|
| Greenside | 7.40 | 7.65 | 5.34 | 8.95 | 9.81 | 6.35 | 8.95 |
| Sigma | | | | | 4.70 | 6.31 | 7.50 |
| Welgedacht | | | | | 9.01 | 9.90 | 8.90 |
| Delmas | | | | | 9.45 | - | 7.50 |
| Matla | | | | | | 7,79 | 7.50 |

* These figures are an 11-year average and were obtained from the results of a project carried out by the CSIR from 1975 to 1986 entitled "The Lightning Registration Scheme".

## 7 NORMALISED FREQUENCY OF SURGES IN THE VARIOUS MINES

To allow the comparison of this set of data between mines but also with the models developed in Chapters 2 and 3, the data was summarised and normalised through equation 5.5.

$$\textit{Frequency of an event at a mine} = \frac{\textit{Total No. of observations}}{\textit{Total flash density} \times \textit{No. of installations}} \qquad 5.5$$

The normalised frequency of the totals of the three configurations at all the mines is given in Tables 5.9 to 5.11

**Table 5.9** Normalised frequencies for Face 1, vertical

| Face 1, vertical | Rating of blown fuse (A) | | | | | |
|---|---|---|---|---|---|---|
| | 3 | 7 | 10 | 20 | 40 | 90 |
| Total number of blown fuses | 16 | 3 | 1 | 1 | 1 | 1 |
| No. of faces x $N_g$ | 1 325 | 1 325 | 1 325 | 1 325 | 1 325 | 1 325 |
| Normalised frequency | 0.0120 | 0.0022 | 0.0008 | 0.0008 | 0.0008 | 0.0008 |

**Table 5.10** Normalised frequencies for Face 1, horizontal

| Face 1, horizontal | Rating of blown fuse (A) | | | | | |
|---|---|---|---|---|---|---|
| | 3 | 7 | 10 | 20 | 40 | 90 |
| Total number of blown fuses | 9 | 1 | 1 | 1 | 1 | 1 |
| No. of faces x $N_a$ | 1 300 | 1 300 | 1 300 | 1 300 | 1 300 | 1 300 |
| Normalised frequency | 0.0070 | 0.0008 | 0.0008 | 0.0008 | 0.0008 | 0.0008 |

**Table 5.11** Normalised frequencies for Face 2

| Face 2 | Rating of blown fuse (A) | | | | | |
|---|---|---|---|---|---|---|
| | 3 | 7 | 10 | 20 | 40 | 90 |
| Total number of blown fuses | 37 | 10 | 5 | 1 | 1 | 1 |
| No. of faces x $N_a$ | 1 289 | 1 289 | 1 289 | 1 289 | 1 289 | 1 289 |
| Normalised frequency | 0.0287 | 0.0077 | 0.0039 | 0.0008 | 0.0008 | 0.0008 |

**Table 5.12** Normalised frequencies for Face 2 at the individual mines

| Mine | Rating of blown fuse (A) | | | | | |
|---|---|---|---|---|---|---|
| | 3 | 7 | 10 | 20 | 40 | 90 |
| Arnot | 0.0186 | 0 | 0 | 0 | 0 | 0 |
| Delmas | 0 | 0 | 0 | 0 | 0 | 0 |
| Douglas | 0.00963 | 0.00963 | 0.00484 | 0 | 0 | 0 |
| Goedehoop | 0.00448 | 0 | 0 | 0 | 0 | 0 |
| Greenside | 0.03663 | 0.01581 | 0.01108 | 0.00557 | 0.00557 | 0.00557 |
| Kriel | 0.03154 | 0.00741 | 0.00795 | 0 | 0 | 0 |
| Landau | 0.04410 | 0 | 0.00741 | 0 | 0 | 0 |
| Matla | 0.01161 | 0 | 0 | 0 | 0 | 0 |
| Sigma | 0.0978 | 0.00822 | 0 | 0 | 0 | 0 |
| South Witbank | 0.01200 | 0.0022 | 0 | 0 | 0 | 0 |

The frequencies for Face 2 at the individual mines was also calculated and are given in Table 5.12.

# 8 RESULTS: SOME COMPARISONS

## 8.1 The configuration of Faces 1 and 2

From Tables 5.9 to 5.11, it can be seen that the configurations of "Face 2" are twice as likely to experience an event than any of the configurations of "Face 1". This is to be expected and is supported by the analysis in Chapter 3.

This result is further supported by Figure 5.4. This is a histogram of the 3 A frequency at all the mines comparing the three face configurations. The frequencies at Face 2 are in all cases much higher than the frequencies at Face 1. Furthermore, it shows that the Face 1 horizontal configuration experienced a very low frequency of surges.

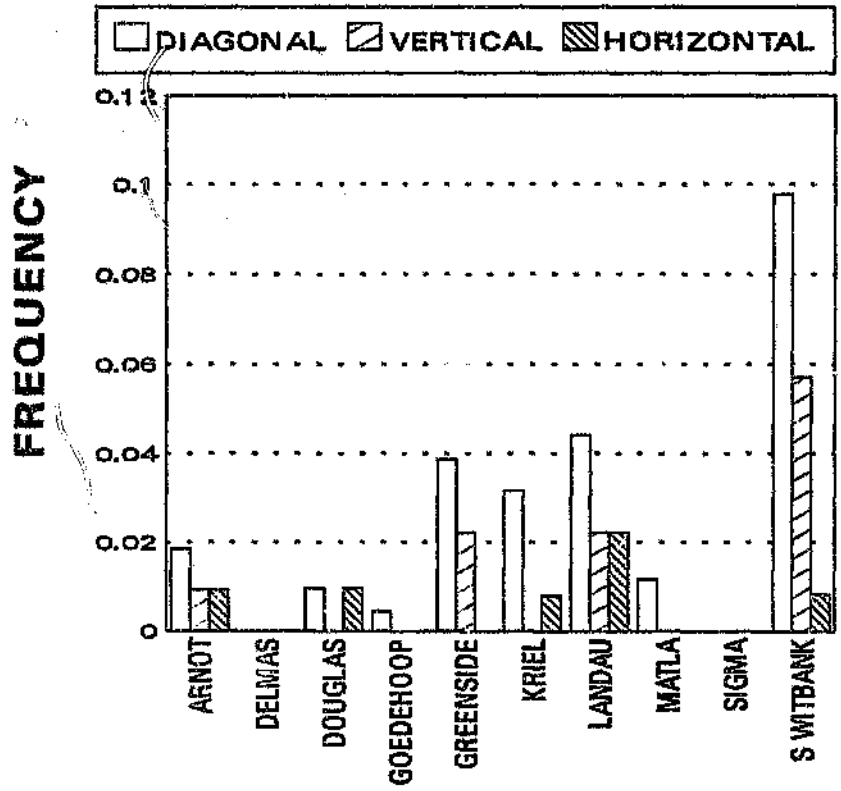



**Figure 5.4** The normalised frequency of 3 A of Face 1, vertical or horizontal and Face 2 at the various mines.

The frequencies for Face 2 at the individual mines was also calculated and are given in Table 5.12.

# 8 RESULTS: SOME COMPARISONS

## 8.1 The configuration of Faces 1 and 2

From Tables 5.9 to 5.11, it can be seen that the configurations of "Face 2" are twice as likely to experience an event than any of the configurations of "Face 1". This is to be expected and is supported by the analysis in Chapter 3.

This result is further supported by Figure 5.4. This is a histogram of the 3 A frequency at all the mines comparing the three face configurations. The frequencies at Face 2 are in all cases much higher than the frequencies at Face 1. Furthermore, it shows that the Face 1 horizontal configuration experienced a very low frequency of surges.

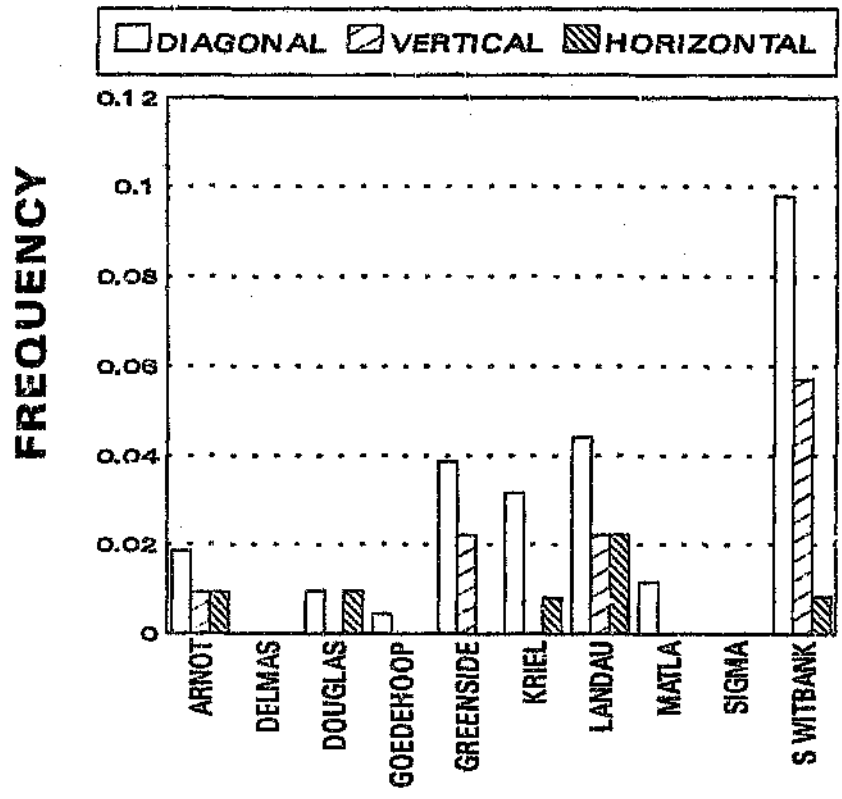



**Figure 5.4** The normalised frequency of 3 A of Face 1, vertical or horizontal and Face 2 at the various mines.

## 8.2 Comparison with the simple model

Based on the simple model of Chapter 2, Geldenhuys et al (Oct. 1987) did a Monte Carlo study to predict the frequency of surges. The results of this study are plotted in Figure 5.5 giving the average results obtained in all the mines. Furthermore, the results obtained in specific mines (especially the higher frequencies) are plotted on the same axis as (+).

When comparing the simple model to the results obtained, the inverse relationship between frequency and current peak are confirmed. The average of the FSD programme is almost a factor 10 less frequent than the model. However, in some cases, the highest results in specific mines exceed the prediction of the model. From the large scatter in the data, it is obvious that other factors have a big influence on the current induced into a detonator circuit.

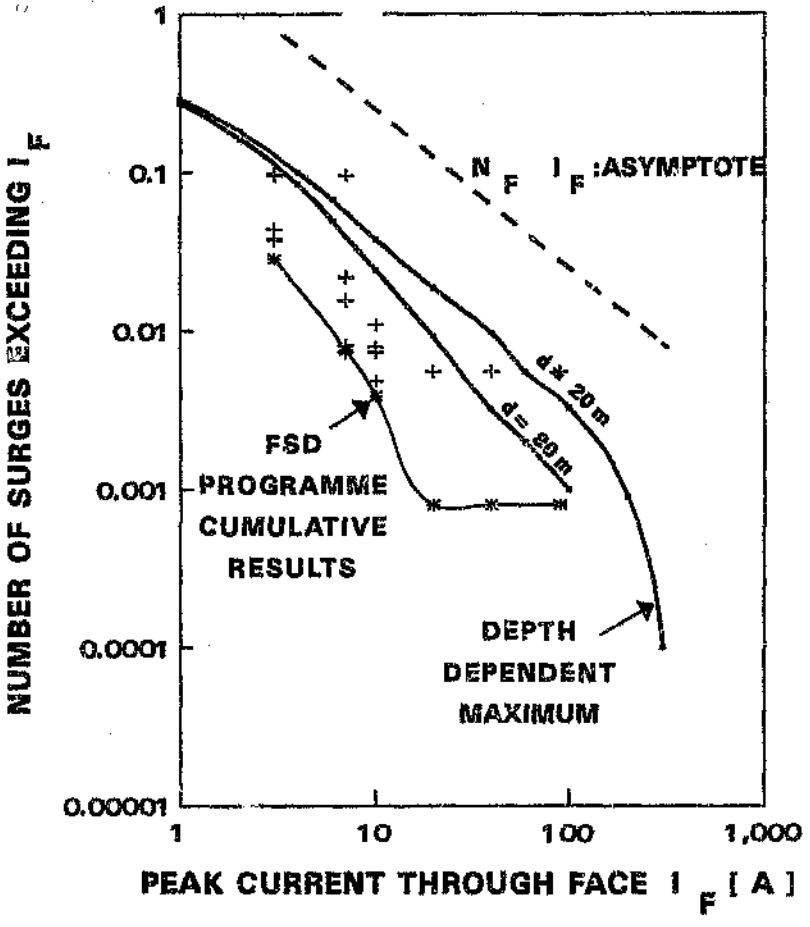



Figure 5.5 The predicted frequencies (Geldenhuys et al, Oct. 1987) at diagonal faces at depths (d) of 20 m and 80 m. The average results of all the mines in the FSD programme are plotted on the same axis as the line marked with *.
+ These points are frequencies that have been observed in particular mines.

## 5.3 Comparison between the mines and depth dependence

Figure 5.6 gives a comparison of the normalised frequencies of 3 A, 7 A and 10 A that blew fuses in Face 2 at various mines. In two mines, not even a single 3 A fuse blew (Delmas and Sigma Collieries). Another odd result is the very high 3 A frequency in South Witbank, where no 10 A fuse blew.

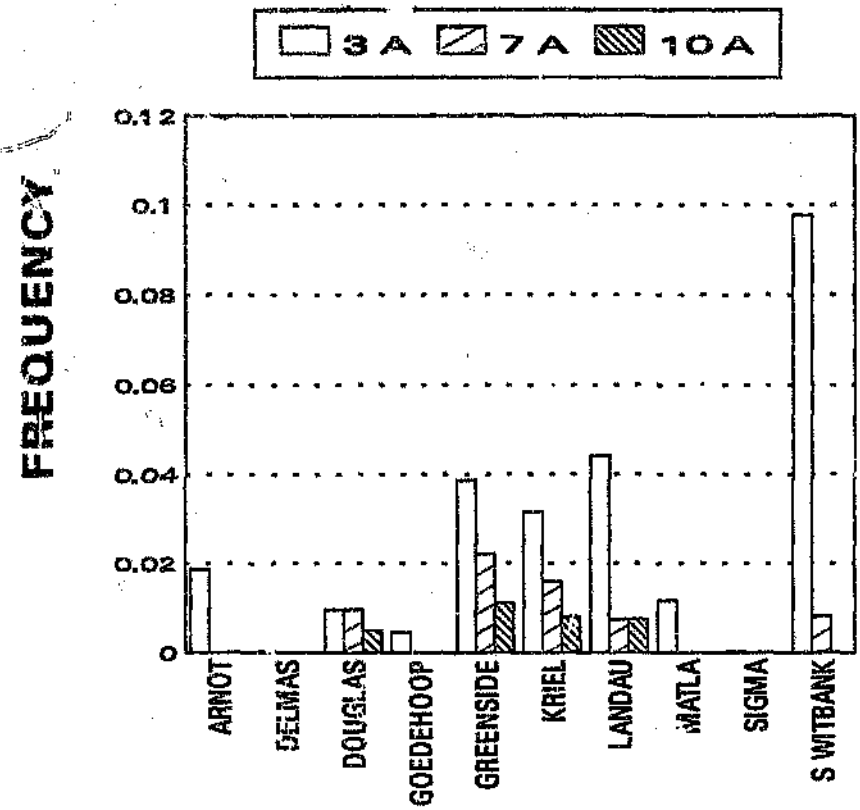



**Figure 5.6** The normalised frequencies of 3 A, 7 A and 10 A that blew fuses in Face 2 (diagonal current) in the various mines.

The cause of this variation must be sought in a number of factors, such as

The depth of the mines
The thickness of the seams
The resistivity of the overlying strata (e.g. coal layers)
The resistivity of the strata below
Geological faults

In this chapter, only depth has been analysed. Figure 5.7 shows the normalised frequencies at Face 2 for 3 A, 7 A and 10 A. The two mines that had no blown fuses are the two mines with the deepest average depth (Table 5.4 and Figure 5.5). Furthermore, only mines shallower than 50 m experienced 10 A currents. The data supports the depth-dependency concept strongly.

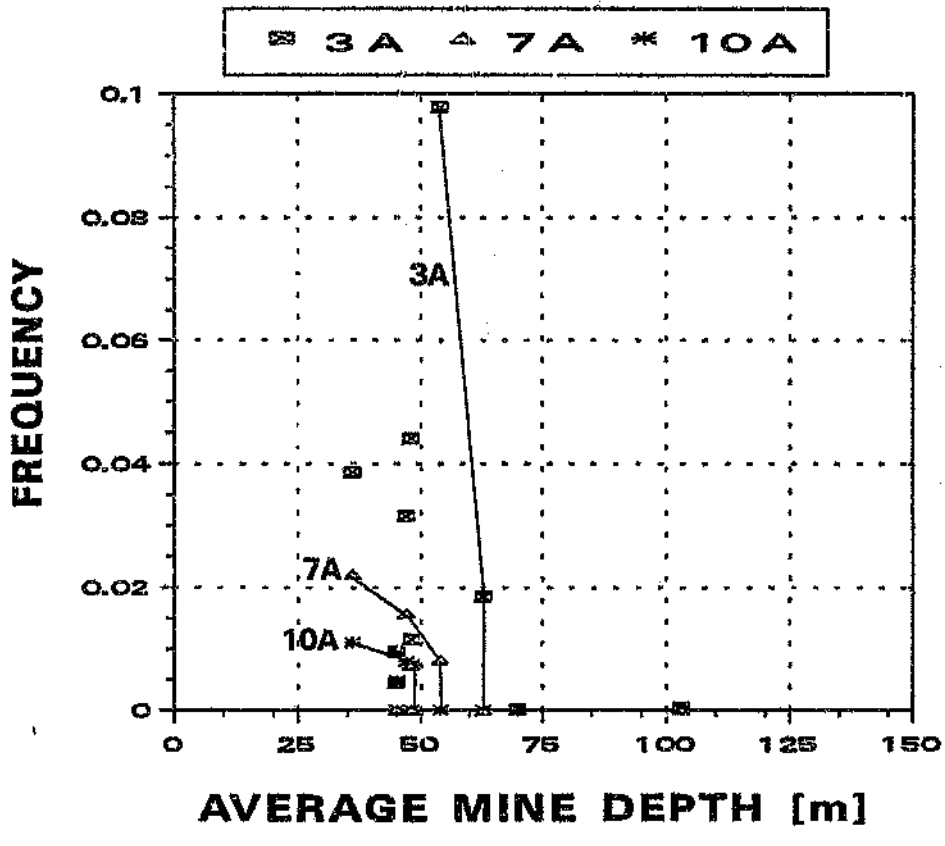



Figure 5.7 The normalised frequencies of 3 A, 7 A and 10 A that blew fuses in Face 2, plotted against the average depth of the FSD installation in the various mines. The maximum frequency of a specific current versus depth is also shown through the interconnecting lines.

# CHAPTER 6

# METHANE SENSITIVITY TO LIGHTNING-INDUCED SPARKS

## 1 INTRODUCTION

The first line of defence against methane explosions is adequate ventilation. However, should ventilation fail for some reason, the second line of defence is to prevent ignition sources which could initiate an explosion. Lightning-induced sparks underground are a possible ignition source. This chapter investigates the level of lightning sparks that could ignite methane air mixtures.

Lightning can induce voltage differences between a metal object to a metal object, or a metal object to the strata. This may lead to sparking between the metal objects or to the strata. In high-resistivity shallow mines in particular, lightning may even cause sparks in the strata and on the mine roof or wall, due to the high field gradient in the strata. Any such sparking is a potential source of ignition.

The Coal Mine Controlling Council initiated an investigation into the conditions required for lightning sparks to ignite methane. The results of this investigation were reported by Pretorius (1991). This chapter will summarise those results and put them into the context of this thesis.

## 2 THE NATURE OF LIGHTNING SPARKS UNDERGROUND

### 2.1 Sparking on the strata surface

Sparks will occur on the surface or interface of the strata when the electric field induced is of the order of 500 kV/m or more.

From the simple spherical model in equation 3.1 of Chapter 3, the electric field gradient can be calculated. If we set equation 3.1 equal to 500 kV/m, the maximum radius at which such ionisation/sparking can occur can be calculated as a function of the resistivity of the strata. The result of this calculation is given in Table 6.1. The lightning current peak was assumed to be 100 kA.

**Table 6.1** Ionisation radius of a lightning current of 100 kA versus strata resistivity

| $\rho$ Ω.m | Ionisation Radius m |
|---|---|
| 10 000 | 17.8 m |
| 3 000 | 9.8 m |
| 1 000 | 5.6 m |
| 300 | 3.1 m |

The actual strata configuration with coal layers will increase the ionisation radius slightly. However, the resistivity must be extremely high before this mechanism can induce sparking underground.

It is clear that this mechanism will initiate sparks underground only when there is a combination of very high resistivities (exceeding 10 000 Ω.m) and very high lightning current. The mechanism will produce filamentary spark channels in which the current will be similar to the current waveshape of the main lightning strike. The length of the spark channel will be at least several centimetres or even some metres long and the current will be at least several amperes.

## 2.2 Sparking involving conductors

Equipment and construction material used underground are more often than not made of conducting material. One example of this is the use of catenary wires (normally steel wire) strung along the roof suspended on roofbolts. These wires are used to support electrical cables, water pipes, etc.

Due to their length, these wires can "integrate: the induced electric field along the roof of the underground workings or between the roof and the floor (as is the case with detonators).

The electric field/potential induced into the strata has been dealt with in Chapters 2 and 3 extensively, especially where detonators are concerned. This analysis is repeated in this chapter but is focused on lengths of wires and underground structures.

The potential induced into the roof of an underground mine is shown in Figure 6.1. Table 6.2 is derived from Figure 6.1 (given at different depths) and gives the maximum voltage difference induced into the ends of a conductor of a specific length.

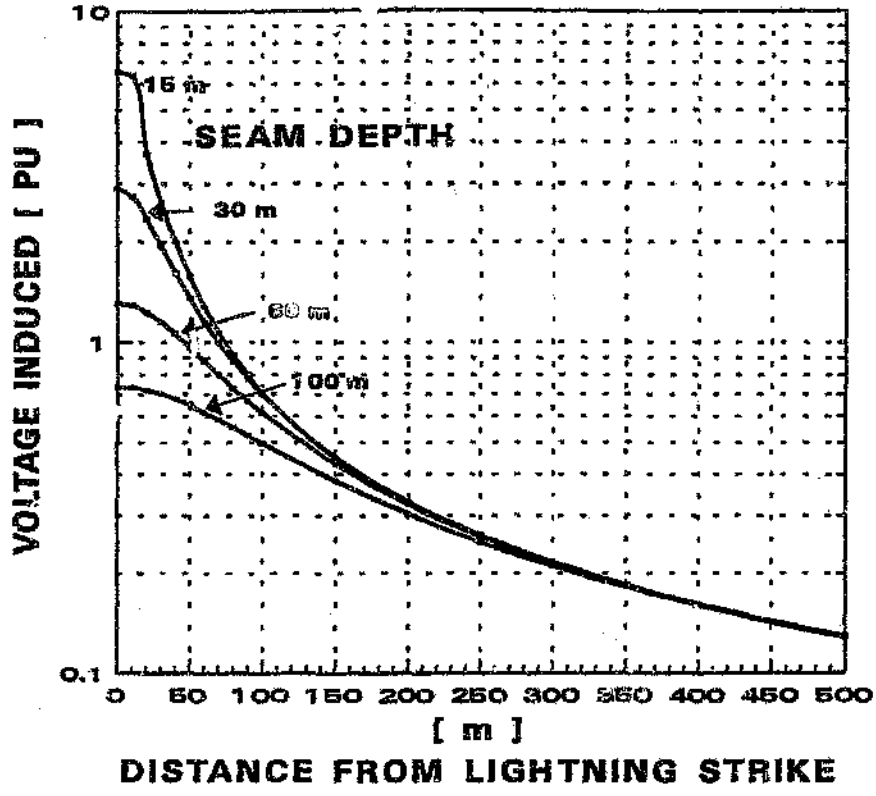



**Figure 6.1** The potential induced into the roof of an underground working.
t = 3 m, $\rho_C$ = 3 000 Ω.m.
$\rho_1 = \rho_2$ = 400 Ω.m.
$I_L$ = 1 A.

**Table 6.2** The maximum voltage difference induced into the roof of a 15-m deep coal seam and a 30-m deep coal seam by a lightning current of 100 kA.

| Wire length $\ell$ | Mine depth | |
|---|---|---|
| | d = 15 m | d = 30 m |
| | $U_{max}$ (kV) | $U_{max}$ kV |
| 10 | 164 kV | 40 kV |
| 20 | 285 kV | 79 kV |
| 50 | 499 kV | 159 kV |
| 100 | 585 kV | 221 kV |
| 200 | 623 kV | 265 kV |
| 500 | 643 kV | 278 kV |

The maximum horizontal voltage gradient in a 15 m deep mine or a 30 m deep mine was derived from the data in Figure 6.1. This is only 16.4 kV/m, which is much less than the 500 kV/m required to cause spontaneous sparking on the strata-air boundary.
The maximum vertical field gradient for a 15 m deep seam and a 30 m deep seam can be

derived from Figure 3.14. The result is 164 kV/m.

From Chapter 3, it is known that the voltage difference listed in Table 6.2 depends on the depth of the mine seam and the resistivity of the strata. The values in Table 6.2 can be regarded as being the higher end of seams in typical Witbank mines. These voltages will induce current in the conductors. The magnitude of this current will depend on the "quality" of the conductor's contact with the surrounding strata. If the conductor is connected to roofbolts, the induced current will be even more than in the case of a detonator in an equivalent circuit configuration due to its lower resistance. Similar calculations can be made as has been done in Chapter 8 to determine the frequency with which such surges will occur.

Only one example is given here to illustrate a typical result:

Assume that we want to calculate the current in a wire with a 10 m length at a seam depth of 30 m. We know from Table 6.2 that 40 kV is induced at the ends of the wire. Assume that the ends of the 10 m cable are connected to a roofbolt of 1.8 m at each side.

The current can be calculated through the Oettlé model (discussed in more detail in Chapter 8) by transforming equation 8.8 into a relationship to determine current directly:

$$I = \left[\frac{U\ h^{0.4}}{12\ \rho^{0.74}}\right]^{0.77} \quad \ldots\ldots\ldots\

mining environments (SABS 549 1987, IEC Publication 1979, BASEFA 1972, Widginton 1966 and 1968, Tolson 1980, Cawley 1988, Krzytolik et al 1983).

The implication of this was that the nature of the electrical sparks in these studies are typical of electrical/electronic AC or DC circuits (make and break of electrical circuits with defined circuit resistance, inductance, capacitance and voltage sources.) Some of the authors focus on sparks generated by static electricity (stored in capacitors).

The circuits and spark currents in the work mentioned above are very different from the type of current that lightning induces.

Some work has been done on gaps of fixed distance which are sparked over by relatively high voltages of up to 6 kV (Widginton 1963; Bartels, 1975; Bartels and Riddlestone, 1966; and Lintin and Wooding, 1959). This work has some bearing on lightning-type sparks but cannot be used directly.

The most important points from these references are the following:

## 3.1 Energy

Most of the references report on the "energy" required to ignite methane. The way that the energy is determined is often not given. This raises some concern as to whether it is the total energy in the circuit (dissipated in internal stray resistances, etc.) or whether it is truly the energy in the spark. However, minimum energies of about 0.4-1 mJ are quoted to ignite methane.

"Energy" cannot simply be translated into gap size, current waveshape and peak current. This is therefore a parameter which is useless for lightning spark sensitivity.

## 3.2 Current

There is some information available, especially from Bartels (1975). He used tungsten electrodes of 10 mm diameter separated by 1.27 mm. The gap broke down at 5.9 V. The current was supplied by transmission lines which gave him square current pulses. Transmission lines with different impedance characteristics were used to get different peak currents, ranging from 7 A to 45 A and pulse durations of between 98 $\mu$s and 0.75 $\mu$s. Some of Bartels's (1975) data is given in Table 6.3.

**Table 6.3** The voltage current, pulse duration and peak current required to ignite methane-air mixtures in a 1.25 mm gap, taken from Bartels (1975).

| Line impedance | Sparkover voltage | Current pulse duration | Current pulse peak |
|---|---|---|---|
| 78 Ω | 5.9 kV | 20.0 μs | 35.0 A |
| 112 Ω | 5.9 kV | 29.8 μs | 25.0 A |
| 121 Ω | 5.9 kV | 51.5 μs | 24.0 A |
| 213 Ω | 5.9 kV | 69.0 μs | 12.8 A |
| 416 Ω | 5.9 kV | 98.0 μs | 7.1 A |

## 3.3 Rate of energy dissipation

Bartels and Riddleton (1966) conclude in their paper that: "the most important factor affecting the ignition energy level is the rate of energy dissipation in the early stages of the discharge. With high rates of dissipation a low energy level is needed, and vice versa". From the data obtained from the experiment by Pretorius (1991), it is believed that this plays an extremely important role in the current/energy required to ignite methane-air mixtures. This point will be explored later in this chapter.

## 3.4 Electrode material and shape

Some of the authors cited point out that the electrode material plays an important role in the minimum ignition energy. It has also been proved that the shape of the electrode can have an effect on the ignition energy.

# 4 THE CSIR EXPERIMENT

In view of the lack of information on the sensitivity of air-methane mixtures to lightning-like sparks, a programme was undertaken to determine this sensitivity. This work was carried out under the guidance of the author and is fully reported by Pretorius (1991).

## 4.1 The experimental arrangement

On behalf of the coal-mining industry, the CSIR set up a 200-m long tunnel to study coal-dust explosions in coal mines. The tunnel has a diameter of 2.5 m and the first 5 m of the tunnel is normally sealed off and filled with a 9 % (volume) methane-air mixture. This

section is used to initiate the coal-dust explosions. This section of the tunnel was used to conduct the experiment.

Figure 6.2 shows a cross-section of the tunnel. It also shows the manhole through which the impulse was applied to an electrode configuration.

The electrodes used were made of mild steel, except in one instance when brass was used. Mild steel was preferred because it is the most common material used underground and is most likely to be involved in a spark underground.

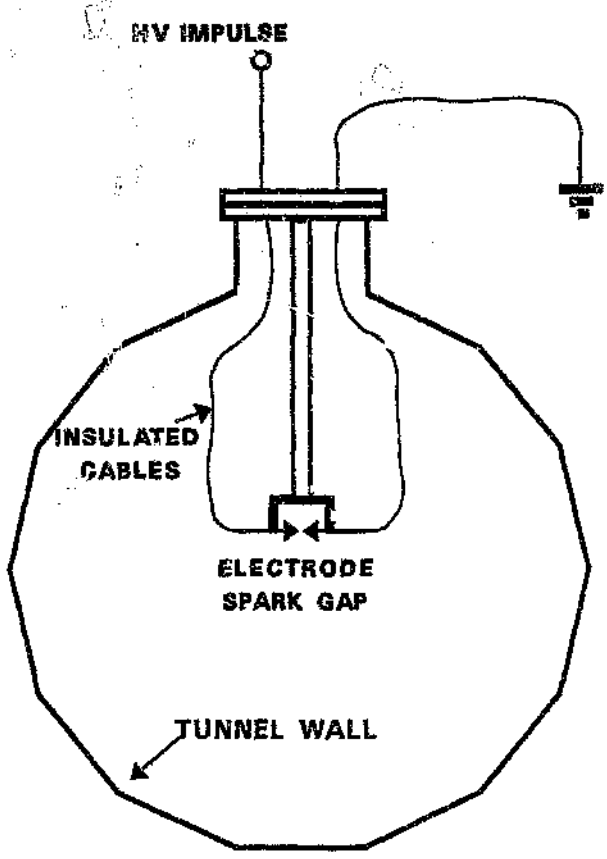



**Figure 6.2** The cross-section of the 2.5 m diameter tunnel in which the experiment was conducted. The electrode spark gap and the manhole through which the wires were fed into the tunnel are also shown.

Figure 6.3 shows an equivalent diagram of the high-voltage impulse circuit that was used in the experiment. A relatively large capacitor (4.3 $\mu$F) discharged through a 15.6 $\Omega$ resistor to give a voltage impulse across the resistor which has a time-to-half value close to 50 $\mu$s. The capacitor-resistor combination was also chosen to minimise the effect that any load currents may have had in the circuit, on the wave-shape.

The rise time in the circuit was not intentionally controlled. It can be estimated that the series inductance (L) that determined the rise time across the 15.6 Ω resistor must have been in the range of 1 $\mu$H to a maximum 5 $\mu$H. This corresponds to a time constant of 0.066 $\mu$s and 0.32 $\mu$s across the resistor.

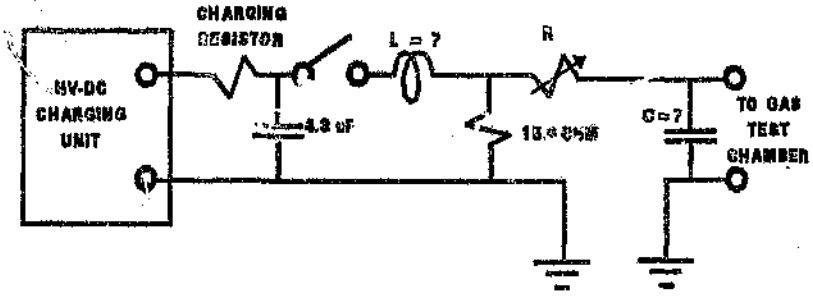



**Figure 6.3** The equivalent circuit diagram of the high-voltage impulse circuit. The HV-DC charging unit could charge the capacitor up to 40 kV.

The rise time across the electrodes in the explosion chamber depend on the resistor R which varied, as shown in Table 6.4. The load capacitance of the leads (and voltage measuring probe) on the electrode side is estimated to be about 10 pF. The RC rise time constant associated with the appropriate value of R is also given in Table 6.4 It is uncertain what the actual rise times were and what the effect of the rise times would be on the experiment. This will need careful attention in any future experiment.

**Table 6.4** The values of R and the RC time constant assuming C = 10 pF

| Resistance R (Ω) | Time constant RC ($\mu$s) |
|---|---|
| 6.00 M | 60.00 |
| 3.00 M | 30.00 |
| 1.80 M | 18.00 |
| 1.00 M | 10.00 |
| 0.44 M | 4.40 |
| 123 k | 1.20 |
| 35 k | 0.85 |
| 54 k | 0.54 |
| 30 k | 0.03 |

## 4.2 Results from the CSIR experiment

The results from the CSIR experimental programme are fully described in the report by Pretorius (1991).

The main conclusions from this chapter are summarised here in Figures 6.4 and 6.5.

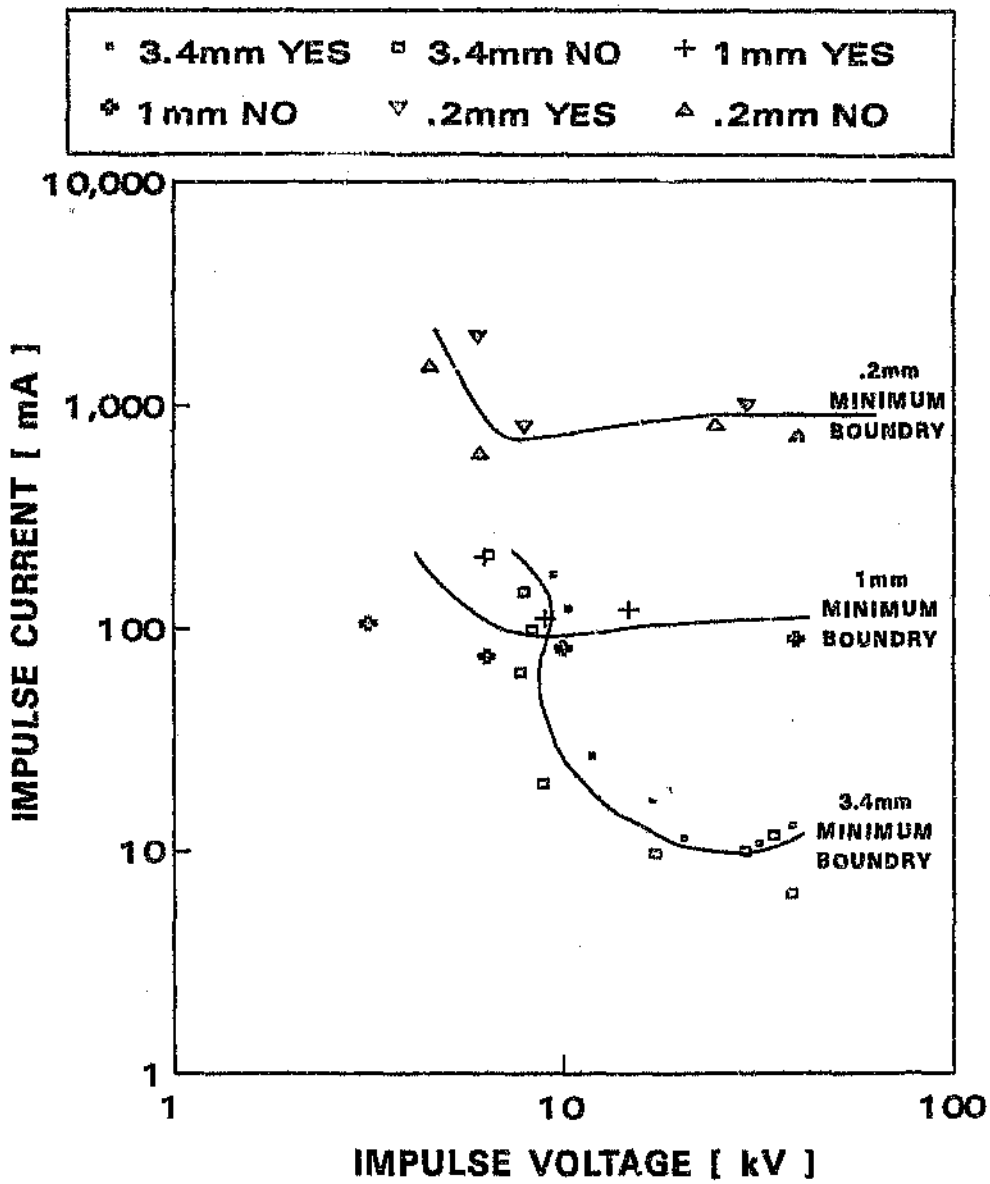



**Figure 6.4** The ignition (YES) and the non-ignition (NO) data points obtained from the CSIR experiment. The lines are drawn on the boundaries of ignition or non-ignition for the three gaps tested. The waveshapes have a time-to-half value of 50 $\mu$s. The electrodes are of steel.

Figure 6.4 shows the results of three electrode gap spacings that were tested: 0.2 mm, 1 mm and 3.4 mm. The picture that emerged from the experiment is a rather complicated one. It is clear that the parameters will have to be known more accurately before a fundamental understanding of the observations will be possible. However some important trends have emerged which are reported here.

To confirm these trends, further in-depth studies will have to be undertaken. The statistical sampling on which the experiment is based is also limited. The experiment was constrained by the availability of funds, but the question could also be asked whether further in-depth knowledge is required for the purpose of this study.

It can be seen from Figure 6.4 that the .2 mm gap behaved reasonably coherently, with a minimum current at about 700 mA. The 1 mm gap behaved equally coherently with a minimum ignition current of about 90 mA.

In the case of the 3.4 mm gap size, the ignition current ranges from 200 mA down to 11 mA in a rather incoherent fashion.

The minimum current associated with a particular gap size is plotted in Figure 6.5. A favourable result from Figure 6.5 is that very small gaps require relatively larger currents to ignite methane. Small gaps are typically possible where poor contact is made between connected wires or wires and roofbolts. However, unfortunately, it can be seen from the figure that the currents (10 mA) required to ignite methane in bigger gaps are very small. This type of spark is possible between a loose wire close to the coal strata, where sparking from the wire to the strata takes place.

It is also important to note the discrepancy between this data and the experiment reported by Bartels (1975). His gap of 1.25 mm is very similar to the 1 mm gap used in this experiment. His minimum current is 7 A for a 98 $\mu$s square wave current pulse and 24 A for a 51.5 $\mu$s square wave pulse, with a charging voltage of 5.9 kV being used in both cases.

In this experiment, a voltage of 6.24 kV is associated with an ignition current of 208 mA. This is rather a large difference.

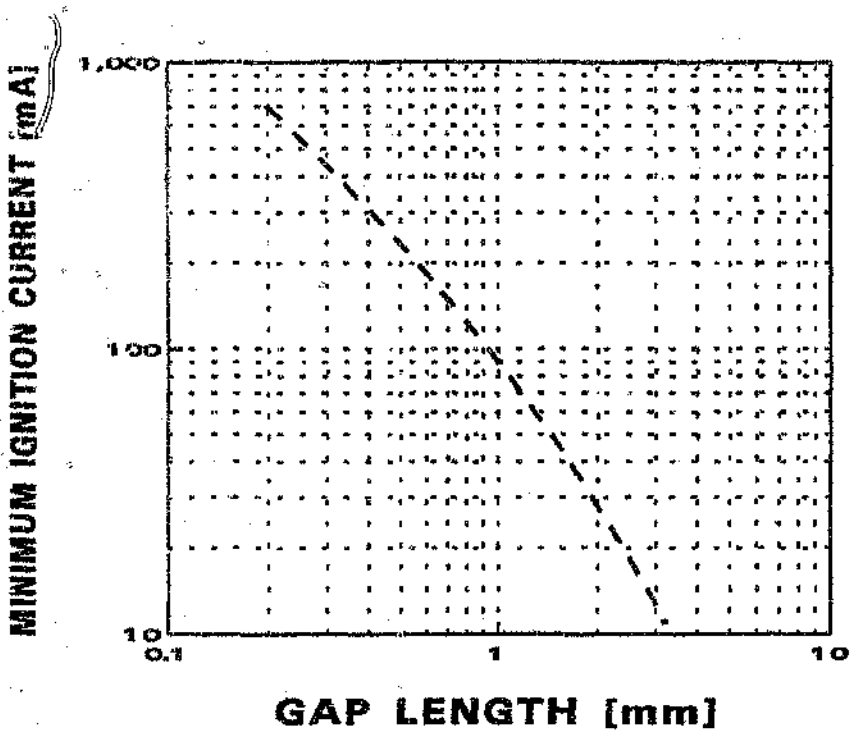



**Figure 6.5** The minimum ignition peak current required to ignite of an air-methane mixture as a function of the spark gap length. The waveshape has a time-to-half value of 50 $\mu$s. Steel electrodes were used.

# 5 CONCLUSIONS

Some useful data has been obtained from the CSIR experiment. The criteria for methane sensitivity (from Figure 6.5) will be used in this thesis.

A more extensive experimental programme and a theoretical understanding of the mechanisms of methane ignition are required to address the discrepancies between the results of the CSIR study and some of the results in the literature.

# CHAPTER 7

# THE SENSITIVITY OF CONVENTIONAL DETONATORS

## 1 CONSTRUCTION OF A CONVENTIONAL ELECTRIC DETONATOR

Figure 7.1 shows the basic construction of a conventional electrical detonator. The detonator consists of the following functional elements:

### 1.1 The operating mechanisms

The operating mechanism is a thin nichrome wire that has been dipped/covered with a temperature-sensitive pyrotechnical explosive. An electrical current is passed through the nichrome wire to heat it to a temperature that is sufficient to ignite the pyrotechnical explosive. This element will be referred to as the fuse head.

### 1.2 Delay element and base charge

When all the detonators in a circuit are initiated by setting off the operating mechanism, it is desirable in some cases to use a delay time to allow sequential shot firing. For this reason, a delay element is included in some of the detonators. A base charge is also required to provide sufficient energy to initiate the explosives in a particular hole.

### 1.3 Housing

The detonator is housed in a tube. In fiery mines, this is normally made of copper to prevent the ignition of any methane gas which may be released by the explosion.

### 1.4 Static protection

It can be seen from Figure 7.1 that an insulating sleeve has been used to protect the fuse head from electrical sparks. This insulating sleeve is around the fuse head and there are spur electrodes on the lead wires to aid sparkover between the spurs and the detonator tube.

The electrical sensitivity of the detonator is simply adjusted by changing the thickness of the nichrome wire. This sensitivity relationship has already been discussed in Chapter 5 and is part of the FSD design.

Geldenhuys (1981) was commissioned to investigate the lightning sensitivity of the detonators which were used in South African Collieries in the early 1980s. This chapter will summarise the results of that investigation.

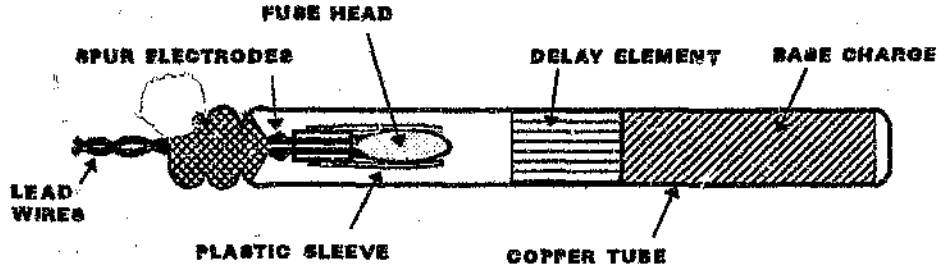



**Figure 7.1** The construction of an electrostatically-protected electrical detonator.

## 2 TYPES OF DETONATORS TESTED

Two types of differently constructed detonators were tested at two different levels of energy required to set off the detonators.

The difference in construction of the two types is that one of the two designs incorporated static-electricity protection, as shown in Figure 7.1, and the other design did not.

The three different types are listed in Table 7.1.

Table 7.1 Different types of conventional detonators tested

| Type of detonator | Sensitivity level | Construction | Bridge wire resistance |
|---|---|---|---|
| Instantaneous detonator, Type 0 | 0 | No static protection | 1.41 Ω |
| Carrick Type 0 | 0 | Static-protected | 1.41 Ω |
| Carrick Type 1 | 1 | Static-protected | 0.25 Ω |

Figure 7.2 shows an equivalent electrical circuit diagram of a conventional electrical detonator, showing the bridge wire resistance ($R_F$) and the resistance of the detonator lead wires ($R_W$). The average resistance of both of the lead wires together, each with a length of 1.5 m, was 0.57 Ω. This implies that $R_W$ = 0.28 Ω. The figure also shows the insulation characteristic of the detonator shell to the internal electrical circuit. The voltage required to cause a spark breakdown between the detonator shell and the wires is $U_B$.

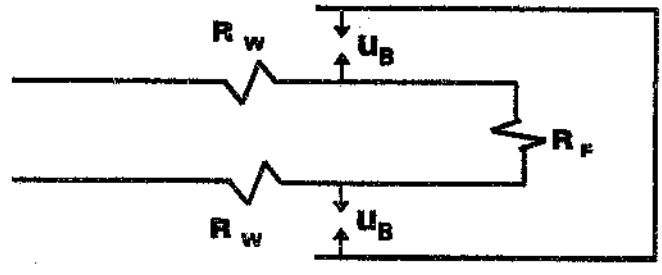



Figure 7.2 The electrical equivalent circuit of a conventional electrical detonator

## 3 SPARKS TO THE FUSE HEAD

If there is an electrical spark to the chemical compound of the fuse head, it can set off the detonator at much lower levels of current and energy than normally required through the bridge wire.

A paper by Marshall (1941) gives much attention to the problem of sparks occurring to the fuse head. The solution proposed in his paper is the bonding of one of the lead wires to

the metal shell of the detonator. This solution can be quite successful but has two drawbacks:

(1) if the shells of two detonators are in electrical contact, so much current may flow via this alternative path that the detonator fails to operate when it should;

(2) If the insulation protecting the detonator from the environment has been removed, low stray voltages (capable of producing high currents) can set off detonators inadvertently.

The static-protection scheme shown in Figure 7.1 is regarded as a better protection method because it is as effective as the shunt method and does not suffer from the above drawbacks.

The instantaneous detonator used in South African collieries up to the middle 1980s did not have any static protection built into the detonator. For this reason, this type of detonator was evaluated for the mechanism where there is a spark to the fuse head. This detonator was compared with two other detonators that contained static protection.

The test was conducted as shown in Figure 7.3. A high-voltage pulse with a 0.5/700 $\mu$s waveshape was applied to the detonator shell with both the leads shorted together and earthed. A rather large resistor was connected in series with the circuit to limit the potential energy to levels below the normal ignition energy of the detonators.

The results are given in Table 7.2 where it can be seen that not a single detonator with static protection failed, whereas, in a high percentage of cases, the detonator without static protection failed at very low spark current levels.

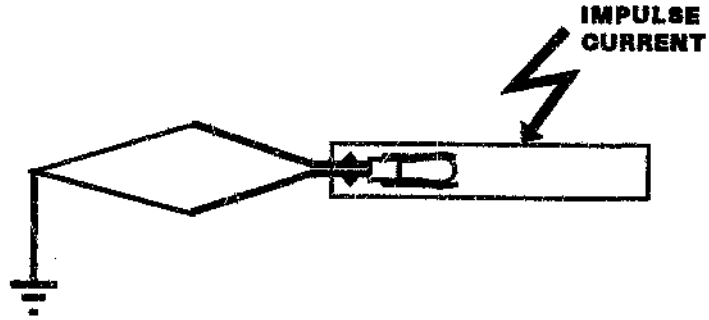



**Figure 7.3** Electrical sparking to the fuse-head test configuration. The high-voltage impulse current was limited by a resistor and the waveshape was 0.5/700 $\mu$s.

It is believed that several of the accidents that occurred in the early 1980s were due to the instantaneous Type 0 detonator being set off by this mechanism.

This type of detonator was withdrawn from shallow collieries in the late 1980s.

**Table 7.2** Results of electrical sparking to the detonator fuse head. The voltage applied had a peak of 6 kV and a 0.5/700 $\mu$s waveshape.

| R (Ω) | Instantaneous Type 0 detonator - % ignited | Type 0 Carrick detonator - % ignited | Type 1 Carrick detonator - % ignited |
|---|---|---|---|
| 2.2 k | 90 % | 0 % | 0 % |
| 6.6 k | 70 % | 0 % | 0 % |
| 17.6 k | 60 % | 0 % | 0 % |
| 100.0 k | 40 % | 0 % | 0 % |
| 800.0 k | 25 % | 0 % | 0 % |

## 4 LIGHTNING-TYPE IMPULSE CURRENT IN NORMAL MODE

The mechanisms through which detonators are set off in the normal mode where current flows through the bridge wire were discussed earlier in this chapter. The mathematical relationship between electrical parameters and the ignition of the detonator is the same as that described in equation 5.1 in Chapter 5 (responsible for blown fuses in the FSDs). The energy ($E_D$) released in the fuse head can be calculated from the resistance of the bridge wire and the waveshape and amplitude of the current passing through the detonator.

$$E_D = R_F \int i^2 (t)\, dt \quad \ldots\ldots\ldots\

were tested as well. A very slight increase in energy required on the longer pulses indicate that ignition takes place at a constant energy input for pulses with shorter durations than 700 $\mu$s. The thermal time constant was not established, but it is quite likely that for maximum durations of multiple flashes (1 s) the energy required will be constant.

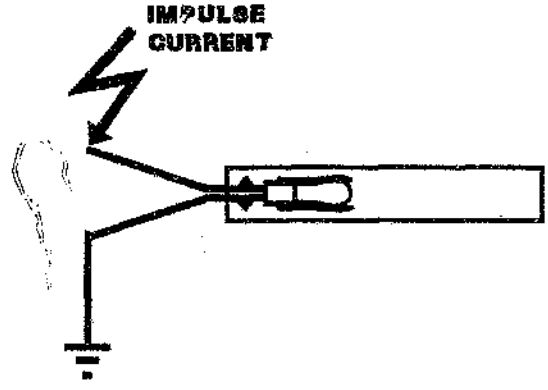



**Figure 7.4** The normal mode of current flow through a detonator

**Table 7.3** The peak current and energy required to set off the different types of detonators

| Current waveform | Ignition current peak and energy of detonator | | |
|---|---|---|---|
| | Instantaneous Type 0 | Carrick Type 0 | Carrick Type 1 |
| 1.2/44 $\mu$s | I = 9.05 ± 0.18 A<br>E = 3.52 mJ | I = 9.38 ± 0.18 A<br>E = 3.78 mJ | I = 42.8 ± 1.7 A<br>E = 11.6 mJ |
| 0.5/700 $\mu$s | I = 2,43 ± 0.05 A<br>E = 4.25 mJ | N/A | I = 12 ± 0.26 A<br>E = 12.1 mJ |
| 100/860 $\mu$s | I = 2.19 ± 0.05 A<br>E = 4.18 mJ | N/A | N/A |

The results of Table 3 are used throughout this thesis where the current required to set off a Type 0 or 1 detonator is of concern.

# 5 BREAKDOWN VOLTAGE FROM THE TUBE TO THE ELECTRICAL CIRCUIT

The impulse breakdown voltage ($U_B$) between the detonator tube and the lead wires was determined for all three types of detonators. A 1.2/50 $\mu$s voltage waveshape was used for this purpose. The data are based on a statistical breakdown method.

Figures 7.5 and 7.6 give the results of this test.

The results indicate that "stray" voltages of up to 1 kV peak cannot penetrate the detonator circuit from the tube end. This provides a substantial protection against AC power and other low-voltage sources.

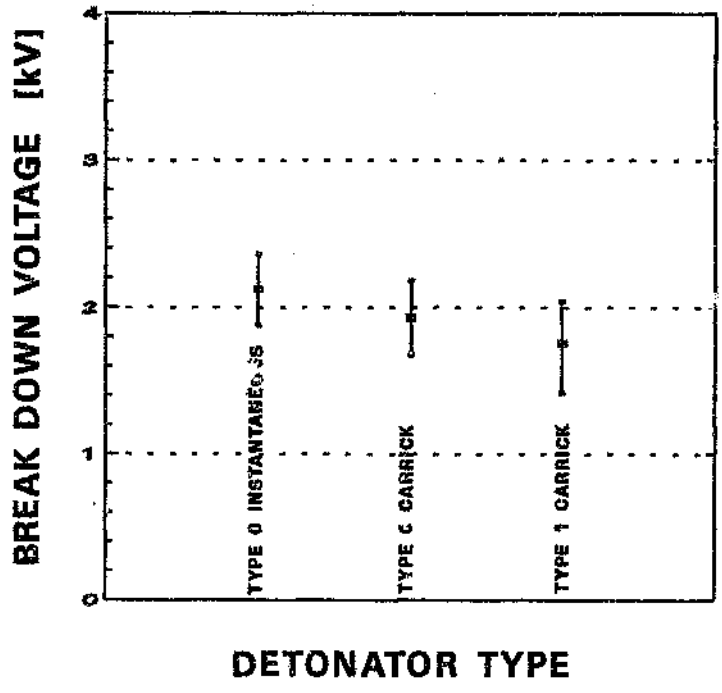



**Figure 7.5** The impulse breakdown voltage of the different detonator types. A 1.2/50 $\mu$s waveshape was used. The tube was positive and the wires negative. The line represents one standard deviation.

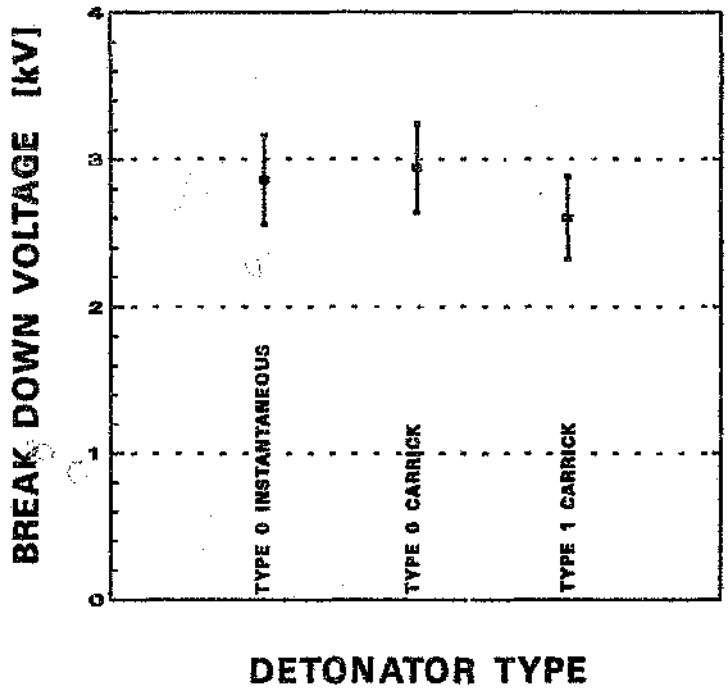



**Figure 7.6** The impulse breakdown voltage of the differe.t detonator types. A 1.2/50 $\mu$s waveshape was used. The tube was negative and the wires positive. The line represents one standard deviation.

# CHAPTER 3

# THE LIGHTNING SURGE VOLTAGE REQUIRED TO SET OFF AN ELECTRICAL DETONATOR

## 1 INTRODUCTION

In this chapter, the question is addressed of what voltage and electric field gradient are required to set off a detonator underground in a colliery.

The lightning surge current required to set off a conventional detonator is given in Chapter 7. This information can be used to determine the corresponding voltage/electric field gradient in the strata to induce the required surge current in a detonator circuit.

The answer to this question will be a direct input to the criteria set for "lightning-safe" detonator specifications and for determining safety-level criteria for the "Mine Lightning Risk Index".

An experimental study was performed to answer the question. Two large blocks of coal were taken from two collieries to the High-voltage Laboratory at the CSIR. High-voltage impulses were applied to the coal blocks in various ways. "Detonators" were made up out of brass tubes of the same size of standard detonators. Two types of dummy explosives were used in the experiment; much care was taken to ensure that the resistivity of the dummy explosives matched the resistivity of the actual commercial explosives.

The first approach to the problem was to study the individual components separately, i.e. the detonator-to-explosive conduction; and second, the conduction through the coal. Then a typical detonator circuit was set up and the full combined detonator-explosive-to-coal configuration was studied.

# 2 AN EQUIVALENT ELECTRICAL CIRCUIT FOR DETERMINING THE CURRENT THAT LIGHTNING INDUCES INTO A DETONATOR CIRCUIT

A simplified, schematic representation of an exploder-detonator layout underground in a colliery is shown in Figure 8.1.

The detonator is embedded in the explosive which, in turn, is inserted into a predrilled hole in the coal. About twenty detonators are connected in series in the coal face. These are led back to the point where the exploder is placed, normally on the floor of the underground workings.

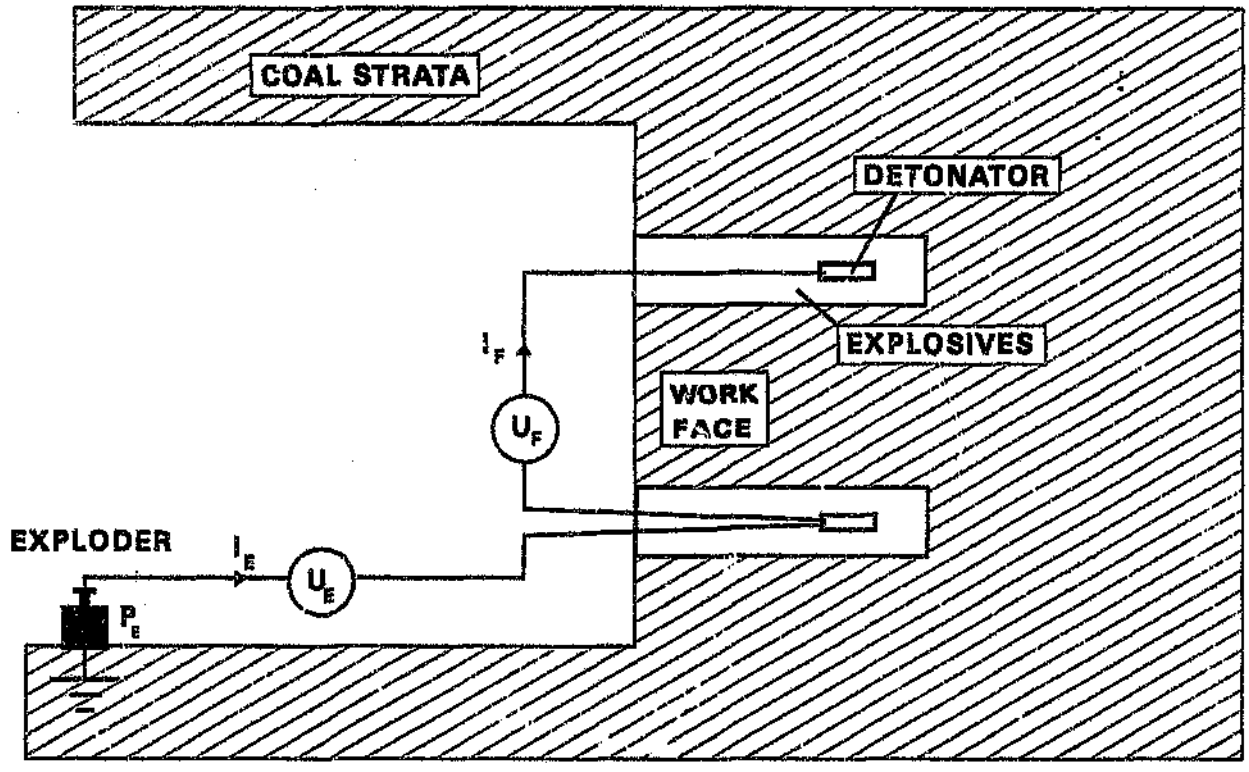



**Figure 8.1** A schematic representation of the voltage and current induced by lightning in an underground coal-seam mining operation.

Figure 8.2 shows an electrical circuit equivalent to the detonator-exploder configuration shown in Figure 8.1.

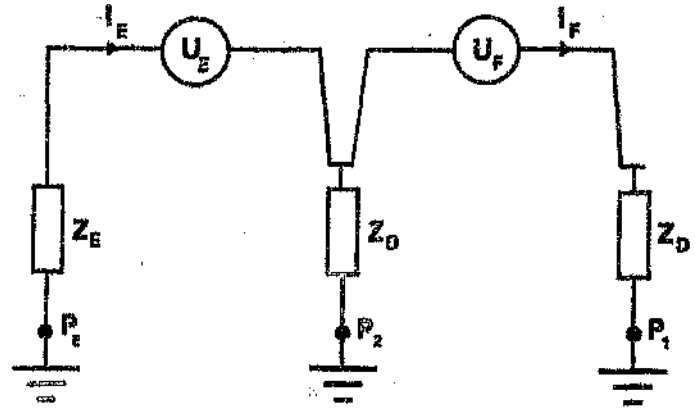



**Figure 8.2** An electrical equivalent representation of the detonator-exploder configuration.

The elements of the circuit are as follows:

$Z_D$ - dynamic impedance of the detonator to the body of the earth
$Z_E$ - dynamic impedance of the exploder-to-coal floor connection

**NOTE:** These impedances are functions of time and current

$U_D$ - is the voltage induced by lightning between the exploder and the coal face.
$U_V$ - is the voltage induced by lightning between adjacent detonators.

The voltage U(t) induced by lightning between any two points $P_1$ and $P_2$ can be calculated by taking the line integral of the electric field E(t) induced by lightning:

$$U(t) = \int_{P_1}^{P_2} E(t)\, dx \quad \ldots\ldots\ldots\

### 2.1 The current flow between the two detonators $I_F$

If the exploder is not connected, the current induced into the circuit $I_F$ is:

$$I_F = U_V / 2 Z_D \quad \ldots\ldots 8.3$$

### 2.2 The current flow between the exploder and the detonators in the work face

It can be assumed that $U_D$ is much smaller than $U_V$ because the distance between detonators is only about 2 m, whereas the distance from the exploder to the face is in excess of 15 m. This implies, with reasonable accuracy, that:

$$I_E = U_D / (Z_E + 0.5 Z_D) \quad \ldots\ldots 8.4$$

## 3 THE IMPEDANCE (TIME AND CURRENT) BEHAVIOUR OF THE ELEMENTS OF A DETONATOR CIRCUIT UNDER LIGHTNING CURRENT IMPULSES

Two elements directly determine the current flow through the detonator circuit:

(1) The explosives
(2) The coal

In this section, the behaviour of both materials under lightning current impulse conditions is investigated; first separately, and then combined in a typical detonator-explosive configuration.

### 3.1 Explosives

#### 3.1.1 The DC resistivity of two commercial explosives

The resistivity of commercial explosives (Coalex and Ajax) was first measured to broadly categorise the electrical parameters of explosives. The electrode configuration used is shown in Figure 8.3.

Dimensions of cartridge and location of electrodes:

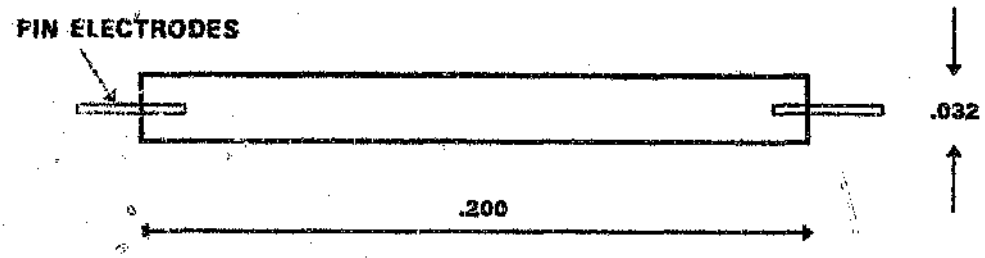



**Figure 8.3** The electrode configuration used to measure the resistance through a stick of explosives

The resistivity of two commercial explosives was determined by inserting a pin on both sides of a stick of explosives, as shown in Figure 8.3, and then measuring the resistance (R) with a Hipotronics Megohm meter.

It is assumed that the resistivity ($\rho$) can be calculated as follows:

$$\rho = \frac{RA}{\ell}$$

$$A = \frac{\pi d^2}{4} \quad \textit{(the cross-sectional area of the explosives)} \cdots\cdots\cdots\cdots\cdots\cdots \quad 8.6$$

d = diameter of the stick of explosives = .032 m
A = $8.04 \times 10^{-4}$ m$^2$
$\ell$ = 0.2 m (the length of the explosives)

The results are given in Table 8.1. Three explosion cartridges of each type of explosive were measured.

Table 8.1 Measurements obtained with the Hipotronics Megohm meter:

| Type of Explosive | Resistance (MΩ) | Resistivity |
|---|---|---|
| Coalex (i) | 450 (at 5 kV) | $1.81 \times 10^6$ Ω.m |
| (ii) | 600 (at 5 kV) | $2.41 \times 10^6$ Ω.m |
| (iii) | 520 (at 5 kV) | $2.09 \times 10^6$ Ω.m |
| Ajax (i) | 0.27 (at 1 kV) | $1.09 \times 10^3$ Ω.m |
| (ii) | 0.24 (at 1 kV) | $.965 \times 10^3$ Ω.m |
| (iii) | 0.30 (at 1 kV) | $1.21 \times 10^3$ Ω.m |

The implications of these results are:

- There is a major difference between the resistivities of Coalex and Ajax (commonly used in coal mines).
- The resistivity of Coalex is so high that it is possible that it can effectively reduce the induction of lightning current into a detonator circuit.
- The resistivity of Ajax is so low (comparatively) that it is possible that it can enhance the induction of lightning current into a detonator circuit.

### 3.1.2 The impulse impedance behaviour of explosives

**Experimental configuration**

From the DC resistance test, it can be seen that the electrical behaviour of different explosives varies widely. This study was further expanded to investigate the impulse behaviour of explosives under typical lightning current conditions and the current density conditions required to set Type 0 and Type 1 detonators off.

The study was conducted by inserting a detonator tube into a dummy cartridge of explosives. This dummy cartridge was then tamped in the normal way inside a metal tube. This is schematically shown in Figure 8.4. The dummy cartridge was first tested to ensure that the resistivity closely matched the resistivity of real explosives, as measured in the previous section.

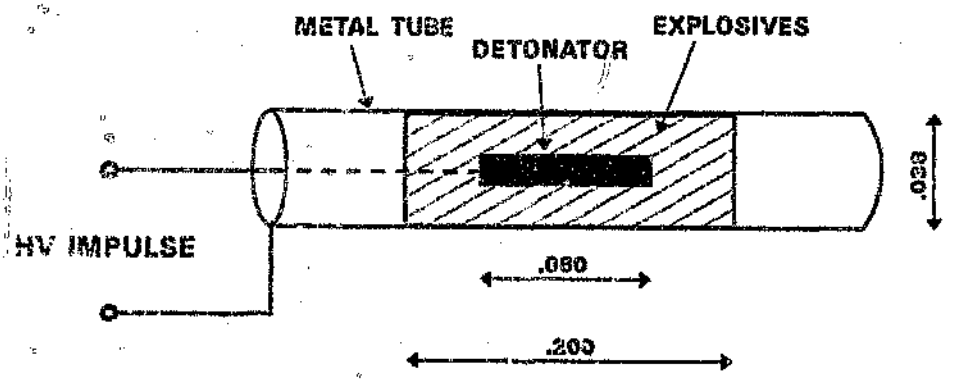



**Figure 8.4** A schematic diagram showing the dummy explosive cartridge tamped inside a metal tube. A detonator was placed inside the explosive as in normal practice and an high-voltage impulse was applied between the detonator and the metal pipe.

### 3.1.3 Calculated (expected) resistance based on the DC resistivity measurements

The resistance between the detonator and the metal tube of Figure 4 can be approximated by the equation:

$$R = \frac{\rho}{2\pi}\left[\frac{1}{\ell_d}(\ln r_2 - \ln r_1) \parallel \frac{1}{2}\left[\frac{1}{r_2} - \frac{1}{r_1}\right]\right] \quad \ldots\ldots\ldots\ldots\ldots\ldots \quad 8.7$$

with
$\ell_d$ = 0.06 m = detonator tube length
$r_1$ = detonator radius = 0.003 m
$r_2$ = tube radius = 0.019 m
$\parallel$ = parallel resistance to allow for fringing.

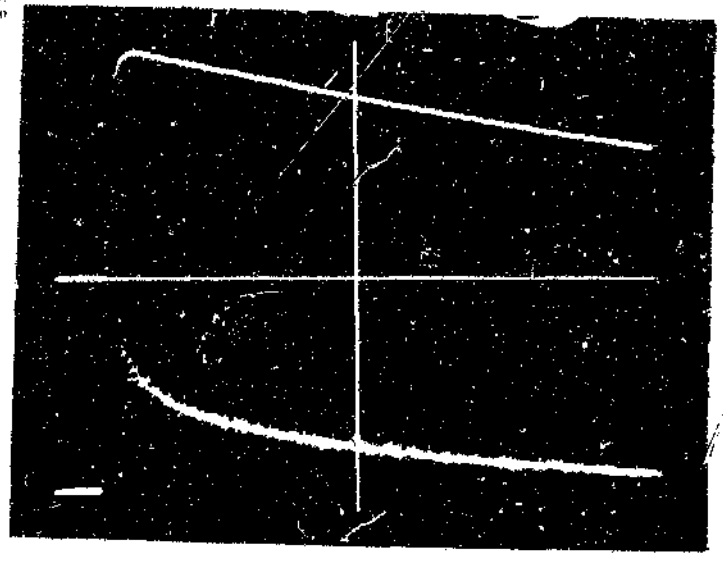
$R = 4.02\,\rho$

Using the values obtained in the resistivity measurement of the explosives, we find that the resistance of a detonator in Ajax is: $\rho = 1 \times 10^3\ 0\ \Omega.m$, $R = 4.0\ k\Omega$

and the resistance of a detonator in Coalex is: $\rho = 2 \times 10^6\ \Omega.m$, $R = 8.0\ M\Omega$

### 3.1.4 Experimental results

Figure 8.5 shows a typical applied voltage waveshape and the discharge current resulting from a voltage impulse.



Applied voltage waveshape

$U_{peak}$ = 19.8 kV

Measured discharge current

$I_{peak}$ = 1 A

50 $\mu$s sweep

**Figure 8.5** Oscillogram showing the applied voltage waveshape and measured impulse current on Ajax (before breakdown)

**Table 8.2** Impedance in Figure 8.5 against time

| Time ($\mu$s) | Z (k$\Omega$) |
|---|---|
| 2.8 | 10 |
| 5.0 | 24 |
| 10.0 | 31 |
| 20.0 | 42 |
| 40.0 | 72 |

**Ajax**

The impedance was calculated at different points of the impulse. This varied from 10 k$\Omega$ at the voltage peak and increased up to 70 k$\Omega$ at 40 $\mu$s. These values are much higher than the calculated 4 k$\Omega$ but are nevertheless in the right order of magnitude.

Two factors could be responsible for this difference. First, it was difficult to get the dummy explosive resistivity to be the same as the "real" explosives. Second, the wax-paper covering of the explosive was not taken into consideration when calculating the resistance. It is rather difficult to evaluate its contribution. However, it effectively acts as an insulator and will increase resistance effectively and substantially.

When the voltage was gradually increased, a "breakdown" of the resistance occurred above 19 kV. A type of hysteresis was found in that once breakdown occurred, subsequent breakdown occurred at a lower level. If the set-up was given time to rest, it recovered to the same breakdown strength as before.

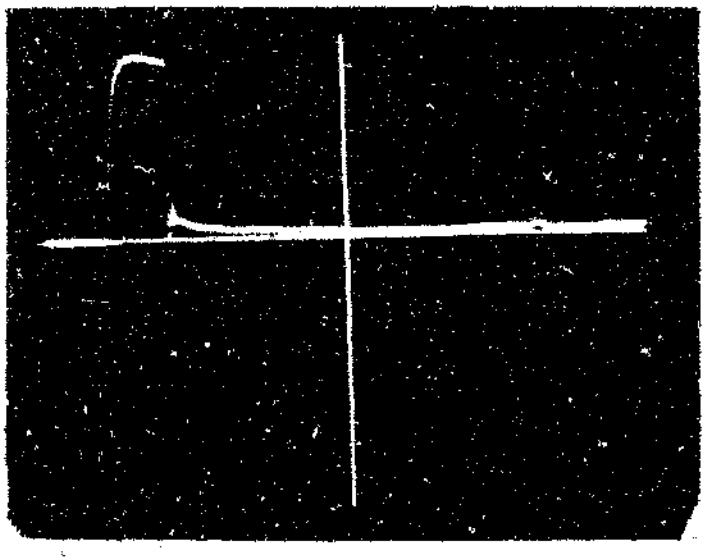
The breakdown is shown in Figure 8.6. After breakdown the resistance drops to 50 Ω.

**Coalex**

The same experiment was conducted on Coalex. The results are shown in Figure 8.7. The results obtained were again very similar to those of Ajax.

The first oscillogram shows the Coalex before breakdown. However, here a small capacitance current is observed initially, whereafter the current drops to practically zero - which is in line with the calculated 8 MΩ.

Again, breakdown occurs; this time at a slightly lower voltage of about 12 kV.

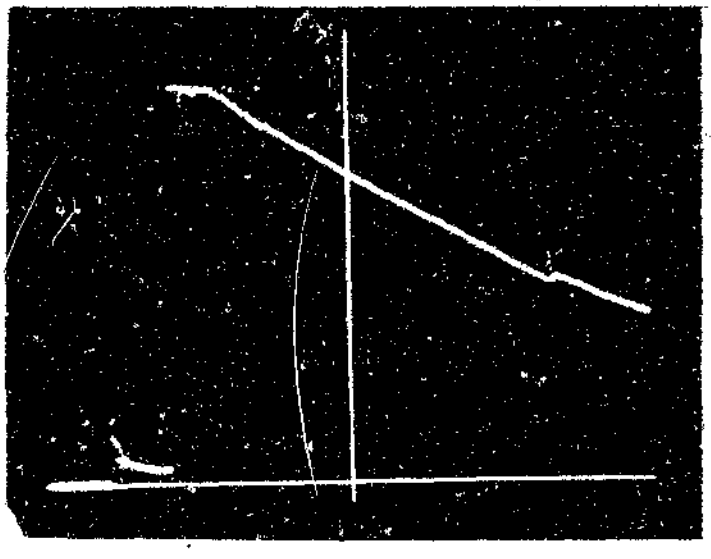


Applied voltage:

U = 16.16 kV

I = 640 mA

Z = 25 kΩ



Current:

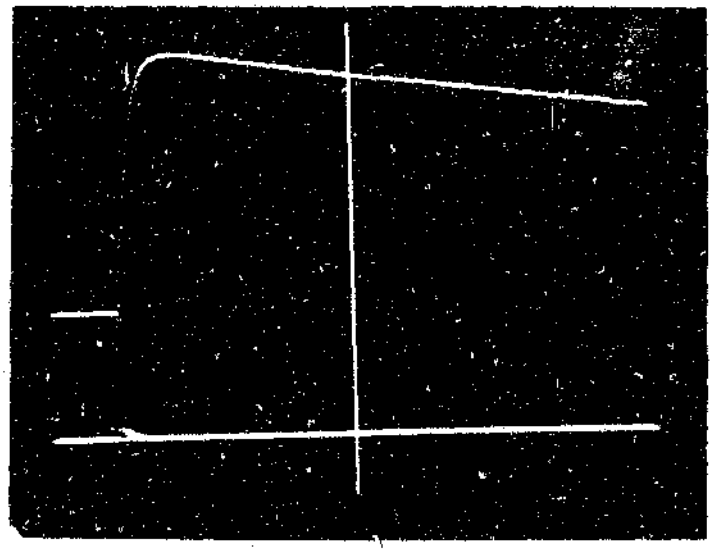
Before breakdown at $U_{peak}$, I = 640 mA

After breakdown, $I_{peak}$ = 16.7 A

| Time | U (kV) | I (A) | Z (Ω) |
|---|---|---|---|
| Before breakdown 2.8 $\mu s$ | 16.16 | 0.64 | 25 k |
| After breakdown | | | |
| 10.0 $\mu s$ | 0.96 | 16.70 | 57 |
| 20.0 $\mu s$ | 0.48 | 13.50 | 36 |
| 40.0 $\mu s$ | 0.48 | 8.16 | 59 |

Figure 8.6 Oscillogram showing the applied voltage (top), which breaks down and collapses to almost 0 V, with an associated step in current (bottom). The impedance after breakdown is also shown.

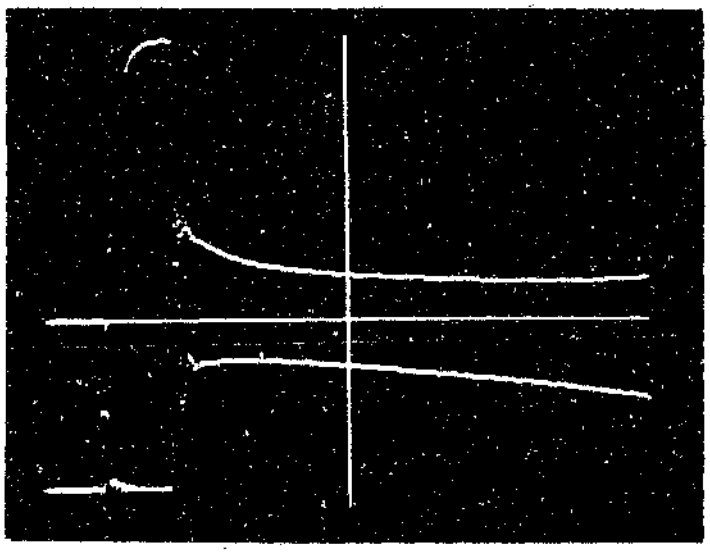
Before breakdown.



U = 11.3 kV peak

I = 960 mA capacitive current

Conductive current is practically zero



U = 12.3 kV peak

Before breakdown:

I = 800 mA capacitive current

After breakdown:

U = 2.48 kV @ 6.4 $\mu$s

I = 10.9 A

Z = 228 Ω

Figure 8.7 Oscillogram of voltage impulse applied to Coalex.
A - before breakdown. B - after breakdown.

# 4 THE IMPULSE IMPEDANCE BEHAVIOUR OF COAL

Experiments were conducted to study the impulse impedance behaviour of coal.

## 4.1 The experimental set-up

To study the lightning current impulse behaviour of coal, two large pieces of coal were taken to the CSIR high-voltage laboratory. The physical dimensions of the sample from Greenside Colliery are shown in Figure 8.8 and are summarised in Table 8.3.

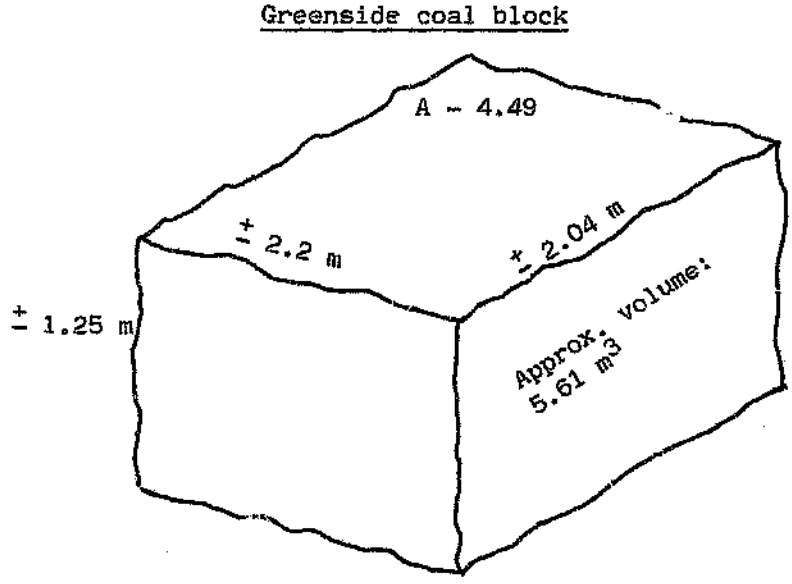



**Figure 8.8** Physical dimensions of the coal block from Greenside Colliery

**Table 8.3** Physical dimensions of the coal blocks used in the experiment.

| | Sigma | Greenside |
|---|---|---|
| Height | 1.30 m | 1.25 m |
| Cross-sectional area | 1.25 $m^2$ | 4.49 $m^2$ |

Impulse voltages ranging from 3 kV to 180 kV were applied across the coal block in the configuration shown in Figure 8.9.

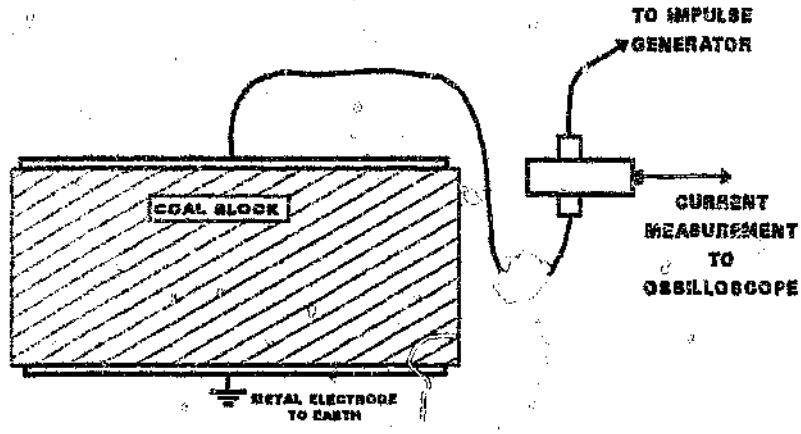



**Figure 8.9** The physical layout of the experiment.

Contact with the top and bottom surfaces of the coal block was made by aluminium foil which was pressed onto the coal surface by a sponge, using mechanical pressure.

The impulse generator circuit used in the experiment is shown in Figure 8.10. A 1/50 $\mu$s waveshape was produced by the generator.

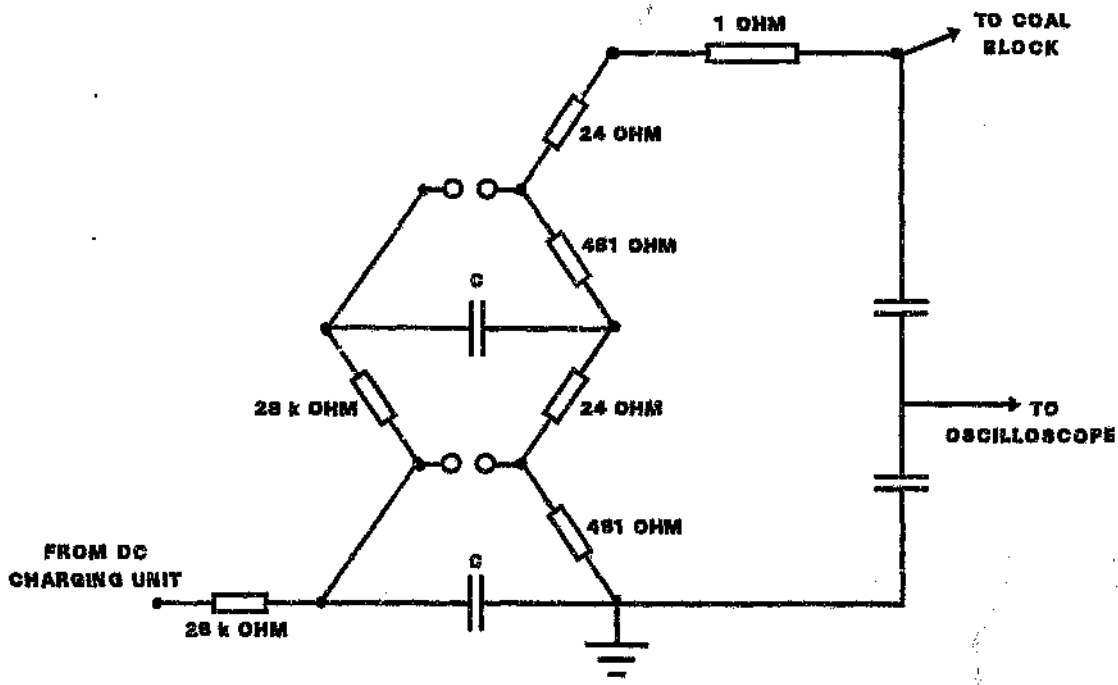



**Figure 8.10** The impulse generator circuit used in the experiment. The generator has a rating of 50 kV per stage. Up to four stages were used.
C = .14 $\mu$F per stage.

## 4.2 Experimental results

The applied voltage and the resulting current were measured and recorded on digital oscilloscopes. The measured values were then converted into electric field intensity (kv/m), current density ($A/m^2$), and resistivity ($\Omega$.m).

It was found that there was a marginal increase in impedance in time - as a particular impulse continued. The resistivity decreased as electric field increased - from an initial value of about 3 k$\Omega$.m down to 1 k$\Omega$.m at higher field intensities. Polarity had almost no effect, as can be seen from the results shown in Figures 8.11 and 8.13.

The results are summarised in Figures 8.11 to 8.14.

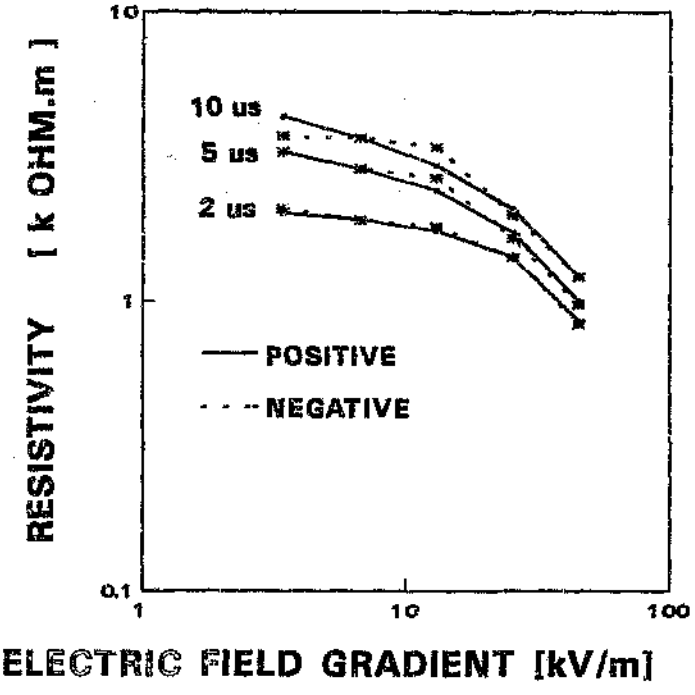



**Figure 8.11** The resistivity as a function of field strength, as measured on the coal block from Sigma Colliery (in a uniform current density field). The results from both positive and negative pulses are shown. Measurements were taken at 2 $\mu$s, 5 $\mu$s and 10 $\mu$s after the impulse peak.

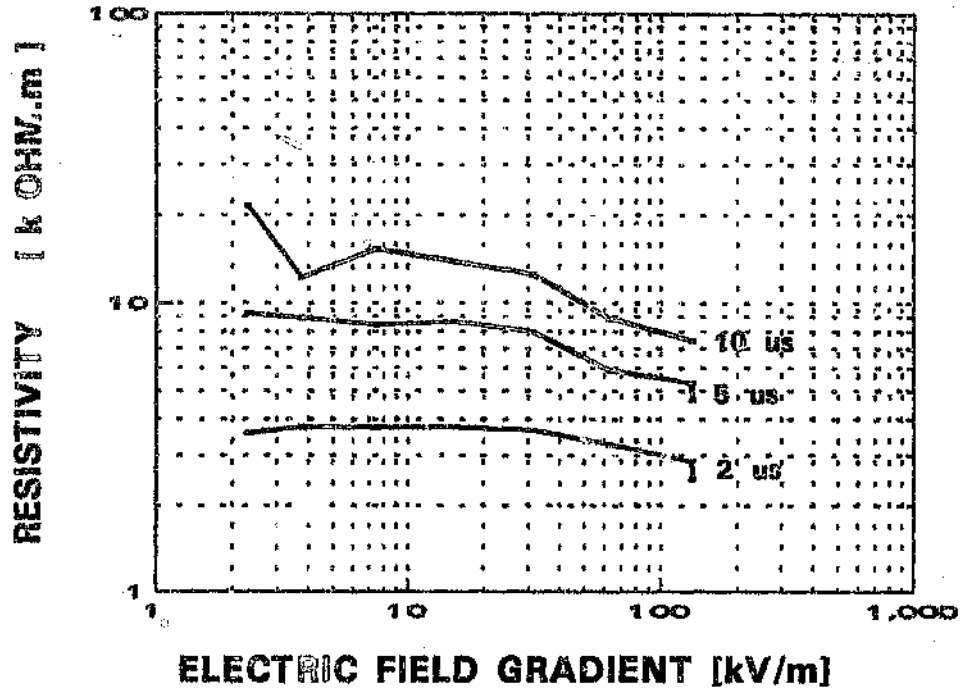



**Figure 8.12** The resistivity as a function of field strength, as measured on the coal block from Greenside Colliery (in a uniform current density field). Measurements were taken at 2 $\mu$s, 5 $\mu$s and 10 $\mu$s after the impulse peak.

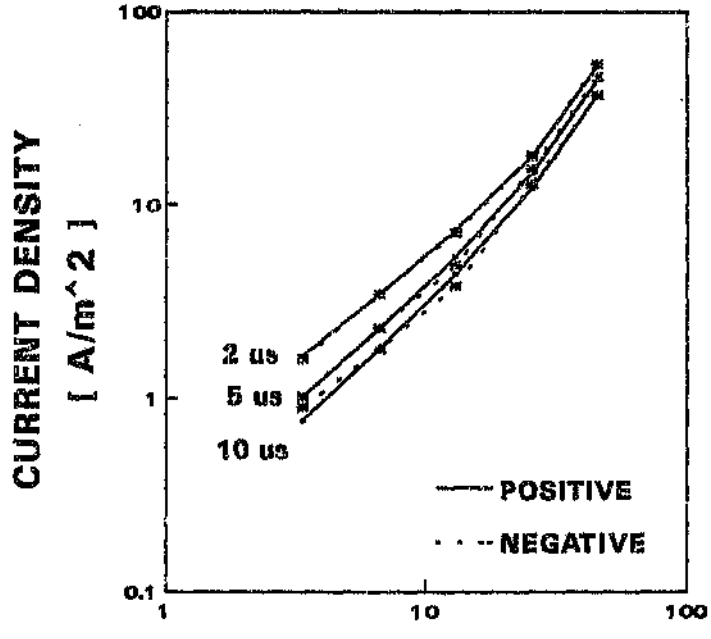



**Figure 8.13** The current density as a function of field strength, as measured on the coal block from Sigma Colliery (in a uniform current density field). The results from both the positive and negative impulses are shown. Measurements were taken at 2 $\mu$s, 5 $\mu$s and 10 $\mu$s after the impulse peak.

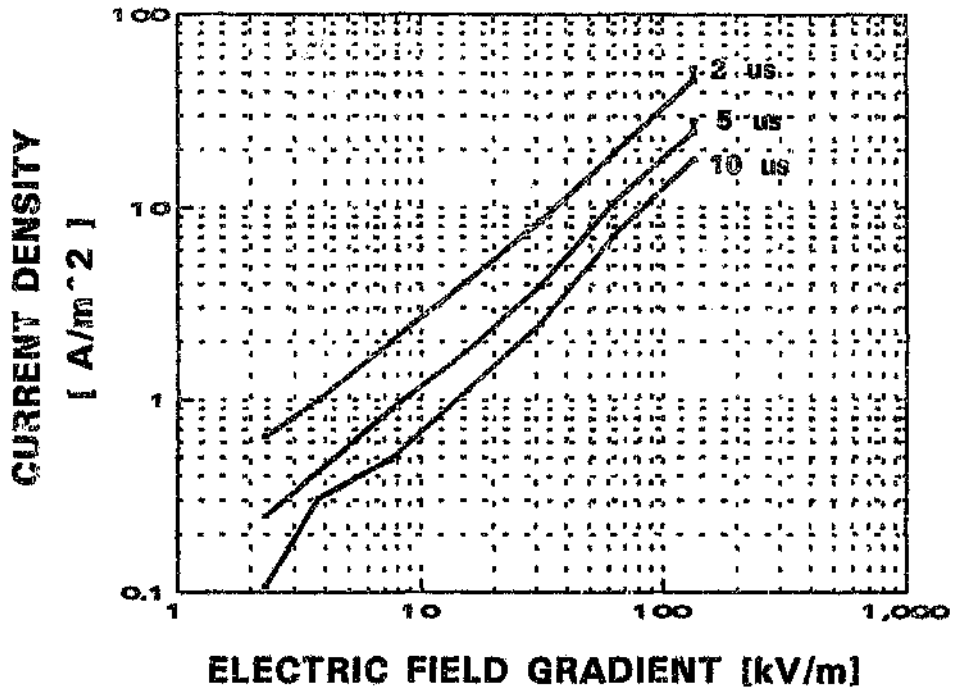



**Figure 8.14** The current density as a function of field strength, as measured on the coal block from Greenside Colliery (in a uniform current density field). Measurements were taken at 2 $\mu$s, 5 $\mu$s and 10 $\mu$s after the impulse peak.

# 5 THE IMPULSE IMPEDANCE BEHAVIOUR OF A DETONATOR IN AN EXPLOSIVES-COAL INSTALLATION

The last experiment conducted in the series was to study the current flow/impedance of a detonator embedded in explosives and stemmed into a hole in the coal, as normally done in underground blasting operations.

The configuration used is shown in Figure 8.15. The Greenside coal block was used in this case. The impulse generator circuit that was used in similar to that shown in Figure 8.10, with an external front resistance of $R_F = 1\ \Omega$. Up to four stages were used, depending on the voltage required. Impulses ranging from 2 kV to 200 kV were applied and the applied voltage and resulting current wave shapes were recorded on floppy discs using digital storage oscilloscopes.

The dummy explosive used was Ajax and the stemming was a clay-based stemming.

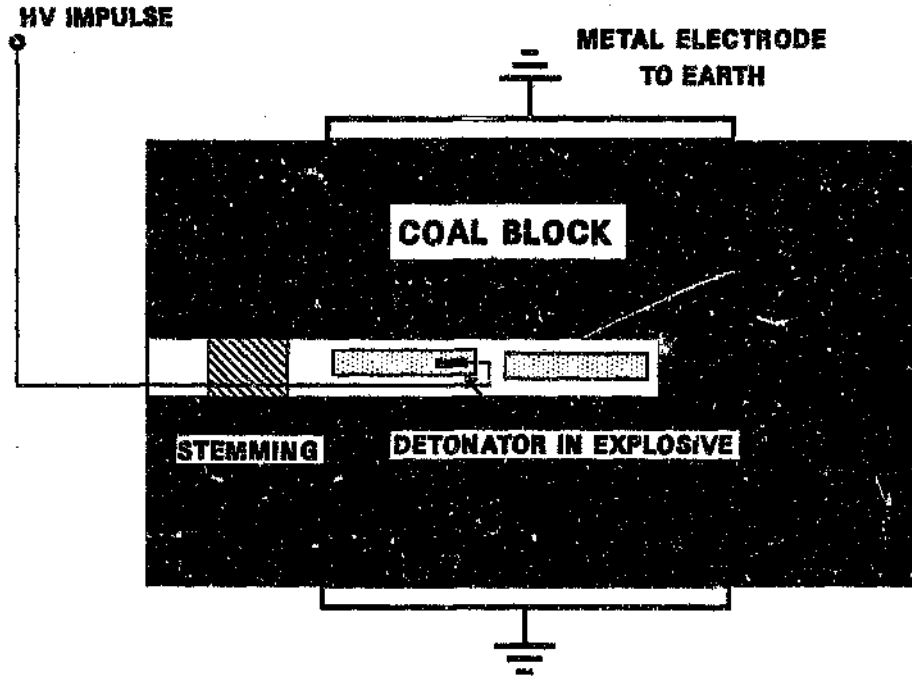



**Figure 8.15.** A cross-sectional schematic diagram showing how the dummy explosive-detonator circuit was constructed in the CSIR HV laboratory.

## 5.1 The experimental results

The experimental results showed a rather complex picture. First, a strong time dependence of impedance was observed in all cases. The impedance increased with time. Second, as the applied voltage was increased, the impedance reduced. This complex picture can be

rationalised into three categories. Table 4 shows a list of the impulses applied to this configuration.

**Table 8.4** The impulses applied to the coal block in chronological order. + Indicates the positive polarity applied to the detonator.

| Date | No. | Peak voltage | Peak current |
|---|---|---|---|
| 20/8/91 | 1 | + 2.0 kV | - |
| | 2 | + 5.0 kV | - |
| | 3 | + 10.0 kV | - |
| | 4 | + 20.0 kV | - |
| | 5 | + 30.0 kV | - |
| | 6 | + 40.0 kV | 0.32 A |
| | 7 | + 60.0 kV | 1.60 A |
| | 8 | + 80.0 kV | 3.20 A |
| | 9 | + 100.0 kV | 9.60 A |
| | 10 | + 125.0 kV | 14.40 A |
| | 11 | + 150.0 kV | 19.20 A |
| | 12 | + 175.0 kV | 28.80 |
| | 13 | + 200.0 kV | Breakdown |
| | 14 | + 180.0 kV | " |
| | 15 | + 160.0 kV | " |
| | 16 | + 140.0 kV | " |
| | 17 | + 3.2 kV | 0.024 A |
| 22/8/91 | 18 | + 5.0 kV | 0.056 A |
| | 19 | + 10.0 kV | 0.104 A |
| | 20 | + 20.0 kV | 0.860 A |
| | 21 | + 30.0 kV | 1.500 A |
| | 22 | + 40.0 kV | 1.740 A |
| | 23 | + 60.0 kV | 14.700 A |
| | 24 | + 80.0 kV | Breakdown |
| | 25 | + 100.0 kV | " |
| | 26 | + 125.0 kV | " |
| | 27 | + 140.0 kV | " |
| | 28 | + 150.0 kV | " |
| | 29 | + 160.0 kV | " |
| | 30 | + 175.0 kV | " |
| | 31 | + 200.0 kV | " |
| | 32 | - 40.0 kV | " |

### 5.1.1 Time dependence of impedance

In all cases, the impedance of the coal increases rapidly in time. For example, Figure 8.16 shows an applied impulse with a peak of 20 kV. Initially, after 2.3 $\mu$s, the impedance is 23.8 kΩ. By the end of the impulse, the impedance has increased to 406 kΩ. The time increase effect of impedance will tend to limit the current that passes through a detonator. The result of an increase of impedance with pulse duration is inconsistent with the work by Oettlé (1988) in uniform granular soil where the impedance decreased significantly with the pulse duration.

### 5.1.2 Voltage dependence of current

A synthesis of the results shows that three distinct phenomena were observed. They fell into the following zones:

**Zone 1 - No breakdown/ionisation (0 kV to approximately 40 kV)**

In this zone, the current in the circuit is limited by the combined resistance of the coal and the explosives. However, because the explosive resistance is greater, it dominates the combined resistance. This is shown in Figure 8.16 which shows an impulse with a peak amplitude of 20 kV. This result is almost identical to the result of Figure 8.5 which supports the above statement: that the configuration is dominated by the explosive.

**Zone 2 - Breakdown through the explosives (from 40 kV to 160 kV)**

In this zone, the current in the circuit is limited mainly by the resistance of the coal. The explosives have broken down electrically and are ionised and appear as a low impedance.

The sparkover-ionisation process can be observed in Figure 8.17, where the applied voltage peak is 40 kV.

The current jumps up to a higher level and collapses again as the ionisation process initiates and extinguishes. At 100 kV, the ionisation is so well established that the only evidence of it is the fact that the initial resistance has dropped from 20 kΩ to less than 10 kΩ (see Figure 8.18).

**Zone 3 - Breakdown through the explosives and the coal block (above 160 kV)**

In this zone, complete sparkover occurs from the detonator, through the coal to the metal electrodes. However, this will never happen in a circuit at a work face in a mine as the electrodes do not exist in nature.

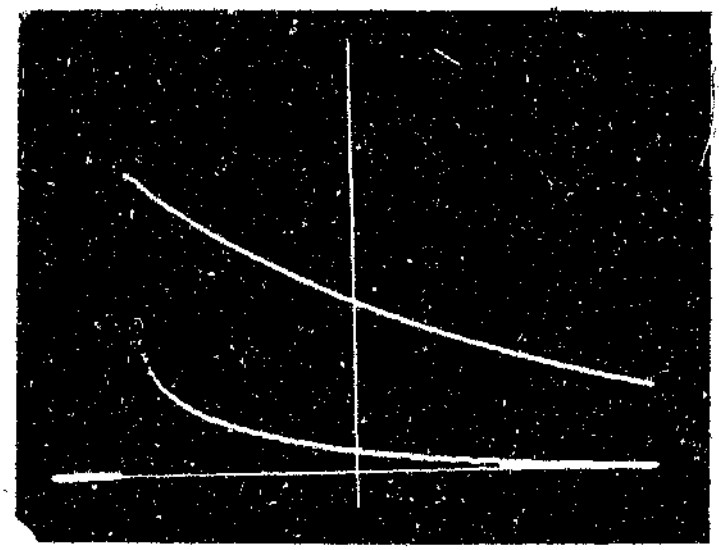



**Figure 8.16** Zone 1: The current impulse waveshape resulting from the application of a 20 kV peak 1/50 μs impulse to the configuration of Figure 8.15 (Impulse No. 20 of Table 8.4). Positive voltage polarity was applied to the detonator.

Voltage, current and impedance values are shown in the table below at the different time intervals.

| Time (μs) | Voltage (kV) | Current (A) | Impedance (kΩ) |
|---|---|---|---|
| 2.3 | 20.4 | 0.856 | 23.8 |
| 5.0 | 19.5 | 0.432 | 45.1 |
| 10.0 | 18.0 | 0.312 | 57.7 |
| 20.0 | 15.5 | 0.192 | 80.7 |
| 40.0 | 11.6 | 0.088 | 132.0 |
| 80.0 | 6.5 | 0.016 | 406.0 |

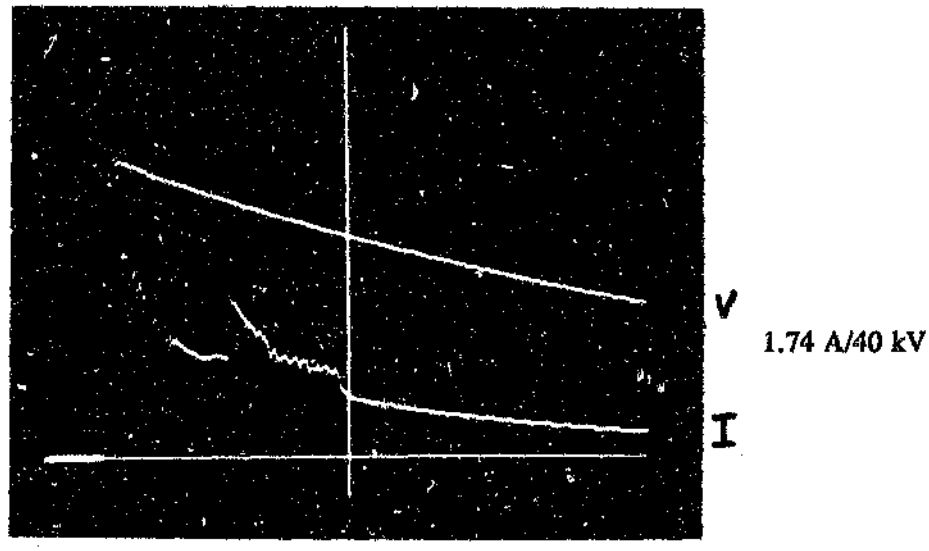
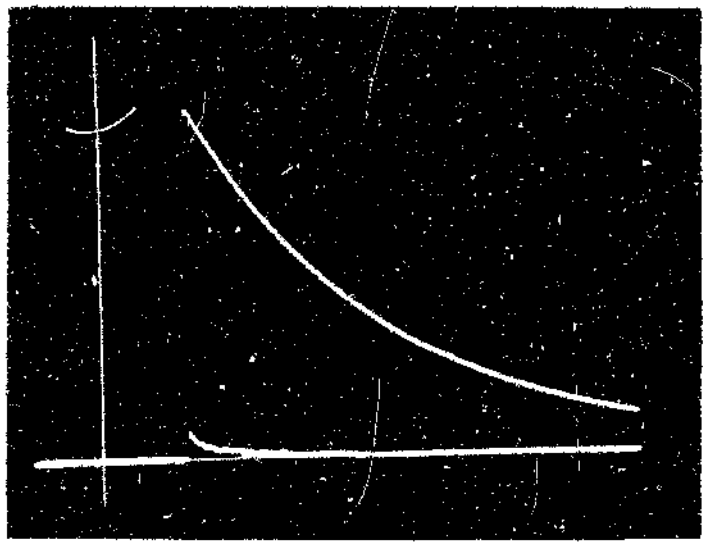



**Figure 8.17** Transition from Zone 1 to Zone 2: The current impulse waveshape resulting from the application of a 40 kV peak 1/50 μs impulse to the configuration of Figure 8.15 (Impulse No. 22 of Table 8.4). Positive voltage polarity was applied to the detonator.

Voltage, current and impedance values are shown in the table below at the different time intervals.

| Time (μs) | Voltage (kV) | Current (A) | Impedance (kΩ) |
|---|---|---|---|
| 2.30 | 40.2 | 1.74 | 23.1 |
| 6.05 | 37.7 | 0.98 | 38.9 |
| 10.80 | 34.9 | 1.33 | 26.2 |
| 20.00 | 30.6 | 0.75 | 40.8 |
| 40.00 | 23.1 | 0.26 | 90.0 |
| 80.00 | 13.1 | 0.048 | 272.0 |



9.6 A/95 kV

200 $\mu$s sweep

**Figure 8.18** Zone 2: The current impulse waveshape resulting from the application of a 100 kV peak 1/50 $\mu$s impulse to the configuration of Figure 8.15 (Impulse No. 9 of Table 8.4). Positive voltage polarity was applied to the detonator.

Voltage, current and impedance values are shown in the table below at the different time intervals.

| Time ($\mu$s) | Voltage (kV) | Current (A) | Impedance (k$\Omega$) |
|---|---|---|---|
| 2.30 | 95.0 | 9.60 | 9.9 |
| 5.00 | 91.0 | 6.40 | 14.2 |
| 10.00 | 84.4 | 3.20 | 26.4 |
| 20.00 | 72.4 | 2.40 | 28.9 |
| 40.00 | 53.8 | 0.80 | 67.2 |
| 30.00 | 29.6 | - | - |

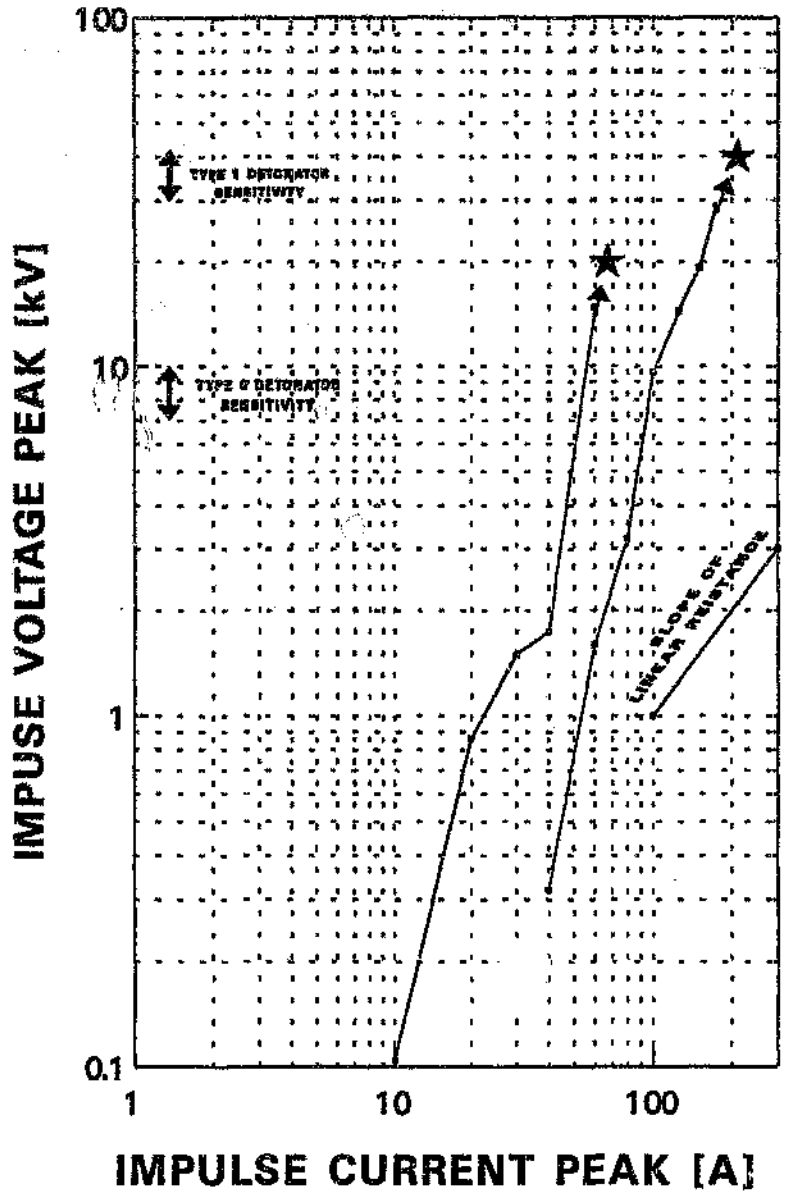



**Figure 8.19** The applied voltage peak versus the peak current measured through the detonator circuit for the sequence of impulses as applied in Table 8.4. Note the difference between the first and second series of tests.

★ The next impulse resulted in a complete breakdown from the detonator to the earth electrode.

## 5.2 Ageing of the test configuration

The sequential results indicated that the experimental configuration "aged" with each applied impulse. This is quite apparent if the first and second 60 kV impulses are compared (see Table 8.4 or Figure 8.19). The observed reduction in resistance could be postulated to be caused by carbonisation of the coal during impulse which gradually reduces the resistance of the configuration. This effect must be taken into consideration in order to avoid erroneous conclusions being drawn from the results.

## 5.3 Effect of polarity

The effect of polarity was not checked and is not known at present. The results in the uniform case (Section 8.4) did not indicate a polarity effect. However, this may not be true for the non-uniform case.

## 5.4 An empirical mathematical relationship between current and voltage

In order to interpolate and slightly extrapolate the data obtained in the experiment, a mathematical regression relationship is required. The least squared method was used to do this and the results are shown in Figure 8.20. A power relationship gives the best regression coefficient:

$$I = 5.67 \times 10^{-6} V^{3.03}$$

or

$$V = 53.9 I^{0.33}$$

$$r^2 = 98.01$$

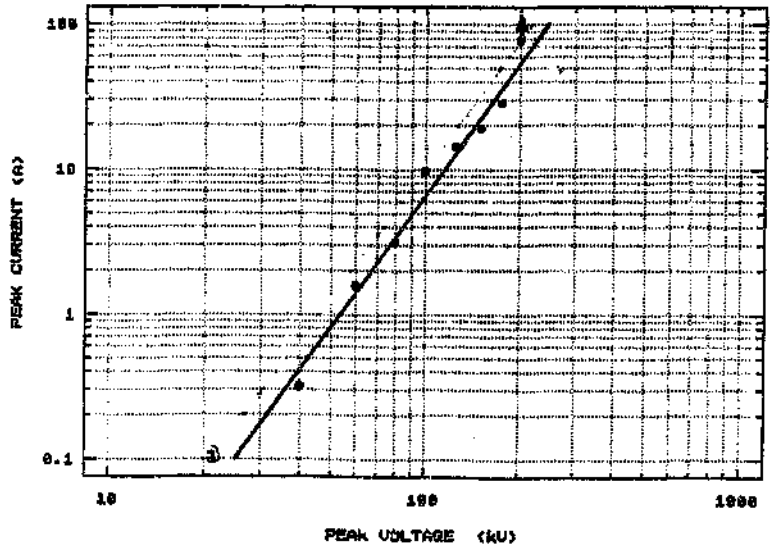



**Figure 8.20** Mathematical regression line fitted to the data of Figure 8.19.

The regression was done on the first round of test data. The reason for this is that this is the state in which the detonator circuit will be when stressed by lightning.

# 6 GENERALISATION OF THE RESULTS

To apply the results to different coal-seam resistivities and detonators, a generalised model is required. (The results obtained here only apply to the specific coal block and detonator in Section 8.4.)

## 6.1 Explosives-detonator-coal model

From the results obtained, it is clear that there are two mechanisms at work in a detonator circuit:

- The impedance of the explosives
- The impedance of the coal

The explosives act mainly as an insulation medium and are therefore modelled as a sparkover gap.

The impedance of the coal acts as a current-dependent, time-dependent and resistivity-dependent medium.

## 6.2 Comparison with the Oettlé model

Oettlé (1988) refined a model for the calculation of the effect of ionisation in concentrated earth electrodes. Geldenhuys et Oettlé (1987) subsequently carried out further analysis and derived an expression for impulse impedance:

$$\alpha = 12\frac{\rho^{0.74}}{h^{0.4}\ I^{0.3}} \qquad \ldots\ldots 8.8$$

where $\alpha$ = impulse impedance
$\rho$ = DC resistivity
h = "characteristic dimension of the electrode"
I = peak impulse current

This model has been compared to the results obtained in the present experiment. The results of the comparison are shown in Figure 8.21.

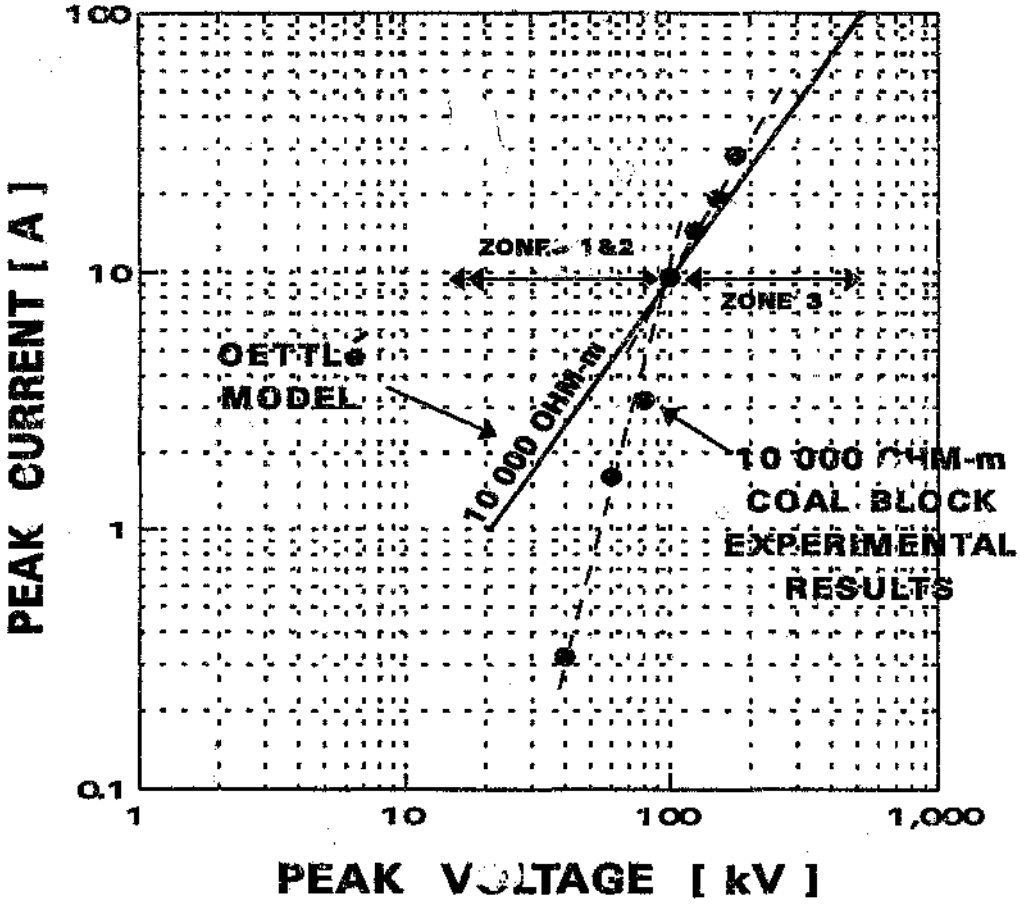



**Figure 8.21** Comparison between the experimental data and the Oettlé model.

To fit the Oettlé model reasonably well to the experimental data, the "characteristic dimension" h was set to h = 0.2; using this, the Oettlé model fits the experimental data above 100 kV particularly well.

Because of the lack of more experimental data, the Oettlé model has been adopted for the purpose of determining the effect of coal with different resistivities:

$h = 0.2$ m

$\alpha = 22.8\ \rho^{0.74}/I^{0.3}\ \Omega$

The Oettlé model (for various different resistivities) is shown in Figure 8.22.

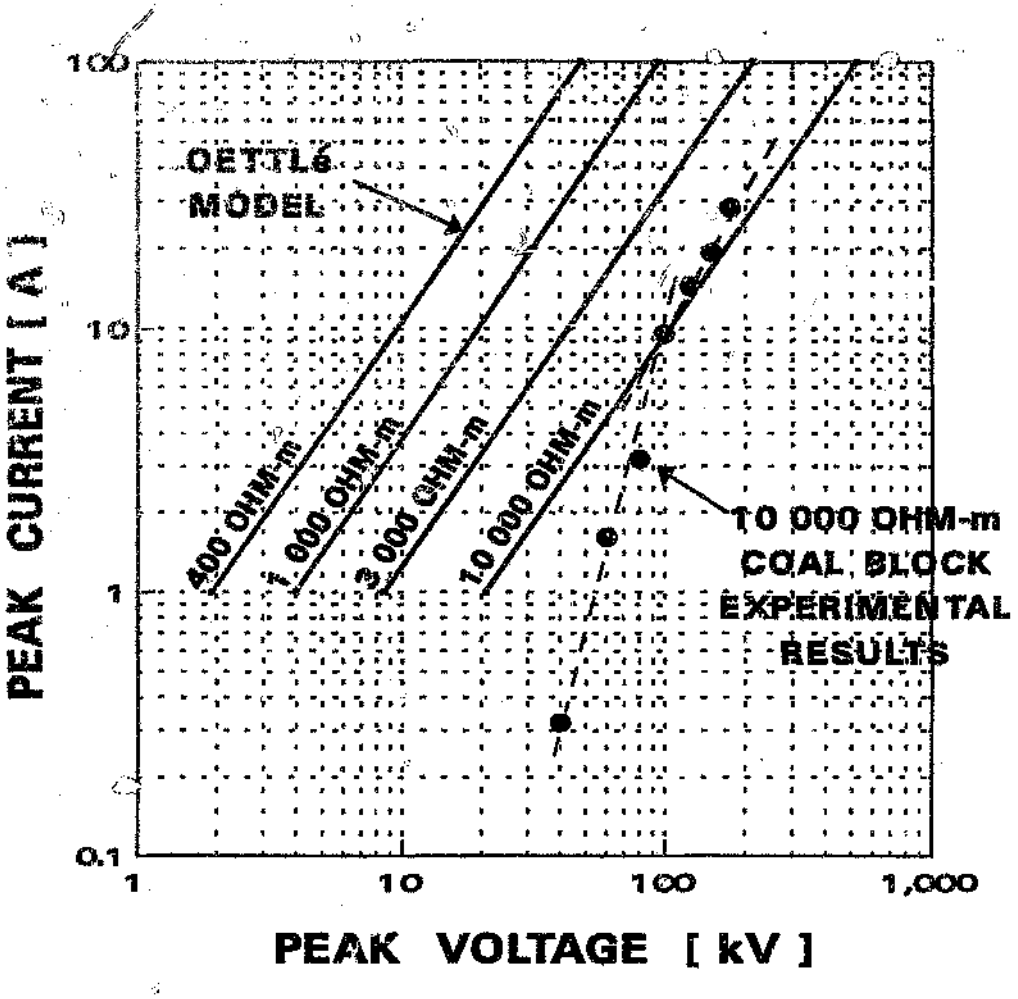



**Figure 8.22** The Oettlé model used for various coal resistivities

## 6.3 A model for the exploder and the detonator

Following the discussion of 6.1 and the adoption of the Oettlé model in 6.2, it is obvious that models for a detonator and an exploder on the mine floor would be as shown in Figure 8.23.

The relationship between coal resistivity and the voltage required to produce various magnitudes of impulse current is shown in Figure 8.24.

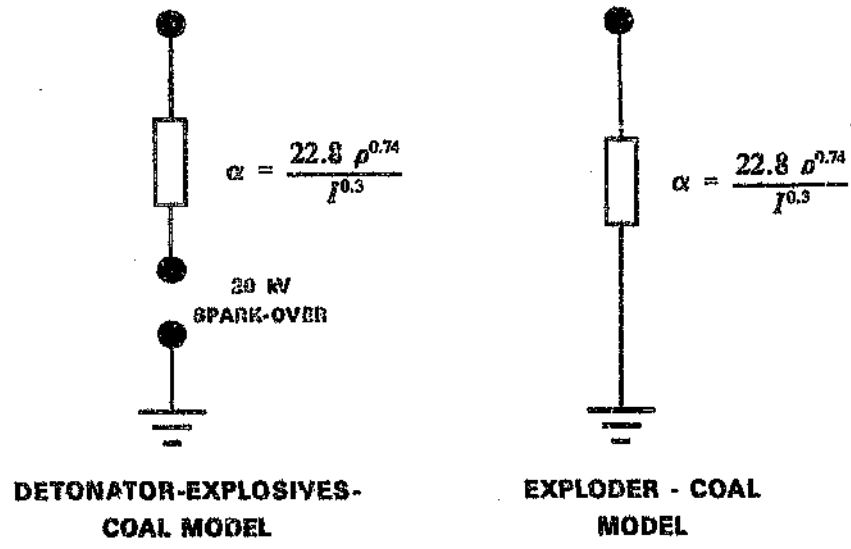



**Figure 8.23** The impulse impedance model for a detonator in explosives in coal and a model for an exploder standing on the mine floor

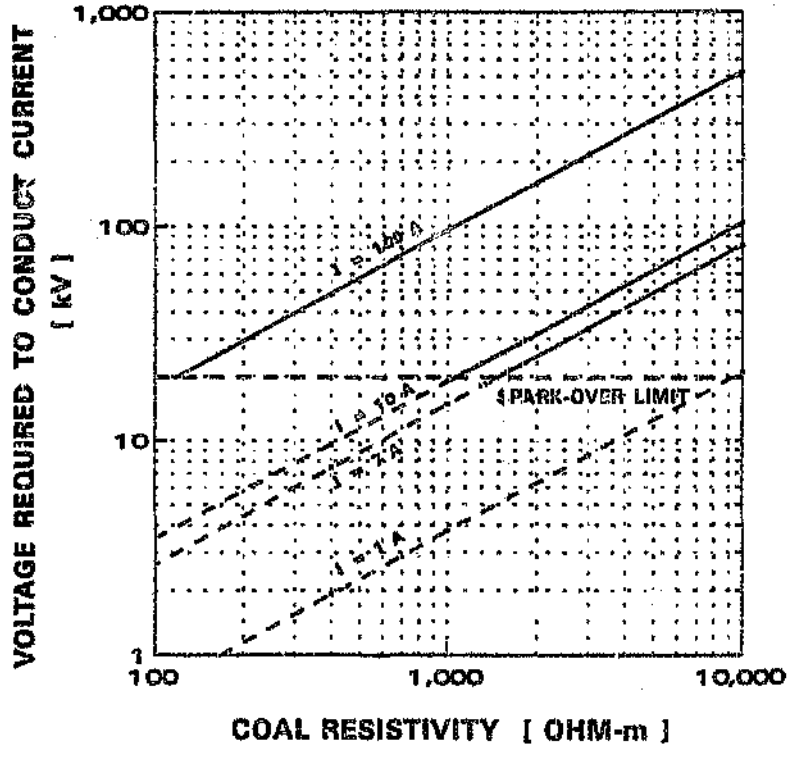



**Figure 8.24** The detonator-explosion-coal impulse impedance model showing the sparkover at 20 kV due to the explosives insulation characteristic

# 7 THE VOLTAGE AND ELECTRIC FIELD GRADIENT REQUIRED TO SET OFF DETONATORS

From the model given in 6.3, it was now possible to calculate the voltage and electric field gradient required to set off a detonator.

Two configurations were considered: the first configuration modelled was a situation that is typical of a work face (from top to bottom); the second was the situation between the work face and a shot exploder.

## 7.1 Face (top to bottom)

### 7.1.1 Five detonators in parallel in series with five parallel detonators

In this case, the current was induced into five detonators in the roof relative to five detonators in the floor of the work face (assuming a floor-to-roof height of 3 m). The conditions required to set off a detonator are as follows:

Assume the coal resistivity to be: $\rho$ = 3 000 Ω.m:

### 7.1.2 Type O detonator:

Current per detonator: 7 A/5 = 1.4 A per detonator is required.

Total voltage required to set off the detonator: $U = 2 \times (22.8\ \rho^{.74}\ I^{.7})$
$= 21.6$ kV

However, because this is less than the 2 x sparkover voltage of 2 x 20 kV, the minimum sparkover voltage is assumed to be U = 40 kV

Electric field gradient required to set off the detonator: 40 kV/3 m = 13 kV/m

The equivalent test voltage for a single detonator would be 40 kV/2 = 20 kV, and the equivalent test resistance to produce 7 A would be 20 kV/7 A = 2.9 kΩ

### 7.1.3 Type 1 detonator

Current per detonator: 32 A/5 = 6.4 A

Voltage required to set off the detonator: $U = 2 \times (22.8\ \rho^{.74}\ I^{.7})$
$= 62.6$ kV

Electric field gradient required to set off the detonator: 62.6 kV/3 m = 20.9 kV/m

The equivalent test voltage for a single detonator would be 62.9 kV/2 = 31 kV, and the equivalent test resistance to produce 32 A would be 31 kV/32 A = 970 Ω.

The same calculation was made for resistivities of 1 000 Ω.m and 10 000 Ω.m. The results are given in Table 8.5.

**Table 8.5** Face (top to bottom): The voltage, electric field gradient and equivalent test parameters required to set off a detonator, for different coal resistivities

| | Coal resistivity (Ω.m) | | |
|---|---|---|---|
| Type O detonator | 1 000 | 3 000 | 10 000 |
| Voltage (kV) | 40.00 | 40.00 | 52.70 |
| Field gradient (kV/m) | 13.00 | 13.00 | 17.60 |
| Equivalent test resistance (kΩ) | 2.90 | 2.90 | 3.80 |
| Test voltage (kV) | 20.00 | 20.00 | 26.00 |
| | Coal resistivity (Ω.m) | | |
| Type 1 detonator | 1 000 | 3 000 | 10 000 |
| Voltage (kV) | 40.00 | 62.60 | 153.00 |
| Field gradient (kV/m) | 13.00 | 20.90 | 51.00 |
| Equivalent test resistance (kΩ) | 0.63 | 0.98 | 2.39 |
| Test voltage (kV) | 20.00 | 31.30 | 76.00 |

## 7.2 15 parallel detonators in series with a shot exploder

In this case, the current was induced into 15 detonators installed into the face, all contributing to the current flowing to the shot exploder. It was assumed that the shot exploder was a distance of 15 m away from the face. It was also assumed that the process whereby the current enters a shot exploder is the same as for detonators.

The conditions required to set off a detonator will then be (assuming the coal resistivity to be $\rho$= 3 000 Ω.m):

### 7.2.1 Type 0 detonator

Current per detonator: 7 A/15 = 0.47 A per detonator is required.

Total voltage required to set off the detonator: $U = 22.8\ \rho^{.74}\ (0.47^{.7} + 7^{.7})$
$= 5.08\ kV + 33.3\ kV$
$= 38.3\ kV$

Electric field gradient required to set off the detonator: 38 kV/15 m = 2.56 kV/m

The equivalent test voltage from a single detonator would be 20 kV and the equivalent test resistance to produce 7 A would be 20 kV/7 A = 2.86 kΩ.

### 7.2.2 Type 1 detonator

Current per detonator: 32 A/15 = 2.13 A.

Total voltage required to set off the detonator: $U = 22.8\ \rho^{.74}\ (2.13^{.7} + 32^{.7})$
$= 14.5\ kV + 96.5\ kV$
$= 111\ kV$

Electric field gradient required to set off the detonator: 111 kV/15 m = 7.4 kV/m

The equivalent test voltage for a single detonator would be 111 kV and the equivalent test resistance to produce 32 A would be 111 kV/32 A = 3.47 kΩ.

The same calculation was repeated for resistivities of 1 000 Ω.m and 10 000 Ω.m. The results are given in Table 6.6.

**Table 8.6** Face to exploder. The voltage, electric field gradient and equivalent test parameters required to set off a detonator, for different coal resistivities

| | Coal resistivity (Ω.m) | | |
|---|---|---|---|
| Type O detonator | 1 000 | 3 000 | 10 000 |
| Voltage (kV) | 20.00 | 38.00 | 93.50 |
| Field gradient (kV/m) | 1.33 | 2.56 | 6.23 |
| Equivalent test resistance (kΩ) | 2.86 | 5.40 | 13.40 |
| Test voltage (kV) | 20.00 | 38.00 | 93.50 |
| | Coal resistivity (Ω.m) | | |
| Type 1 detonator | 1 000 | 3 000 | 10 000 |
| Voltage (kV) | 49.00 | 111.00 | 270.00 |
| Field gradient (kV/m) | 3.30 | 7.40 | 18.00 |
| Equivalent test resistance (kΩ) | 1.53 | 3.47 | 8.44 |
| Test voltage (kV) | 49.00 | 111.00 | 270.00 |

## 7.3 The minimum voltage and minimum electric field gradient

It is much more convenient and demonstrative to plot the results of Tables 8.5 and 8.6. The most important result is summarised in Figure 8.27. It is clear from this figure that, when the face-to-exploder configuration is used, the chance of a detonator being ignited is as much as ten times more than when other configurations are used. It is also clear that resistivity plays an important role.

Figures 8.25 to 8.27 will be used extensively in the rest of the thesis where a criterion for detonator sensitivity is required.

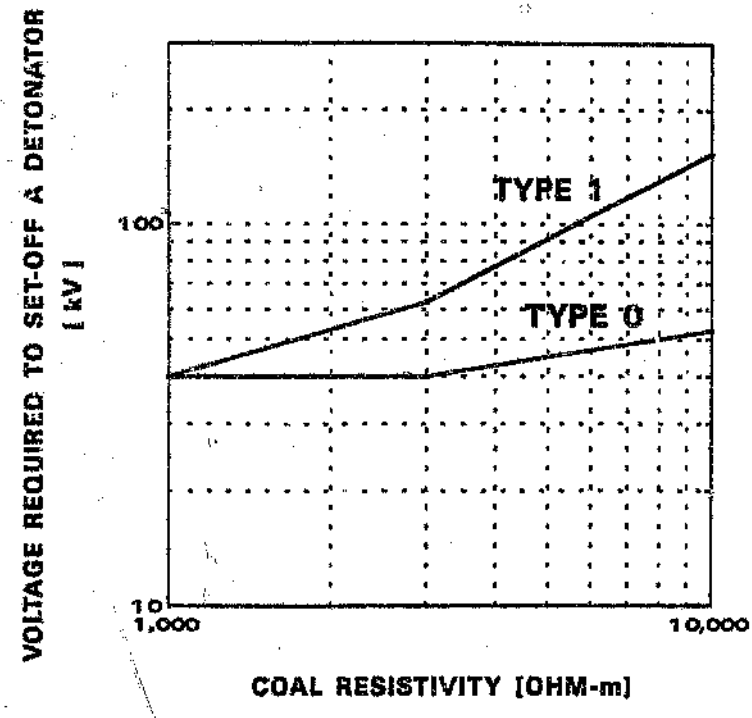



**Figure 8.25** The minimum voltage required to set off a detonator in the face top-to-bottom configuration.

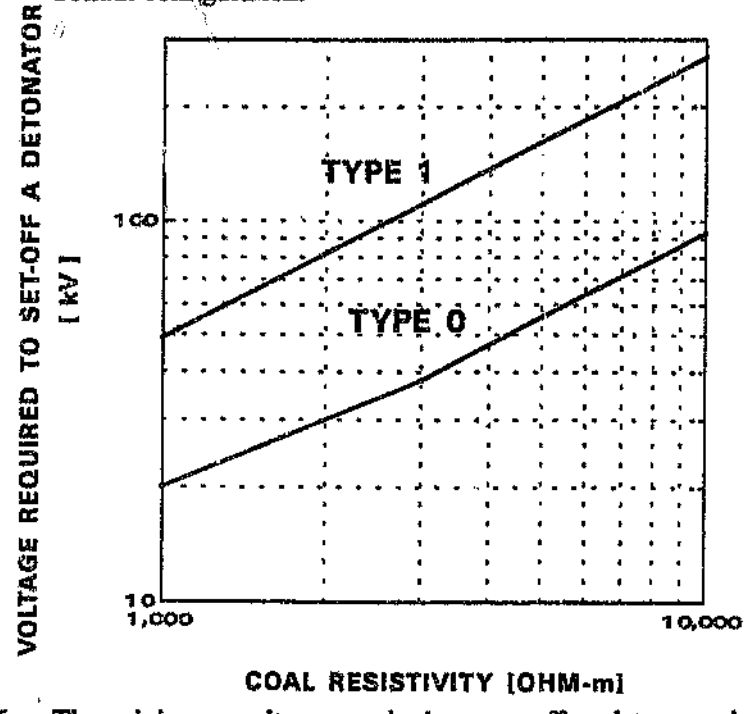



**Figure 8.26** The minimum voltage required to set off a detonator in the face-to-exploder configuration.

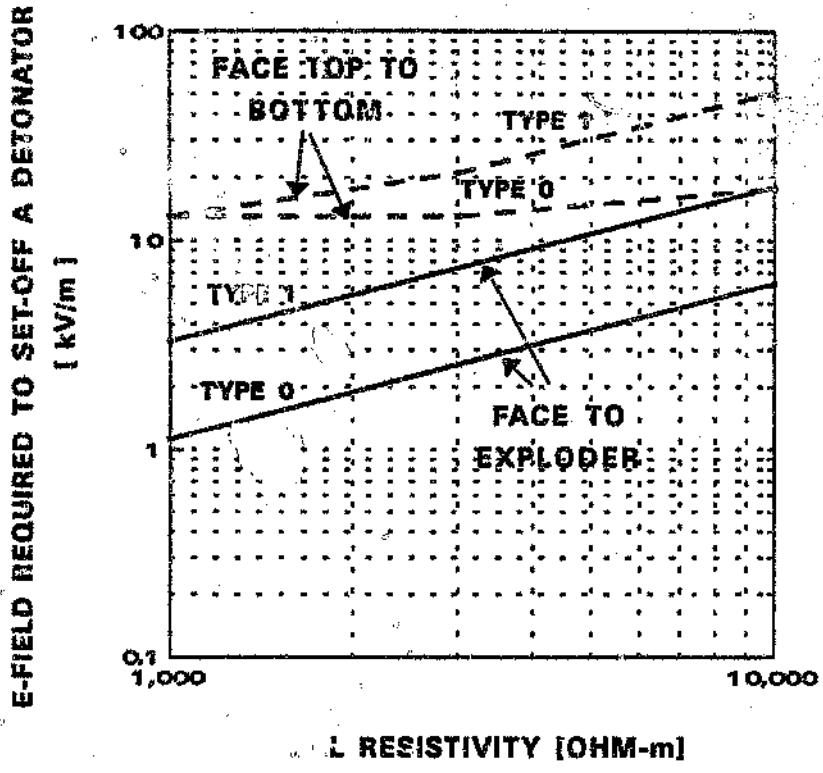



**Figure 8.27** The minimum el... field gradient required to set off a detonator in the two configurations analysed.

# CHAPTER 9

# AN IMPROVED ELECTRICAL SAFETY SPECIFICATION FOR COLLIERY DETONATORS

## 1 INTRODUCTION

In Chapter 7, the lightning sensitivity of conventional electrical detonators used in South African collieries was examined. The safety characteristics of these types of detonators depended on the fundamental design and construction of the detonators and are a function of the specific technology developed.

The advances made in technology and blasting have resulted in the use of alternatively designed and constructed detonators that have improved blasting techniques considerably. The criteria for safety that developed for conventional detonators are no longer sufficient to protect the alternatively designed detonators.

An enhanced test specification is proposed in this chapter to generalise lightning-safety testing methods to enable them to be applied to any detonator, independent of any specific detonator design.

(NOTE: The words ***static electricity*** used in this thesis refer specifically to the phenomenon (and hazard) of electrical charge accumulating on the surface of insulation materials or on insulated conductive objects. These must be clearly distinguished from the effects of **lightning**. Whereas both are fundamental electrostatic processes, their manifestation in electrical circuits are very different. The large difference between the two phenomena are often not recognised by the mining fraternity and there is confusion because the processes are regarded as being much the same.)

## 2 HISTORIC SAFETY TESTS

Historically, protection against the hazard of high voltages (static) were addressed by tests that were specifically designed for static electricity.

An example of this type of test that is used for explosives in South African collieries is the so-called "French" test, where a 2 000 pF capacitor is charged to 10 kV; this capacitor is then discharged between the detonator leads and between the detonator shell and the leads. The total energy stored in this test is 100 mJ.

This test is suitable for evaluating the static hazards to which a detonator could be exposed, but does not adequately evaluate the lightning safety of a detonator. The following example explains why lightning safety is not evaluated:

Consider a conventionally designed detonator (the electrical circuit diagram of this type of detonator is shown in Figure 7.2 in Chapter 7) and consider the test configuration using the "French" test, shown in Figure 9.1.

The energy released into the bridge-wire resistance ($R_P$) of the detonator does not depend on the bridge wire only but also depends on the resistance of the detonator lead wires.

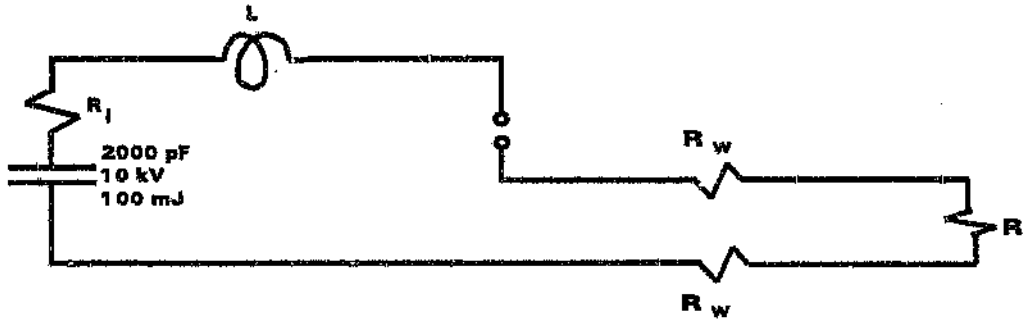



**Figure 9.1** A "French" test performed on a conventional electrical detonator. $R_i$ = internal resistance of the capacitor; L = circuit stray resistance

The effect of the lead wire resistance ($R_W$) can be seen in Table 9.1. In the case where $R_W$ = 0.28 Ω and $R_P$ = 1.41 Ω, the energy dissipated in the fuse head is 71.9 mJ. This is more than sufficient to set the detonator off. However, by simply increasing the resistance of the lead wire to $R_W$ = 24 Ω, the energy in the fuse head drops to 2.85 mJ which is the level at which the detonator will pass the test.

This result is perfectly valid for protection against static electricity. However, lightning

current acts like a current source and the additional lead-wire resistance will have a minimal effect on the energy dissipated by lightning in the detonator. The detonator will therefore still be just as sensitive to lightning as before. An alternative test is therefore required to represent the effect of lightning on a detonator.

**Table 9.1** The energy dissipated in a detonator with a bridge-wire resistance of 1.41 Ω and different lead wire resistances.

| Lead-wire resistance $R_w$ | Energy in the detonator $E_F$ |
|---|---|
| 0.28 Ω | 71.9 mJ |
| 24.00 Ω | 2.85 mJ |

Another problem with the "French" test is the internal resistance of the capacitor. The inductance of the test circuit is likely to be about 1 μH. The resonance frequency will be about 4 MHz and the characteristic impedance of the circuit will be about 22 Ω. If the internal resistance of the capacitor is not carefully chosen, it can influence the results obtained in the test. This is an issue which is not generally understood by the explosives industry and it is uncertain whether the various test configurations in use produce the same results.

## 3 INSULATION PROTECTION AND SHORT-CIRCUIT PROTECTION

There are two fundamental techniques which are employed to protect electrical and electronic systems against lightning:

**Isolation or short circuit**

In the case of isolation, the designer attempts to prevent lightning surge current (and energy) to be conducted through the system.

In the case of short-circuit, the designer attempts to prevent lightning surge voltage (and energy) from stressing the system. This is done by providing a shunt path for the lightning current (with a sufficiently low resistance and impedance), often referred to as earthing and bonding.

The quality of the isolation protection is evaluated by voltage tests.

The quality of short-circuit protection is evaluated by defined current tests.

These two possible protection methodologies will be provided for by the generalised test proposed in this chapter.

## 4 A LIGHTNING SENSITIVITY TEST

The two extreme poles of lightning-protection methods, isolation protection and short-circuit protection, each require a specific test to measure their effectiveness.

For isolation protection, a voltage source with a defined waveshape (1.2/50$\mu$s) is used: the peak amplitude represents an effective protection measure.

For short-circuit protection, a current source with a defined waveshape (1.2/50 $\mu$s) is used: the peak amplitude represents an effective protection measure.

These two tests can be incorporated into one generalised test by configuring a test set-up which produces 1.2/50 $\mu$s open-circuit voltage pulses and 1.2/50 $\mu$s current pulses when it is short-circuited. This test is schematically represented in Figure 9.2.

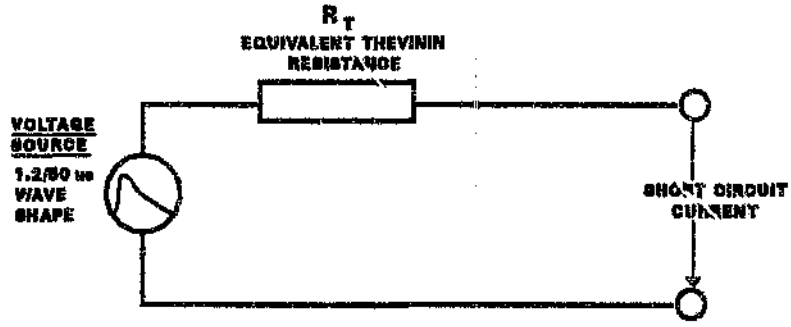



**Figure 9.2** A schematical circuit diagram pf a lightning-sensitivity test set-up for detonators.

One question remains unanswered: what should the value of the equivalent Thevinin resistance be? The same question can be phrased quite differently: What resistance will produce a voltage and a current which will occur with the same frequency?

The examples of typical work faces given in Chapter 8 and summarised in Tables 8.5 and 8.6 give a partial answer to this question. These tables contain a variable called "equivalent test resistance".

This "equivalent test resistance" is derived as follows. The amplitude of the current of each test is determined: 7 A in the case of a Type 0 detonator and 32 A in the case of a Type 1 detonator. The second parameter to be determined is the voltage that could potentially stress the insulation of a detonator. In Table 8.5 (Chapter 8), it is the total voltage divided by 2, because there are detonators at both ends of the circuit.

In Table 8.6, it is the total voltage in the circuit, because there are detonators at only one end of the circuit.

The "equivalent test resistance" is therefore the total voltage divided by the test current.

The various "equivalent test resistances" ($R_T$) given in Chapter 8 are summarised in Table 9.2.

**Table 9.2** The equivalent test resistance, $R_T$, obtained from the vertical and diagonal detonator analysis in Chapter 8, for Type 0 (7 A) and Type 1 (32 A) detonators.

| | | Coal resistivity (Ω.m) | | |
|---|---|---|---|---|
| | | 1 000 | 3 000 | 10 000 |
| Vertical configuration | I = 7 A | 2.90 Ω | 2.90 Ω | 3.80 Ω |
| | I = 32 A | 0.63 Ω | 0.98 Ω | 2.39 Ω |
| Diagonal configuration | I = 7 A | 2.86 Ω | 5.40 Ω | 13.40 Ω |
| | I = 32 A | 1.53 Ω | 3.47 Ω | 8.44 Ω |

The diagonal configuration $R_T$ is plotted in Figure 9.3. Only this diagonal configuration $R_T$ will be considered when deciding on a value for $R_T$. The reason for this is that the diagonal configuration is the critical one because of the high frequency of surges that occur in this configuration.

The value of $R_T$ is affected by the resistivity of the strata around a charged detonator hole. The current dependence is due to the ionisation-reduction of resistance, as discussed in Chapter 8.

The approach followed uses current as the fundamental reference.

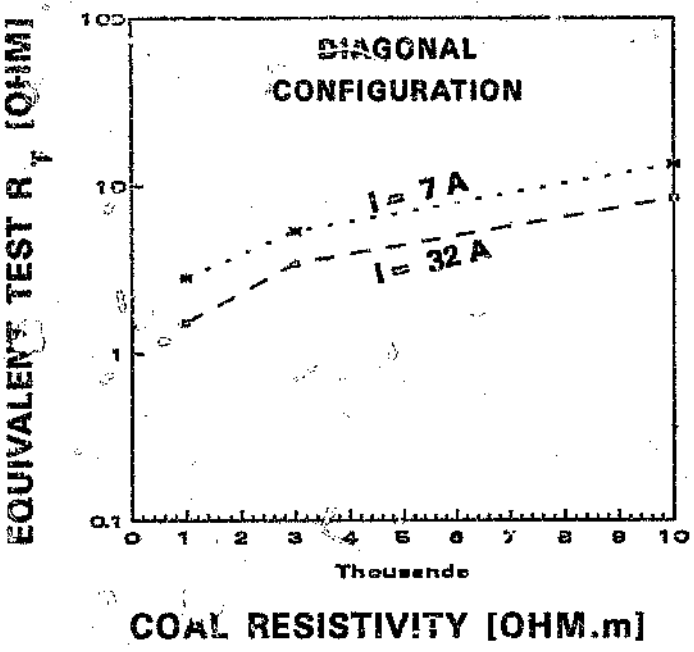



**Figure 9.3** The equivalent test resistance, $R_T$, for the diagonal configuration.

It is more appropriate to use the frequency of occurrence of both current and voltage surges as a fundamental reference. This comparison was, in effect, made using Figure 3.23. This figure is reproduced here as Figure 9.4, with the relevant subscripts.

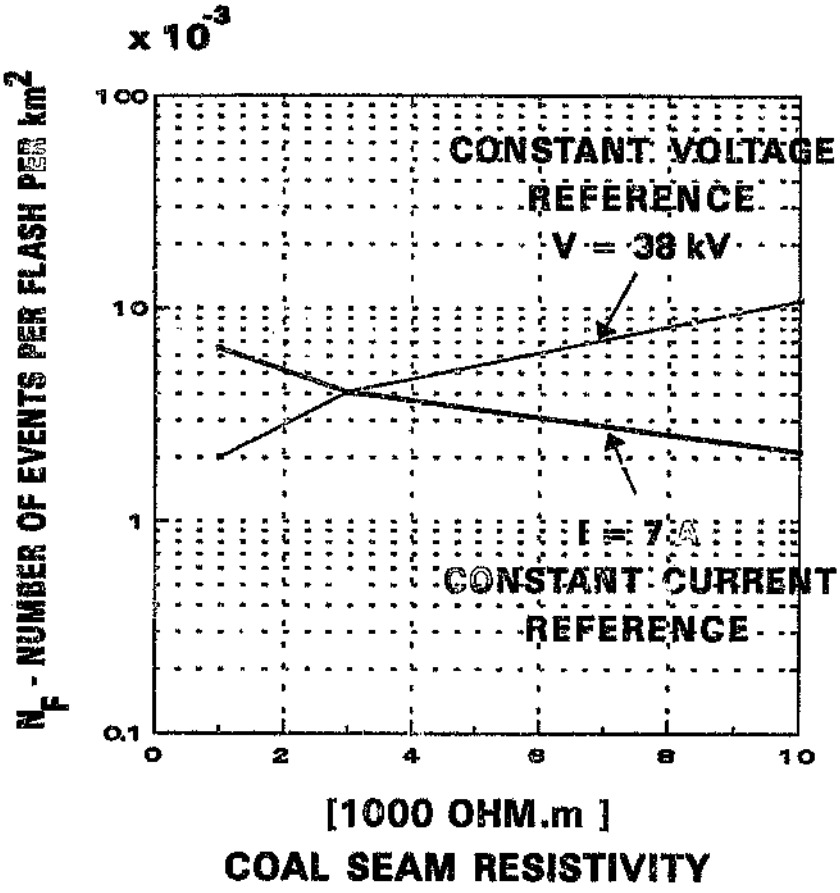



**Figure 9.4** The frequency of surges in the case where the current induced into a detonator circuit and where the current is kept constant, as reference I = 7 A. The second curve is the case where the voltage is kept constant, as reference V = 38 kV.
t = 3 m; d = 30 m; $\rho = \rho_2 = 400$ Ω.m

From Figure 9.4, it can be seen that if voltage is used as the reference it results in a high frequency of surges exceeding the chosen level in high-resistivity strata and in a low frequency of surges in low-resistivity strata. Exactly the opposite is true when current is used as the reference.

The average value of coal resistivity in the mines concerned is regarded as being 3 000 Ω.m. It is suggested, therefore, that if $R_T$ is chosen as

$$R_T = \frac{U_T\ (\rho_c = 3000\ \Omega.m)}{I_T\ (\rho_c = 3000\ \Omega.m)} = \frac{38kV}{7\ A} = 5.4\ k\Omega \quad \ldots\ldots\ldots\ldots\ldots\ldots\ldots\ldots\ 9.1$$

If 3 000 Ω.m is the average resistivity, it could be argued that the underprotection and overprotection of the two approaches will cancel out on average. For this reason, $R_T$ = 5 kΩ is accepted as the norm here. This implies that the two detonator types studied in

this thesis (Type 0 and Type 1) will have the same safety level as a device insulated to levels of 35 kV and 160 kV respectively. (7A x 5kΩ = 35 kV, 32A 160 kV)

## 5 SPARK PENETRATION TEST

The "French" test for electrostatic hazards and the lightning tests may, by default, ignite a detonator which is prone to sparks directly to the fuse head. However, they are not specifically designed to identify any weakness in this regard. This test should be designed specifically for this purpose.

Two criteria are set for the spark penetration test. The first requirement is that several waveshapes be applied, varying the rise time of the test waveshapes; 0.1 $\mu$s, 1 $\mu$s and 10 $\mu$s are proposed. The insulation co-ordination between different gaps is a time-dependent property and the different rise times are proposed to cover this aspect. A time-to-half value of 50 $\mu$s should be used.

The second requirement is that the waveshapes should not be able to set the detonator off in the "normal" mode. A series resistance of 10 kΩ and an amplitude equal to the lightning test pass level is proposed. This will ensure that the impulse cannot set off the detonator in the "normal" mode.

Due to the nature of this mechanism, this test should be performed on a statistically large enough sample to ensure that any defect of this kind is detected, even when it occurs in only a small percentage of units.

## 6 METHODS OF APPLYING THE TESTS

The methods of applying the tests depend on the construction of the detonator. Various types of construction used in the industry will be dealt with here. Any new innovative approaches that do not fit these broad descriptions will have to be dealt with in the context of this analysis.

Examples of possible detonator designs are given in Figure 9.5.

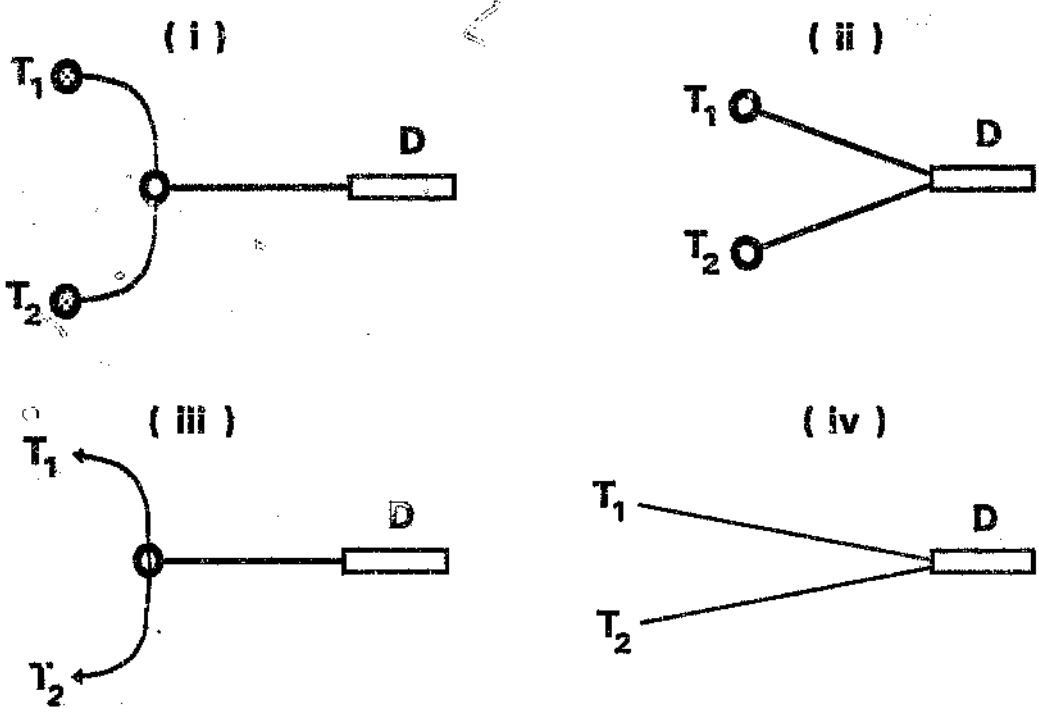


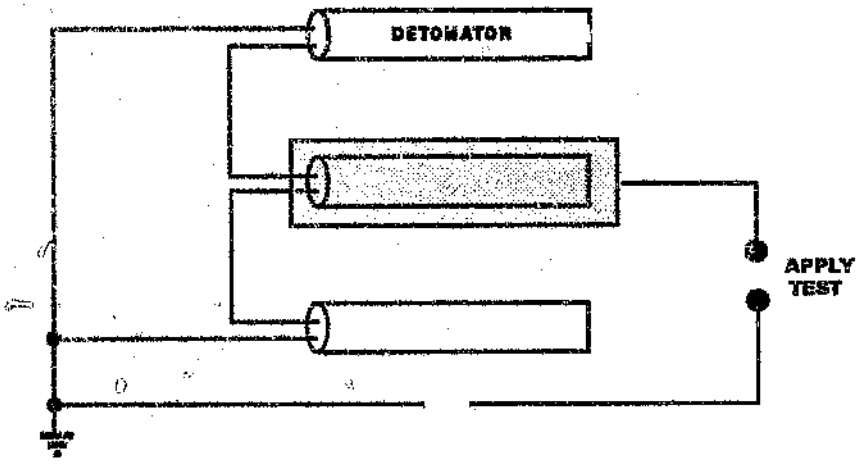

**Figure 9.5** Different designs of detonators:

(i) Multi-wire, T-off
(ii) Multi-wire, in out
(iii) Transformer coupled
(iv) Conventional design

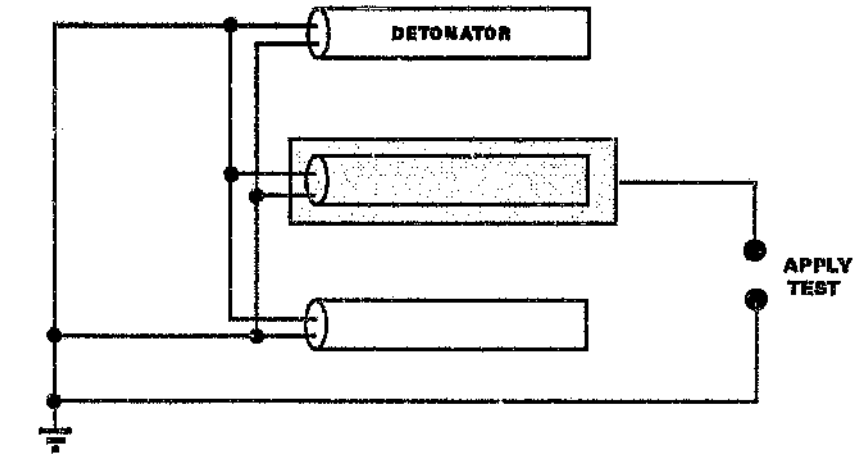
All known detonators have a detonator shell, D, which is inserted into the rock face. It also has an in-terminal, $T_1$, and an out-terminal, $T_2$. These terminals ($T_1$ and $T_2$) may contain multiple wires or may have only a single wire, as in the case of a conventional detonator.

## 6.1 Common-mode test

A harness containing at least three detonators should be prepared for this test. The three detonators should be connected in series or in parallel, depending on the normal method of connection as shown in Figure 9.6.




(i) Series connection




(ii) Parallel connection

**Figure 9.6** Common-mode test configuration for detonators connected in series and in parallel

The leads of the outer detonators should be taken down to ground. If the detonators have multiple leads, all the outer wires should be taken down to ground.

The voltage is applied to the detonator in the middle of the harness. The voltage is applied by "embedding" (wrapping) the detonator and the lead (which is normally embedded in explosives) in a sheet of aluminium foil.

# CHAPTER 10

# A LIGHTNING-RISK INDEX FOR A MINE

## 1 INTRODUCTION

The hazards to which a mine are exposed have to be understood before appropriate actions can be taken to prevent them. These counter measures usually involve additional costs and preventing the risk of lightning is no exception.

To ensure that adequate preventative measures are taken but, at the same time, to avoid unnecessary expense, a risk assessment is of great benefit. This chapter proposes such a risk index for collieries.

As indicated in Chapter 1, lightning contributes to two hazards, explosions where methane has been ignited and explosions caused by the initiation of detonators. Whether these explosions occur depends on the circumstances at a particular mine; i.e. whether methane can accumulate in the mine and whether electrical/ electronic detonators that can be ignited by lightning are used.

## 2 TYPES OF HAZARDS

### 2.1 Methane

This thesis makes only a superficial contribution towards determining the methane/lightning hazard. It has shown that very low currents (11 mA) of "long sparks" (3 - 4 mm) can ignite methane. When this criterion is compared to the lightning current required to set off a Type 0 detonator (7 A), it can be seen that this low current is very small: a factor of 640 times.

No attempt will be made here to further analyse this risk in any quantitative format. However, by following the same argument used for setting off detonators, the risk of methane ignition can be evaluated.

### 2.2 Detonators/explosives

The lightning risk developed in this chapter is essentially based on the use of Type 0 detonators. The so-called "Stat-Safe" detonators being used in collieries are only

marginally better than the Type 0 detonators and, for practical purposes, are at the same risk.

The following factors have an influence on the risk of a detonator underground being set off:

The sensitivity of detonators
The lightning flash density
The resistivity and structure of the strata
The depth of the mine
The characteristics of the coal seam, such as thickness and resistivity

## 3 A PROPOSED RISK INDEX

The requirements for a risk index are that it should indicate a real risk, based on information that is readily available, and it should give results that can be applied by mining practitioners. These factors are all taken into consideration in the proposed index.

The index is essentially based on the analysis made in Chapter 3. The range over which they are analysed and their relative sensitivity are given. The relative sensitivity of a factor is the ratio between the change in the factor to the change this factor has on the frequency at which surges occur.

**Table 10.1** The factors analysed in Chapter 3. The ranges of the factors are given and their relative effect on the frequency that surges will occur.

| Factor | Range analysed | Range ratio | Frequency Range | Frequency influencing ratio | Frequency ratio/Range ratio |
|---|---|---|---|---|---|
| Mine depth | 15 - 100 m | 6.67 | 0.00600 - 0.00270 | 22.00 | 3.330 |
| Strata resistivity | 200 - 1 600 Ω.m | 8.00 | 0.00194 - 0.01720 | 8.87 | 1.110 |
| Coal resistivity | 1 kΩ.m - 10 kΩ.m | 10.00 | 0.00650 - 0.00200 | 3.25 | 0.325 |
| Seam thickness | 2.5 m - 10 m | 4.00 | 0.00270 - 0.00040 | 6.75 | 1.690 |

Table 10.1 shows that mine depth has the greatest influence followed by seam thickness, strata resistivities and, last, coal resistivity.

The parameters that are readily available are mine depth and coal-seam thickness, which can be obtained from the Geological Office at the mine, in the form of borehole information.

It is more difficult to obtain the resistivities of the strata and almost impossible to determine the resistivity of the coal seam.

It is suggested that the resistivities of the strata be obtained by using either the Venner or Schlumberger method. The resistivity of the surface layer can be determined with a high degree of certainty. The resistivities of the deeper strata can be determined by using this resistivity measurement in conjunction with the information obtained from the borehole samples.

It is further suggested that, in the light of the difficulty in determining the coal resistivity and its relatively small effect on the total, it be omitted as a factor in determining the risk index.

The frequency $N_F$ of surges expected at a particular face in a specific mine is given as

$$N_F = N_g \cdot N(d) \cdot K_\rho \cdot K_T \quad \ldots\ldots\ldots\

## 3.2 N(d) - Surge frequency at depth (d)

The effect of mining depth is analysed in Chapter 3.7.1. Figure 3.15 gives a relationship between the number of surges exceeding the sensitivity of the Type 0 detonator. The curve of Figure 3.15 can be represented reasonably accurately by the equation

$$N(d) = 10^{-(1.05 + 0.0162\ d)} \quad \ldots\ldots\ldots\

## 3.3 $K_\rho$ - the effect of strata resistivity

The analysis in Chapter 3 was done using a strata configuration of three layers. If the strata surrounding the coal seam can be reduced to an equivalent three-layer model, Figure 10.2 can be used to determine $K_\rho$.

Figure 10.2 is based on the results of Chapter 3, paragraph 7.2. It has been normalised for a depth of 30 m and $\rho_1 = \rho_2 = 400$ Ω.m.

The thick line in Figure 10.2 represents the correction factor $K_\rho$ where the resistivity of the strata above and below the coal layer is the same. This line fits a power relationship excellently ($r^2 = 100$).

$$K_\rho = 1.92 \times 10^{-3} \rho^{1.0423} \quad \ldots\ldots\ldots\

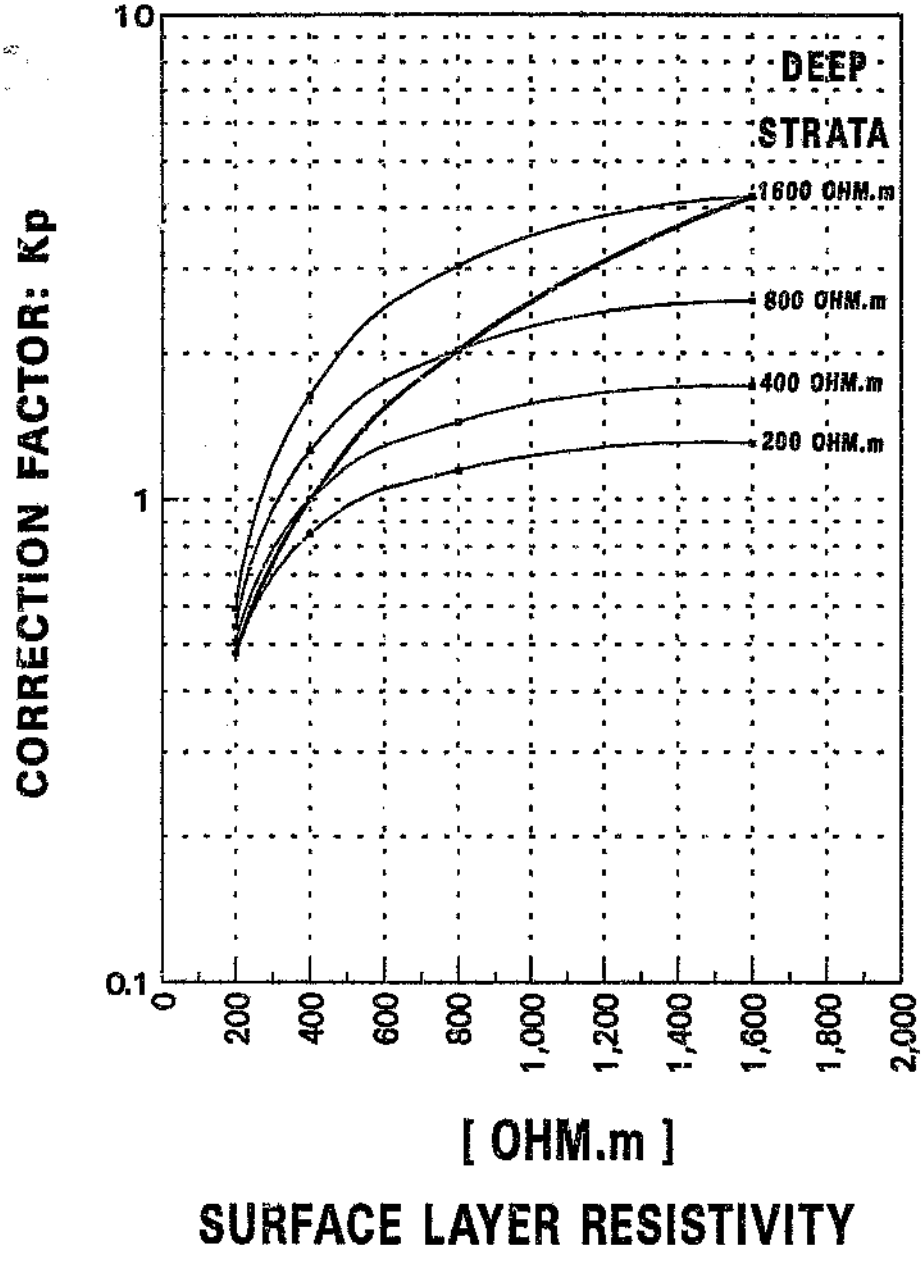



**Figure 10.2** The correction factor, $K\rho$ that makes provision for the effect of strata resistivity. The thick line represents the case where the resistivity above and below the coal seam is the same.

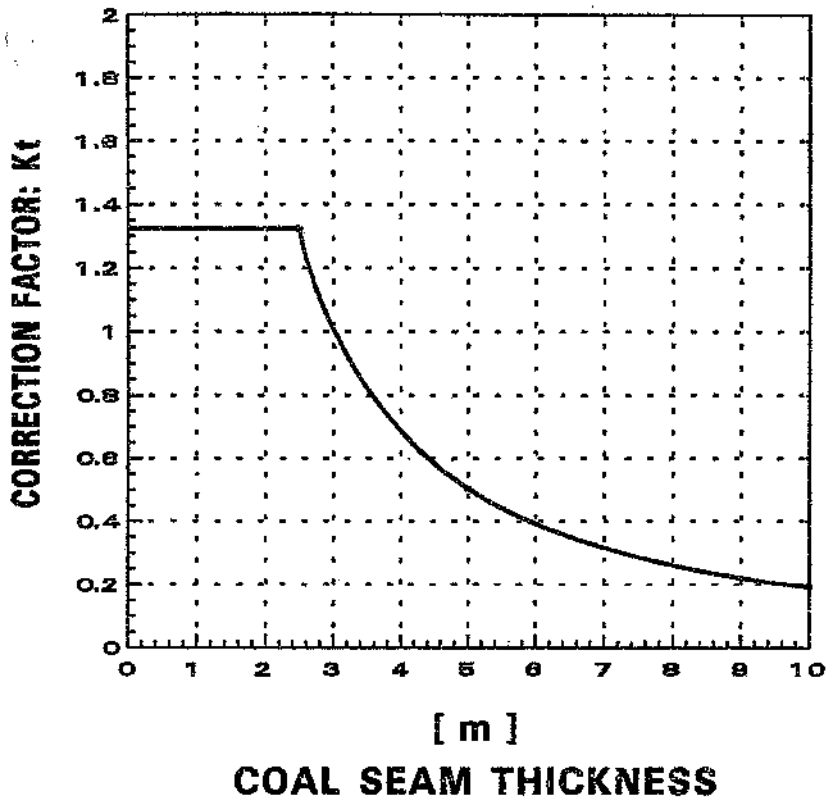



**Figure 10.3** The correction factor, $K_t$ that makes provision for the effect of coal-seam resistivity.

## 4 RISK INDEX ANALYSIS USED IN MINES ON THE FUSE SURGE DETECTOR PROGRAMME

In this thesis, an analytical model for calculating risk was developed. Empirical studies have also been done using the results from the Fuse Surge Detector (FSD) programme. This allows the testing of the analytical model to calculate frequency by comparing the calculated frequency with the observed frequency using the FSD programme.

The depth of the mine and the thickness of the coal seam in mines using the FSD programme are given in Table 5.4. This was obtained by using the resistivity profiles obtained from using the Venner method and the information gained from the borehole samples which were available in some of the mines and is given in Appendix VII. Table 10.2 summarises the data of depth, thickness and resistivity.

The predicted frequency based on depth and seam thickness is also given in Table 10.2.

In the cases where the resistivity profiles are available, the surface resistivity can be determined with a high level of certainty due to the nature of the Venner method. However, because of the multi-layer nature of the strata, it is impossible to say with any certainty what the resistivities of the deeper layers are. The estimates given in the table have been guessed from the depth profiles.

**Table 10.2** The predicted frequency of surges occurring in mines where the FSD programme was used. Resistivity data was only available in some of the mines and $K\rho$ was calculated only for these mines.

| Mine | Average depth (m) | Average seam thickness (m) | N(d) x $k_t$ (x $10^{-3}$) | Surface resistivity $\rho_1$ | Deep strata resistivity $\rho_2$ | $K_\rho$ | N(d) x $K_t$ x $K_\rho$ (x $10^{-3}$) |
|---|---|---|---|---|---|---|---|
| Arnot | 63 | 2.8 | 1.120 | 400 | 600 | 1.1 | 1.23 |
| Delmas | 103 | 6.7 | 0.084 | N/A | | | |
| Douglas | 45 | 5.1 | 1.000 | N/A | | | |
| Goedehoop | 45 | 3.2 | 1.990 | N/A | | | |
| Greenside | 36 | 1.7 | 3.950 | 600 | 800 | 1.6 | 6.32 |
| Kriel | 47 | 3.9 | 1.360 | N/A | | | |
| Landau | 48 | 6.2 | 0.690 | 1 100 | 1 100 | 2.6 | 1.79 |
| Matla | 48 | 6.6 | 0.650 | N/A | | | |
| Sigma | 70 | 4.0 | 0.570 | 300 | 400 | 0.7 | 0.40 |
| South Witbank | 54 | 4.6 | 0.820 | 600 | 800 | 1.6 | 1.31 |

The measured/observed frequency (in face 2 of Chapter 5) is listed in Table 10.3 for the 3 A, 7 A and 10 A waveshapes (1/44 $\mu$s - the sensitivities of the FSD). From Chapters 5 and 7, it is known that the Type 0 detonator is slightly less sensitive than the "10 A" fuse wire of the FSD. In the ideal case, therefore, there should be a correlation of 1 : 1 between the predicted frequency and the FSD, 10 A observed frequency.

The FSD frequency ("observation resolution") is the inverse of the number of faces x flash density obtained over the total observation period of the FSD measurement programme. This is equal to the observed frequency obtained if one observation was made during the period of study.

The importance of this number (e.g. at Delmas Colliery) is that the "observation resolution" is 37.3 x $10^{-3}$, but the predicted frequency is .084 x $10^{-3}$. This implies that an average observation period must be extended by 444 times to expect one observation. The 0 in Table 10.2 is significant in that the actual observed frequency will be less than the

Table 10.3 The predicted frequency ($N_g$ = 1) versus the observed frequency of surges in the mines taking part in the FSD programme.
* All the frequencies must be multiplied by $10^{-3}$.

| Mine | Predicted frequency* excluding $K_p$ | Predicted frequency* including $K_p$ | FSD frequency* observation resolution | * FSD observed frequency | | |
|---|---|---|---|---|---|---|
| | | | | 3 A | 7 A | 10 A |
| Arnot | 1.120 | 1.23 | 4.60 | 18.4 | 0 | 0 |
| Delmas | 0.084 | | 37.30 | 0 | 0 | 0 |
| Douglas | 1.000 | | 4.78 | 9.6 | 9.6 | 4.8 |
| Goedehoop | 1.990 | | 4.44 | 4.4 | 0 | 0 |
| Greenside | 3.950 | 6.32 | 5.50 | 38.5 | 22.0 | 11.0 |
| Kriel | 1.360 | | 7.87 | 21.5 | 15.7 | 7.9 |
| Landau | 0.690 | 1.79 | 7.35 | 44.1 | 7.4 | 7.4 |
| Matla | 0.650 | | 11.50 | 11.5 | 0 | 0 |
| Sigma | 0.570 | 0.40 | 12.70 | 0 | 0 | 0 |
| South Witbank | 0.820 | 1.31 | 8.13 | 97.6 | 8.1 | 0 |

A regression analysis was performed between the predicted frequency and the FSD results at 3 A, 7 A and 10 A.

As stated earlier, the expected result in the case where the model is 100 % perfect, is that there is a 1 : 1 relationship between the 10 A FSD result and the model.

Table 10.4 Results of the linear regression between the predicted and FSD-measured results ($y = mx + C$)

| | FSD data set | | |
|---|---|---|---|
| | 3 A | 7 A | 10 A |
| Correlation coefficient | 0.50 | 0.83 | 0.89 |
| $R^2$ | 0.25 | 0.58 | 0.80 |
| Linear slope (m) | 4.00 | 2.30 | 0.91 |
| Y axis value (C) | 14.40 | 7.15 | 5.39 |

From the data set, the result from the 3 A FSD at South Witbank is extremely high for such a deep mine; also, the result is not confirmed by the results from the 7 A and 10 A FSDs. It is suspected that the high result could be caused by an unknown factor, or perhaps, even power frequency fault currents. For this reason, this single data point was omitted from the data set.

The regressions are also plotted in Figures 10.4, 10.5 and 10.6.

From Figure 10.4, it is clear that there is some correlation between the model and the observations; however, the statistical spread is rather large, resulting in a poor correlation of 0.5.

In the case of the 7 A and 10 A FSDs, the correlation is much better (0.83 and 0.89). The statistical spread is accordingly smaller. This may, of course, be due to the fewer data points available. It is also worth noting the large influence that the Greenside result has in the regressions and correlations.

It can be concluded that the regressions and correlations show that the model produced results of the correct order of magnitude. It can also be stated that the results from the FSDs significantly support the model.

Lastly, it can be stated that the actual results are influenced by many more factors which the model is not capable of taking into consideration, leading to a relatively large scatter in the results.

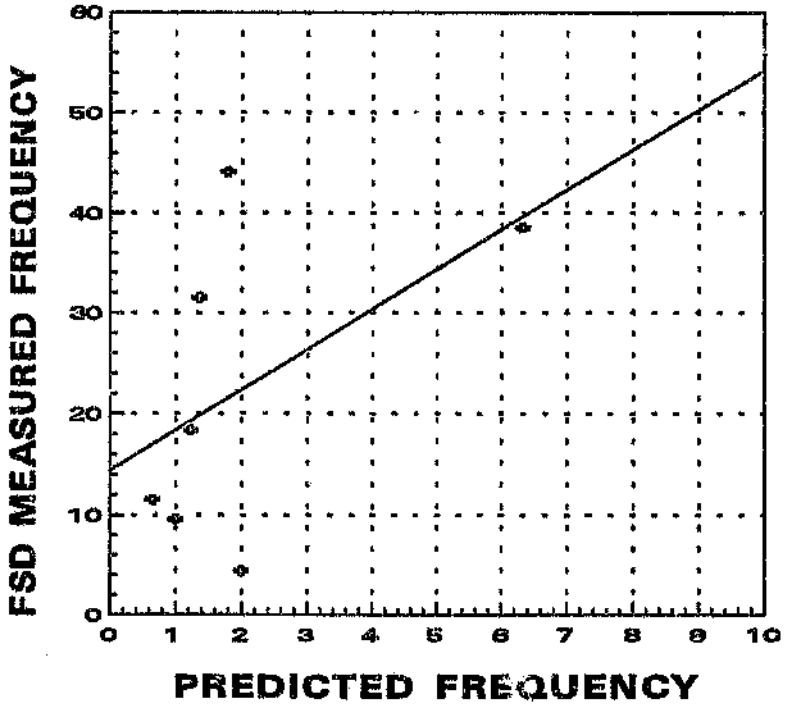



**Figure 10.4** The linear regression between the predicted frequency of the model and the frequency measured by the 3 A FSD.

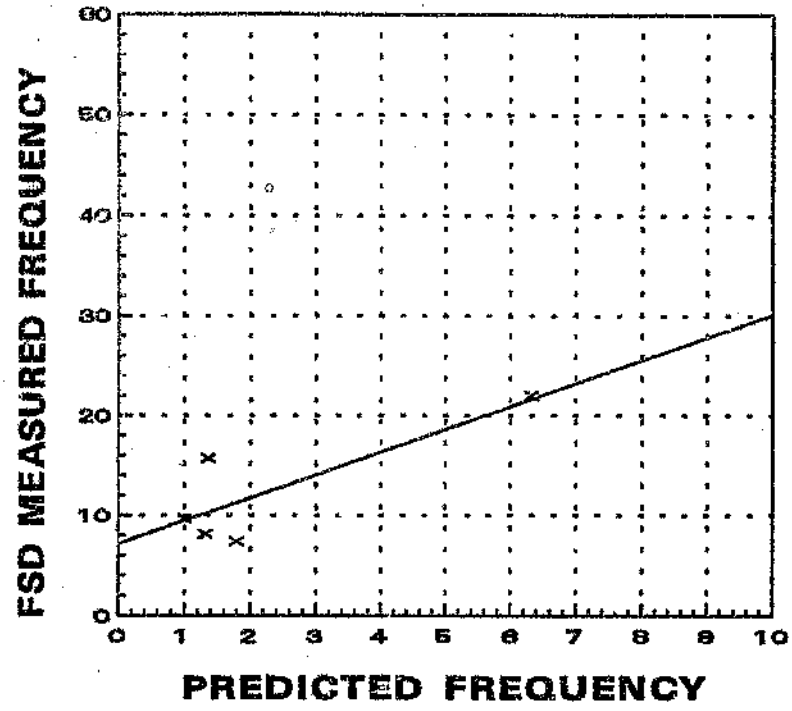



**Figure 10.5** The linear regression between the predicted frequency of the model and the measured frequency of the 7 A FSD.

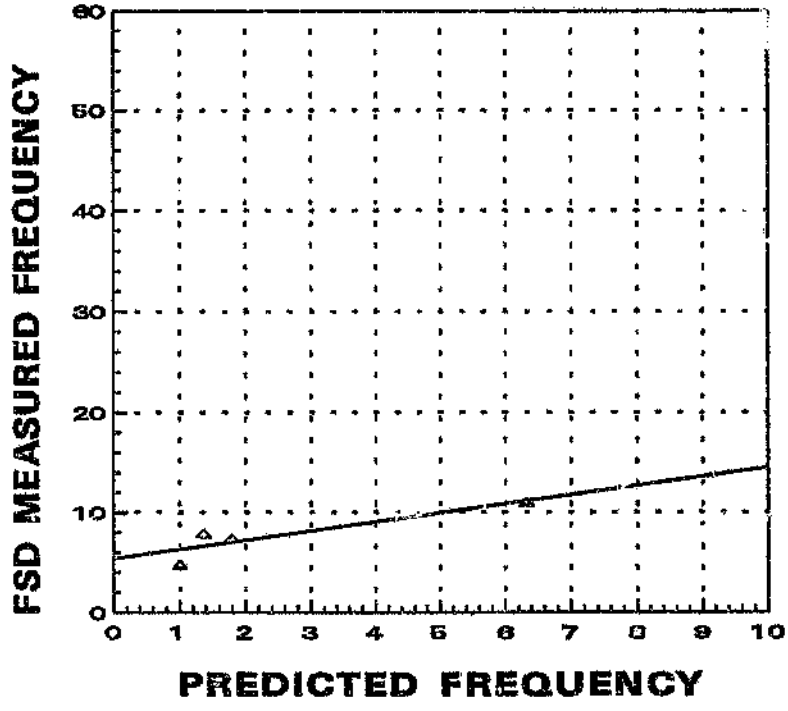



**Figure 10.6** The linear regression between the predicted frequency of the model and the measured frequency of the 10 A FSD

# 5 RISK INDEX

Up to this point in the thesis, the capability to calculate the frequency at which surges can occur underground has been developed. The question now arises: what frequencies can be regarded as being extremely hazardous, moderately hazardous or safe?

## 5.1 Accident statistics

The prevailing frequency of accidents in collieries establishes a reference, enabling a decision to be made to evaluate the hazard category of a mine.

When evaluating the risk in an industrial environment, managers often have to decide whether or not they should implement safety measures which are expensive and would increase production costs. Means of improving safety include good housekeeping, protective clothing, protective machinery, etc.

Table 10.5 summarises the accident statistics obtained from the Office of the Government Mining Engineer in the Eastern Transvaal for the period 1 January 1988 to 30 September 1994 (a total of 6.75 years) (Cloete, 1994). The total number of employees in collieries in the Eastern Transvaal in 1994 was 26 100. This implies that the data base is based on 176 000 man-years. The number of employees for the other years is not available and was assumed to be the same.

These statistics cover open-cast mining, surface operations and underground accidents. The combined total is also given. For this thesis, only the underground operations are of interest, and for this reason only the total number of accidents and the total of accidents underground are given. Further, it is assumed that the ratio of the number of employees involved in underground operations to the total number of accidents is the same ratio as accidents underground to total accidents.

It is proposed here that a frequency equal to 10 % of the present accident frequency (per man year) is a very high risk, 1 % is a moderate risk and 0.1 % is a low risk. This implies that a frequency of $0.68 \times 10^{-3}$ per man year corresponds to a high risk. Due to the somewhat arbitrary choice and for the sake of simplicity this number is approximated as $0.5 \times 10^{-3}$. We then have

High risk $\leq 0.5 \times 10^{-3}$ per man year

Moderate risk $= (0.5 \text{ to } 0.05) \times 10^{-3}$ per man year

Low risk = (0.05 - 0.005) x $10^{-3}$ per man year

Very low risk ≤ 0.005 x $10^{-3}$ per man year

**Table 10.5** Accident statistics from the Government Mining Engineer, Eastern Transvaal area for the period 1/1/88 to 30/9/94. This represents a total of 176 000 man years

| | No. of Accidents | Killed | Injured |
|---|---|---|---|
| Total accidents | 1 203 | 178 | 984 |
| Frequency (per man year) | 6.84 x $10^{-3}$ | 1.01 x $10^{-3}$ | 5.59 x $10^{-3}$ |
| Underground accidents | 870 | 152 | 728 |
| Frequency (per man year) | 6.85 x $10^{-3}$ | 1.20 x $10^{-3}$ | 5.73 x $10^{-3}$ |

## 6 THE RISK OF AN UNDERGROUND DETONATOR ACCIDENT

The frequency of detonator incidents per man year is not simply the frequency at which such surges occur, the actions of the worker must be taken into consideration as well.

A particular man is only exposed during the eight-our shift that he works. This could be either from 07:00 to 15:00, or from 15:00 to 23:00, or - if a third shift is worked in the mine, from 23:00 to 07:00. From Eriksson's analysis (1976b), we know that most lightning storms occur during the afternoon shift of from 15:00 to 23:00. An analysis of his data indicates that 60 % of lightning storms occur in this period. It should also be taken into account that a worker only works five days per week.

The preparation of a coal face for blasting requires the holes to be drilled first. Thereafter, the individual detonators and groups of explosive sticks are tamped into these holes. Finally, the detonator wires are twisted together and the face is ready for blasting. During this period, it is estimated that the period that the face is wired up and could be affected by lightning surges is only 25 % of the time of the shift.

The risk to which a particular miner is exposed to a lightning-induced premature explosion is therefore

Lightning flashes during shift x five days per week x period that the fuse is ready x surge frequency

= 0.6 x 5/7 x 0.25 x N(f)

= 0.107 N(f)

The risk to a particular miner is therefore

$$N_M = 0.107\ N(g) \times N(d) \times K_p \times K_t \quad \ldots\ldots\ldots\ldots\ldots\ldots\ldots\ldots\ldots\ldots\ldots\ldots\ 10.4$$

This risk is calculated for the mines in which the FSDs had been installed and the result is given in Table 10.6. The table also gives the risk index of these mines.

**Table 10.6** The risk index of the mines involved in the FSD measurement programme.

| Mines | $N_f$ (x $10^{-3}$) | $N_g$ | $N_m$ (x $10^{-3}$) | Risk category |
|---|---|---|---|---|
| Arnot | 1.230 | 6.1 | 0.830 | High risk |
| Delmas | 0.084 | 7.0 | 0.065 | Moderate risk |
| Douglas | 1.000 | 7.0 | 0.770 | High risk |
| Goedehoop | 1.990 | 7.0 | 1.530 | High risk |
| Greenside | 6.320 | 6.5 | 4.520 | High risk |
| Kriel | 1.360 | 7.0 | 1.050 | High risk |
| Landau | 1.790 | 6.5 | 1.280 | High risk |
| Matla | 0.650 | 7.0 | 0.500 | High risk |
| Sigma | 0.400 | 7.5 | 0.330 | Moderate risk |
| South Witbank | 1.310 | 7.0 | 1.010 | High risk |

# 7 DISCUSSION

The frequency at which currents can be induced into detonator-circuits has been dealt with in this chapter, up to the level of calculating the risk to which a particular miner is exposed. The choice of high, moderate and low risk indices is somewhat arbitrary and must be debated with the coal-mining industry. The relationship between the developed model and the risk index is not absolute either. It is open to "calibration" and is part of the discussion on the risk index.

# CHAPTER 11

# RECOMMENDATIONS AND FINALE

This chapter concludes this thesis. Firstly, it proposes some amendments to be made to the existing Code of Practice and that other required actions be taken, such as incorporating the recommendations into permitted detonator standards.

Secondly, the chapter focuses on the assumptions and simplifications made in this thesis and highlights areas where further work will be beneficial.

Lastly, the unique contributions made by the thesis are emphasised.

## 1 AMENDMENTS TO THE CODE OF PRACTICE

This section focuses on improvements that can be made to the Code of Practice, discusses and proposes amendments to the Code. However, it should be clearly stated that the existing Code has contributed significantly towards improving safety in shallow coal mines in South Africa.

One of the main factors that made the biggest contribution to the improvement in safety was the installation of lightning-warning devices in the mines, ensuring that the handling of explosives ceases during thunderstorms. A second factor was the introduction of Type 1 "Stat Safe" detonators in the collieries which decreases the risk of a detonator explosion by a factor of four (not 15 as claimed by the manufacturer).

### 1.1 Mine risk index

The thesis culminates (in Chapter 10) in a proposed method for determining the frequency to which a miner (using Type 0 detonators) is exposed, assuming that no particular safety measures have been implemented. This is then related to the risk to which a miner is exposed at present. This, in turn, is then translated into a Mine Risk Index indicating whether the risk of a particular mine experiencing lightning-related accidents is high or low.

The strictly correct way of determining the risk of accidents involving Type 1 detonators and accidents caused by the ignition of methane will be to repeat the analysis of Chapters 3 and 10. However, in the absence of this analysis, it would be reasonable to use the

analysis done for Type 0 detonators, as a relative measure of the risk of methane explosions or of Type 1 detonators being set off; (i.e. as a more generalised indication of the risk of a lightning-related accident occurring in a mine). There will be a factor difference between the predicted frequency in these two cases.

It is proposed that this Risk Index be incorporated into the Code of Practice to assist mine management to manage risk intelligently, thereby optimising the economy of the mining operation.

## 1.2 Detonators

Collieries in the affected areas have replaced Type 0 detonators with Type 1 detonators. This change seems to have made a significant difference to the number of detonator accidents that occurred in collieries in the Eastern Transvaal. This is proved by the absence of lightning-related accidents in the accident statistics obtained from Cloete (1994), compared to the list of lightning-accidents in the 1980's.

It is proposed that the code be amended to ***strongly recommend*** (almost compel) managers of mines in the high-risk category to use Type 1 detonators. It is also recommended that mines in the moderate-risk category also use Type 1 detonators (or equivalently rated detonators).

## 1.3 Connection of detonators

The number of detonators exposed to lightning currents, and the magnitude of the currents through the detonators, can be minimised by cleverly connecting the circuit: if the pattern of current flow between the face and the exploder is inspected (see Figure 10.1), it is evident that the current flow is between the top of the face and the bottom of the face, and between the top of the face and the position of the exploder.

Lightning current to individual detonators can be minimised by connecting the exploder wires to the middle of the top row of detonators. The current flowing diagonally across will be conducted mainly by the exploder cable, and not vertically down the face circuit (through detonators), as would be the case if the exploder cable was connected to the set of detonators in the middle of the row close to the floor.

This blasting technique methodology will have to be taught to the miners to establish this method as the standard method of wiring up a coal face.

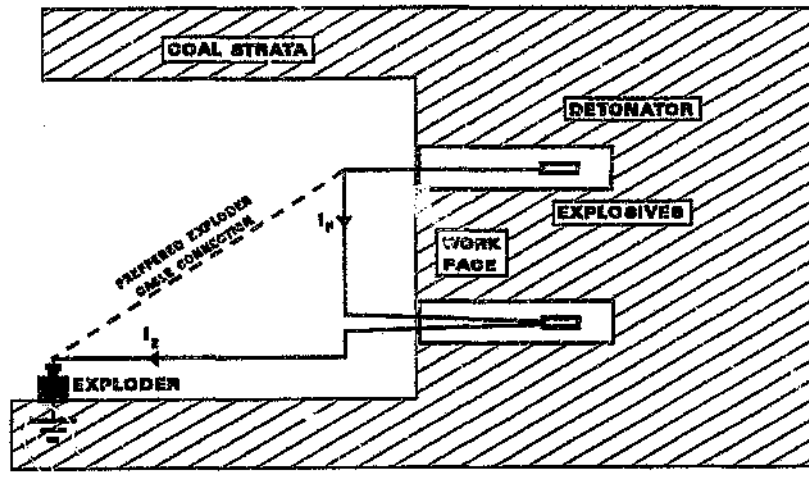



**Figure 11.1** The lightning surge current flow between the face and the exploder. Connecting the exploder cable to the top is preferred.

## 1.4 Methane

In the present Code of Practice, there is no clear discrimination between mines that have a high risk of methane emissions and those mines that have a low risk of methane emissions.

Mines that have a "methane problem" must be aware of the risk of a ventilation failure occurring at the same time that there are lightning storms on the surface and that this combination of circumstances is very dangerous. The probability of losing power for an extended period of time is small, but significant. Lightning is often the cause of power failures and the coincidence of these two factors occurring at the same time is possible. If power does fail, mines must either restore ventilation in a reasonable time or consider evacuating the mine.

The results of the tests on methane sensitivity and current penetration indicate that methane in quite deep mining depths can possibly be ignited by lightning.

It is proposed that a panel of experts, including methane-explosion and mining experts, should be brought together to develop appropriate counter measures.

## 1.5 The relevance of mine depth

In the present Code of Practice, it is stated that mines deeper than 200 m are minimally affected by lightning. From the data resulting from the FSD programme and the models that were developed, it can be stated that mines below the depth of 150 m are definitely safe, and that the risk is low at 100 m.

## 1.6 Earthing of the shaft entrance

In the present Code of Practice, there is no reference to any specific value of earth-electrode resistance that should be used as a standard. It is also suggested in the Code that the underground service structures, such as conveyer belts and power cables, be bonded to roof bolts at intervals not exceeding 200 m.

From the analysis from Chapter 2, it is suggested that the target earth resistance to aim for is 5 Ω.

Concerning the bonding of the underground service structures, the effect of these structures is most pronounced when underground operations are close to a shaft entrance and the risk gradually diminishes when service structures are further and further away from the shaft. It is proposed that the roofbolts close to the shaft be earthed more regularly than those further away from the shaft. In the first 500 m from the shaft, roofbolts should be earthed at every 50 m. It should also be stressed that the roofbolt-earths must be connected to the roof of the mine as well as to the floor (vertically up and down.) This will allow the equalization of potential of the strata above and below the high-resistivity coal seam. At distances further than 500 m away from the shaft, earthing at intervals of 200 m can be used, as recommended at present.

## 1.7 Mechanisms through which lightning can affect mines

In the Code of Practice, it is stated that radiation is one of the ways in which lightning can affect underground operations. The analysis in Chapter 2 suggests that one of the two other mechanisms will always have a stronger effect than radiation. It is suggested that this paragraph in the Code be scrapped.

# 2 A SAFETY STANDARD FOR COLLIERY DETONATORS

It is suggested that the tests discussed in Chapter 9 to evaluate the lightning safety of detonators be included in the Code of Practice for permitted detonators in collieries. The lightning tests described in paragraph 4 and paragraph 5 of Chapter 9 (on the proposed fuse-head spark test) are particularly important.

The inclusion of these tests will ensure that conventionally designed detonators as well as new innovative detonators will be compatible with the environment in which they will operate. This will also assist the designers of new detonators to follow the right design strategy from the start of the development to avoid possible costly re-engineering that could occur when the products, after being used in the field, have been found to be incapable of dealing adequately with the environmental stresses.

This detonator safety standard will then be linked to the Code of Practice which prescribes the levels of safety in mines, depending on their risk index.

# 3 FURTHER WORK REQUIRED TO REFINE THE FINDINGS OF THIS THESIS

Several of the models developed in this thesis, and some of the experimental work that was used to develop the models, need to be studied further to enhance the accuracy of the models. Some of the main issues that require further study are listed below and discussed.

## 3.1 The frequency of surges - model

At the time that the above model was developed, the author did not have the insight into the real complexity of the strata layers; this understanding was gained through the development of this thesis. It became clear towards the end of the study that several other models, apart from the three-layer-strata model that is analysed here, need to be analysed.

With reference to the coal fields of the Eastern Transvaal where there are five main seams, the model can be applied reasonably well when the top coal seam nearest to the surface is mined. However when one of the deeper layers is mined, the upper coal layers must have an appreciable shielding effect on the layers further down. The present model does not make provision for this.

Further, the author suspects that the deeper layers may even have an enhanced effect on the surges experienced in the uppermost layer. This is also suggested by the rather high

surge magnitude versus distance factor that was observed in the results of the "Accurate Measurement" programme (at Greenside Colliery), reported in paragraph 6 of Chapter 4.

However, this thesis lays the basis of the methodology that can now be applied to any strata configuration, depending on the extent to which the resistivities of the layers are know

## 3.2 Coal resistivity and the Oettlè model

The voltage required to set off a detonator was studied in Chapter 8. It was based on one block of coal in particular that had a specific resistivity. Earth resistivity tests on only one block of coal are not enough to arrive at a model that makes provision for different coal resistivities. To supplement the data, the author drew on the work of Oettlè.

This was a rather poor solution for this problem; there is evidence that the physical difference between the conduction in the granular-type of soil that Oettlè's work was based on and the conduction in coal are significantly different. The evidence is shown by the impedance-versus-time effects in the two experiments: in coal, the instantaneous impedance increases in time but, in the media tested by Oettlè, it decreased with time. However, because of the lack of better information, the Oettlè model is used here.

This model is important because it lays the foundation of the "equivalent test resistance" used in the generalised lightning safety test for detonators.

It is therefore suggested that the impulse resistivity of various different coals with different resistivities, under divergent current density conditions, be studied in the laboratory. The knowledge obtained from this will then have to be generalised to fill the gap in the data base.

## 3.3 The effect of underground structures on the distribution of lightning surge currents

The model developed in Chapter 3 does not take the effect of any underground structures into consideration. The underground structures must play a significant role in the way that current penetrates the strata close to such structures. It is suspected that it may have a focusing effect, concentrating more current in some areas than in others.

To analyse this effect a true three-dimensional analysis is required. Programmes that are capable of three-dimensional analysis are not readily available and are costly. This may

make this analysis difficult to realise.

The distance that service structures ought to be away from the coal face must also be addressed by this analysis. At present the Code of Practice recommends that no remotely "earthed" objects (such as electric coal drills, shuttle cars etc.) should be within 25 m of the explosives-charging operation. In the view of the author, these earthed objects ought to be further away; however, there is no concrete definitive study to verify this opinion.

## 3.4 The effect of the mined-out section on current distribution

The model of Chapter 3 does not take the mined-out sections of the mine into consideration. This is a refinement that can be done with relative ease in future.

It can be stated that the mined-out area will, on average, have the effect of increasing the resistivity of the coal layer by the ratio of the volume of coal removed in the mining operation. (On average, 65% of the coal in the area is removed and 35% of the coal remains.) There will also be a localised increase in the current density through the remaining coal. In general, this is expected to increase the occurrence of surges.

## 3.5 Depths exceeding 100 m

The analysis in Chapter 3 was only done for depths of 100 m. The effect of current at depths of 150 m and at 200 m should also be analysed to get a more comprehensive picture. Mines in the moderately dangerous group and in the lower index groups have depths of 100 m and more.

## 3.6 Extrapolation of the effects of resistivity and coal seams

In the postulation of calculating the frequency of surges in the mine risk index (Chapter 10), it is assumed that the effects of resistivity and the thickness of the coal seam scale linearly to other mine depths. This postulation has not been tested. It is important to test this assumption by analysis.

## 3.7 Methane - lightning sensitivity

The results of the experimental work reported in this thesis differ significantly from work that has been obtained by other researchers. It is necessary to find out whether these

differences are due to experimental differences between the reported work or whether they are due to experimental error.

## 4 HIGHLIGHTS OF THE THESIS

In this thesis, the author has succeeded in quantifying the frequency at which surges can be expected in different mines. A method of calculating this frequency practically has been proposed. This model can be applied in mines immediately and can be refined by further work.

The model is supported by the results of some unique laboratory experiments to determine what voltage is required to induce sufficient current into a detonator to set it off.

The frequency calculation is validated by the data from FSD programme. In support of the analytical frequency analysis, the FSD device can be applied to determine the vulnerability of particular mines empirically.

The frequency is related to a risk index which will allow mine management to take appropriate preventative measures, depending on the mine's risk index.

In this thesis, a lightning test for electrical/electronic detonators is proposed. This test has been generalised to cater for innovative new detonators. Provision has been made for conduction protection (short-circuit protection) and, if a designer chooses to insulate the detonator against the effects of lightning, the test can still be applied.

The sensitivity of methane has been studied and the results lay the foundation for further work to be done.

**REFERENCES**

Anderson, J G. Lightning performance of transmission lines. Chapter 12 of *Transmission Line Reference Book*, Electric Power Research Institute, Palo Alta, California, pp. 545-558.

Anderson, R B and Eriksson, A J. Lightning parameters for engineering application. *Electra*, vol. 69, 1980, pp. 65-102.

Anderson, R B et al. Development and field evaluation of a lightning earth-flash counter. *IEE Proceedings*, vol. 131, 1984 pt A, no. 2,

Ballard, A J, Geldenhuys, H J. *Report on progress made on the accurate measurement of surges at Springbok and Greenside Collieries and on the Fuse Surge Detector Programme for the period 1 February to 4 May 1988.* CSIR Division of Energy Technology Report No. CENER 8818, May 1988. *

Ballard, A J, Bourn, G W, and Lagesse, R B. *Interim report on the accurate measurement programme of stray current recording and the surge detector programme during the 1988/89 lightning season.* CSIR Report No. ENER-C 89042. *

Bartels, A L. Ignition energies of methane/air mixtures as a function of electrical discharge-type. *2nd International Conference on Electrical Safety in Hazardous Environments*, pp. 148-152, London, 1975.

Bartels, A L, Riddlestone, H G. *The ignition of methane-air gas mixtures by pulse discharges*, ERA Report 5135, 1966.

BASEFA. *Intrinsic safety.* Certification Standard, SFA 3012:1972

Berger, K. Protection of underground blasting operations. Chapter 20 from *Lightning*, ed. R H Golde, London, Academic Press, 1977.

Bourn, G W, Smith M A. *Report on the measurement of underground surges in coal mines caused by lightning during the 1980/81 season.* CSIR NEERI Report No. Ek/8/81, August 1981. *

Cawley, J C and Peterson, J S. *The relative safety factors obtained by using various materials as spark electrodes in methane-air atmospheres.* IEEE Industry Applications Society Annual Meeting, part II, 1988.

De Wet, E R. *Report of an investigation into explosions of explosives in the Landau III Colliery of SA Coal Estates Ltd.* Report from Chief Inspector of Mines, Witbank Area, South Africa, 1980.

Eriksson, A J. *The lightning ground flash - an engineering study.* Ph.D Thesis, University of Natal, South Africa, 1979.

Eriksson, A J. *Summary of underground disturbance measurements carried out at Arnot Collieries.* CSIR NEERI Report No. Ek/1/79, January 1979. *

Eriksson, A J et al. An improved lightning warning system. *SAIEE Symposium on Electronics in Mining*, 1984.

Eriksson, A J. The incidence of lightning strikes to power lines. *IEEE Transactions on Power Delivery*, vol. PWRD-2, no. 3, July 1987.

Forsyth, W and J R Gordon. *Protection of electric detonators against electrostatic discharges*, Imperial Chemical Industries Limited Report, June 1959.

Geldenhuys, H J. *The sensitivity of electrical detonators to lightning stray currents with specific reference to coal mines.* CSIR Report No C ELEK 307, 1982. *

Geldenhuys H J. *Report on the measurement of underground surges in coal mines caused by lightning during the 1981/82 season.* CSIR NEERI Report No. C ELEK 307, August 1982 *

Geldenhuys H J and Oettlé, E E. A discussion of recent work on the prediction of the impulse impedance of earth electrodes. *Cigré Colloquium*, Japan, 1987.

Geldenhuys, H J. The measurement of underground lightning-induced surges in a colliery. *Symposium on Safety in Coal Mining*, Pretoria, 5-8 Oct. 1987.

Geldenhuys, H J et al. The design and use of simple fuse surge detectors top evaluate the occurrence of electrical lightning-induced surges underground in collieries. *Proceedings of the Symposium on Safety in Coal Mining*, Pretoria, October 1987.

Geldenhuys, H J and Ballard, A J. *Report on progress made on the accurate measurement of underground surges at Springbok and on the fuse surge detector programme.* CSIR Internal Report No. I ELEK 322, January 1988. *

Geldenhuys, H J and Bourn, G W. *Report on the performance of Fuse Surge Detectors during the period August 1987 to May 1988.* CSIR Report No. ENER-C 8827. *

Geldenhuys, Eriksson, A J and Bourn, G W. Fifteen years' data of lightning current measurements on a 60 m mast. *SAIEE Transactions*, Sept. 1989, vol. 80, No.1, pp 89 to 103.

Geldenhuys, H J. Further progress on research into lightning-related incidents in shallow South African Coal Mines. *Proceedings of the 23rd International Conference of Safety in Mines Research Institutes*, Washington, DC, Sept. 11-15, 1989.

Geldenhuys, H J and Lagesse, R B. New electrical safety specifications for colliery detonators. *Third International Symposium on Explosives Technology and Ballistics*, Pretoria, 1991.

Golledge, P. Sources of ignition in coal mines. *Australian IMM, Illawarra Branch Symposium*, Australia, 1981.

Hayt Jr, W H. *Engineering Electromagnetics*, 3rd ed. Tokyo; McGraw-Hill Kogakusha Ltd, 1974.

IEC Publication 79. *Electrical apparatus for explosive gas atmospheres.*

Ireland, K S. Private communication. AECI Explosives and Chemicals Limited, 1984.

Johnson, R C, Janota, D E and Hay, J E. An operational comparison of lightning warning systems. *J. Met.*, vol. 3, 1982.

Krzystolik, P A, Dworok, R Investigating the influence exerted by the electric parameters RLC of the shotfiring circuit upon its degree of intrinsic safety. *20th International Conference of Safety in Mines Research Institutes*, vol. 3, Sheffield, 1983.

Kuffel, E and Zaengl, W S. *High Voltage Engineering Fundamentals*. Pergamon Press, pp 266-294, 1984.

Lagesse, R B, Ballard, A J and Geldenhuys H J. *Report on the progress made on the accurate measurement of underground surges*. CSIR Division of Energy Technology Report ENER C 89092, October 1989. *

Lagesse, R B and Bourn, G W. *The performance of Fuse Surge Detectors during the period August 1986 to May 1990*. CSIR Report No. 90052. *

Lagesse, R B and Bourn, G W. *The performance of Fuse Surge Detectors during the period August 1986 to May 1991*. CSIR Report No. 91050. *

Lintin, D R and Wooding. Investigation of the ignition of a gas by an electric spark. *British Journal of Applied Physics*, vol. 10, April 1959.

Marshall, C A. Safety first in the Witwatersrand Gold Mining Industry. *The Transactions of the South African Institute of Electrical Engineers*, vol. no. Feb. 1941.

Naudé, L. *Report of accident which occurred at Greenside Colliery on 23 October 1984*. Report from the Chief Inspector of Mines, Witbank Area, South Africa, 1984.

Naudé, L. *Enquiry into the premature ignition of one shot hole during an electrical storm at Arnot Colliery on 30 September 1985*, Report of the Chief Inspector of Mines, Witbank, South Africa.

Oettlé, E E. A new general estimation curve for predicting the impulse impedance of concentrated earth electrodes. *IEEE Transactions on Power Delivery*, vol. 3, no. 4, Oct. 1988, pp. 2020-2029.

Petrick A J, van Rensburg W C J and Vos A D. *Report of the Commission of Enquiry in regard to the coal sources of the Republic of South Africa*. Department of Mining Report, ISBN 0621024384, Pretoria, April 1974.

Pretorius, M. *The ignition of incendive methane-air mixtures by lightning-related electric sparks*. CSIR Report No. ENER-C 91044, Pretoria, June 1991. *

Santis, L D. Lightning warning system pay off. *Journal of Explosives Engineering*, vol. 6, Sept-Oct. 1988.

Santis, L D. Instrumentation for lightning warning in blasting operations. *IEEE Industry Applications Society Conference*, San Diego, Ca, Oct. 1989.

Schuch, J H. *Investigation into the incident at S A Coal Estates (Landau Colliery) on 23 October 1984.* Report from the Chief Inspector of Mines, Witbank Area, Area, 1984.

The South African Bureau of Standards. *Standard Specification for Intrinsically Safe Electrical Apparatus*, SABS 549, Pretoria, 1987.

The South African Coal Mining Research Controlling Council. *Code of Practice for the avoidance of hazards underground in collieries due to lightning.* Compiled by the Lightning Stray Current Research Subcommittee of the Explosion Hazards Advisory Committee, 1981.

Tolson, P. The stored energy needed to ignite methane by discharges from a charged person. *Journal of Electrostatics*, vol. 8, pp. 289-293, 1980.

Widginton, D W. *Ignition of methane by electrical discharges.* SMRE Research Report 240, January 1966.

Widginton, D W. *Some aspects of the design of intrinsically safe circuits.* SMRE Research Report 256, 1968.

Widginton, D W. *Electrical ignition of gases: Use of controlled Discharges for investigating minimum ignition energies.* Nature, no. 4884, 8 June 1963.

* Note: Reports available from

CSIR
P O Box 395
Pretoria
0001
South Africa

# APPENDICES


I The Accurate Measurement Research Station at Springbok Colliery

II The Accurate Measurement Research Station at Greenside Colliery

III Accurate measurements taken in Configuration 1 at Landau Colliery

IV Accurate measurements taken in Configuration 3 at Springbok Colliery

V Accurate measurements taken in Configuration 4 at Springbok Colliery

VI Accurate measurements taken in Configuration 5 at Springbok Colliery and Greenside Colliery

VII The location of Fuse Surge Detectors in mines taking part in the Fuse Surge Detector Programme and information about the strata

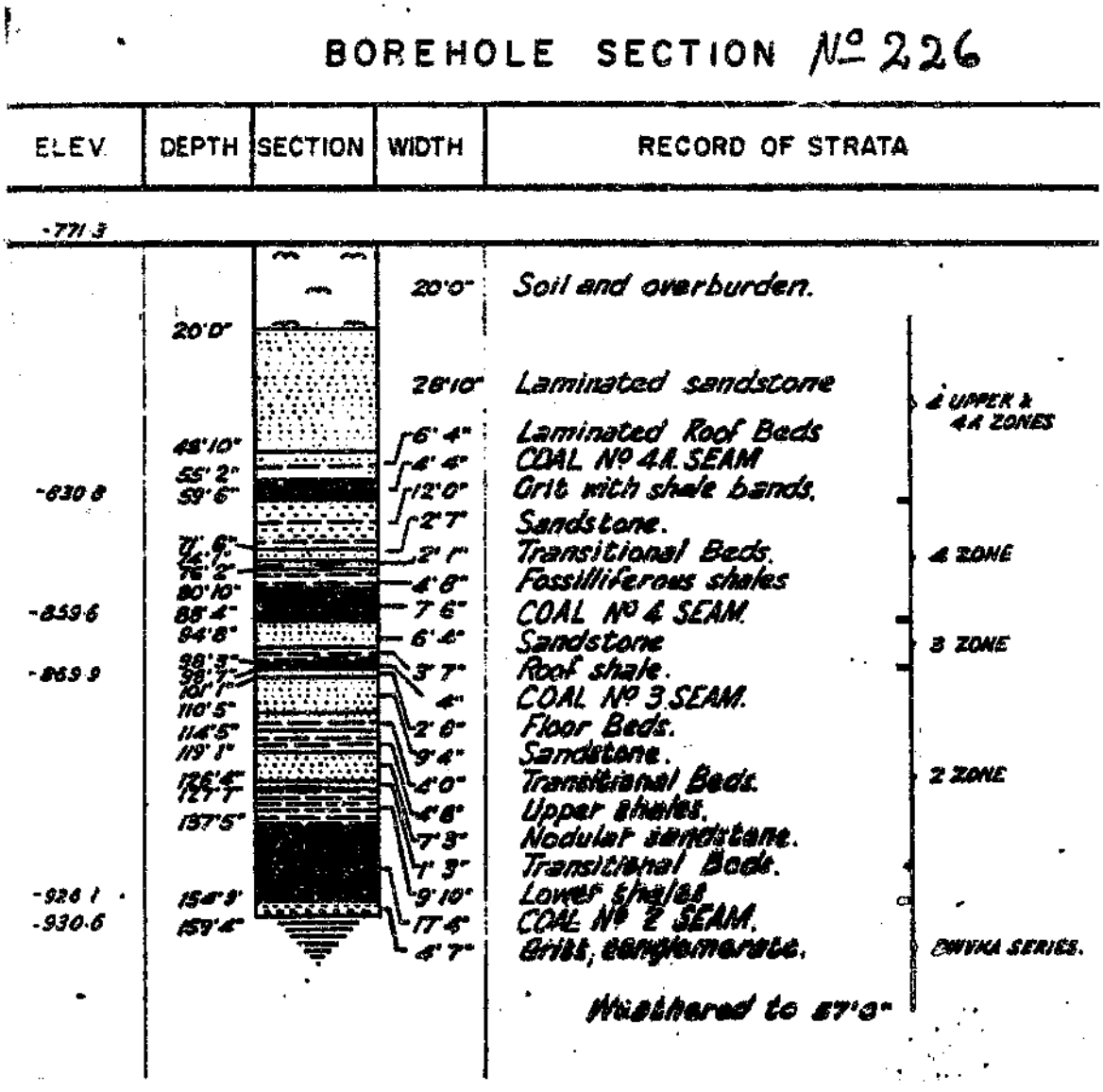
**APPENDIX I**

# THE ACCURATE MEASUREMENT RESEARCH STATION AT SPRINGBOK COLLIERY

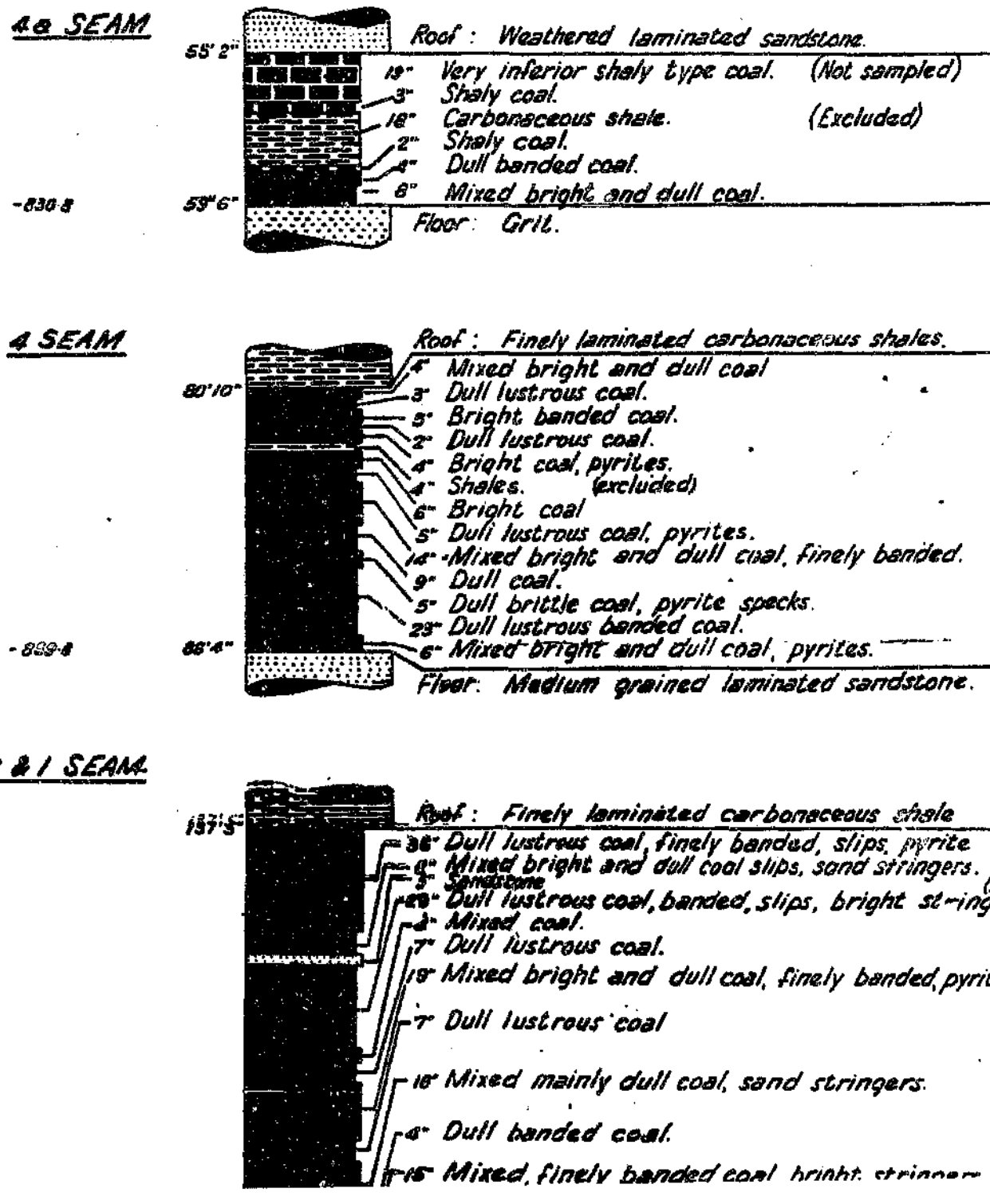
Geographic information

Geological information about the strata

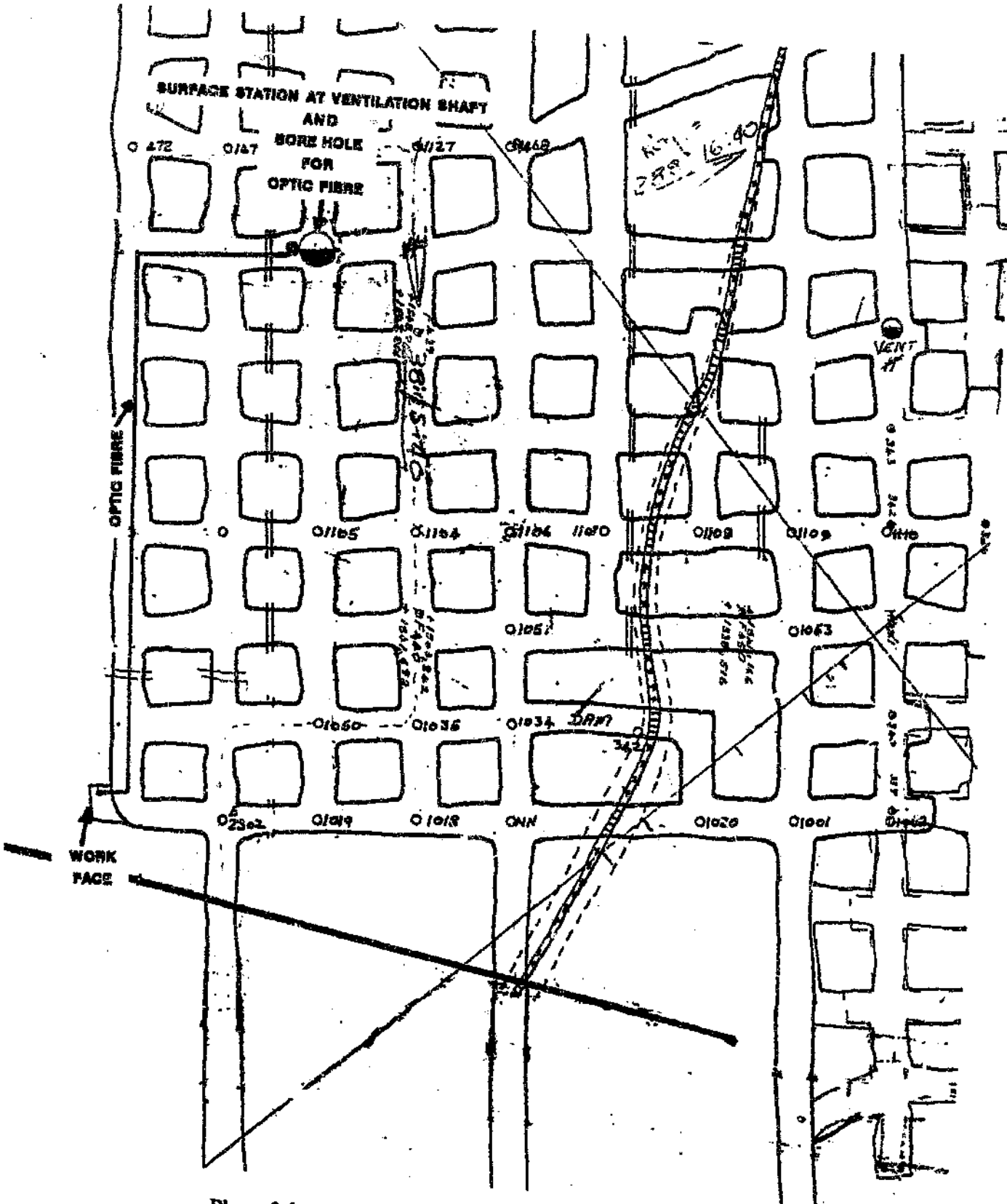
Earth resistivity measurements



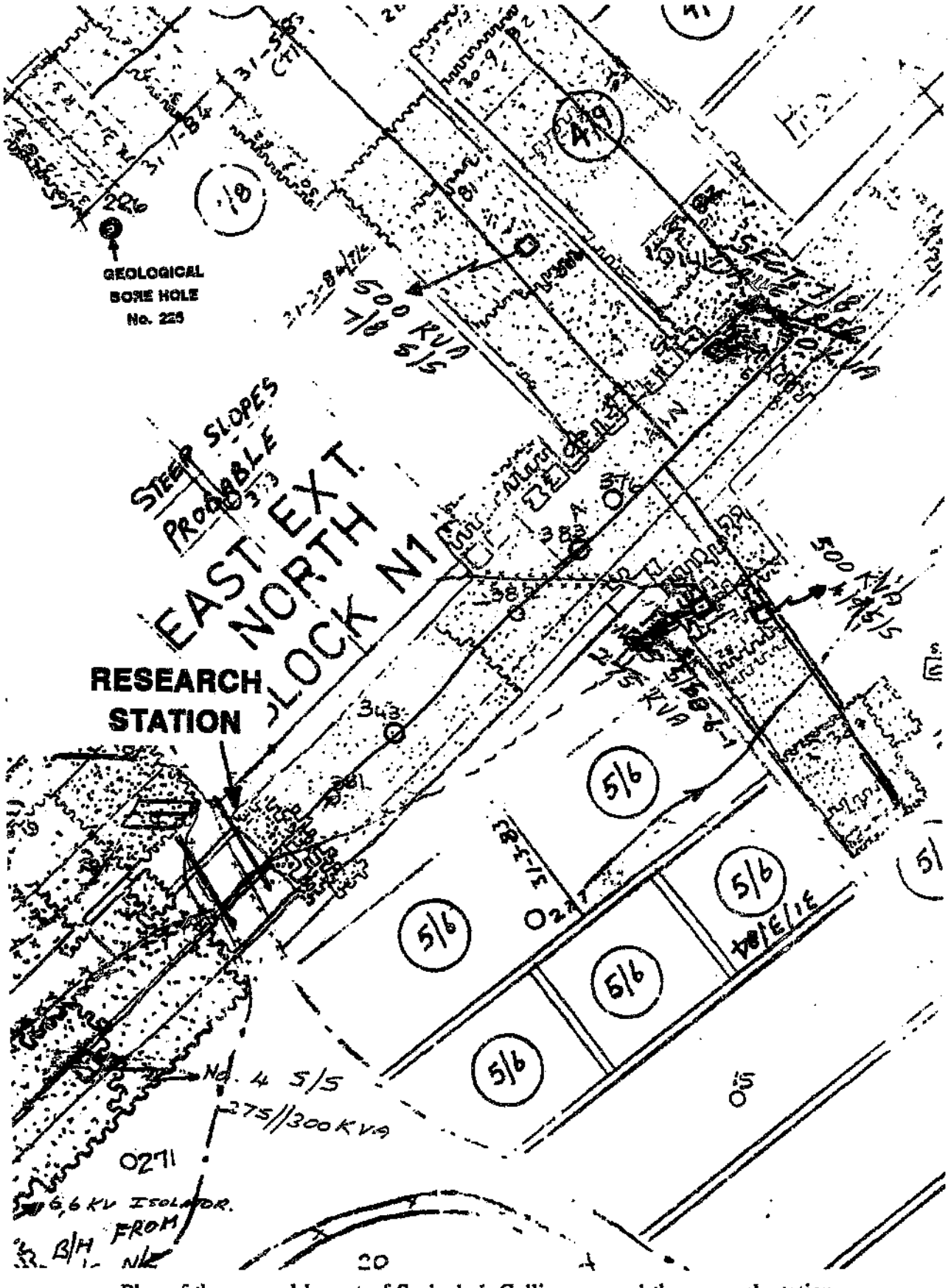

Analysis of the geological borehole situated
about 800 m from the research station at Springbok Colliery




Details of the coal seams in Springbok Colliery.
Note the high shale content of 40 Seam.




Plan of the area around the research station at Springbok Colliery




Plan of the general layout of Springbok Colliery around the research station. The position of the geological borehole is also shown.

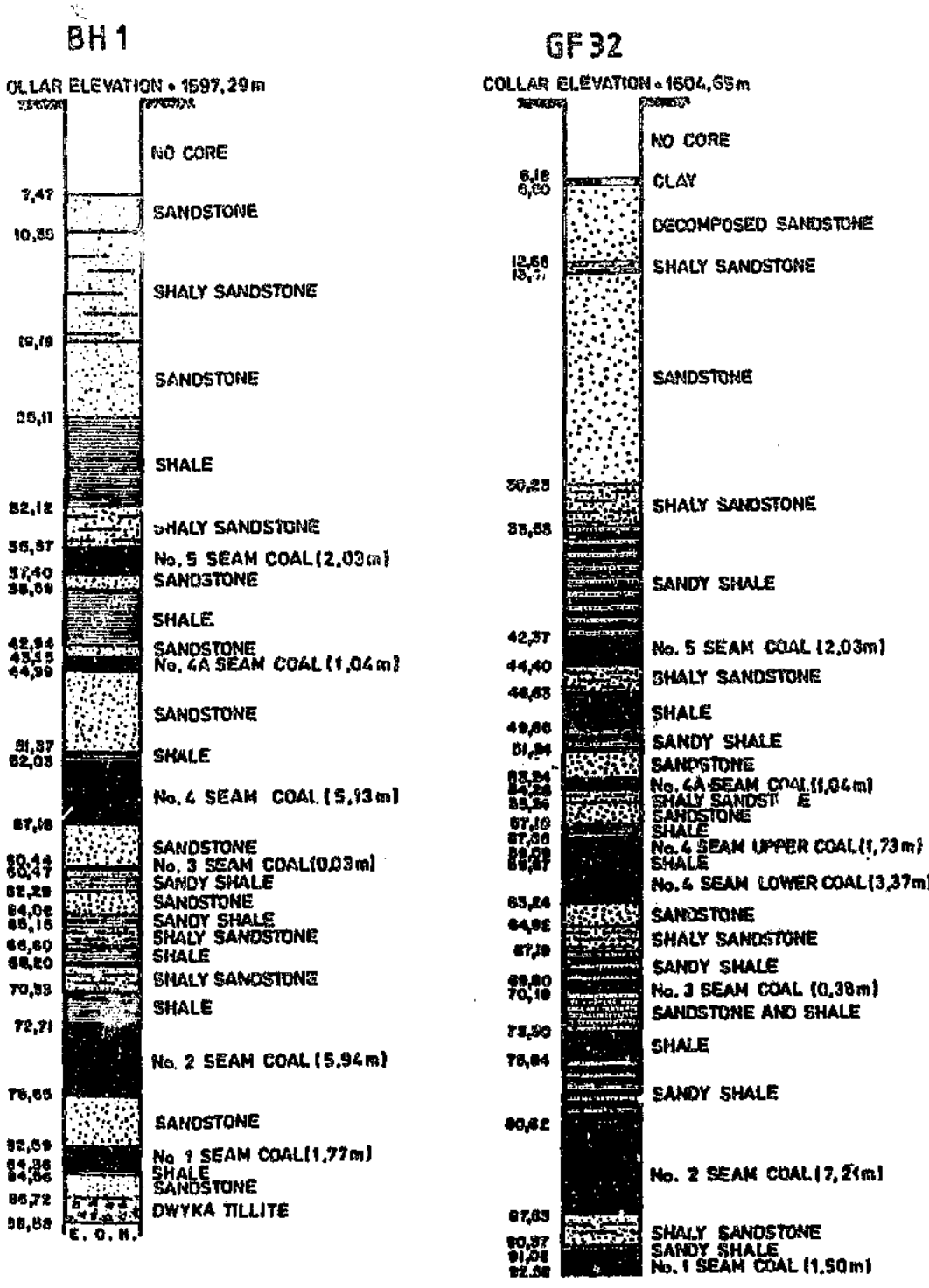
**APPENDIX II**

# THE ACCURATE MEASUREMENT RESEARCH STATION AT GREENSIDE COLLIERY

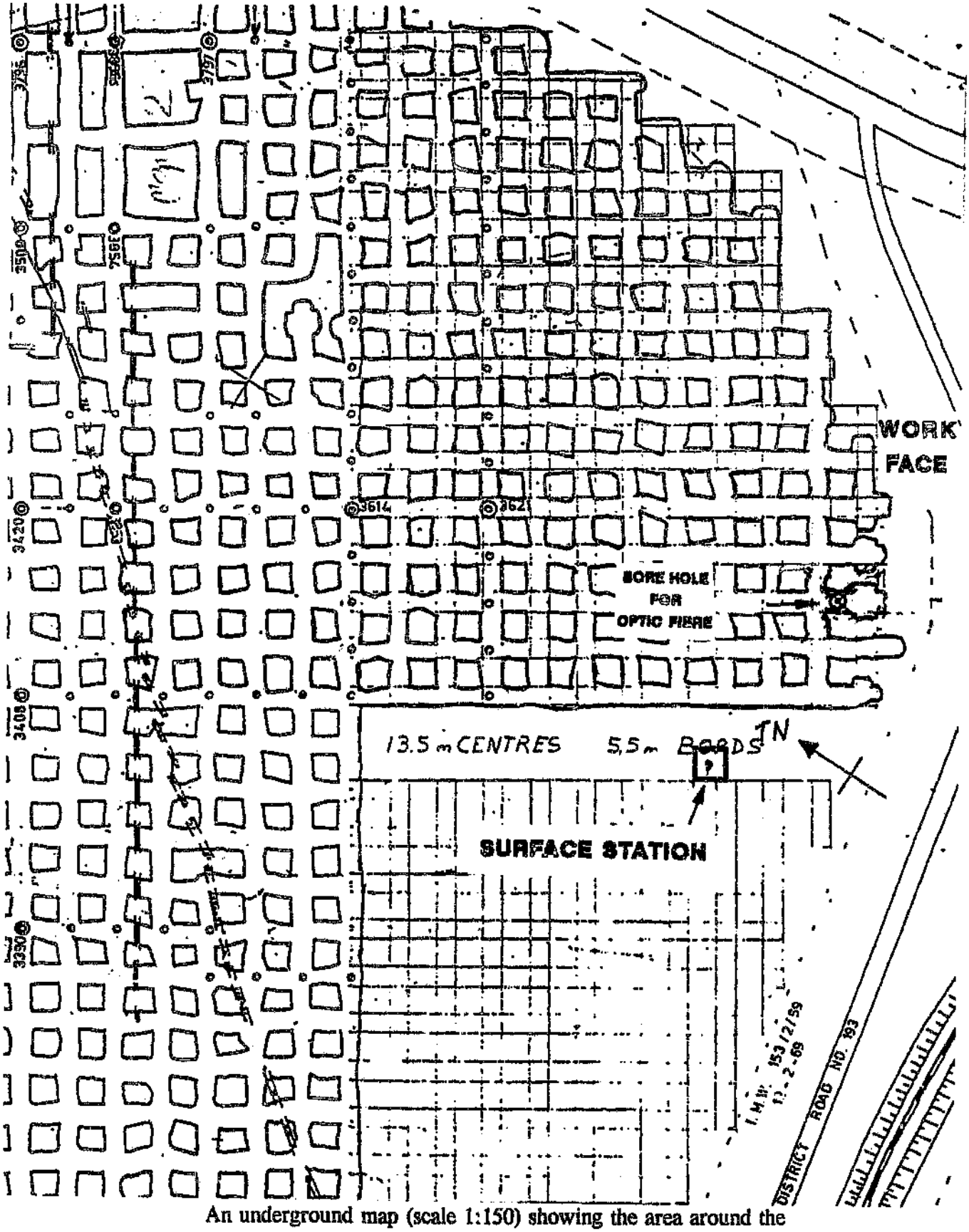
Geographic information

Geological information about the strata

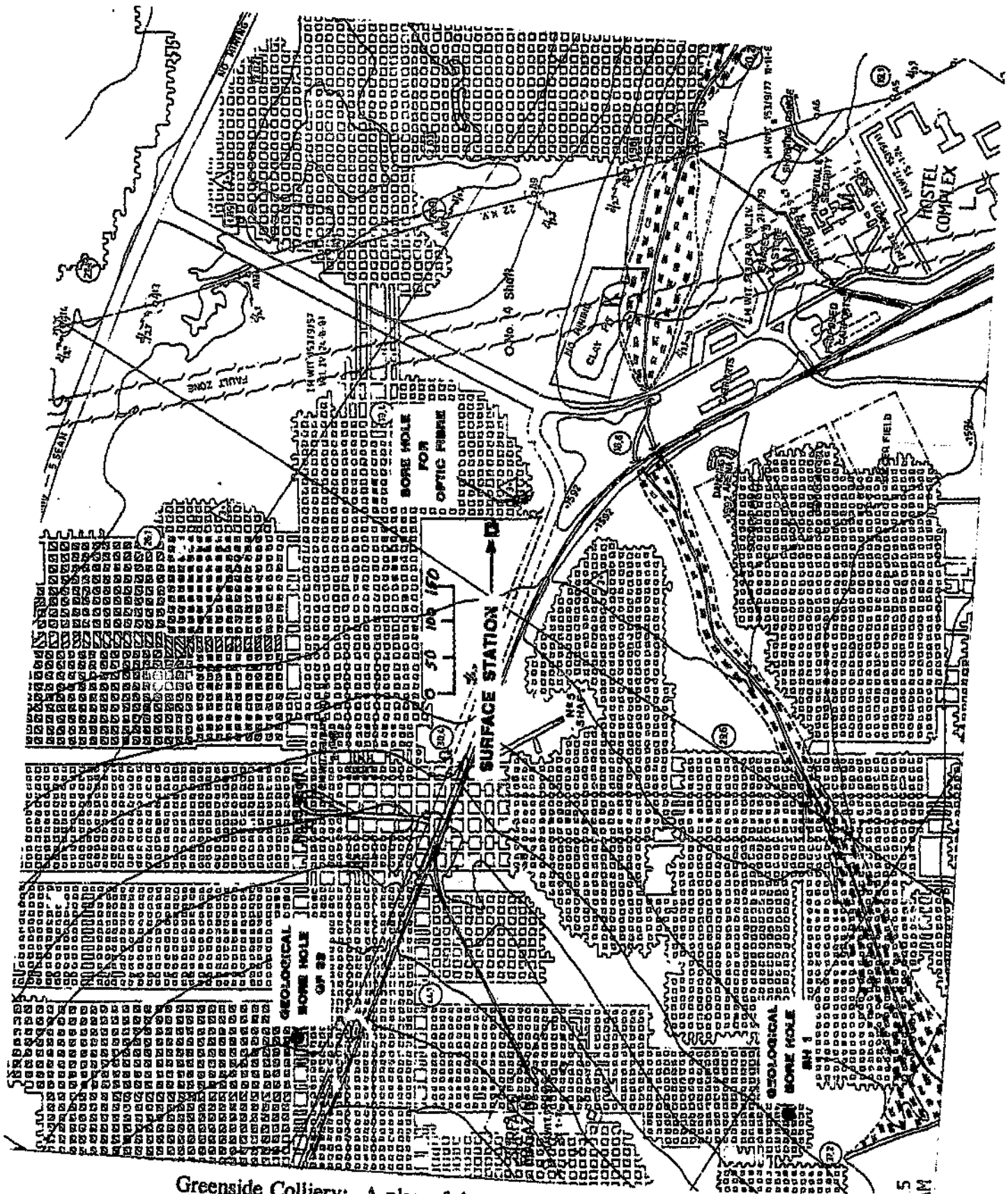
Earth resistivity measurements




The geological boreholes (BH 1 and GF 32) near the research station at Greenside Colliery

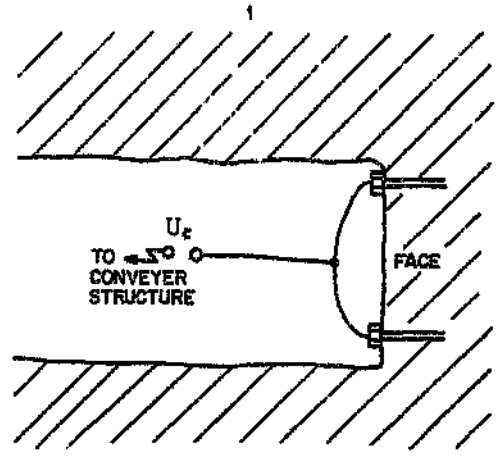



An underground map (scale 1:150) showing the area around the research station at Greenside Colliery




Greenside Colliery: A plan of the general area of the mine near the the research station. The positions of geological boreholes GF 32 and BH 1 are also shown. (Scale 1:7 000.)

# ACCURATE MEASUREMENTS TAKEN IN CONFIGURATION 1 AT LANLAU COLLIERY




CONFIGURATION 1
$U_c$ – CONVEYER VOLTAGE

Configuration 1: The voltage measured between the face and the conveyor structure

DATALOGGER

86/03/10 13:48:49

Storm 1

| 86/03/11 | | | 15:50:38 |
|---|---|---|---|
| Surge no. | | | Time |
| 1 | : 1 | 1 | 16:04:32 |
| 1 | : 2 | 2 | 16:31:16 |
| Storm 1 | | 2 | surges |
| 86/03/11 | | | 17:51:24 |

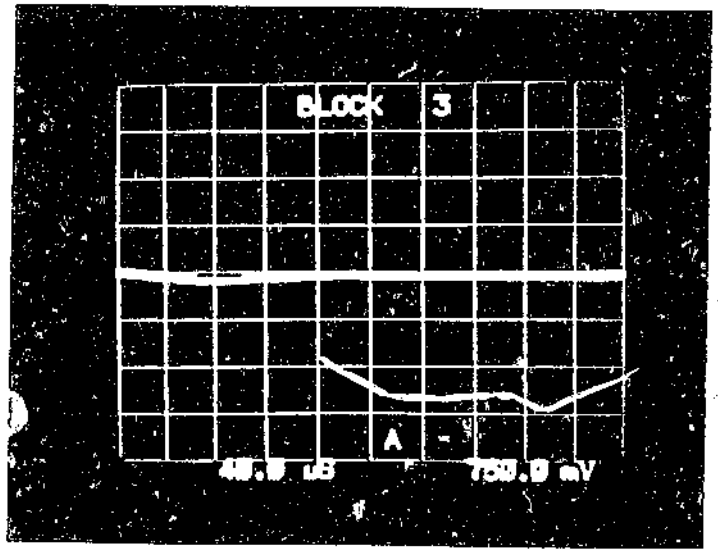
Storm 2

| 86/03/12 | | | 14:13:13 |
|---|---|---|---|
| Surge no. | | | Time |
| 2 | : 1 | 3 | 14:33:01 |
| Storm 2 | | 1 | surges |
| 86/03/12 | | | 16:07:42 |

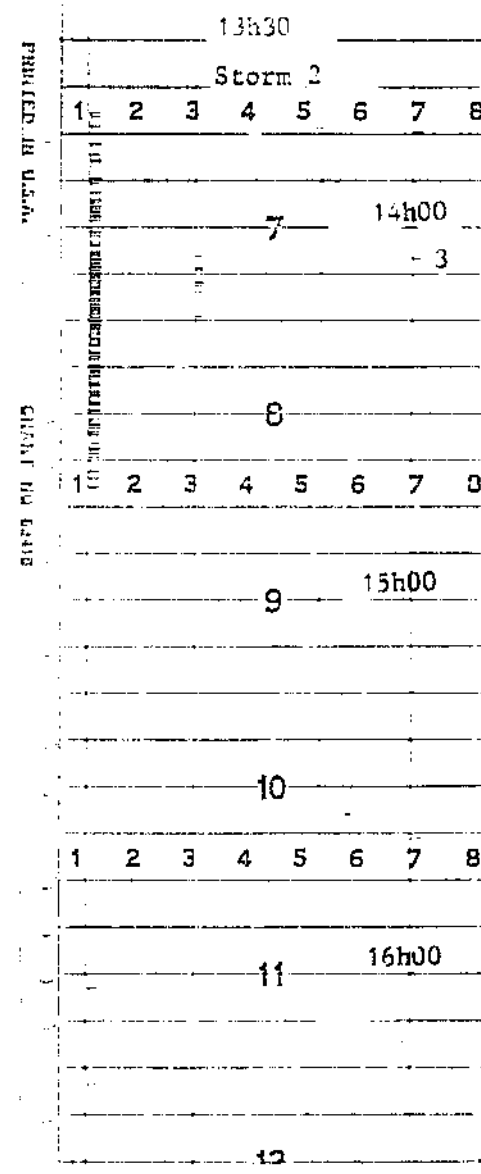
Storm 3

| 86/03/12 | | | 21:26:01 |
|---|---|---|---|
| Surge no. | | | Time |
| 3 | : 1 | 4 | 21:37:19 |
| 3 | : 2 | 5 | 21:54:59 |
| 3 | : 3 | 6 | 22:10:29 |
| 3 | : 4 | 7 | 22:30:05 |
| 3 | : 5 | 8 | 22:37:37 |
| Storm 3 | | 5 | surges |
| 86/03/12 | | | 23:59:39 |

1. Computer printout




Wednesday, 12 March 1986




2. Event recorder chart:

Pen 1: RSA 10 - 20 km
Pen 2: RSA 10 - 5 km
Pen 3: Diesel on
Pen 4: Surge

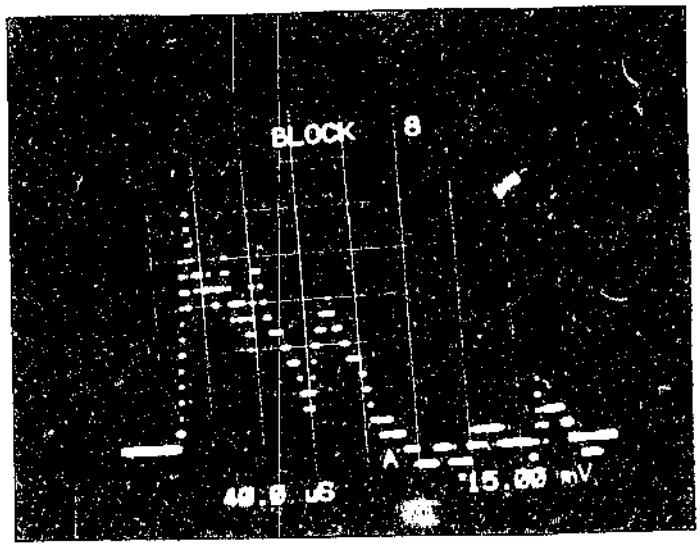
3. Oscilloscope:

3rd Surge of storm

Scale: 40 us/div (H)
750 mV/div (V)

V Peak -300 V

Typical examples of the format of the results obtained in the accurate measurement programme

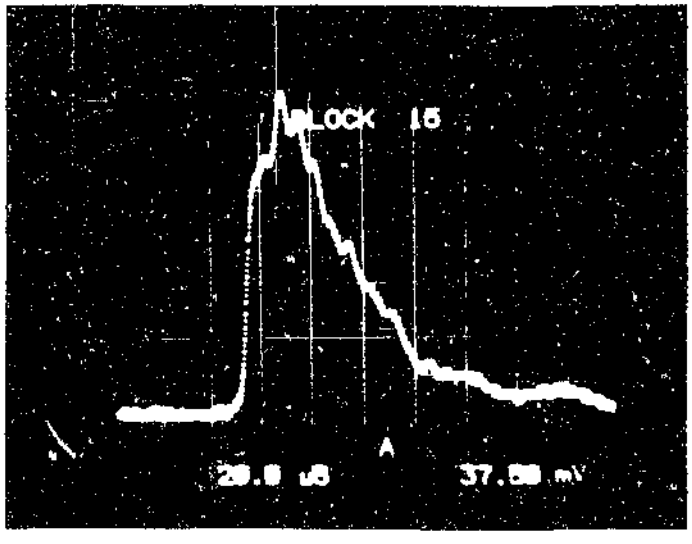



Surge No. 8: 227 V peak, 40 µs/div

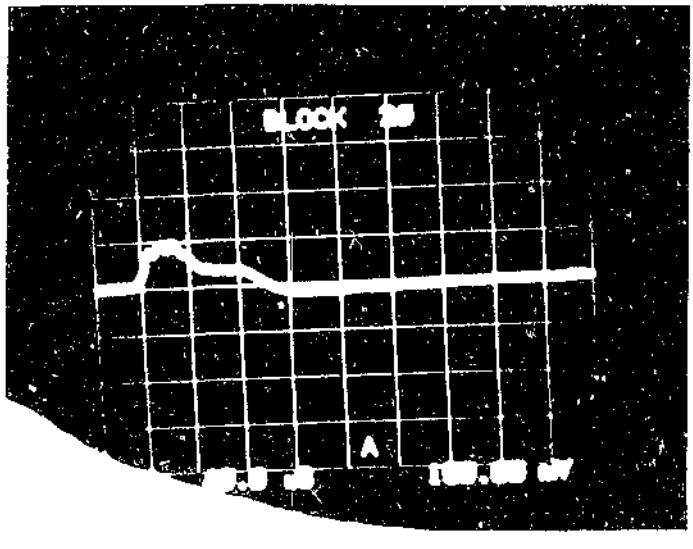
STORM 1

Monday, 24 March 1986, 07h11

Voltage divider: 1 000 : 1




Surge No. 15: 773 V peak, 20 µs/div




Surge No. 20: 409 V peak, 20 µs/div.

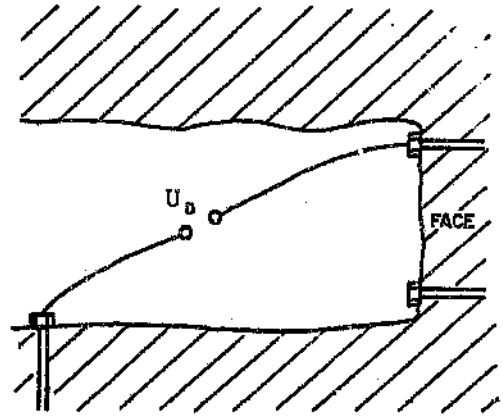
DATALOGGER

86/03/21 14:17:01

Storm 1

| 86/03/24 | | 07:11:24 |
|---|---|---|
| Surge no. | | Time |
| 1 | 1 | 07:14:24 |
| 2 | 2 | 07:15:47 |
| 3 | 3 | 07:16:56 |
| 4 | 4 | 07:17:79 |
| 5 | 5 | 07:17:55 |
| 6 | 6 | 07:18:49 |
| 7 | 7 | 07:20:17 |
| 8 | 8 | 07:20:59 |
| 9 | 9 | 07:21:31 |
| 10 | 10 | 07:22:26 |
| 11 | 11 | 07:23:55 |
| 12 | 12 | 07:23:48 |
| 13 | 13 | 07:24:07 |
| 14 | 14 | 07:24:37 |
| 15 | 15 | 07:24:49 |
| 16 | 16 | 07:26:48 |
| 17 | 17 | 07:27:15 |
| 18 | 19 | 07:27:36 |
| 19 | 19 | 07:28:04 |
| 20 | 20 | 07:28:41 |
| 21 | 21 | 07:29:34 |
| 22 | 22 | 07:29:49 |

# ACCURATE MEASUREMENTS TAKEN IN CONFIGURATION 3 AT SPRINGBOK COLLIERY



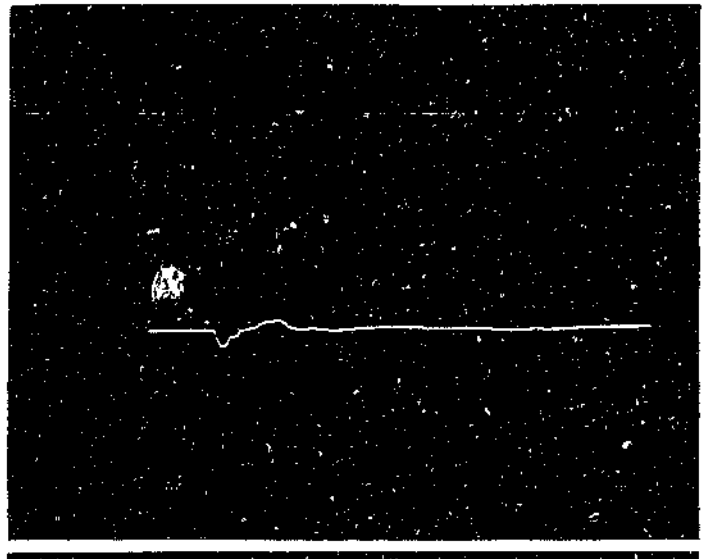

CONFIGURATION 3
$U_D$ – DIAGONAL VOLTAGE

Configuration 3: The voltage measured diagonally ($V_D$) between the top of the face and the "exploder" point



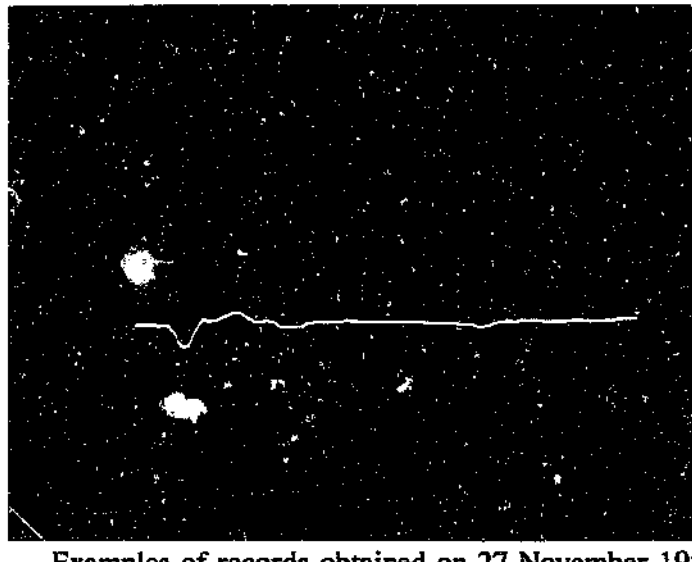
- 1 017 $V_{peak}$

400 $\mu$s sweep



- 484 $V_{peak}$

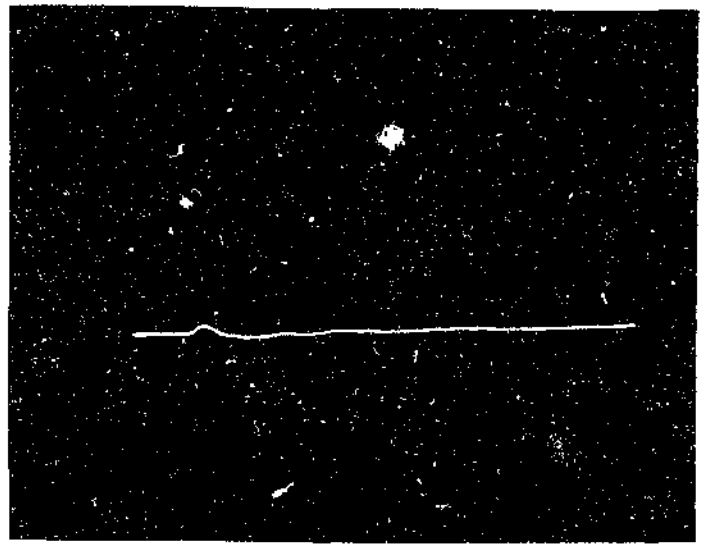
400 $\mu$s sweep



- 688 $V_{peak}$

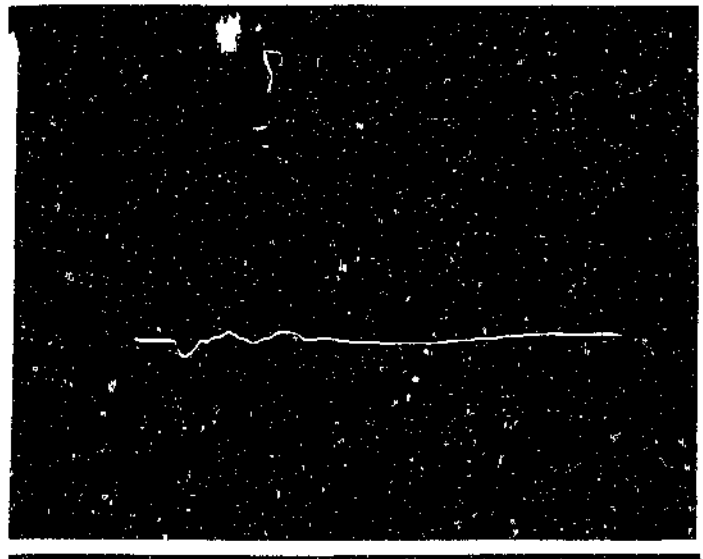
400 $\mu$s peak

Examples of records obtained on 27 November 1986 in Configuration 3 at Springbok Colliery



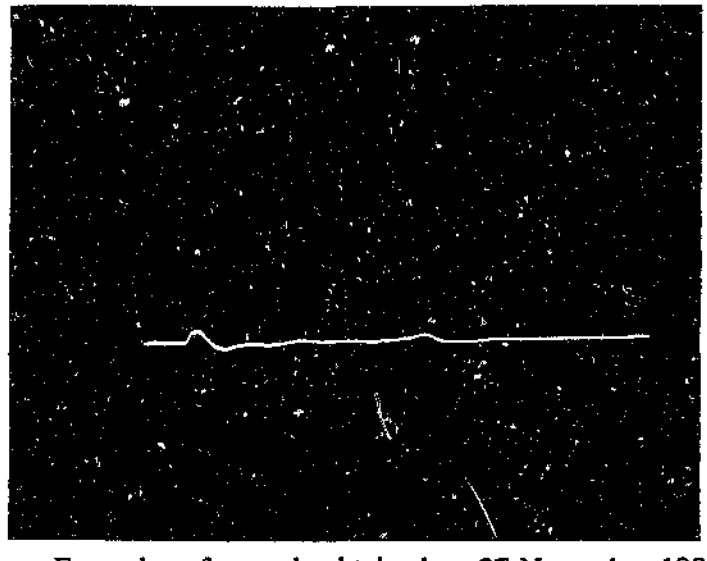
+ 234 $V_{peak}$

400 $\mu$s sweep



- 446 $V_{peak}$

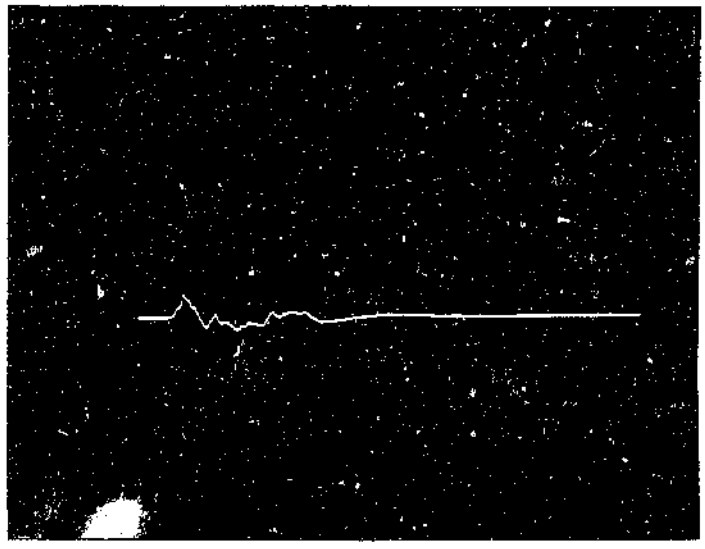
400 $\mu$s sweep



+ 350 $V_{peak}$

400 $\mu$s peak

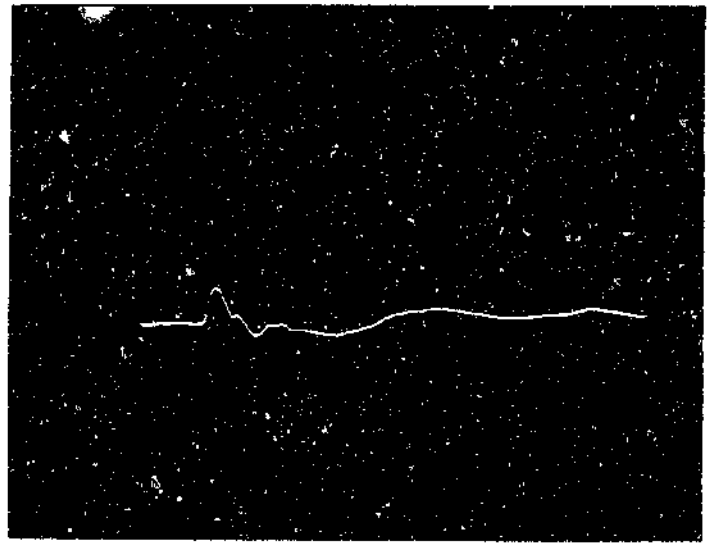
Examples of records obtained on 27 November 1986 in Configuration 3 at Springbok Colliery



+ 601 $V_{peak}$

400 $\mu$s sweep

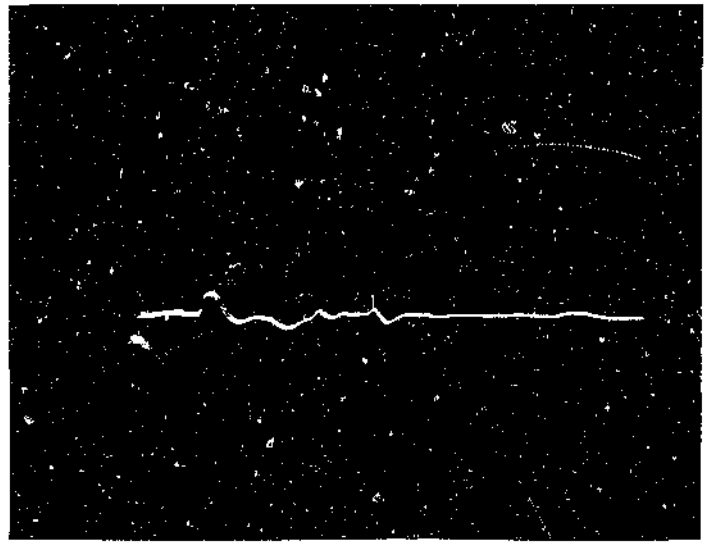
Record 1



+ 892 $V_{peak}$

400 $\mu$s sweep

Record 4

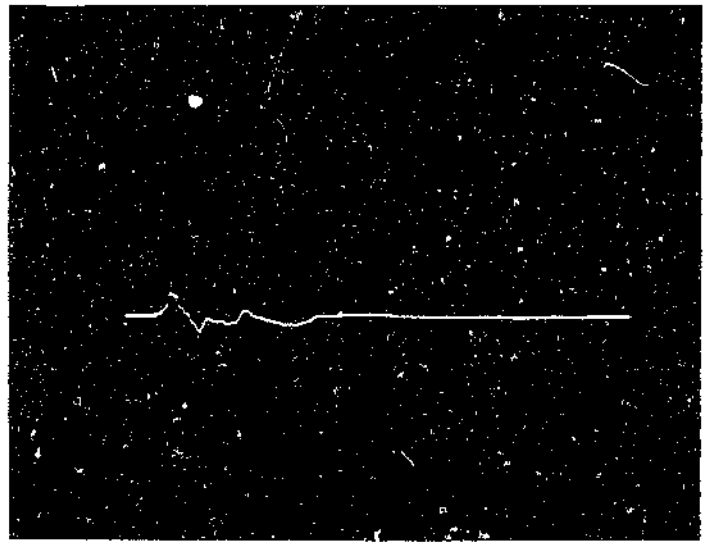


+ 737 $V_{peak}$

400 $\mu$s peak

Record 6

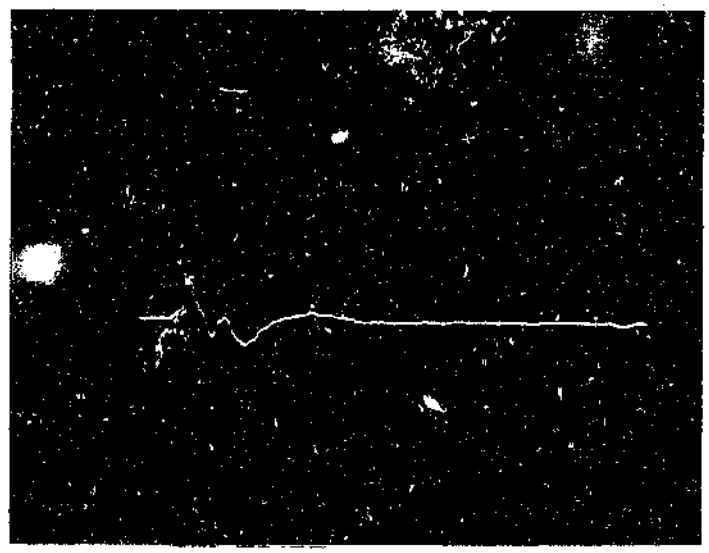
Records obtained on 1 December 1986 in Configuration 3
at Springbok Colliery



+ 504 $V_{peak}$

400 $\mu$s sweep

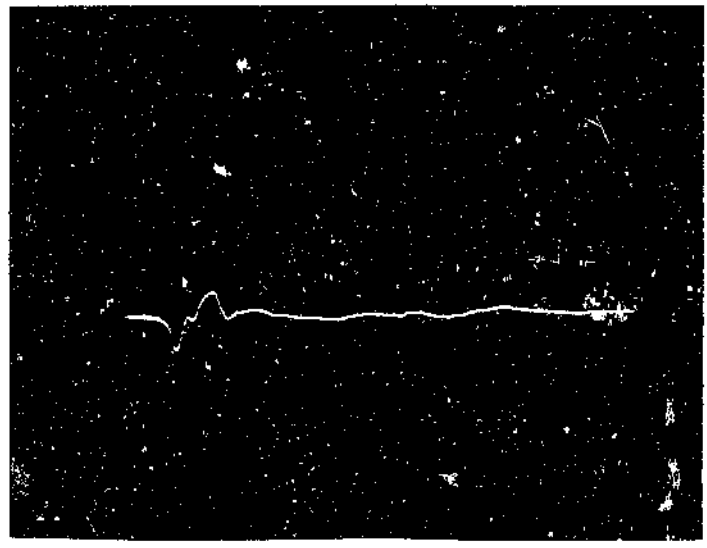
Record 7



+ 970 $V_{peak}$

400 $\mu$s sweep

Record 8

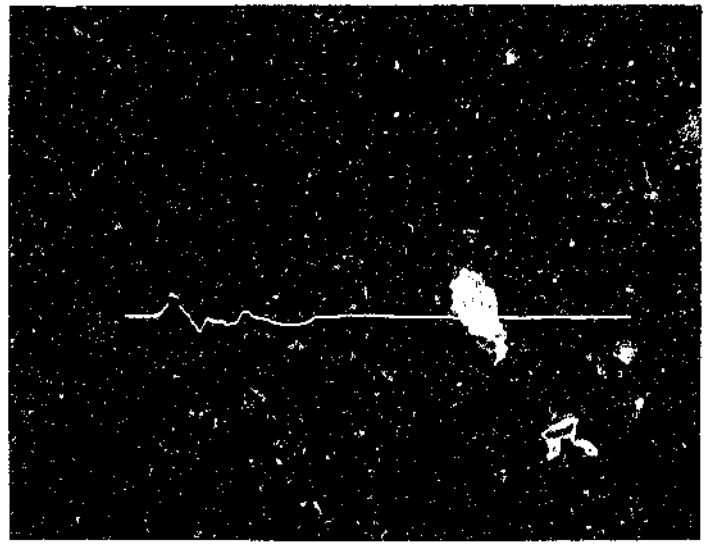


- 834 $V_{peak}$

400 $\mu$s peak

Record 9

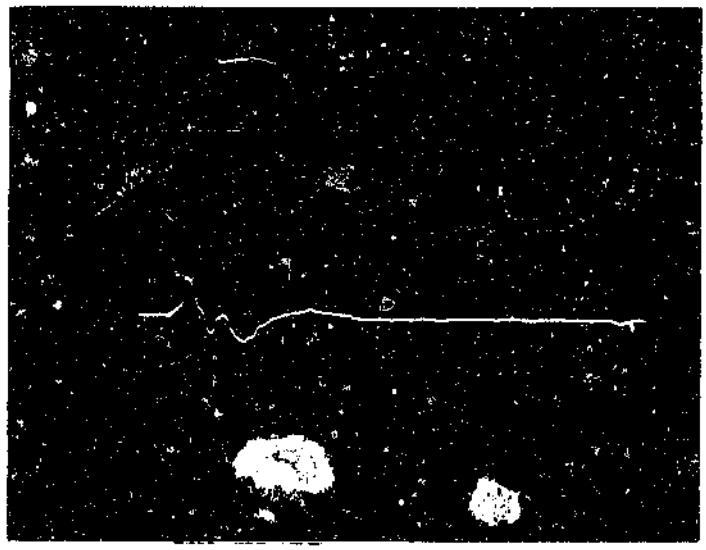
Records obtained on 1 December 1986 in Configuration 3
at Springbok Colliery



+ 504 $V_{peak}$

400 $\mu$s sweep

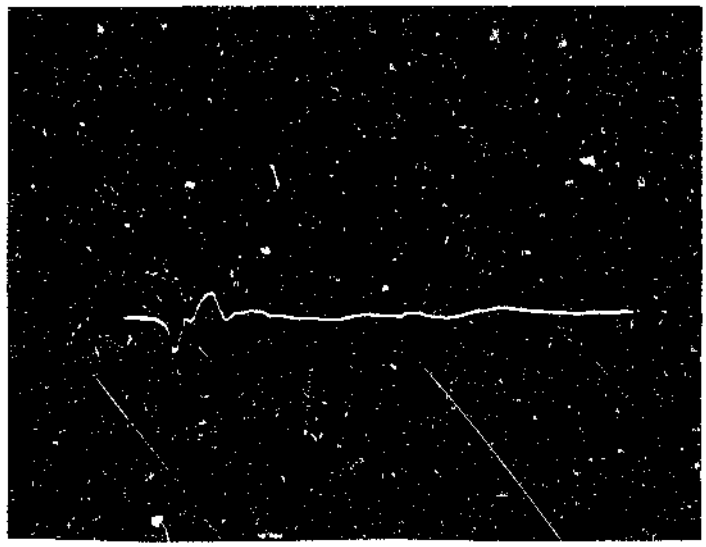
Record 7



+ 970 $V_{peak}$

400 $\mu$s sweep

Record 8

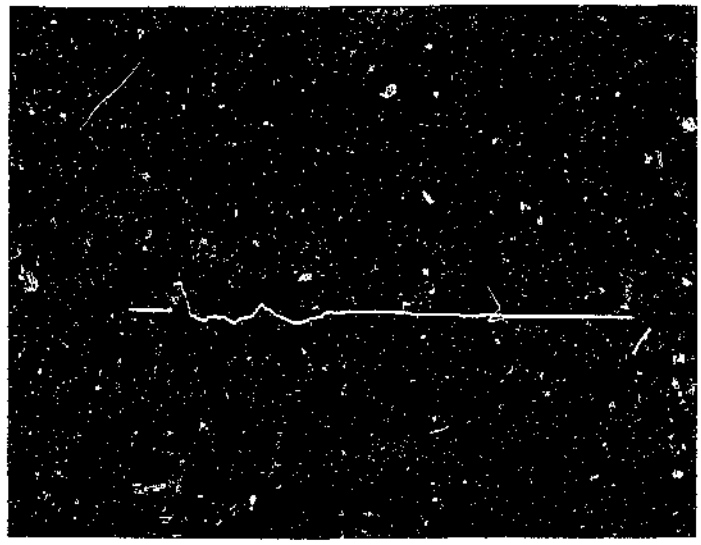


- 834 $V_{peak}$

400 $\mu$s peak

Record 9

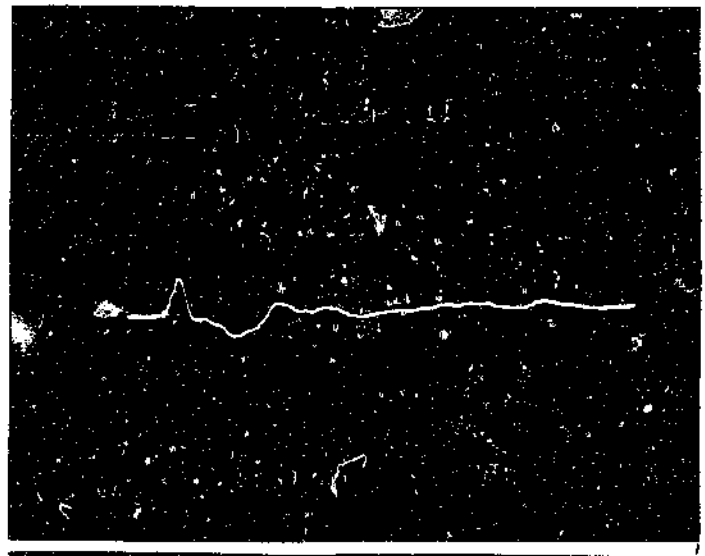
Records obtained on 1 December 1986 in Configuration 3
at Springbok Colliery



+ 660 $V_{peak}$

400 $\mu$s sweep

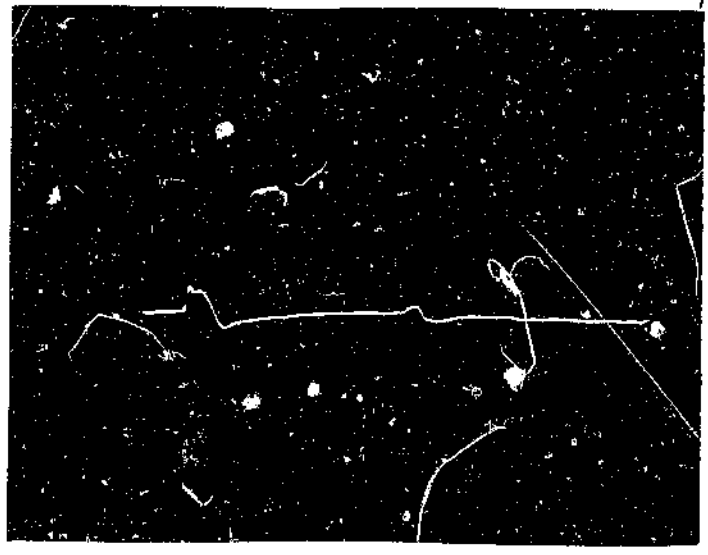
Record 10



+ 970 $V_{peak}$

400 $\mu$s sweep

Record 11

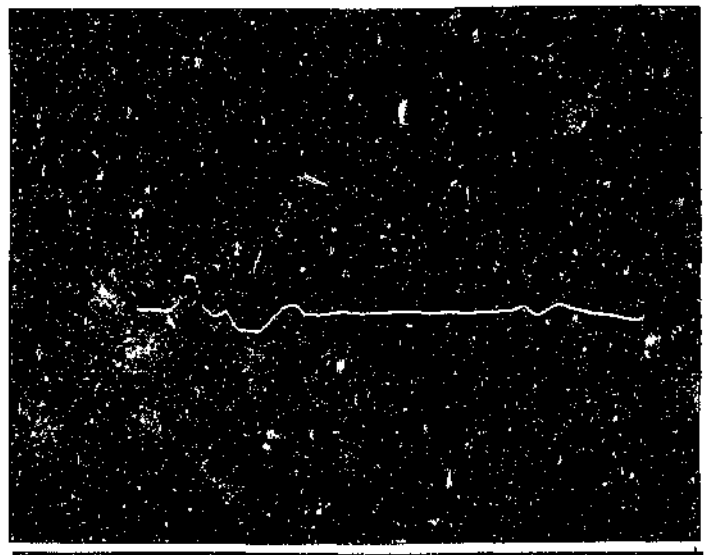


+ 640 $V_{peak}$

400 $\mu$s peak

Record 12

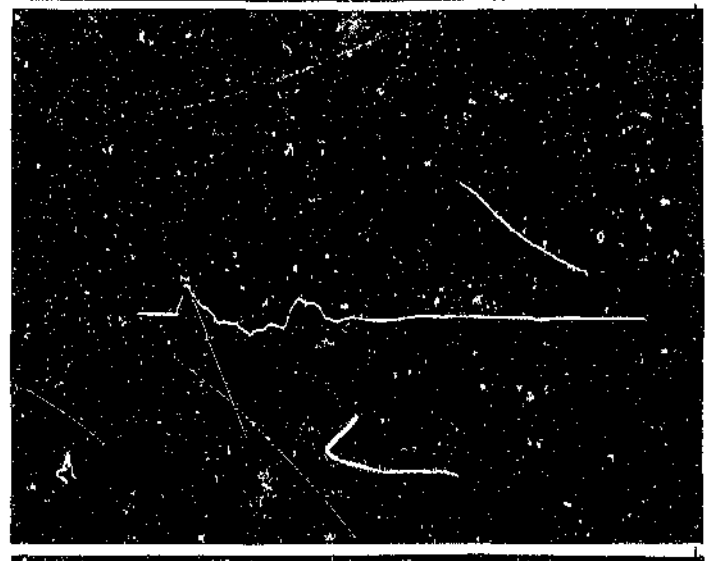
Records obtained on 1 December 1986 in Configuration 3
at Springbok Colliery



+ 834 $V_{peak}$

400 $\mu$s sweep

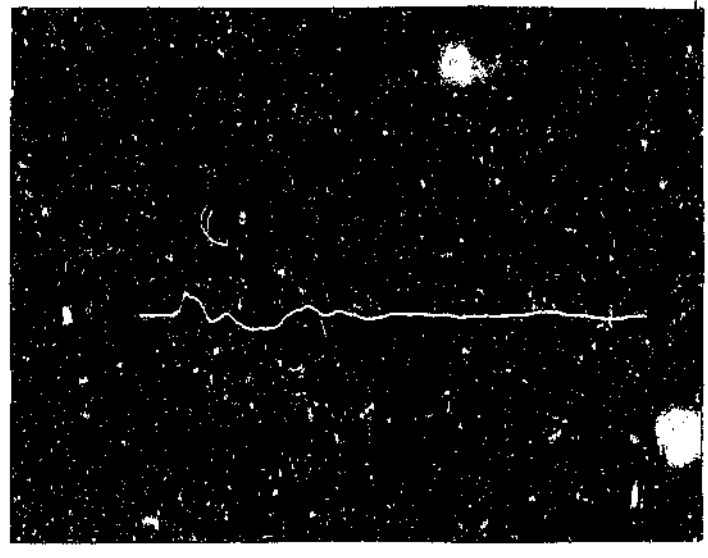
Record 12



+ 737 $V_{peak}$

400 $\mu$s sweep

Record 14



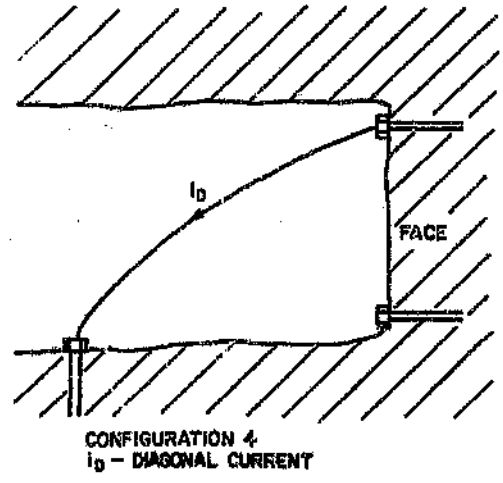
+ 563 $V_{peak}$

400 $\mu$s peak

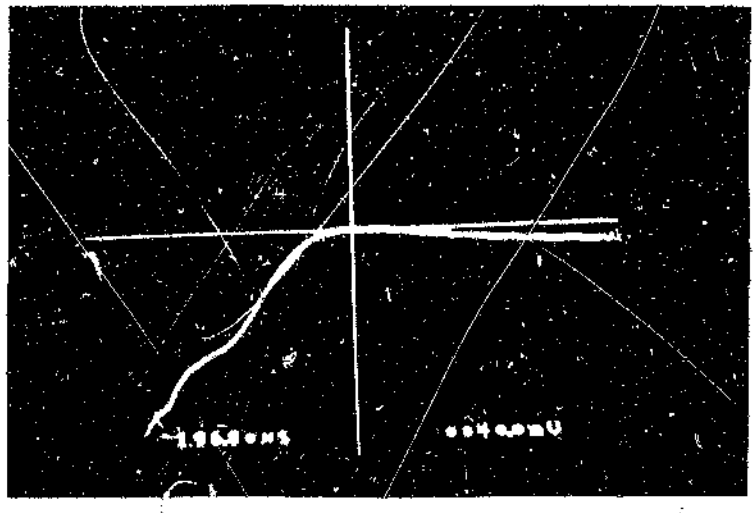
Record 15

Records obtained on 1 December 1986 in Configuration 3
at Springbok Colliery

# ACCURATE MEASUREMENTS TAKEN IN CONFIGURATION 4 AT SPRINGBOK COLLIERY



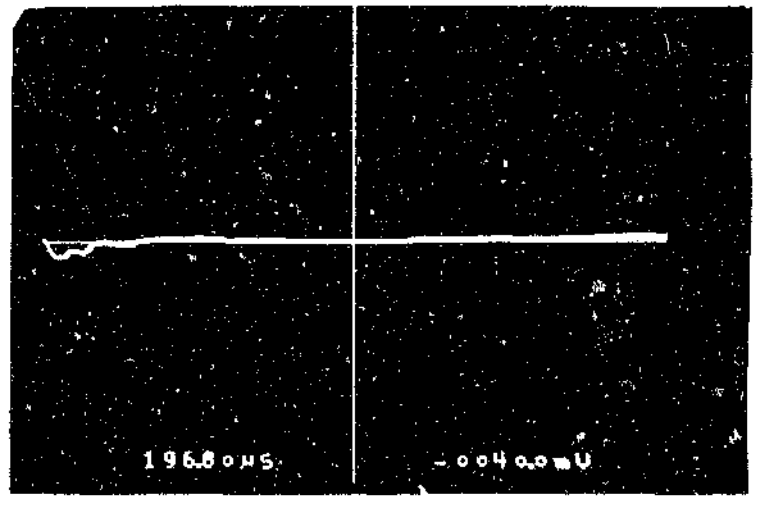

Configuraion 4: The current measured diagonally ($I_D$) between the top of the face and the "exploder point"



- 3.3 $A_{peak}$

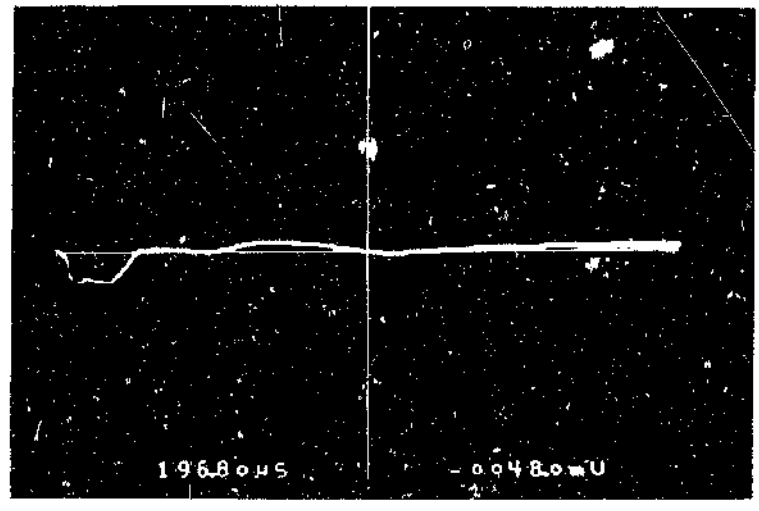
400 $\mu s$ sweep

Record obtained at 18:19 on 25 January 1987. The rise of the waveshape is not visible, it was obscured by the counters in front of the camera



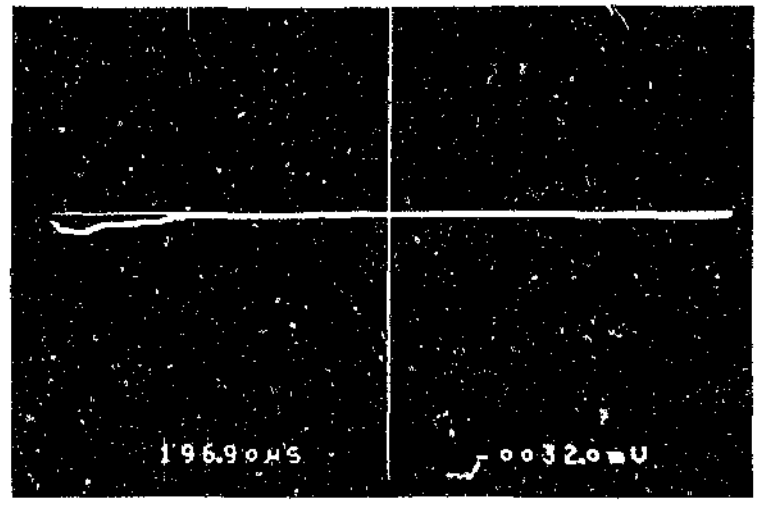

- 0.34 $A_{peak}$

400 $\mu$s sweep




- 0.56 $A_{peak}$

400 $\mu$s sweep




- 0.36 $A_{peak}$

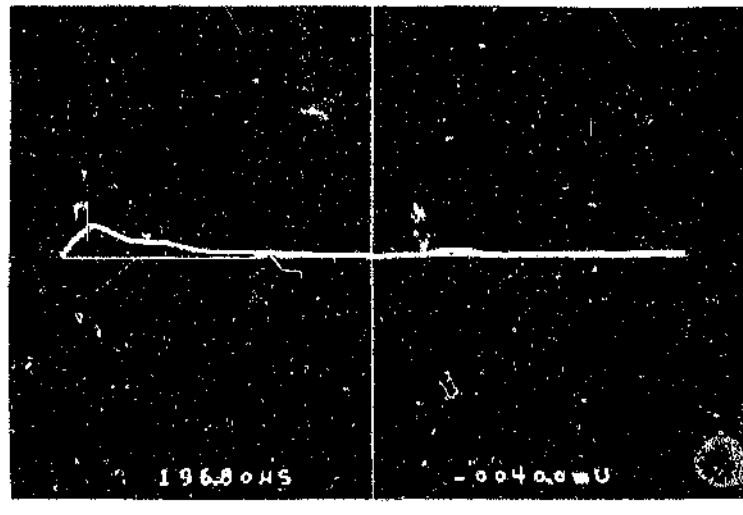
400 $\mu$s peak

Records obtained on 25 January 1987 in Configuration 4
at Springbok Colliery




+ 0.34 $A_{peak}$

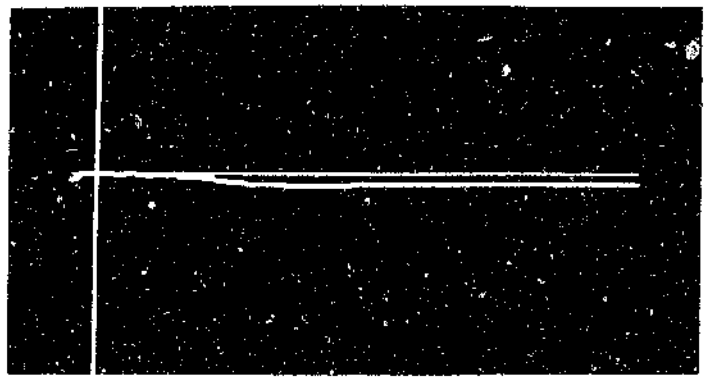
400 μs sweep




+ 0.61 $A_{peak}$

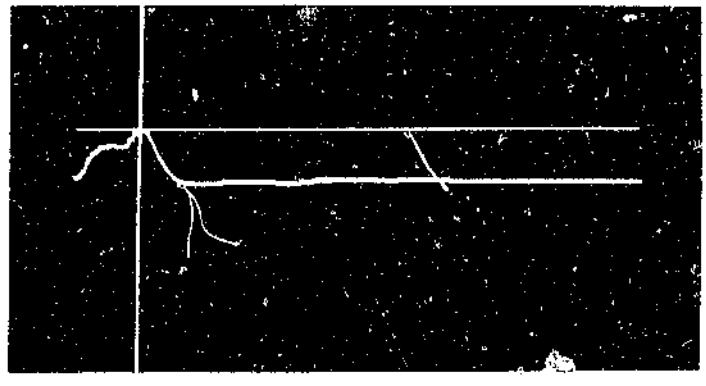
400 μs sweep

Records obtained on 25 January 1987 in Configuration 4
at Springbok Colliery



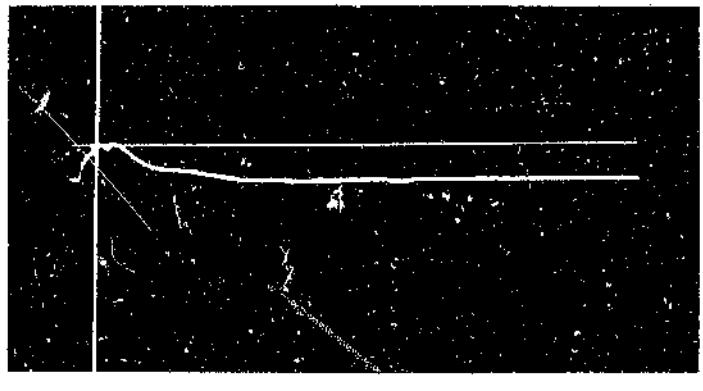
+ 360 mA

400 $\mu$s sweep



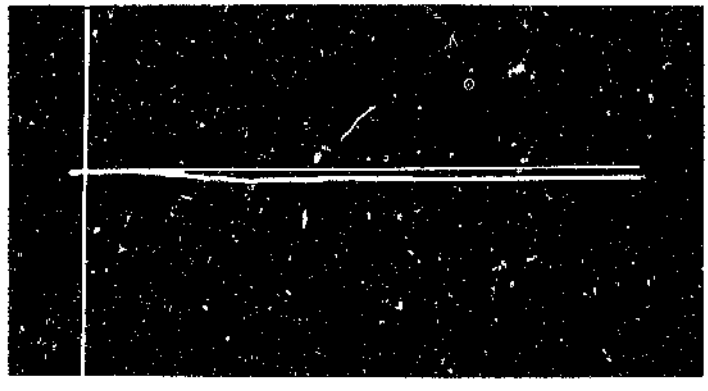
+ 418 mA

400 $\mu$s sweep



+ 57 mA

400 $\mu$s sweep

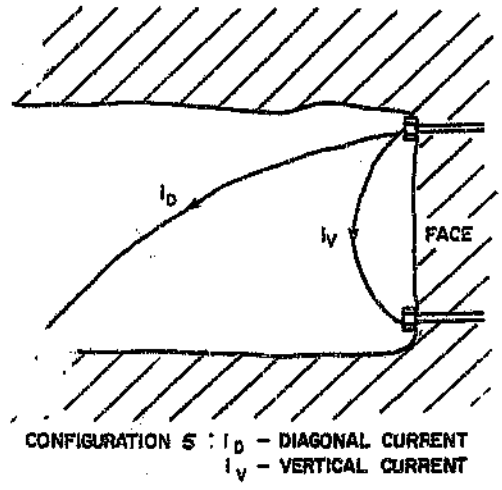


+ 86 mA

400 $\mu$s sweep

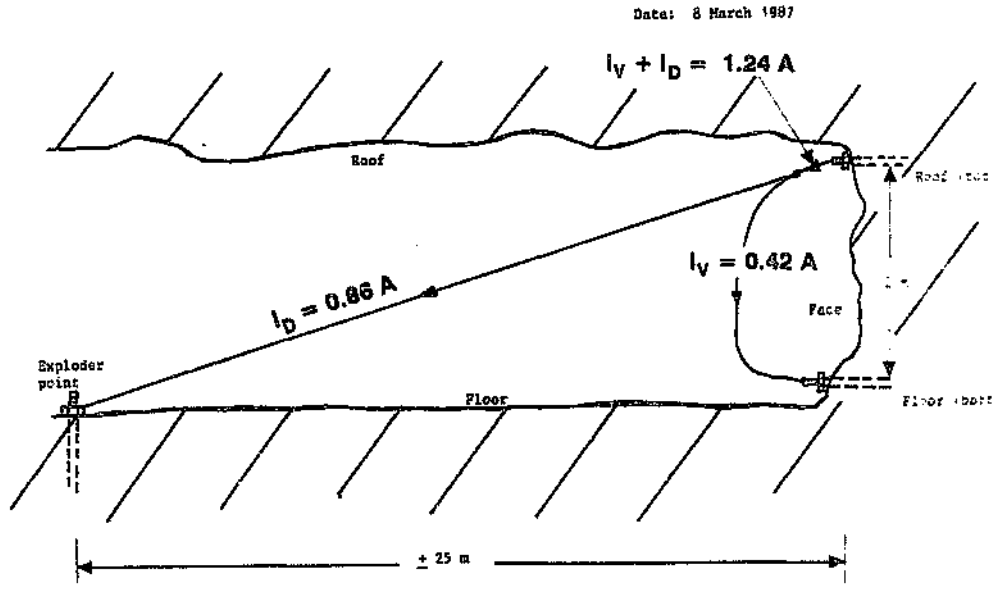
Records obtained between 18:18 and 18:28 on 1 February 1987
in Configuration 4 at Springbok Colliery

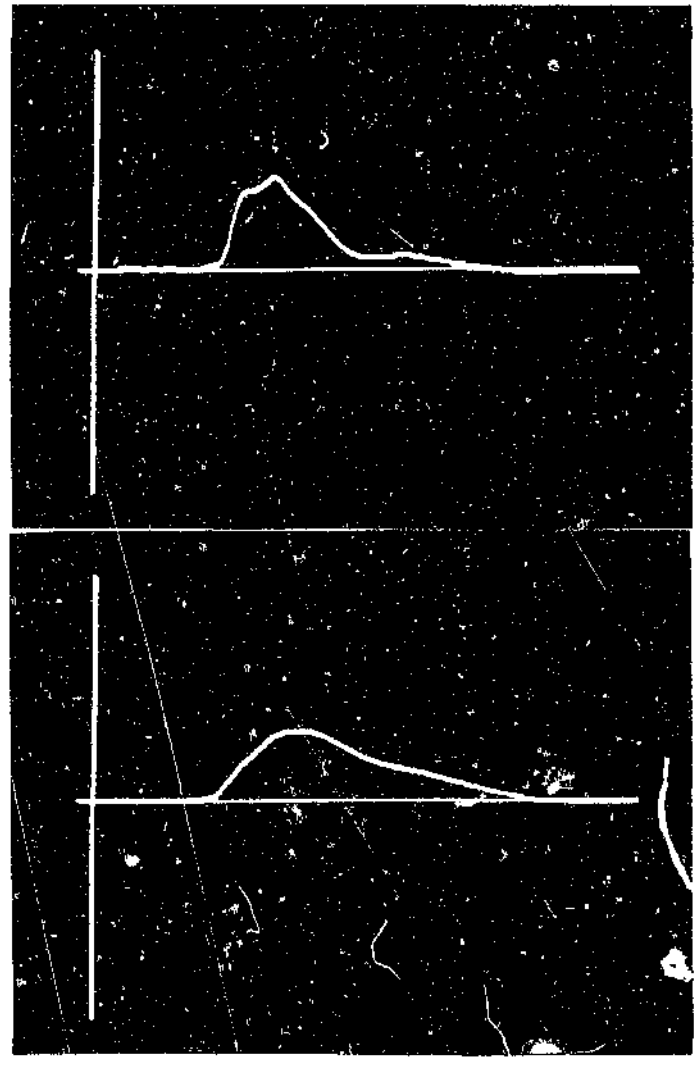
## ACCURATE MEASUREMENTS IN CONFIGURATION 5 AT SPRINGBOK COLLIERY AND GREENSIDE COLLIERY




Configuration 5: The current was measured diagonally ($I_D$) between the top of the face and the "exploder" point.

The current was also measured vertically ($I_V$) between the top of the face and the bottom of the face.



($I_D$) Roof (top) bolts to exploder point

$I_D = 0.86\ A_{peak}$

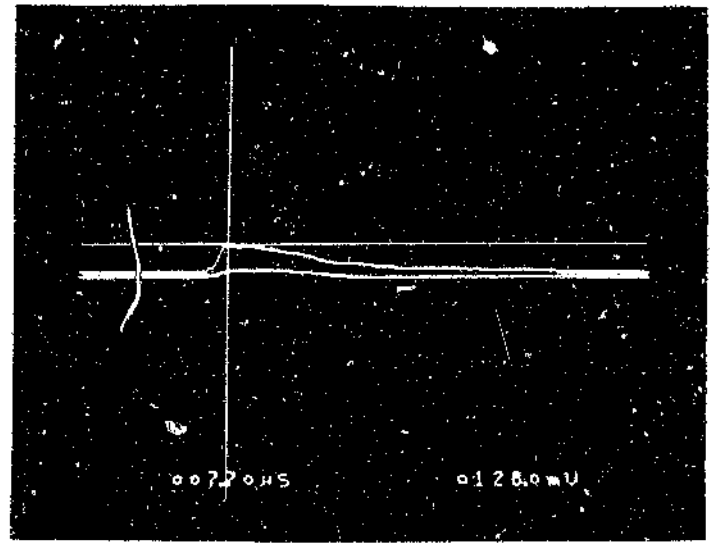
200 $\mu$s sweep

($I_V$) Roof (top) bolts to floor (bottom) bolts

$I_V = 0.42\ A_{peak}$

200 $\mu$s sweep

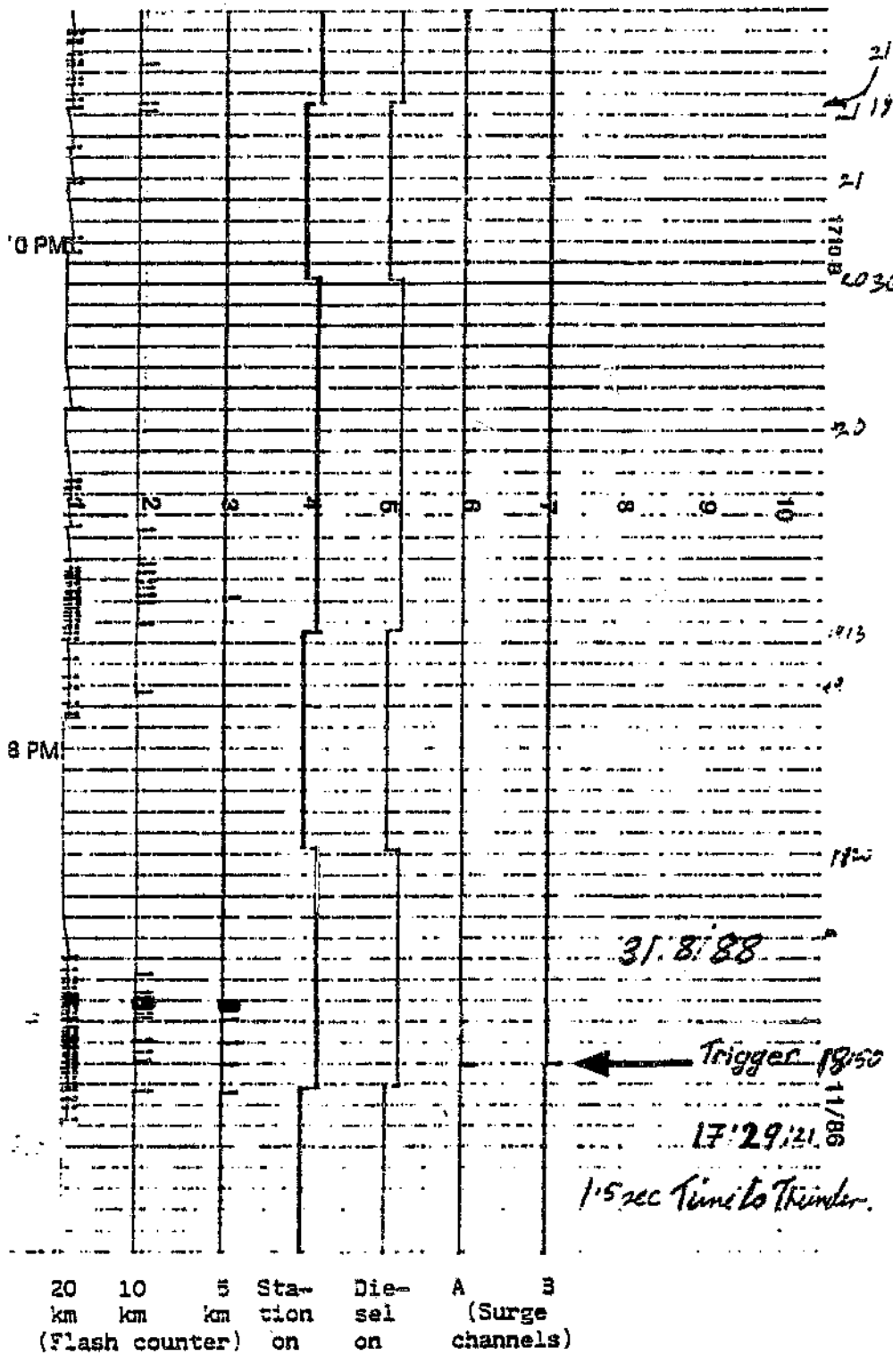
Records obtained on 8 March 1987 in Configuration 5 at Springbok Colliery




$I_D = +0.24\ A_{peak}$

$I_V = +0.04\ A_{peak}$

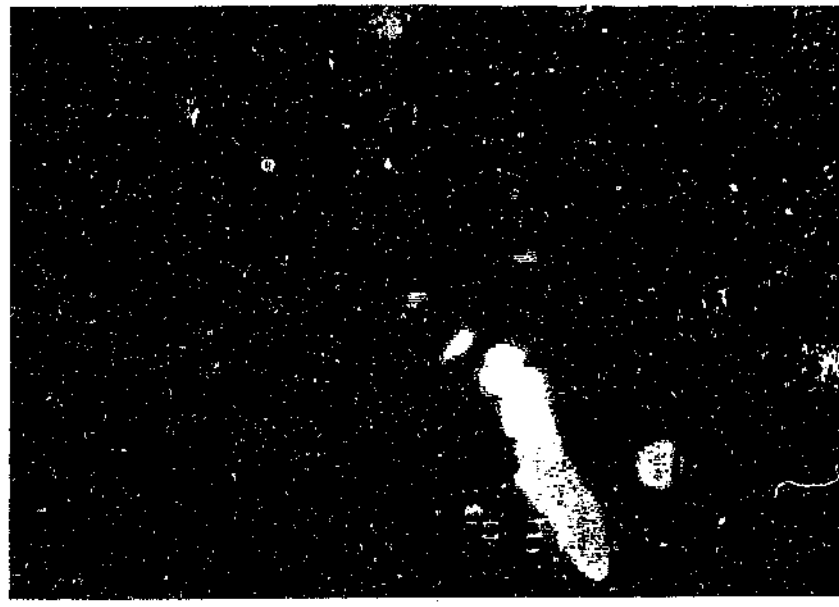
Record obtained on 8 March 1987 in Configuration 5
at Springbok Colliery




Event recording of storm on 31 August 1989 during which surges occurred

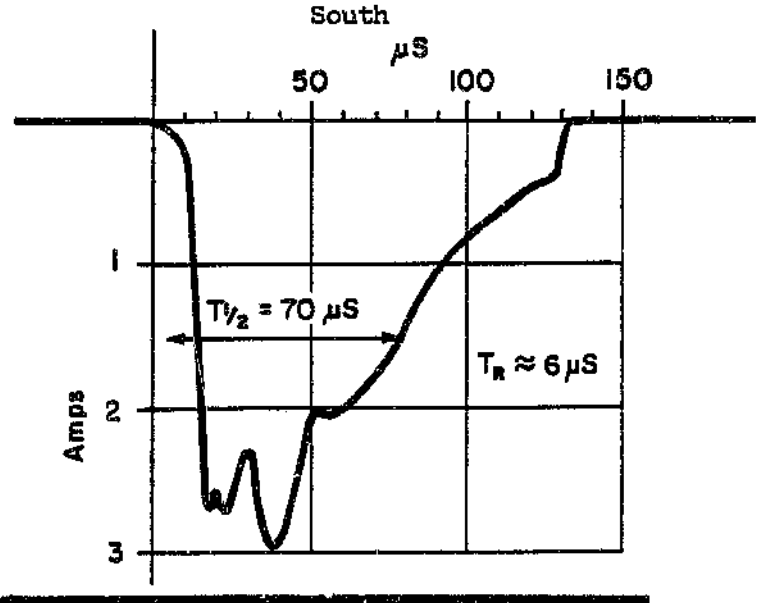
North

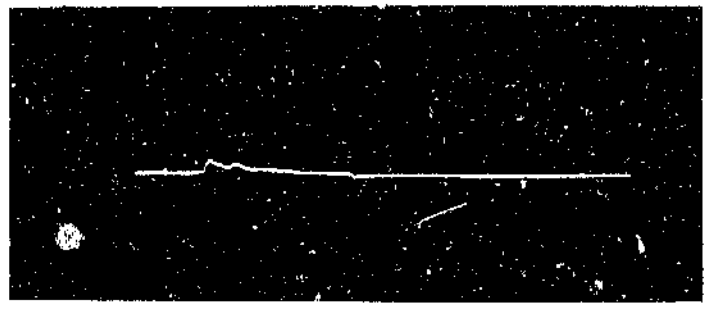
West



East

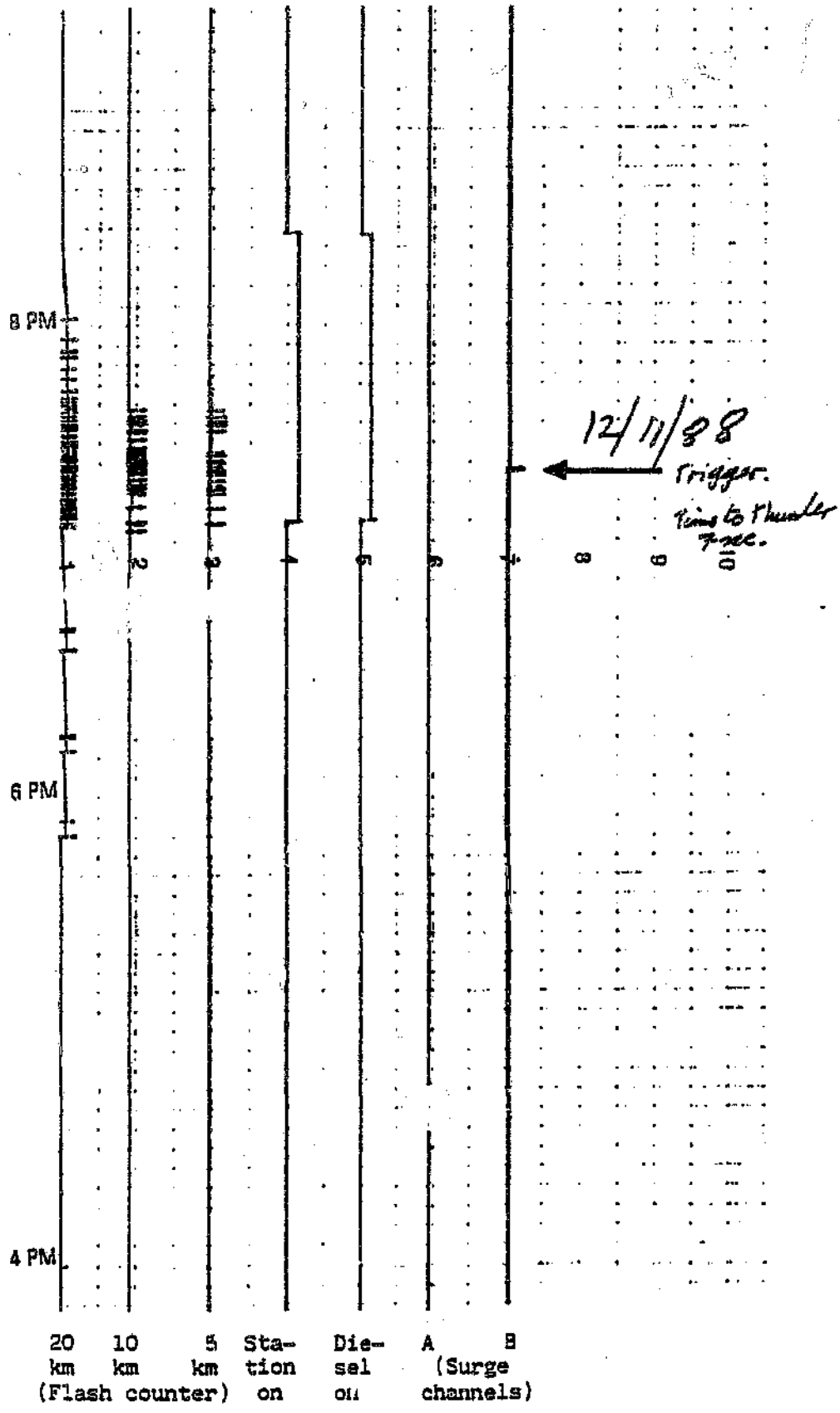
South



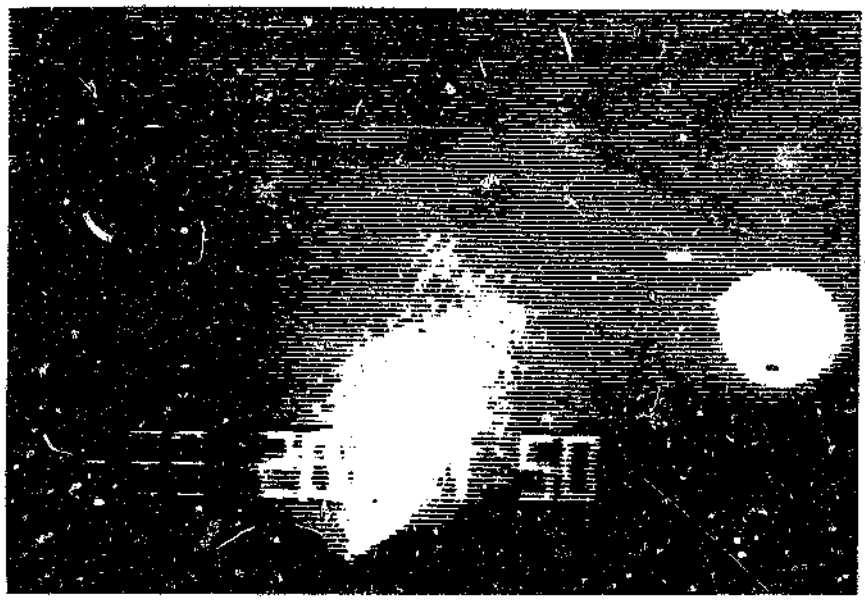
$I_V = 0.14\ A_{peak}$
400 μs sweep

Top: Video recording of strike  Middle: Diagonal current ($I_D$ = - 2.98 $A_{peak}$)
Bottom: Vertical current in face ($I_V$ = + 0.14 $A_{peak}$)
Distance: 4 34 m  Direction: SSE  Date 31/8/88  Time 18:50



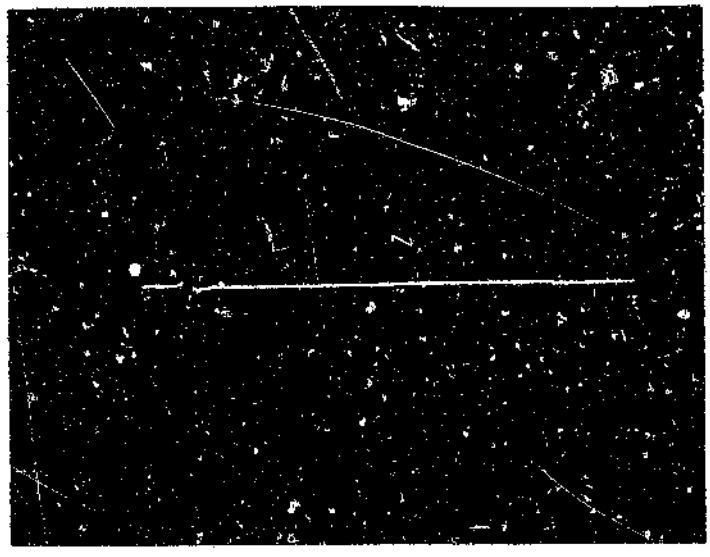

Event recording of the storm on 12 November 1988

North



West East

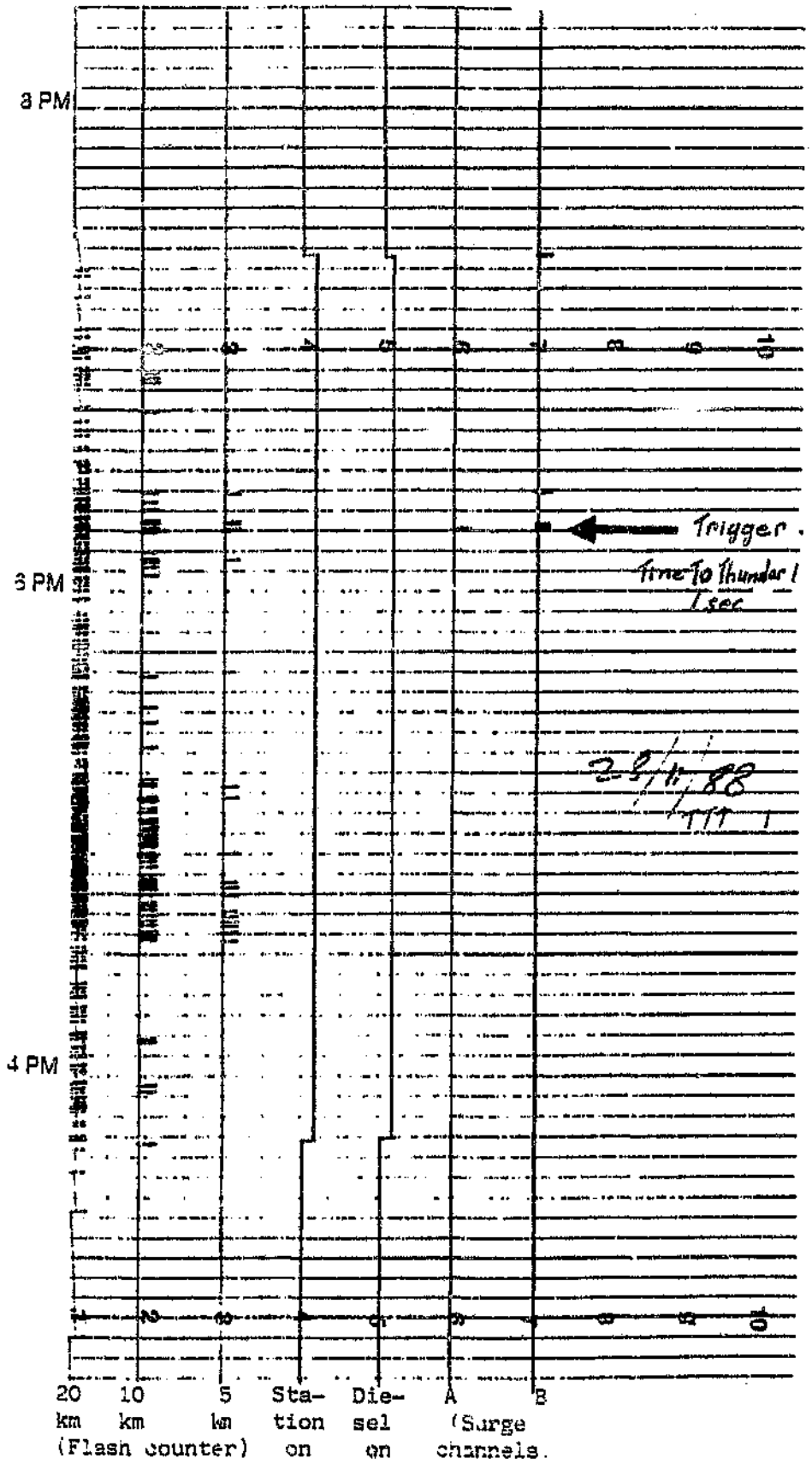
South



400 $\mu$s sweep

Video recording and corresponding current pulse.

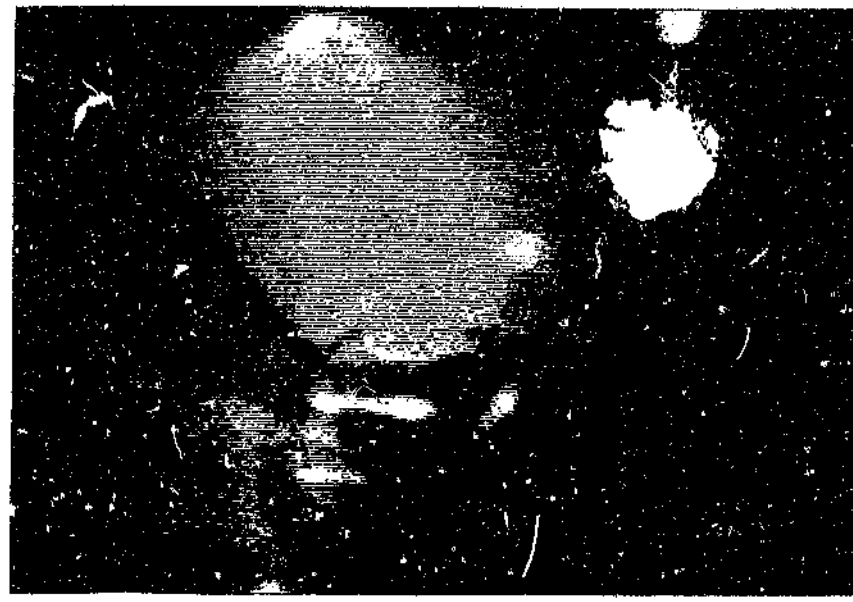
| | |
|---|---|
| Magnitude: + 614 mA | Configuration: Horizontal |
| Distance: ± 2 317 m | Direction: South south west |
| Date: 12 November 1988 | Time: 19:23 |




Event recording of the storm on 28 November 1988

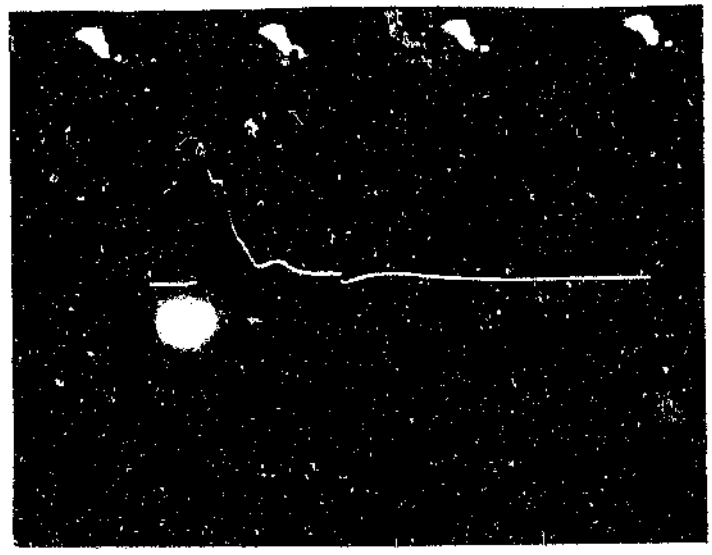
North

West



East

South

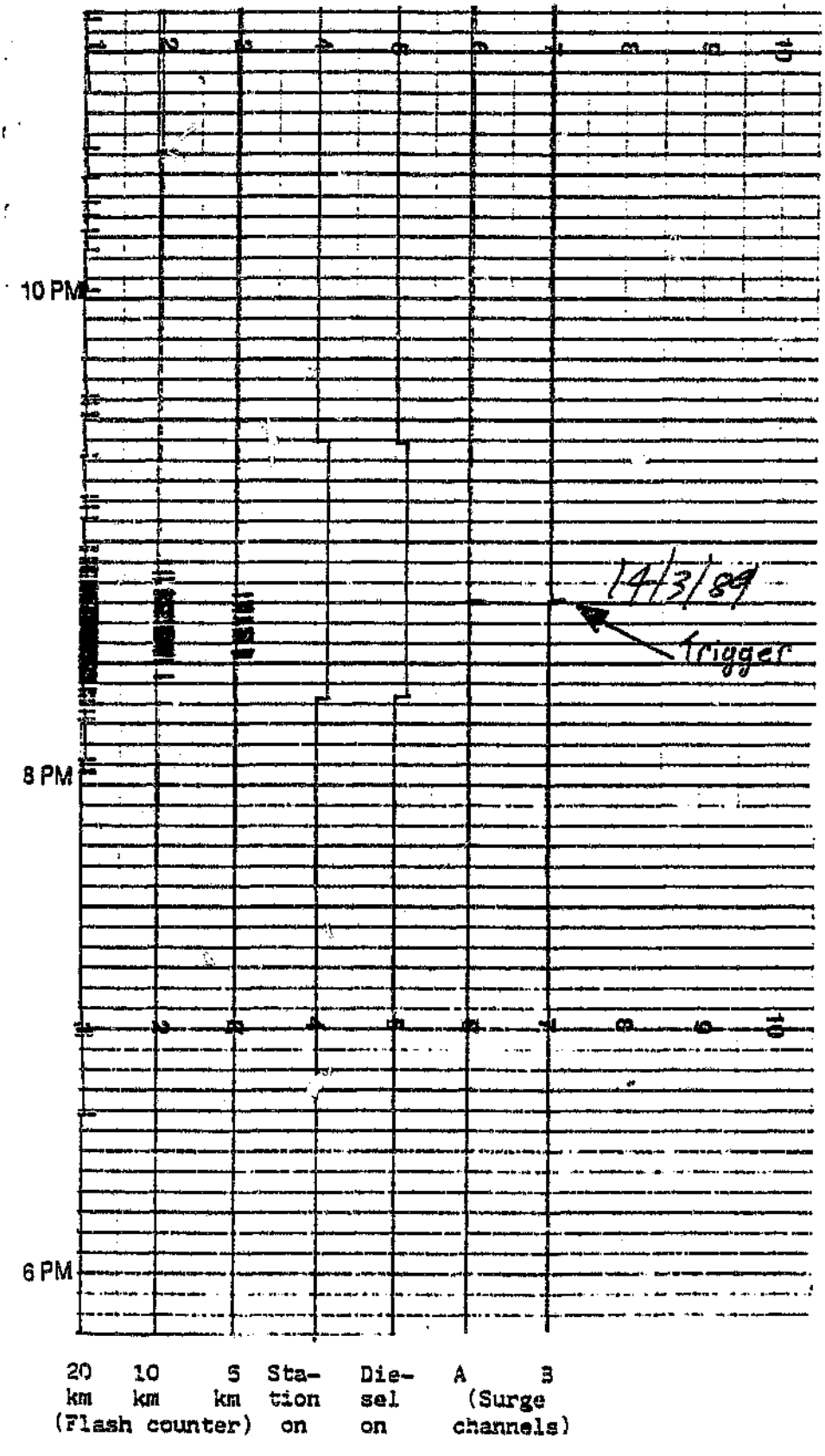


400 $\mu$s sweep

Video recording and corresponding current pulse.

Magnitude: + 2.8 A
Distance: ± 331 m
Date: 28 November 1988

Configuration: Horizontal
Direction: North north west
Time: 18:16




Event recording of the storm on 14 March 1988

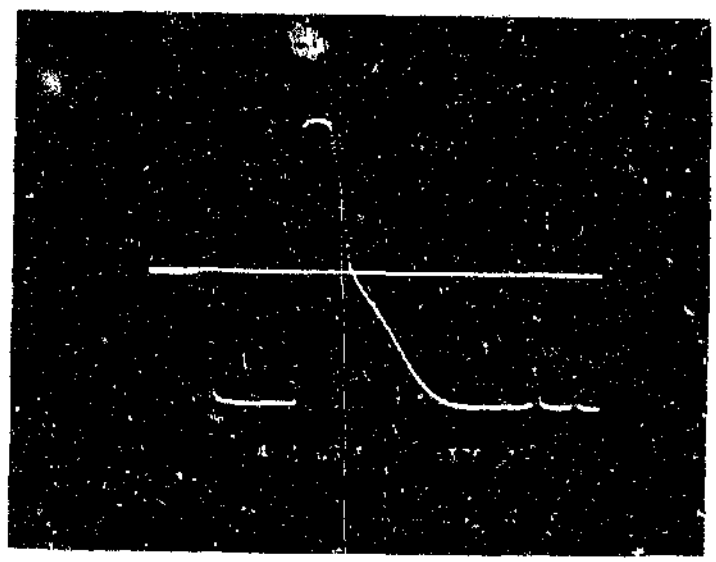
North

West



East

South



40 $\mu$s sweep

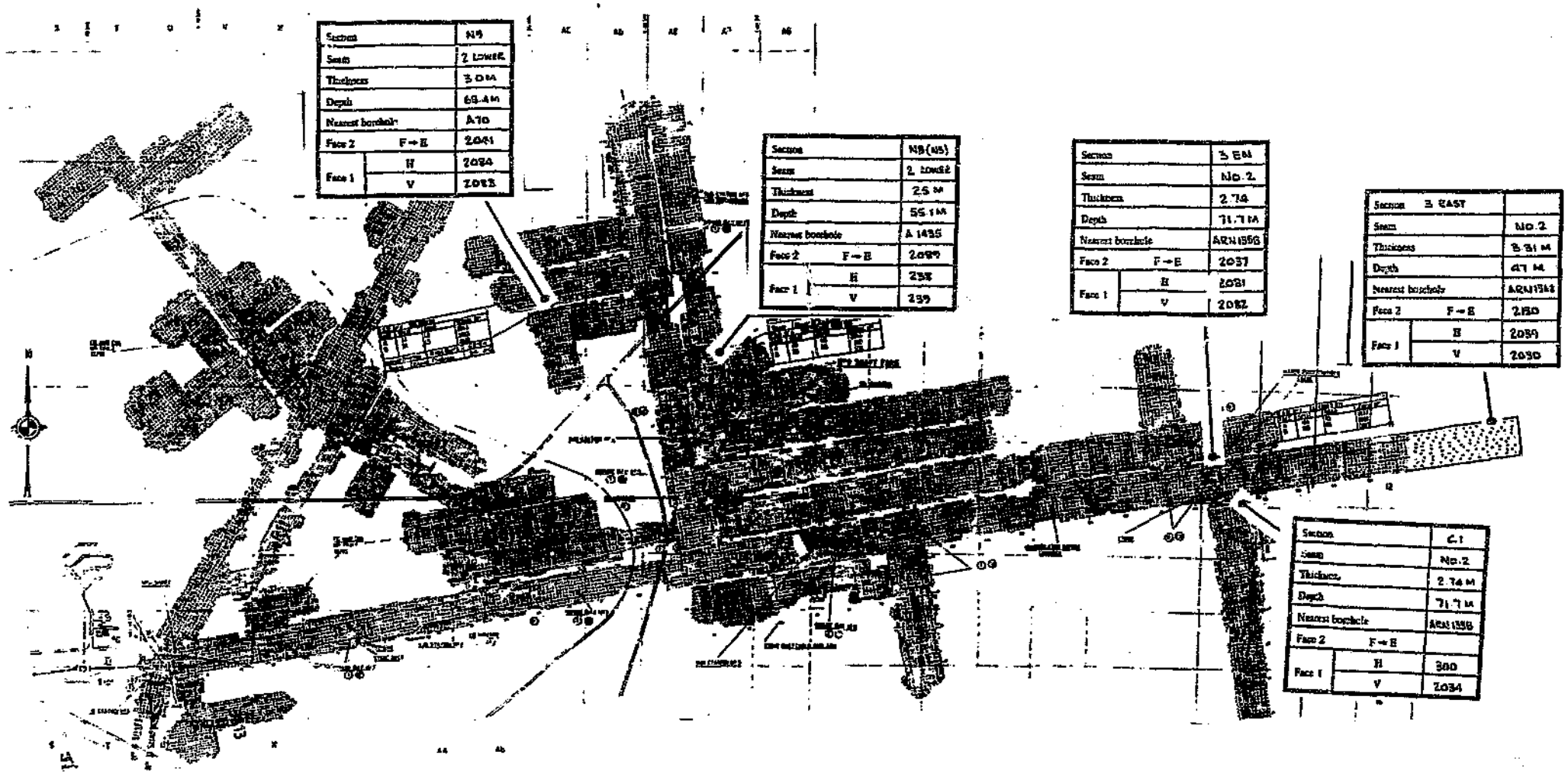
Video recording and corresponding current pulse.

Magnitude: -10 to -20 A
Distance: ± 140 m
Date: 14 March 1989

Configuration: Horizontal
Direction: north east
Time: 20:45

**APPENDIX VII**

# THE LOCATION OF FUSE SURGE DETECTORS IN MINES TAKING PART IN THE FUSE SURGE DETECTOR PROGRAMME AND INFORMATION ABOUT THE STRATA

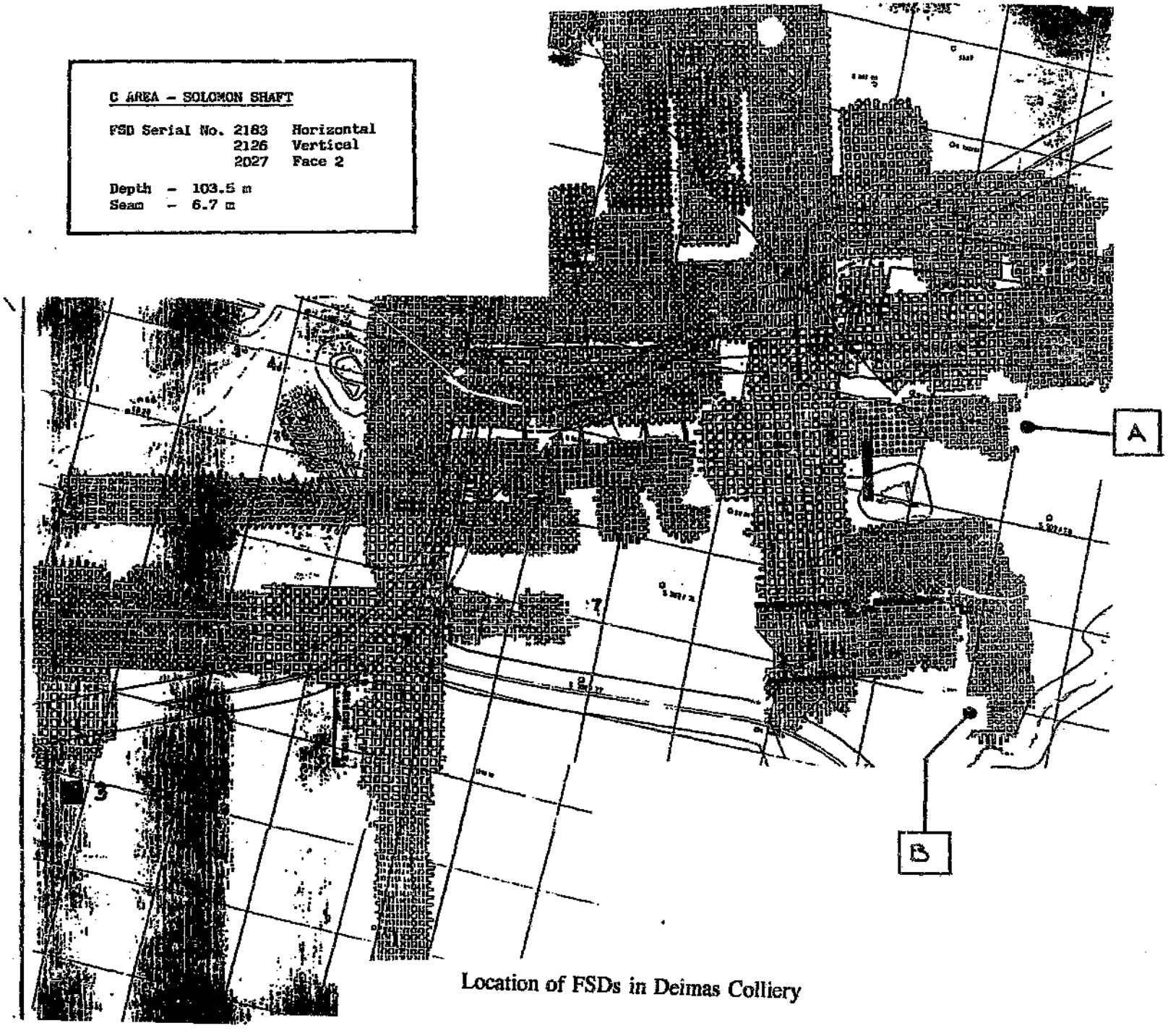



Location of FSDs in Arnot Colliery

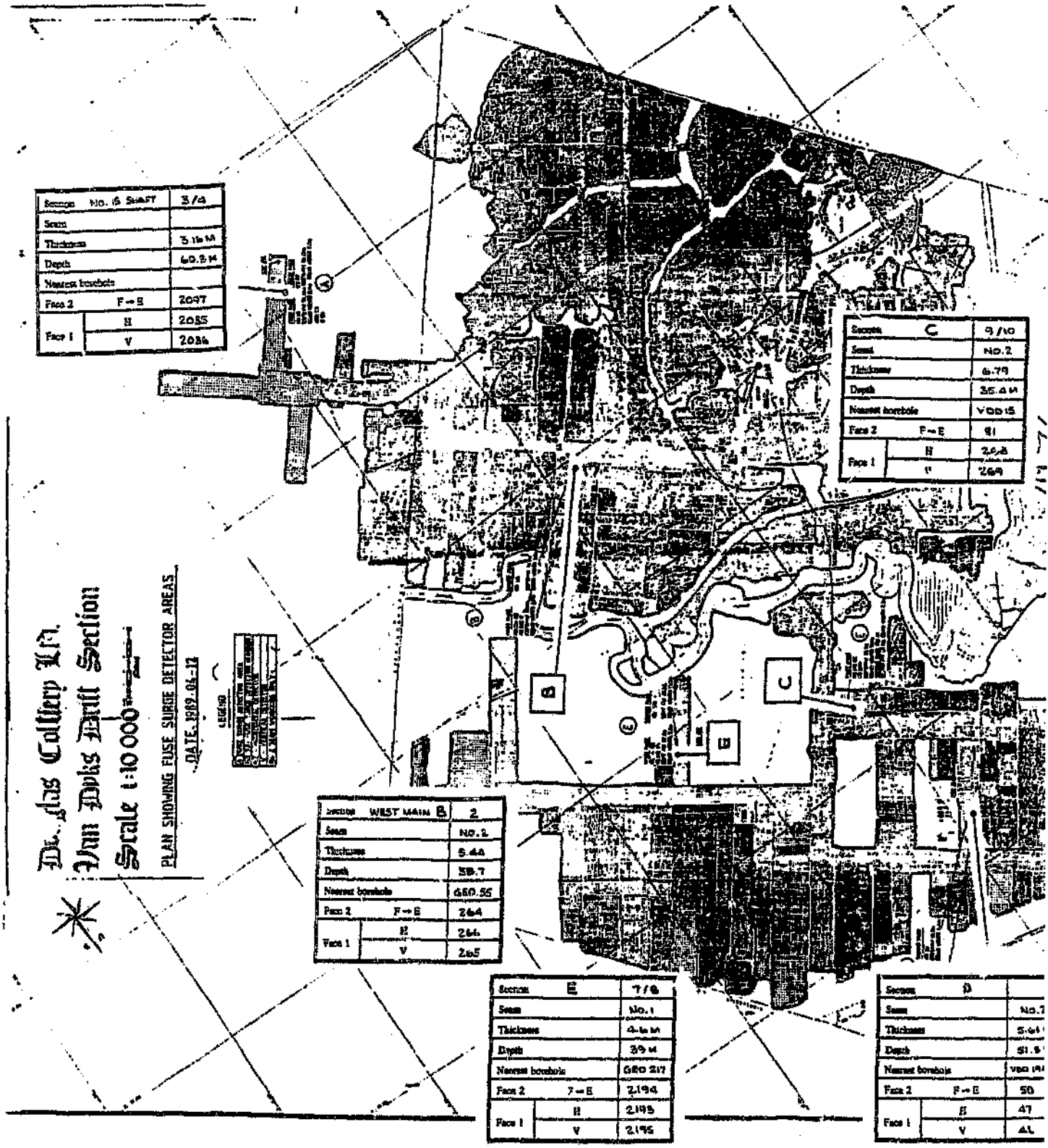
C AREA – SOLOMON SHAFT

FSD Serial No. 2183 Horizontal
2126 Vertical
2027 Face 2

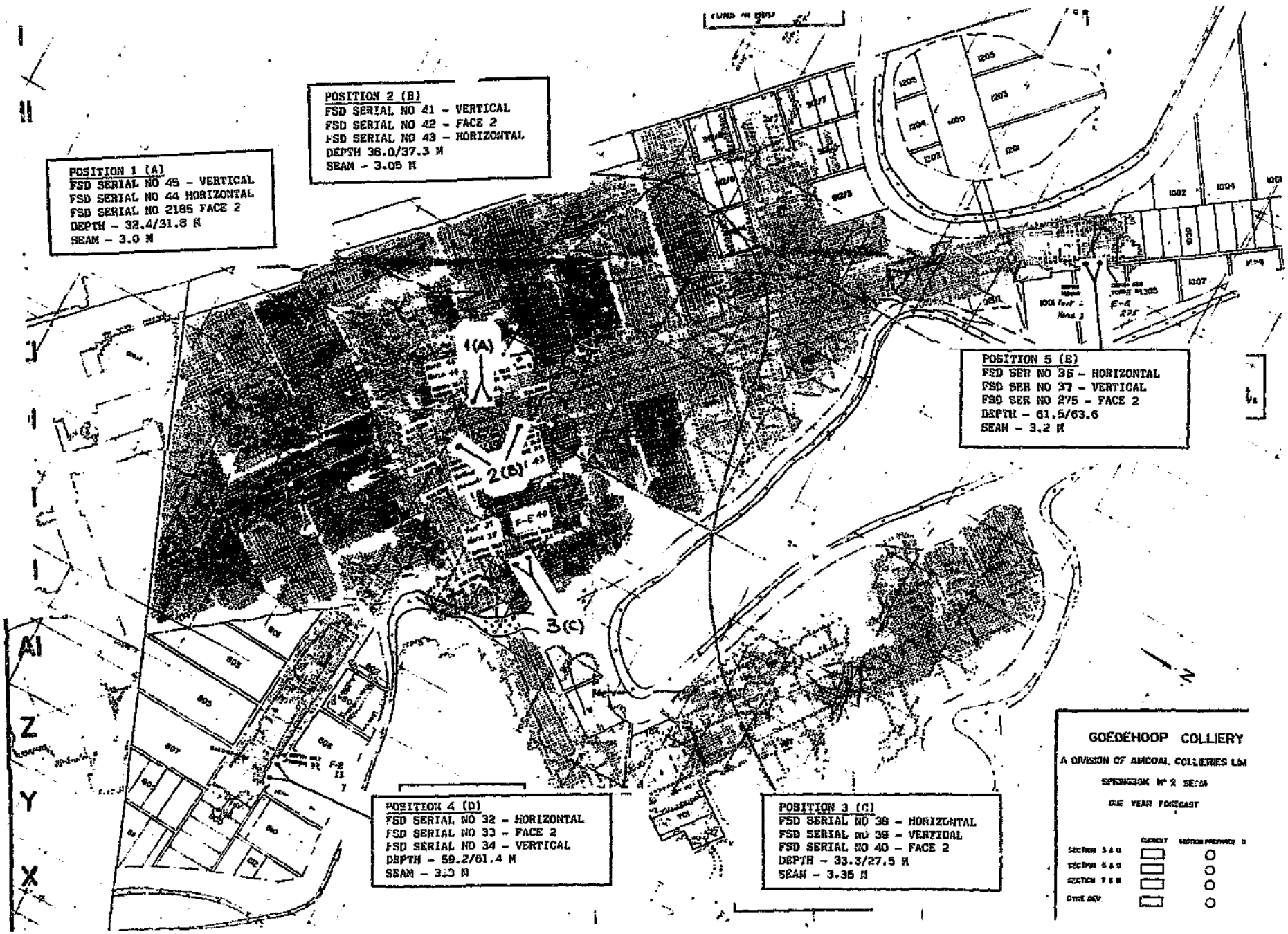
Depth – 103.5 m
Seam – 6.7 m



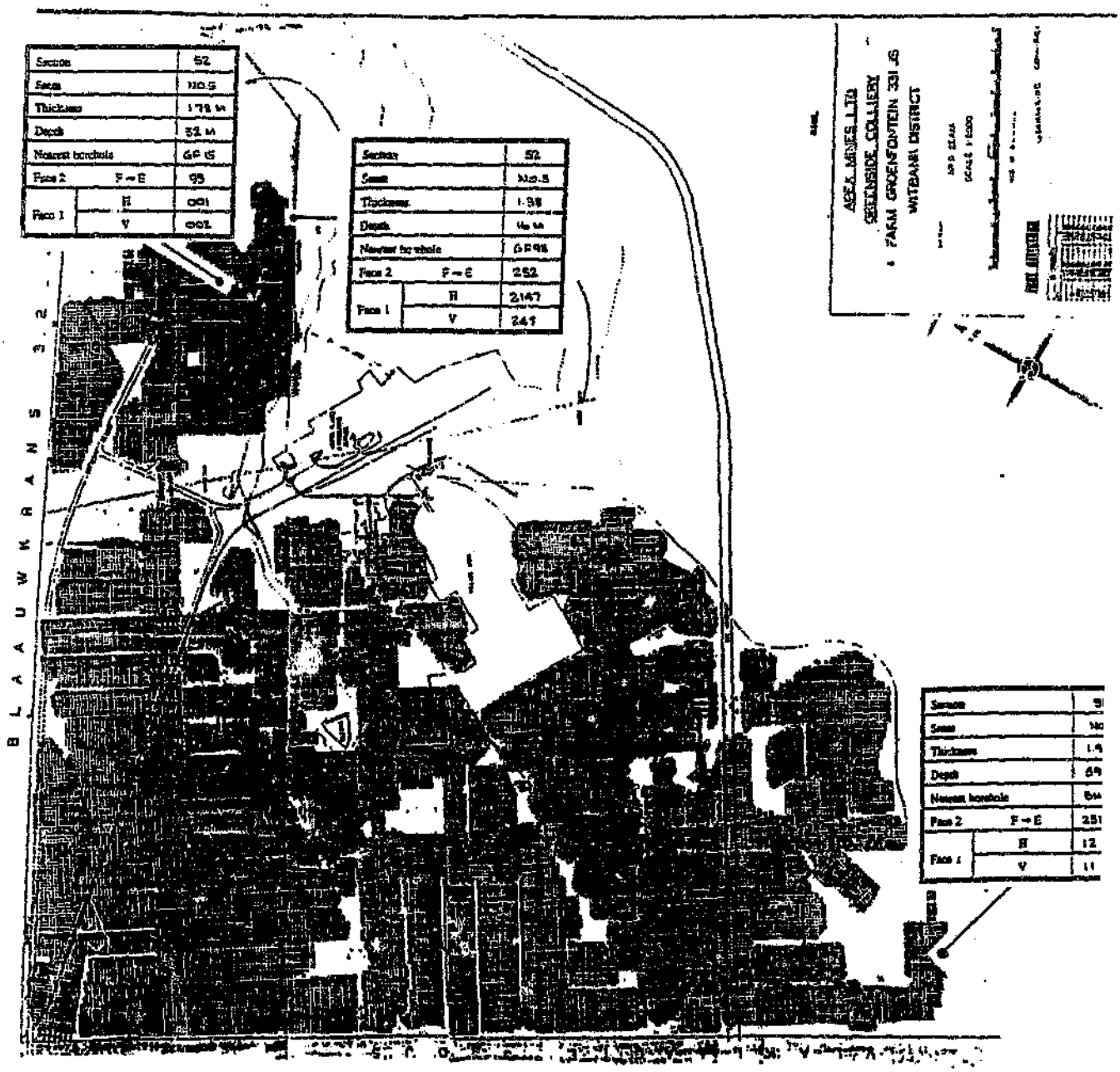

Location of FSDs in Deimas Colliery




Location of FSDs installed in Douglas Colliery

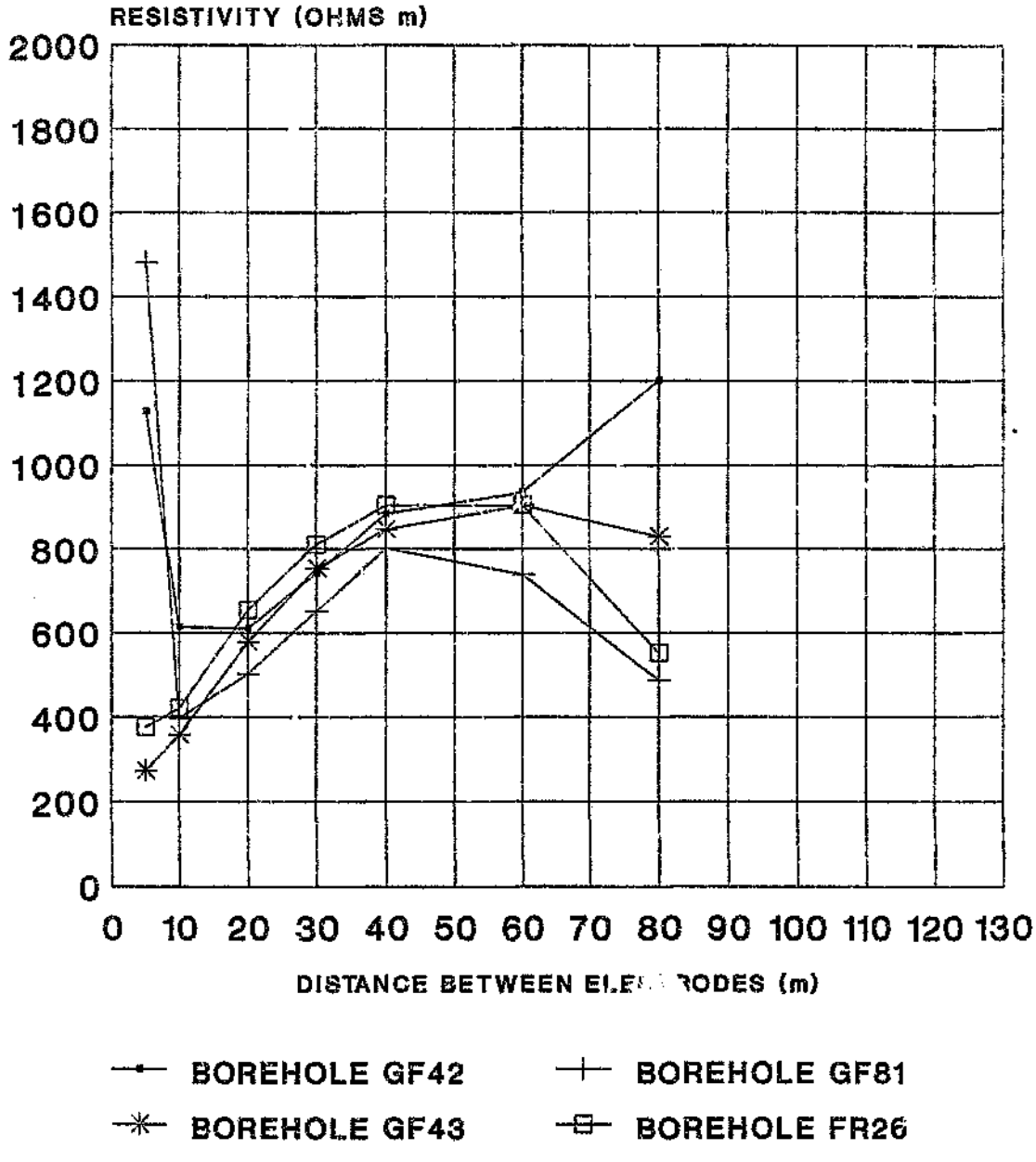



Location of FSDs in Goedehoop Colliery




Location of FSDs installed in Greenside Colliery

# GREENSIDE COLLIERY
## EARTH RESISTIVITY




**NOTE:** The resistivity/depth profiles are shown here. The geological data of the boreholes is given on the next two pages and the locations of the boreholes are shown on the third page.

# BOREHOLE INFORMATION

BOREHOLE No: GF 42 MINE: GREENSIDE
AREA: Nº 16 SHAFT

| DEPTH M | DEPTH CM | GEOL. SECTION | GEOLOGICAL DESCRIPTION OF CORE |
|---|---|---|---|
| | | | No CORE RECOVERY |
| 7 | 01 | | SHALY SANDSTONE |
| 10 | 72 | | SANDY SHALE AND SILTSTONE |
| 18 | 80 | | SHALE & SANDSTONE |
| 18 | 06 | | ARGIL SHALE |
| 20 | 85 | | SANDSTONE |
| 39 | 75 | | SANDSTONE / SHALE |
| 41 | 80 | | COAL Nº5 SEAM |
| 41 | 98 | | SHALE |
| 42 | 11 | | COAL Nº5 SEAM |
| 45 | 26 | | SHALE / SANDSTONE |
| 47 | 00 | | SHALE |
| 53 | 09 | | SANDSTONE / SHALE |
| 56 | 23 | | SANDSTONE |
| 56 | 08 | | SHALE |
| 56 | 89 | | COAL Nº 4A SEAM |
| 62 | 92 | | SHALE |
| 66 | 88 | | SANDSTONE |
| 70 | 10 | | COAL Nº 4 SEAM |
| 74 | 97 | | SANDSTONE |
| 74 | 14 | | COAL Nº 3 SEAM |
| 75 | 26 | | SHALE |
| 77 | 62 | | SANDSTONE SHALE |
| 84 | 82 | | SHALE |
| 91 | 93 | | COAL Nº 2 SEAM |
| 92 | 87 | | SANDSTONE |
| 96 | 49 | | COAL Nº 1 SEAM |
| 99 | 52 | | SHALE |
| 99 | 96 | | DARK TILLITE |
| 77 | 94 | | SANDSTONE |

# BOREHOLE INFORMATION

BOREHOLE No: FR26 MINE: GREENSIDE
AREA: A.M. STATION

| DEPTH M | DEPTH CM | GEOL. SECTION | GEOLOGICAL DESCRIPTION OF CORE |
|---|---|---|---|
| | | | SOIL |
| 6 | 55 | | SANDSTONE WITH SHALE BANDS |
| 24 | 84 | | COAL Nº5 SEAM |
| 25 | 77 | | SANDSTONE |
| 28 | 24 | | SHALE |
| 33 | 35 | | SANDSTONE |
| 34 | 89 | | COAL Nº 4A SEAM |
| 35 | 69 | | SHALE |
| 36 | 45 | | GRIT |
| 36 | 91 | | COAL Nº 4 UPPER SEAM |
| 41 | 07 | | SHALE |
| 41 | 65 | | COAL Nº 4 LOWER SEAM |
| 45 | 11 | | GRIT |
| 46 | 94 | | |

# BOREHOLE INFORMATION

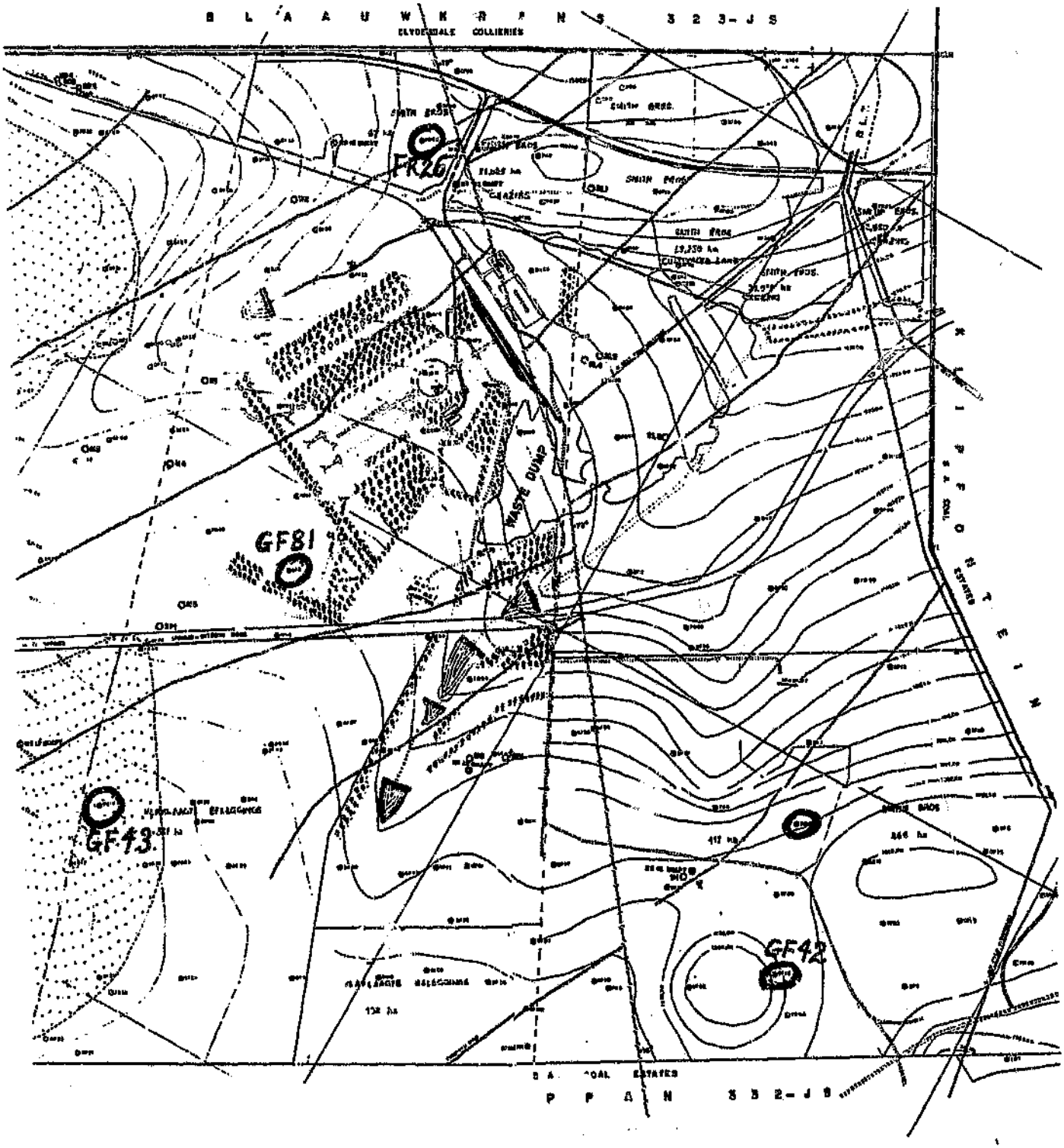
BOREHOLE No: GF 81 MINE: GREENSIDE
AREA:

| DEPTH M | DEPTH CM | GEOL. SECTION | GEOLOGICAL DESCRIPTION OF CORE |
|---|---|---|---|
| 6 | 17 | | SILTSTONE / SANDSTONE |
| 14 | 14 | | SANDSTONE |
| 19 | 39 | | MICROCLINE GRANITE |
| 20 | 49 | | SANDSTONE |
| 32 | 61 | | SANDSTONE / SILTSTONE / MUDSTONE |
| 38 | 12 | | COAL No 5 SEAM |
| 41 | 00 | | SILTSTONE / MUDSTONE / SANDSTONE |
| 42 | 74 | | SHALE / SILTSTONE |
| 47 | 50 | | SANDSTONE |
| 50 | 34 | | MUDSTONE / SILTSTONE |
| 53 | 14 | | COAL No 4A SEAM |
| 56 | 23 | | SANDSTONE / SILTSTONE |
| 62 | 98 | | SHALE / SILTSTONE / MUDSTONE |
| 64 | 07 | | COAL No 4 SEAM |
| 68 | 45 | | SANDSTONE / MUDSTONE |
| 68 | 49 | | COAL No 3 SEAM |
| 69 | 75 | | SANDSTONE / SILTSTONE |
| 70 | 52 | | |

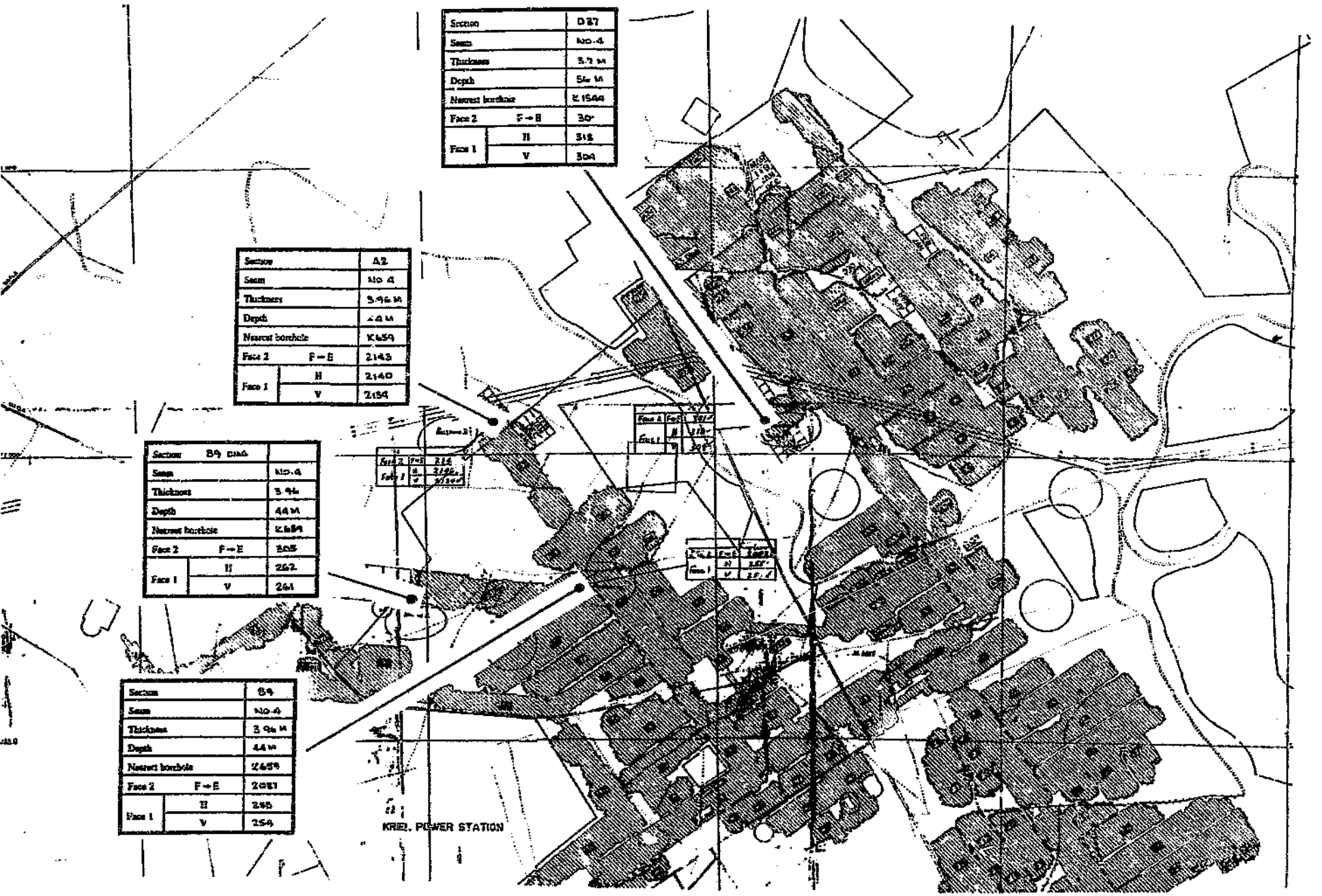
# BOREHOLE INFORMATION

BOREHOLE No: GF 43 MINE: GREENSIDE
AREA:

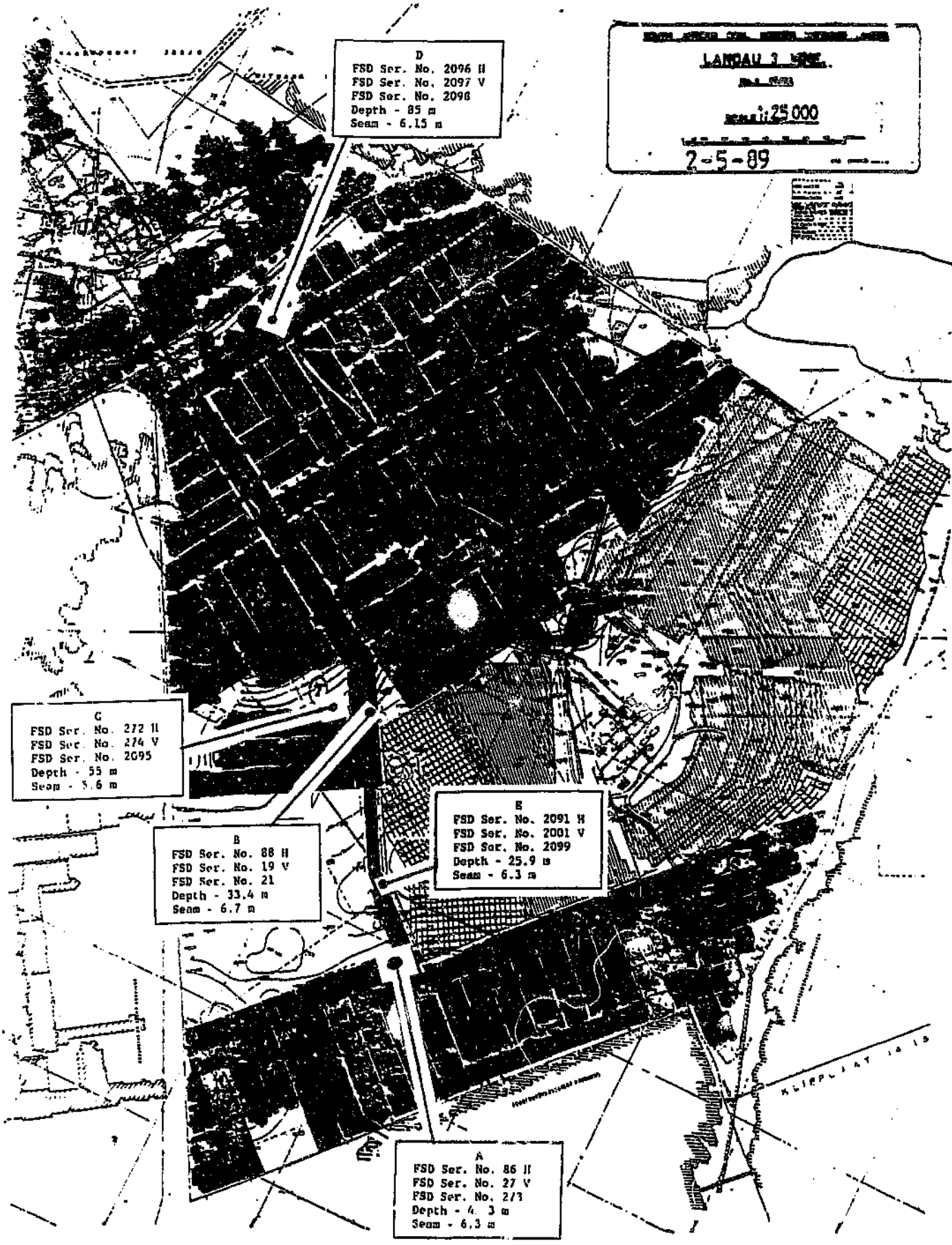
| DEPTH M | DEPTH CM | GEOL. SECTION | GEOLOGICAL DESCRIPTION OF CORE |
|---|---|---|---|
| | | | NO CORE RECOVERED |
| 7 | 57 | | BOULDERS |
| 11 | 85 | | SANDSTONE |
| 16 | 51 | | SHALE / SANDSTONE |
| 31 | 62 | | QUARTZITE |
| 32 | 31 | | SANDSTONE |
| 47 | 55 | | SHALE / SANDSTONE |
| 54 | 00 | | COAL No 5 SEAM |
| 55 | 72 | | SANDSTONE / SHALE |
| 65 | 71 | | COAL No 4A SEAM |
| 66 | 60 | | SANDSTONE / SHALE |
| 68 | 09 | | SHALE |
| 90 | 71 | | SANDSTONE |
| 93 | 29 | | SHALE / SANDSTONE |
| 95 | 03 | | COAL No 4 SEAM |
| 97 | 98 | | SANDSTONE / SHALE |
| 98 | 96 | | COAL No 3 SEAM |
| 99 | 41 | | SANDSTONE / SHALE |
| 100 | 30 | | SHALE |
| 107 | 95 | | COAL No 2 SEAM |
| 113 | 51 | | SANDSTONE / SHALE |
| 118 | 01 | | COAL No 1 SEAM |
| 119 | 61 | | SHALY SANDSTONE |
| 120 | 28 | | |



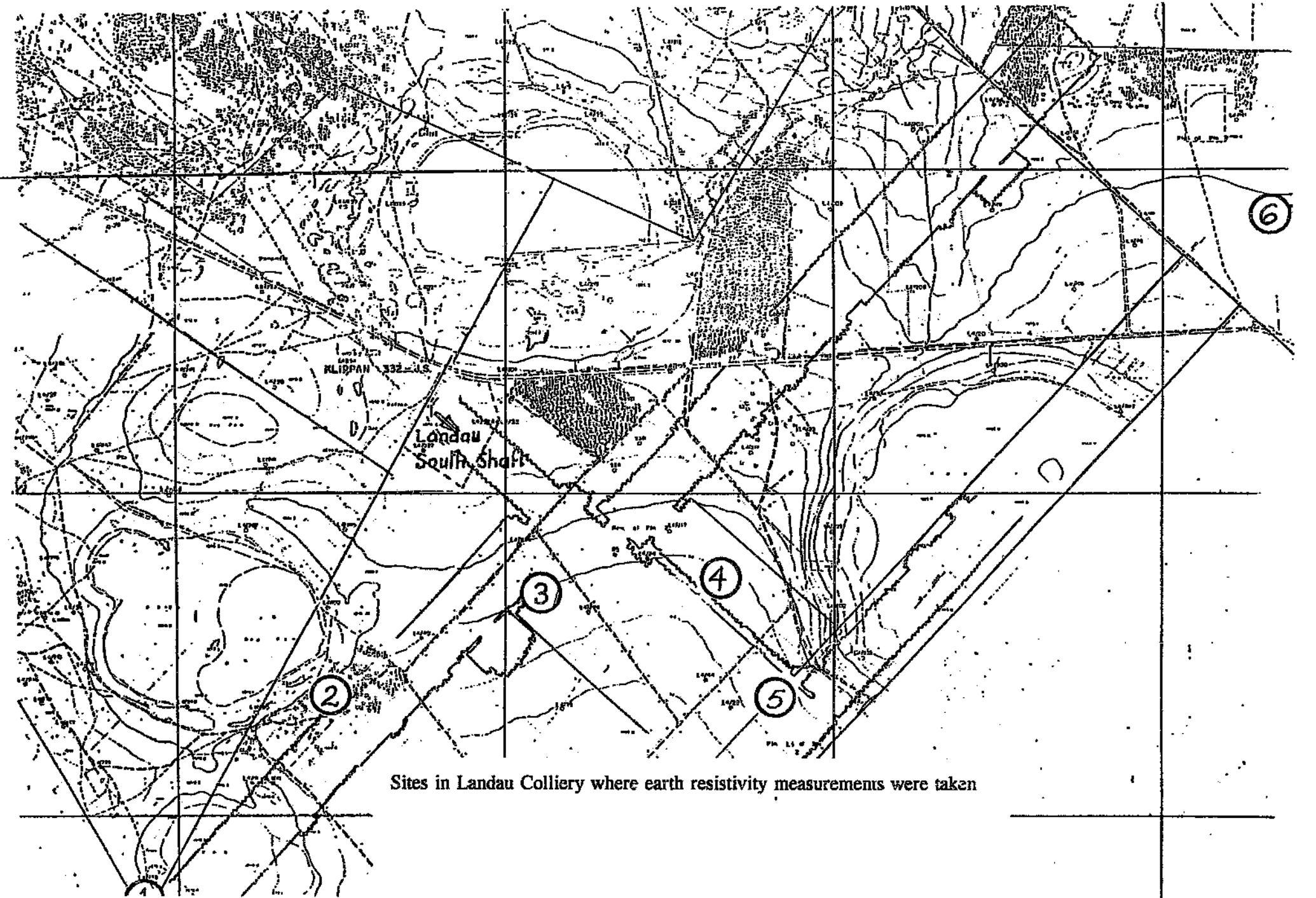

The location of boreholes at Greenside Colliery




The location of FSDs in Kriel Colliery




The location of FSDs installed in Landau Colliery




Sites in Landau Colliery where earth resistivity measurements were taken

## BOREHOLE INFORMATION

BOREHOLE No: R7 MINE: SIGMA
AREA:

| DEPTH M | DEPTH CM | GEOL. SECTION | GEOLOGICAL DESCRIPTION OF CORE |
|---|---|---|---|
| | | | OVERBURDEN |
| 7 | 62 | | SHALE |
| 15 | 00 | | SANDSTONE |
| 23 | 07 | | DOLERITE |
| 59 | 41 | | SANDSTONE |
| 64 | 93 | | SHALE |
| 69 | 73 | | MUDSTONE |
| 71 | 35 | | SHALE |
| 72 | 46 | | MUDSTONE |
| 77 | 09 | | SANDSTONE |
| 77 | 03 | | MUDSTONE |
| 77 | 05 | | SHALE |
| 80 | 47 | | MUDSTONE |
| 81 | 44 | | SHALE |
| 82 | 80 | | COAL - C3 |
| 84 | 79 | | SHALE |
| 86 | 91 | | MUDSTONE |
| 92 | 84 | | SANDSTONE |
| 97 | 46 | | COAL - C2B |
| 101 | 72 | | MUDSTONE |
| 102 | 35 | | COAL - C2A |
| 102 | 75 | | MUDSTONE |
| 104 | 46 | | TILLITE |

## BOREHOLE INFORMATION

BOREHOLE N: C2 MINE: SIGMA
AREA:

| DEPTH M | DEPTH CM | GEOL. SECTION | GEOLOGICAL DESCRIPTION OF CORE |
|---|---|---|---|
| | | | OVERBURDEN |
| 8 | 25 | | SANDSTONE |
| 12 | 80 | | SHALE |
| 25 | 91 | | SANDSTONE |
| 28 | 96 | | SHALE |
| 30 | 89 | | COAL/MARKER |
| 32 | 01 | | SHALE |
| 34 | 29 | | COAL - C3 |
| 36 | 65 | | SHALE |
| 42 | 98 | | SANDSTONE |
| 45 | 42 | | SHALE |
| 46 | 64 | | SANDSTONE |
| 50 | 70 | | COAL - C2B |
| 56 | 38 | | SHALE |
| 57 | 60 | | COAL - C2A |
| 58 | 98 | | CONGLOMERATE |
| 60 | 65 | | SHALE |
| 65 | 53 | | TILLITE |
| 70 | 72 | | |

## BOREHOLE INFORMATION

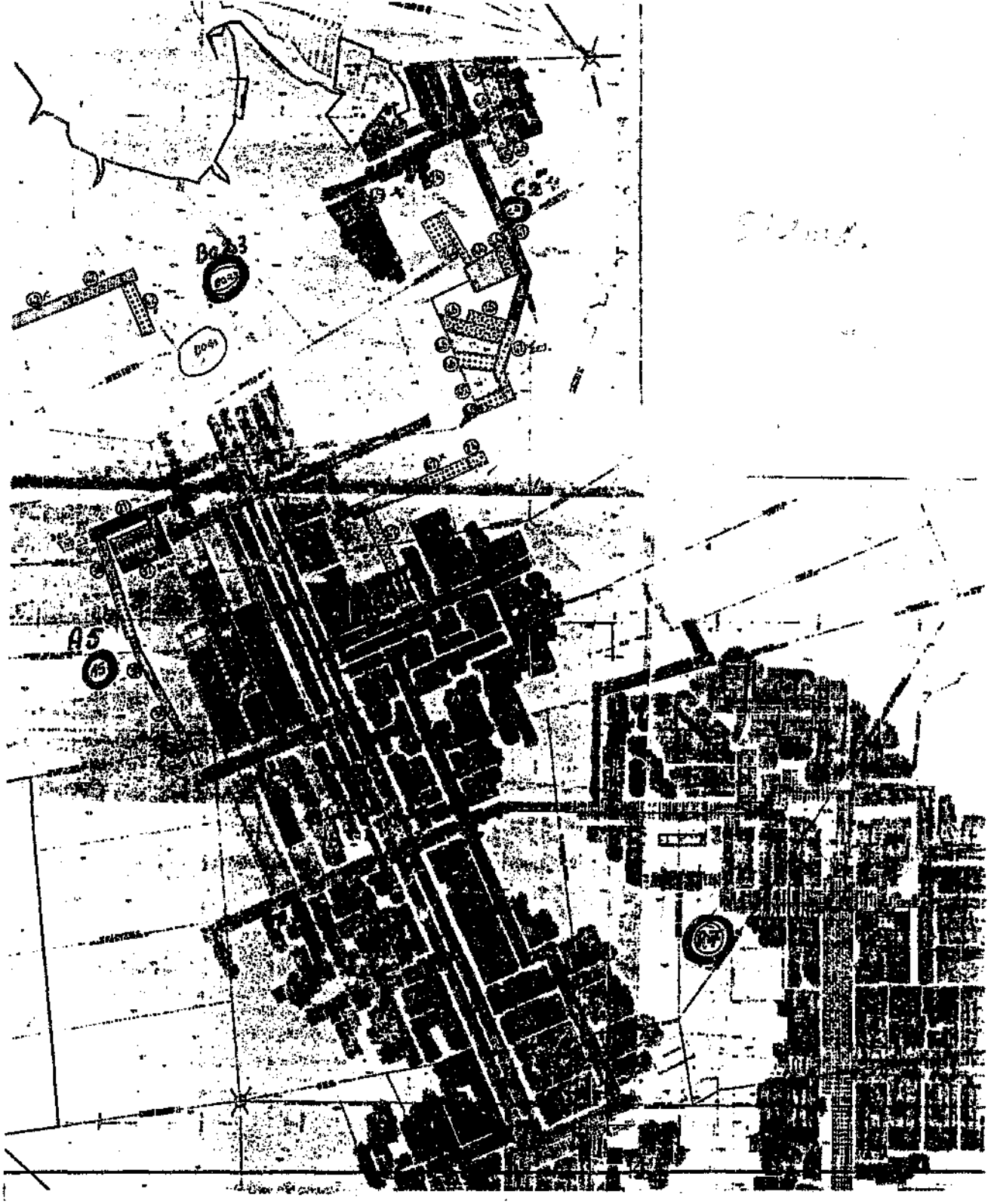
BOREHOLE No: A5 MINE: SIGMA
AREA:

| DEPTH M | DEPTH CM | GEOL. SECTION | GEOLOGICAL DESCRIPTION OF CORE |
|---|---|---|---|
| | | | OVERBURDEN |
| 8 | 00 | | DOLERITE |
| 10 | 66 | | SANDSTONE |
| 59 | 50 | | SHALE |
| 63 | 21 | | SANDSTONE |
| 65 | 70 | | SHALE |
| 80 | 66 | | MUDSTONE |
| 83 | 70 | | COAL - C3 |
| 87 | 45 | | SANDSTONE |
| 94 | 14 | | COAL - C2B |
| 95 | 93 | | MUDSTONE |
| 96 | 62 | | COAL - C2A |
| 100 | 11 | | TILLITE |
| 115 | 03 | | SANDSTONE |
| 119 | 93 | | |

## BOREHOLE INFORMATION

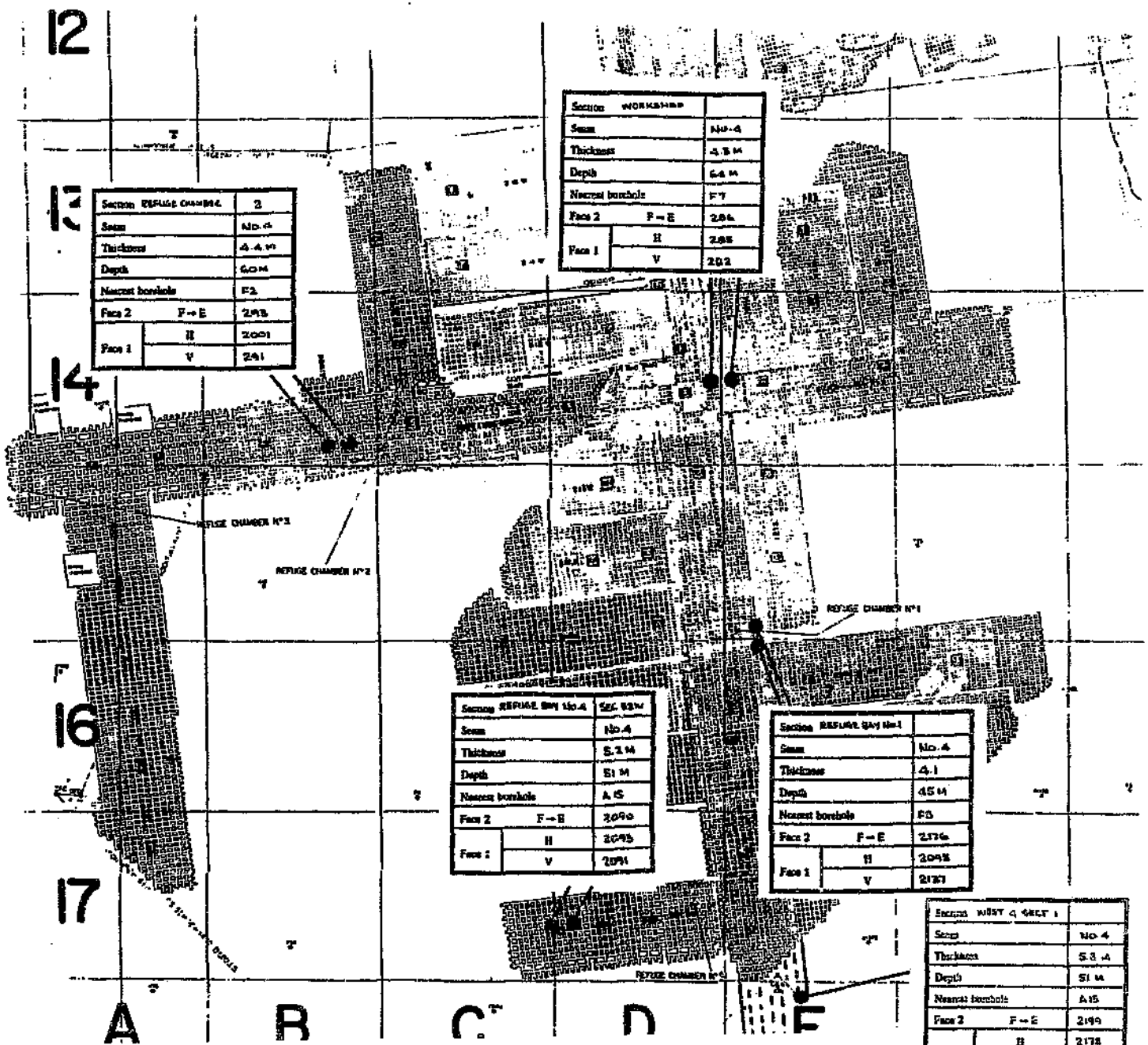
BOREHOLE No: B023 MINE: SIGMA
AREA:

| DEPTH M | DEPTH CM | GEOL. SECTION | GEOLOGICAL DESCRIPTION OF CORE |
|---|---|---|---|
| | | | OVERBURDEN |
| 6 | 95 | | DOLERITE |
| 23 | 00 | | DOLERITE |
| 24 | 50 | | DOLERITE |
| 25 | 45 | | DOLERITE |
| 27 | 20 | | DOLERITE |
| 28 | 30 | | OVERBURDEN |
| 31 | 15 | | SILT STONE |
| 44 | 50 | | SANDSTONE |
| 47 | 30 | | SHALE |
| 51 | 80 | | SILT STONE |
| 58 | 00 | | MUDSTONE |
| 61 | 66 | | SANDSTONE |
| 63 | 40 | | SHALE |
| 64 | 35 | | MUDSTONE |
| 67 | 55 | | COAL - C3 |
| 72 | 20 | | SANDSTONE |
| 75 | 60 | | SILT STONE |
| 79 | 72 | | COAL - C2B |
| 82 | 85 | | SILT STONE |
| 87 | 75 | | OVERBURDEN |
| 90 | 40 | | TILLITE |
| 94 | 30 | | |



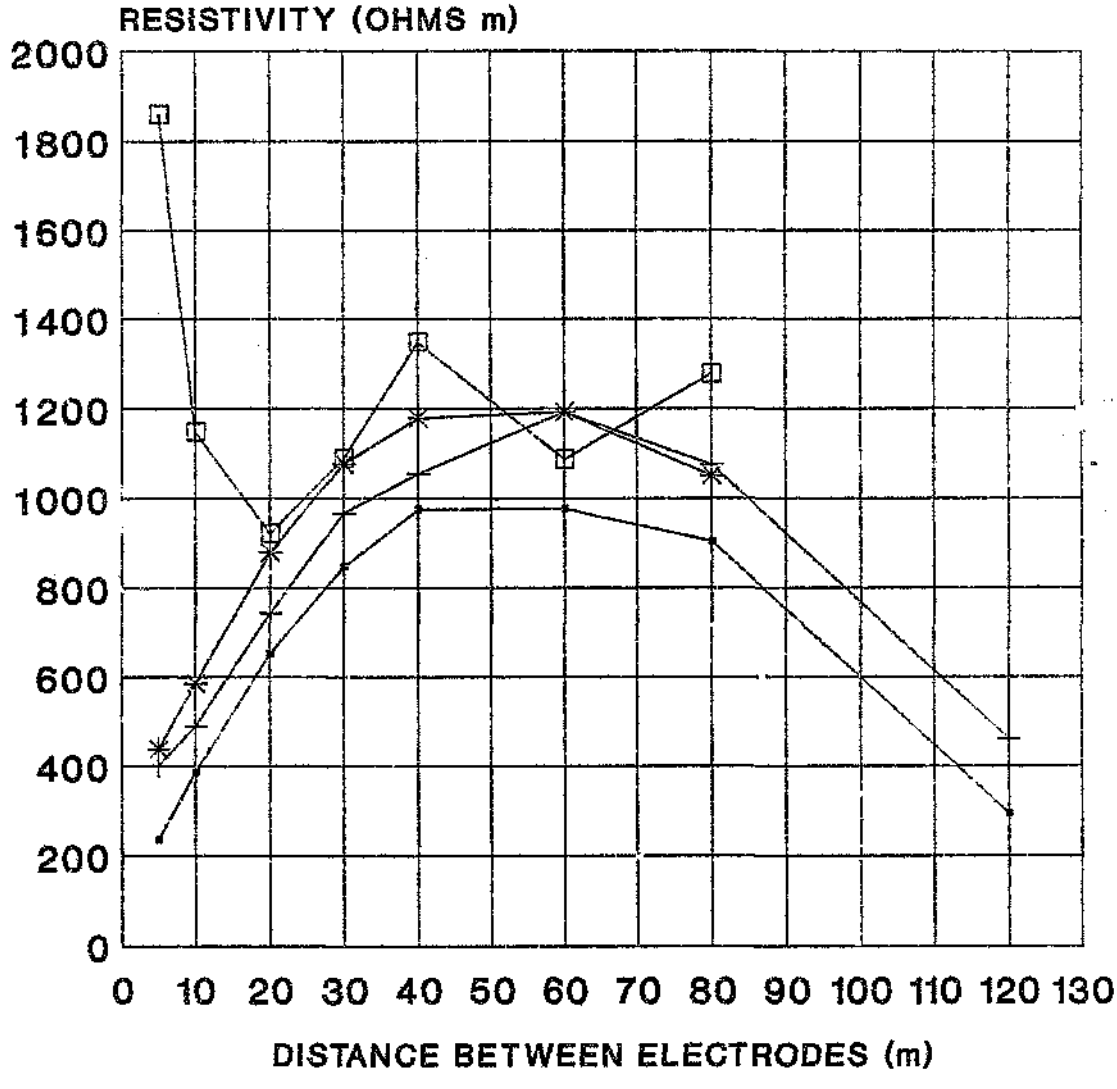

SIGMA COLLIERY

The location of boreholes in Sigma Colliery where earth resistivity measurements were taken




Location of FSDs installed in Tavistock Collieries (South Witbank Coal Mine)

# ARTHUR TAYLOR AND SOUTH WITBANK
## EARTH RESISTIVITY




**NOTE:** The resistivity/depth profiles are shown here. The geological data of the borehole is given on the next two pages and the locations of the boreholes are shown on the third page.

## BOREHOLE INFORMATION

BOREHOLE No: 18 MINE: A.T. & SOUTH WITBANK
AREA:

| DEPTH M | DEPTH CM | GEOL. SECTION | GEOLOGICAL DESCRIPTION OF CORE |
|---|---|---|---|
| | | | NO CORE RECOVERY |
| 20 | 00 | | |
| | | | SANDSTONE |
| 41 | 12 | | |
| 42 | 68 | | COAL No 5 SEAM |
| 44 | 06 | | SILTSTONE |
| | | | SANDSTONE |
| 53 | 36 | | |
| 63 | 40 | | SANDSTONE / SILTSTONE |
| 67 | 65 | | COAL No 4 SEAM |
| | | | SANDSTONE |
| 85 | 73 | | |
| 88 | 61 | | SILTSTONE |
| | | | MIXED LAYERS SANDSTONE / GRIT |
| 109 | 57 | | |
| 111 | 14 | | COAL No 2A SEAM |
| | | | GRIT |
| 117 | 87 | | |
| 120 | 52 | | SILTSTONE |
| | | | SANDSTONE |
| 132 | 94 | | |
| 134 | 77 | | DWYKA TILLITE |

## BOREHOLE INFORMATION

BOREHOLE No: BN7 MINE: A.T. & SOUTH WITBANK
AREA:

| DEPTH M | DEPTH CM | GEOL. SECTION | GEOLOGICAL DESCRIPTION OF CORE |
|---|---|---|---|
| | | | CLAY |
| 8 | 00 | | |
| 11 | 50 | | SILTSTONE / SANDSTONE |
| | | | SANDSTONE |
| 29 | 50 | | |
| 32 | 20 | | SILTSTONE / SANDSTONE |
| | | | COAL No 2 SEAM |
| 36 | 80 | | |
| | | | DOLERITE |
| 40 | 90 | | |

## BOREHOLE INFORMATION

BOREHOLE No: A28 MINE: A.T. & WITBANK SOUTH

AREA:

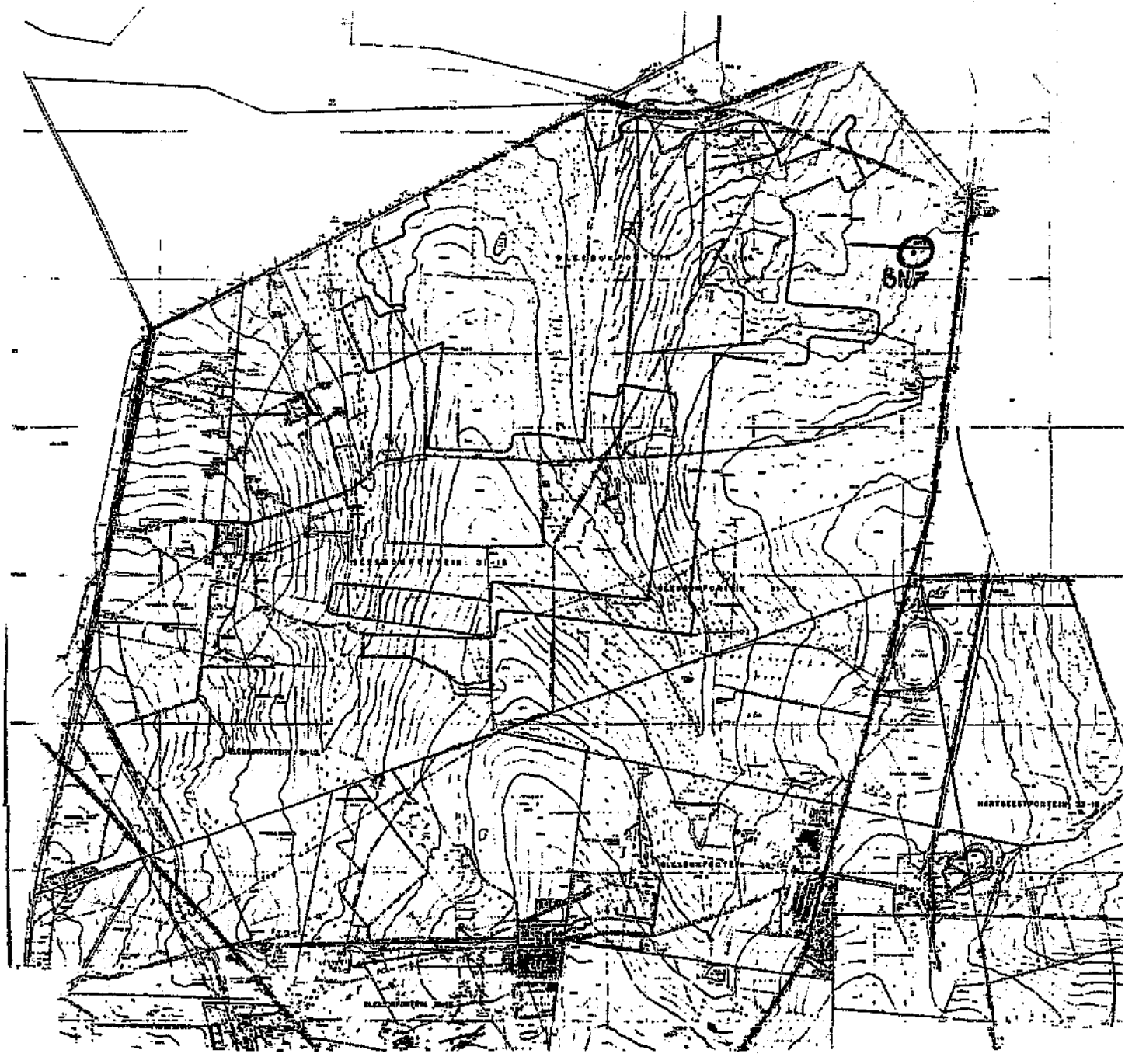
| DEPTH M | DEPTH CM | GEOL. SECTION | GEOLOGICAL DESCRIPTION OF CORE |
|---|---|---|---|
| | | | NO CORE RECOVERY |
| 12 | 56 | | SANDSTONE |
| 23 | 00 | | COAL No 5 SEAM |
| 24 | 58 | | MUDSTONE |
| 26 | 12 | | SANDSTONE |
| 37 | 27 | | SILTSTONE |
| 43 | 53 | | COAL No 4 UPPER SEAM |
| 44 | 05 | | MUDSTONE |
| 44 | 13 | | COAL No 4 LOWER SEAM. |
| | | | SANDSTONE |
| 58 | 43 | | COAL No 3 SEAM |
| 59 | 39 | | MUDSTONE |
| 61 | 00 | | COAL No 2 SEAM |
| 61 | 72 | | SANDSTONE |
| 69 | 82 | | COAL No 2A SEAM |
| 69 | 04 | | SANDSTONE |
| 71 | 02 | | COAL No 1 SEAM |
| 73 | 00 | | MUDSTONE/SANDSTONE |
| 73 | 58 | | TILLITE |
| 96 | 08 | | |

## BOREHOLE INFORMATION

BOREHOLE No: A15 MINE: A.T. & SOUTH WITBANK

AREA:

| DEPTH M | DEPTH CM | GEOL. SECTION | GEOLOGICAL DESCRIPTION OF CORE |
|---|---|---|---|
| 9 | 12 | | NO CORE RECOVERY |
| 16 | 65 | | SANDSTONE |
| 18 | 31 | | COAL No 5 SEAM |
| | | | SANDSTONE |
| 39 | 02 | | SILTSTONE / SANDSTONE |
| 41 | 34 | | COAL No 4 SEAM |
| 46 | 58 | | SANDSTONE |
| 48 | 26 | | COAL No 3 SEAM |
| 48 | 49 | | SILTSTONE/SANDSTONE |
| 50 | 14 | | SANDSTONE |
| 56 | 34 | | SILTSTONE / SANDSTONE |
| 59 | 67 | | COAL No 2 SEAM |
| 60 | 10 | | SILTSTONE |
| 61 | 18 | | SANDSTONE / GRIT |
| 81 | 17 | | COAL No 2A SEAM. |
| 82 | 32 | | SANDSTONE / SILTSTONE / GRIT. |
| 86 | 67 | | QUARTZ - FELDSPAR PORPHYRY |
| 98 | 25 | | |



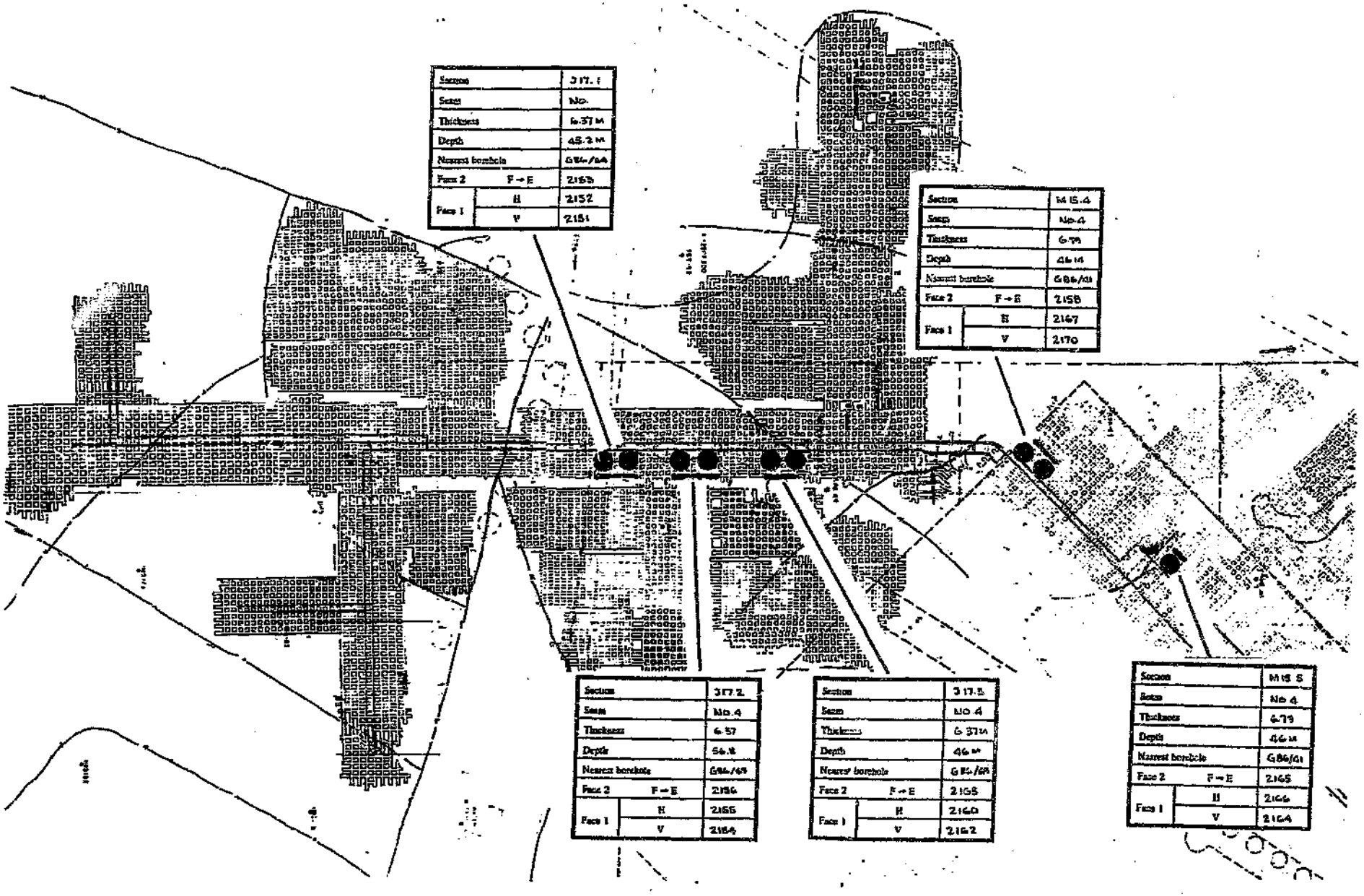

The location of a borehole where earth resistivity measurements were taken in the Arthur Taylor Colliery (part of South Witbank)



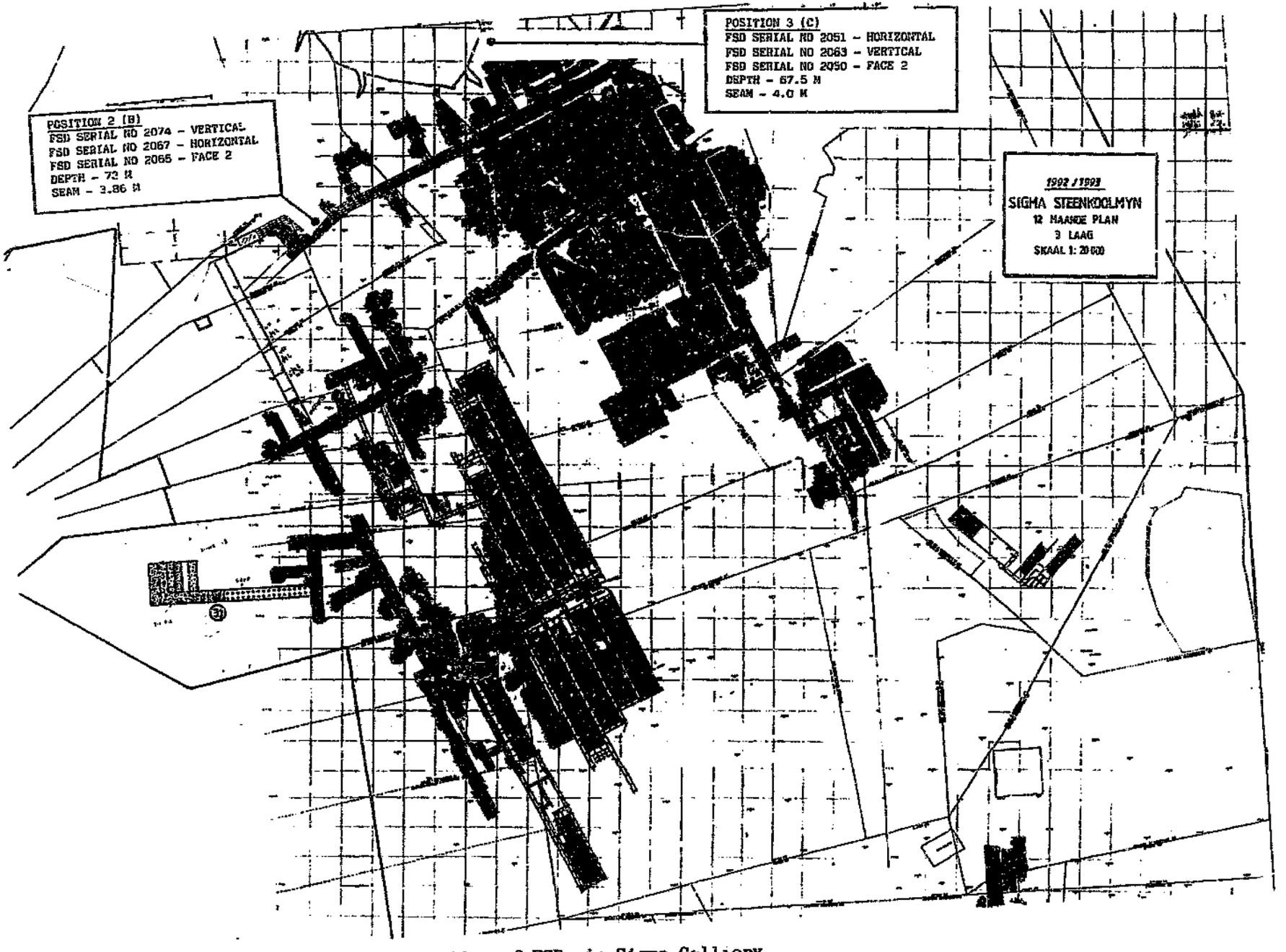

The location of boreholes in South Witbank Colliery where earth resistivity measurements were taken

LANDAU SOUTH SHAFT - EARTH RESISTIVITY TESTS

| SITE NO | a | r | ρ = 2πar |
|---|---|---|---|
| 1 | 5 | 36,3 | 1140 |
| | 10 | 13,5 | 848 |
| | 20 | 4,28 | 538 |
| | 30 | 4,89 | 921 |
| | 40 | 4,14 | 1040 |
| | 60 | 2,23 | 840 |
| 2 | 5 | 37,8 | 1188 |
| | 10 | 18,03 | 1133 |
| | 20 | 7,05 | 886 |
| | 30 | 5,30 | 999 |
| | 40 | 4,2 | 1056 |
| | 60 | 2,75 | 1037 |
| 3 | 5 | 40,3 | 1266 |
| | 10 | 19,66 | 1235 |
| | 20 | 8,36 | 1051 |
| | 30 | 5,77 | 1088 |
| | 40 | 4,54 | 1131 |
| | 60 | 3 | 1131 |
| 4 | 5 | 38,8 | 1219 |
| | 10 | 17,4 | 1093 |
| | 20 | 7,39 | 929 |
| | 30 | 5,12 | 965 |
| | 40 | 3,57 | 897 |
| | 60 | 2,89 | 1090 |
| 5 | 5 | 30,6 | 961 |
| | 10 | 209 | 13 132 |
| | 20 | 171 | 21 488 |
| | 30 | 4,5 | 848 |
| | 40 | 3,7 | 930 |
| | 50 | 212 | 66 602 |
| | 60 | 288 | 198 573 |
| 6 | 5 | 113,9 | 3 641,1 |
| | 10 | 24,4 | 1 533,1 |
| | 20 | 5,7 | 716,3 |
| | 30 | 4,2 | 791,7 |
| | 40 | 447 | 112 343,4 |
| | 60 | 2,84 | 1 070,7 |

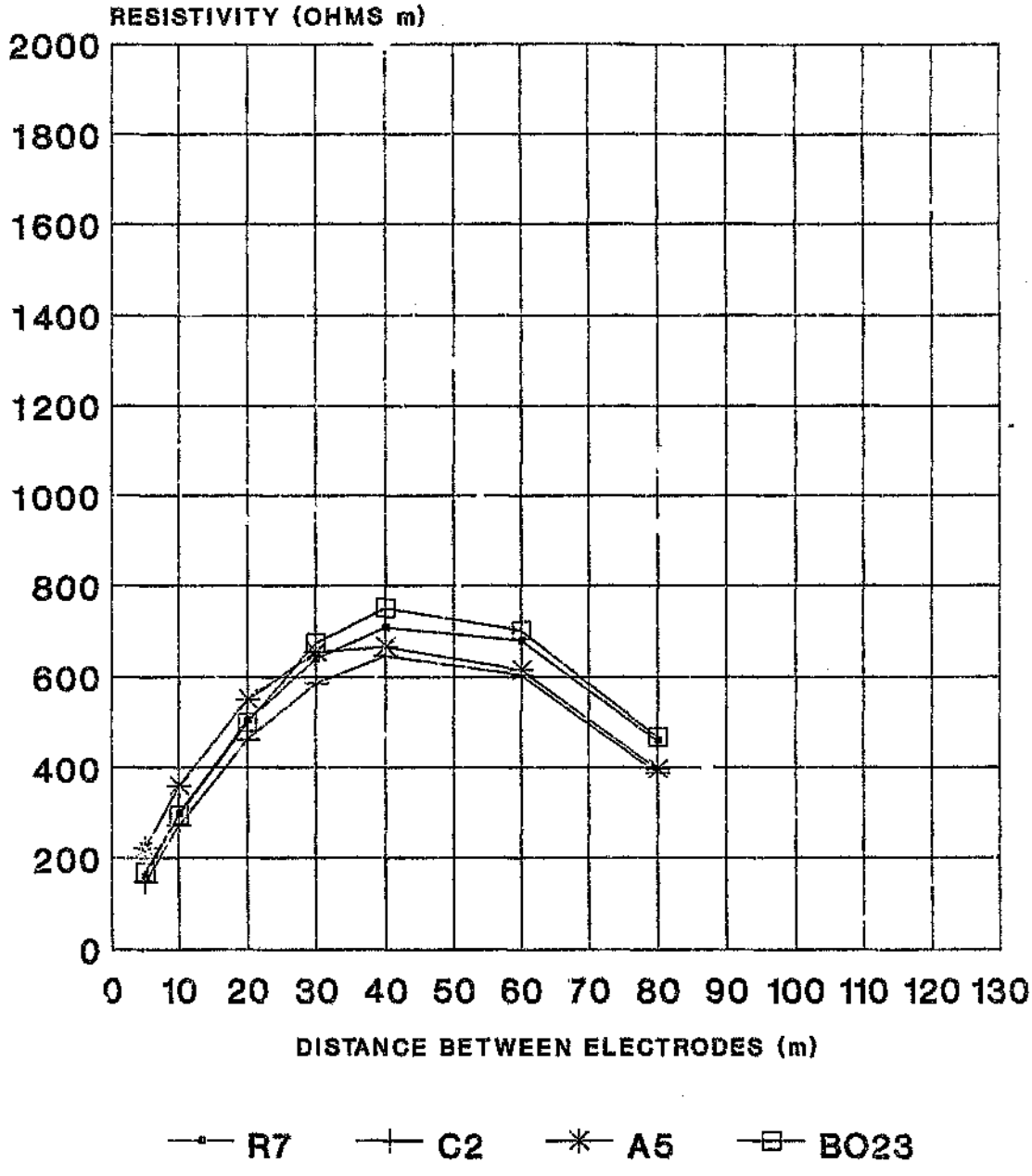



The location of FSDs in Matla Colliery




The location of FSDs in Sigma Colliery

# SIGMA MINE ( SASOL 1 )
## EARTH RESISTIVITY




**NOTE:** The resistivity/depth profiles are shown here. The geological data of the boreholes is given on the next two pages and the locations of the boreholes are shown on the third page.

**Author: Geldenhuys Hendrik Jacobus.**
**Name of thesis: The effects of lightning in shallow coal mines- an engineering study.**

***PUBLISHER:***
**University of the Witwatersrand, Johannesburg**
**©2015**

***LEGALNOTICES:***

**Copyright Notice:** All materials on the University of the Witwatersrand, Johannesburg Library website are protected by South African copyright law and may not be distributed, transmitted, displayed or otherwise published in any format, without the prior written permission of the copyright owner.

**Disclaimer and Terms of Use:** Provided that you maintain all copyright and other notices contained therein, you may download material (one machine readable copy and one print copy per page)for your personal and/or educational non-commercial use only.

The University of the Witwatersrand, Johannesburg, is not responsible for any errors or omissions and excludes any and all liability for any errors in or omissions from the information on the Library website.